

**Coronafacoyl phytotoxin biosynthesis in *Streptomyces scabies* and identification of
common scab-associated *Streptomyces* species in Newfoundland**

By

© Luke Bown

A thesis submitted to the School of Graduate Studies in partial fulfillment for the
requirements for the degree of

Doctor of Philosophy

Department of Biology

Memorial University of Newfoundland

September 2018

St. John's, Newfoundland and Labrador

Abstract

The *Streptomyces* are a genus of Gram-positive Actinomycete bacteria that are best known for their ability to produce a wide variety of secondary metabolite compounds (also known as specialized metabolites). Many of these compounds can allow the *Streptomyces* to interact with other organisms in a symbiotic manner, while other compounds such as antibiotics can have a deleterious effect on organisms that interact with them. A subset of *Streptomyces* species are pathogenic to plants and have been shown to use secondary metabolites as virulence factors for host colonization and infection. For example, *Streptomyces scabies* (syn. *S. scabiei*) is a well-characterized plant pathogen that causes the economically important disease potato common scab, and it produces several secondary metabolites that are known or suspected to contribute to the infection process. One such metabolite is coronafacoyl-L-isoleucine (CFA-Ile), which is a member of the coronafacoyl family of phytotoxins that contribute to the virulence phenotype of several different plant pathogenic bacteria. The best characterized coronafacoyl phytotoxin is coronatine (COR), which is produced by *Pseudomonas syringae*. The biosynthesis of COR and CFA-Ile involves a gene cluster that is highly conserved in both *P. syringae* and *S. scabies*, suggesting that the biosynthetic pathway for producing these metabolites is similar in both organisms. However, there is also evidence that some differences exist in the pathways leading to coronafacoyl phytotoxin production in *P. syringae* and *S. scabies*. The first objective of this study was to further elucidate the biosynthetic pathway for producing CFA-Ile in *S. scabies* by studying the role of three genes, *oxr*, *sdr* and *CYP107AK1*, in the production of this metabolite. This study examined the mechanism of action of the Cfl

enzyme, which is conserved in both *P. syringae* and *S. scabies* and is thought to catalyze the final step in coronafacoyl phytotoxin biosynthesis. The final objective of this study was to investigate the *Streptomyces* species associated with potato common scab in Newfoundland and to characterize the virulence factors that are produced by these species.

The results of this study indicate that the Sdr and CYP107AK1 enzymes are utilized in the introduction of the keto group on the bicyclic hydrindane ring of the CFA polyketide. CYP107AK1 is believed to introduce a hydroxyl group onto the CFA polyketide, which is subsequently oxidized by the Sdr enzyme to form the keto group. Lack of experimental evidence prevented the determination of function for the Oxr enzyme, although it is predicted to be involved in the formation of a C-C double bond in the CFA polyketide based on homology to other F₄₂₀-dependant oxidoreductase genes. The Cfl enzyme was shown to function through a process of adenylation in the ligation of CFA to an amino acid of L-isoleucine. These findings indicate that *S. scabies* utilizes a unique biosynthetic pathway for the biosynthesis of CFA in comparison to *P. syringae*. Observation of *Streptomyces* species associated with potato scab in Newfoundland displayed a prevalence of *S. europaeiscabiei* and an absence of *S. scabies* in the identified samples. This may indicate that *S. europaeiscabiei* is the predominant scab-associated pathogen on the island of Newfoundland.

Acknowledgements

I would like to thank my supervisor Dr. Dawn Bignell for accepting me into her lab, for all the help that she has given me and for everything that she has taught me over the past four years. I would also like to thank my supervisory committee members, Dr. Kapil Tahlan and Dr. Martin Mulligan, for the feedback and help that they have provided me during this project. I want to thank Dr. Celine Schneider, Linda Windsor and Dr. Stefani Egli from CCART for their help with the structural analysis portion of this work. I would also like to thank the former and current members of the Bignell lab who have contributed to this work, Dr. Joanna Fyans, Mead Altowairish, Phoebe Li and especially Lancy Cheng, who provided me with an immense amount of help with all parts of this project and especially with the protein analysis. I also want to thank Brandon Piercey from the Tahlan lab who helped me with the statistical analysis used in the enzyme function portion of this study.

Table of Contents

Abstract.....	ii
Acknowledgements.....	iv
Table of Contents.....	v
List of Figures.....	xiv
List of Tables.....	xx
List of Symbols, Abbreviations and Nomenclature.....	xxi
Chapter 1: Introduction and Overview.....	1
1.1 Background	1
1.2 Lifestyle and Reproduction.....	1
1.3 Secondary Metabolite Production.....	3
1.4 Pathogenic <i>Streptomyces</i>	7
1.5 Virulence Factors.....	9
1.5.1 Nec1.....	10
1.5.2 TomA.....	11
1.5.3 Thaxtomin A.....	12
1.6 Coronafacoyl Phytotoxins.....	13
1.7 Coronafacoyl Phytotoxin Biosynthesis.....	19

1.8 Thesis Objectives.....	23
1.9 References.....	26
1.10 Figures.....	43
Statement of Co-Authorship.....	53
Chapter 2: Production of the <i>Streptomyces scabies</i> coronafacoyl phytotoxins involves a novel biosynthetic pathway with an F ₄₂₀ -dependent oxidoreductase and a short-chain dehydrogenase/reductase.....	57
2.1 Abstract.....	58
2.2 Introduction.....	58
2.3 Results	62
2.3.1 Bioinformatics analyses indicate that <i>oxr</i> and <i>sdr</i> encode a predicted F ₄₂₀ -dependent oxidoreductase and a short chain dehydrogenase/reductase, respectively.....	62
2.3.2 Deletion of <i>oxr</i> and <i>sdr</i> leads to a significant reduction in CFA-Ile production in <i>S. scabies</i>	63
2.3.3 Structural elucidation of the accumulated metabolites in the Δsdr mutant indicates a role for Sdr in coronafacic acid biosynthesis.....	65
2.3.4 The accumulated metabolites in the Δsdr mutant exhibit varying degrees of potato tuber tissue hypertrophy - inducing activity.....	67

2.4 Discussion.....	68
2.5 Experimental Procedures	73
2.5.1 Bacterial strains, growth conditions and maintenance.....	73
2.5.2 Plasmids, cosmids, primers and DNA manipulations.....	74
2.5.3 Construction of the <i>S. scabies</i> Δoxr and Δsdr gene deletion mutants..	75
2.5.4 Complementation of the Δoxr and Δsdr deletion mutants.....	76
2.5.5 Analysis of <i>N</i> -coronafacoyl phytotoxin production.....	76
2.5.6 Potato tuber slice bioassay.....	77
2.5.7 Purification of <i>N</i> -coronafacoyl compounds.....	77
2.5.8 Structural elucidation of <i>N</i> -coronafacoyl compounds from <i>S. scabies</i>	78
2.5.9 Bioinformatics analyses.....	79
2.6 Acknowledgements.....	79
2.7 References.....	80
2.8 Figures and Tables.....	87
2.7 Supplementary Materials.....	101
Chapter 3: Biosynthesis and evolution of coronafacoyl phytotoxin production in the common scab pathogen <i>Streptomyces scabies</i>	119
3.1 Abstract.....	120

3.2 Introduction.....	121
3.3 Results.....	124
3.3.1 <i>CYP107AK1</i> encodes a predicted cytochrome P450 monooxygenase.....	124
3.3.2 Gene deletion analysis confirms that CYP107AK1 plays a direct role in CFA biosynthesis in <i>S. scabies</i>	125
3.3.3 The attached oxygen at position C-2 is important for the bioactivity of CFA-Ile.....	127
3.3.4 The <i>CYP107AK1</i> gene is conserved in a subset of bacterial CFA biosynthetic gene clusters.....	127
3.3.5 Gene content and phylogenetic analyses provide insights into the evolution of coronafacoyl phytotoxin biosynthesis in bacteria.....	129
3.4 Discussion.....	132
3.5 Experimental Procedures.....	137
3.5.1 Bacterial strains and culture conditions.....	137
3.5.2 Construction of the <i>S. scabies</i> Δ <i>CYP107AK1</i> gene deletion mutant.....	138
3.5.3 Analysis of <i>N</i> -coronafacoyl phytotoxin production.....	139

3.5.4 Purification of <i>N</i> -coronafacoyl biosynthetic intermediates.....	139
3.5.5 Structural elucidation of the <i>N</i> -coronafacoyl biosynthetic intermediates.....	139
3.5.6 Potato tuber slice bioassay.....	140
3.5.7 Bioinformatics analyses.....	141
3.6 Acknowledgements.....	142
3.7 References.....	142
3.8 Figures and Tables.....	150
3.9 Supplementary Information.....	161
Chapter 4: Purification of <i>N</i> -Coronafacoyl phytotoxins from <i>Streptomyces scabies</i>	167
4.1 Abstract.....	167
4.2 Introduction.....	167
4.3 Materials and Reagents.....	169
4.4 Equipment.....	171
4.5 Procedure.....	173
4.5.1 Culture growth.....	173
4.5.2 Organic extraction.....	174

4.5.3 Preparative TLC.....	176
4.5.4 Semi-preparative RP-HPLC.....	178
4.6 Notes.....	179
4.7 Recipes.....	182
4.8 Acknowledgments.....	183
4.9 References.....	184
4.10 Figures.....	185
Chapter 5: Coronafacate ligase (Cfl) functions as an adenylate-forming enzyme in the biosynthesis of the coronafacoyl phytotoxin CFA-L-Ile in the plant pathogen <i>Streptomyces scabies</i>	191
5.1 Abstract.....	191
5.2 Introduction.....	192
5.3 Results.....	196
5.3.1 Analysis of the Cfl protein in <i>S. scabies</i> 87-22 and <i>P. syringae</i> pv. <i>tomato</i> DC3000.....	196
5.3.2 Identification of putative <i>cfl</i> genes in <i>Streptomyces</i> spp.....	197
5.3.3 Cloning, expression and purification of the Cfl enzyme.....	198
5.3.4 Cfl exhibits adenylation activity <i>in vitro</i>	199

5.3.5 Confirmation of CFA-Ile production by the Cfl enzyme.....	200
5.4 Discussion.....	201
5.5 Experimental Procedures.....	204
5.5.1 Bioinformatics analysis.....	204
5.5.2 Bacterial strains and growth conditions.....	204
5.5.3 Plasmid, cosmids, primers and DNA manipulation.....	205
5.5.4 Construction of the <i>E. coli cfl</i> expression strain	205
5.5.5 Protein purification protocol.....	206
5.5.6 Western analysis.....	207
5.5.7 Enzyme reaction assay for the detection of adenylation activity.....	208
5.5.8 Analysis of Cfl enzyme ligation products.....	209
5.6 Acknowledgements.....	211
5.7 References.....	211
5.8 Figures and Tables.....	217
5.9 Supplementary Information.....	230
Chapter 6: Isolation and characterization of plant pathogenic <i>Streptomyces</i> species associated with common scab – infected potato tubers in Newfoundland.....	231
6.1 Abstract.....	232

6.2 Introduction.....	232
6.3 Results and Discussion.....	235
6.4 Experimental Procedures.....	241
6.4.1 <i>Streptomyces</i> spp. used in this study.....	241
6.4.2 Isolation of <i>Streptomyces</i> spp. from potato scab lesions.....	241
6.4.3 Morphological and physiological characterization.....	242
6.4.4 Pathogenicity testing.....	243
6.4.5 Bioactivity of the secreted 11-1-2 phytotoxin.....	245
6.4.6 Production of thaxtomin A.....	245
6.4.7 Production of concanamycin A and borrelidin.....	246
6.4.8 Genotypic characterization.....	247
6.4.9 Phylogenetic analysis.....	248
6.4.10 Accession numbers.....	248
6.5 Acknowledgments.....	249
6.6 References.....	249
6.7 Figures and Tables.....	257
Chapter 7: Draft Genome Sequence of the Plant Pathogen <i>Streptomyces</i> sp. 11-1-2.....	271
7.1 Abstract.....	271
7.2 Results and Discussion.....	271

7.3 Acknowledgements.....	274
7.4 References.....	274
Chapter 8: Summary and Future Directions.....	276
8.1 Coronafacoyl phytotoxin production in <i>S. scabies</i>	276
8.2 Plant pathogenic <i>Streptomyces</i> spp. in Newfoundland.....	281
8.3 References.....	284
Appendix 1	
Appendix 2	

List of Figures

Figure 1.1. Life cycle of organisms from the <i>Streptomyces</i> genus.....	43
Figure 1.2. Common scab disease symptoms on a potato tuber.....	44
Figure 1.3. Molecular structure of the thaxtomin A phytotoxin.....	45
Figure 1.4. The CFA and CFA-like biosynthetic gene clusters from <i>P. syringae</i> and <i>S. scabies</i> respectively.	46
Figure 1.5. Molecular structures of (A) coronatine (COR); (B) coronafacoyl-L-isoleucine (CFA-Ile); (C) jasmonoyl-L-isoleucine (JA-Ile).....	48
Figure 1.6. The JA-Ile regulatory pathway.	49
Figure 1.7. Proposed pathway for the biosynthesis of COR in <i>P. syringae</i>	51
Figure 2.1. (A) Biosynthesis of coronafacoyl phytotoxins in <i>Pseudomonas syringae</i> and <i>Streptomyces scabies</i> . (B) Organization of the <i>cfa</i> biosynthetic gene cluster in <i>P. syringae</i> pv <i>tomato</i> DC3000 and the <i>cfa</i> -like biosynthetic gene cluster in <i>S. scabies</i> 87-22	87
Figure 2.2. Phylogenetic relationships among homologues of Oxr (A) and Sdr (B) from the database.	89
Figure 2.3. RP-HPLC analysis of coronafacoyl phytotoxin production by <i>Streptomyces scabies</i> strain $\Delta txtA$ /pRLDB51-1 (A, C), Δoxr (isolate 3) (B) and Δsdr (isolate 1) (D)	90

Figure 2.4. Hypertrophy-inducing activity of organic culture extracts from <i>Streptomyces scabies</i> Δoxr (isolates 2 and 3) (A) and Δsdr (isolates 1 and 2) (B) on potato tuber tissue	91
Figure 2.5. Structure of the metabolites 1 and 2 that accumulated in Δsdr culture supernatants.....	92
Figure 2.6. Hypertrophy-inducing activity of the purified Δsdr metabolites 1 (iv) and 2 (v) (100 nmol each) on potato tuber tissue.	93
Figure 2.7. Hypothetical pathway for the biosynthesis of CFA in <i>Pseudomonas syringae</i> (A) and <i>Streptomyces scabies</i> (B).....	94
Figure S-2.1. Genetic complementation of CFA-Ile production in the Δoxr and Δsdr mutants.	101
Figure S-2.2. (A) RP-HPLC analysis of the purified metabolites 1 and 2 from the Δsdr mutant. (B) RP-HPLC analysis of the purified CFA-Ile end product from the $\Delta txtA$ /pRLDB51-1 strain.	103
Figure S-2.3. HRESIMS/MS analysis of the purified metabolites 1 (A) and 2 (B) from the Δsdr mutant.....	105
Figure S-2.4, related to Table 2.2 and Figure 2.5. NMR spectra of the purified Δsdr metabolite 1.	106
Figure S-2.5, related to Table 2.2 and Figure 2.5. NMR spectra of the purified Δsdr metabolite 2.	109

Figure S-2.6, related to Table 2.2. NMR spectra of the purified CFA-Ile.	112
Figure 3.1. (A) Structure of the coronafacoyl phytotoxins coronatine (COR) and coronafacoyl-L-isoleucine (CFA-Ile) produced by <i>P. syringae</i> and <i>S. scabies</i> , respectively, and of the bioactive plant hormone conjugate (+)-7- <i>iso</i> -jasmonyl-L-isoleucine (JA-Ile). (B) Organization of the CFA biosynthetic gene cluster from <i>S. scabies</i> 87-22	150
Figure 3.2. Proposed biosynthetic pathways for the production of coronafacoyl phytotoxins in <i>P. syringae</i> and <i>S. scabies</i>	151
Figure 3.3. (A) RP-HPLC analysis of culture extracts from the <i>S. scabies</i> $\Delta txtA/pRLDB51-1$ strain (blue line) and the $\Delta CYP107AK1$ mutant (red line). (B) Chemical structure of the purified intermediates i and ii. (C) Hypertrophy-inducing activity of organic culture extracts of <i>S. scabies</i> $\Delta txtA/pRLDB51-1$ (IV) and $\Delta CYP107AK1$ (V) on potato tuber tissue. (D) Hypertrophy-inducing activity of purified CFA-Ile (III) and of the $\Delta CYP107AK1$ mutant intermediates i (IV) and ii (V) on potato tuber tissue	153
Figure 3.4. (A) Heat map showing the protein BLAST identity hits to the <i>S. scabies</i> 87-22 Cfa1-7 and Cfl proteins in different bacterial genomes. (B) Organization of known and putative CFA biosynthetic gene clusters identified in sequenced bacterial genomes. (C) Domain organization of the Cfa6 and Cfa7 type I polyketide synthases encoded in the CFA biosynthetic gene clusters from different bacteria.	155

Figure 3.5. NAD(P)H binding motifs from the Cfa7 ER domains of <i>S. scabies</i> , <i>Azospirillum</i> sp. B510, <i>K. azatica</i> , <i>S. griseoruber</i> and <i>Streptomyces</i> sp. WC-3618.	157
Figure 3.6. Maximum likelihood phylogeny of the core CFA biosynthetic genes (A) and the 16S rRNA gene (B) from different bacteria.	158
Figure S-3.1. LC-HRMS analysis of the purified intermediates i (A) and ii (B) from the <i>S. scabies</i> Δ CYP107AK1 mutant.....	161
Figure S-3.2. Key COSY and HMBC correlations of the purified intermediates i (A) and ii (B) from the <i>S. scabies</i> Δ CYP107AK1 mutant.....	163
Figure S-3.3. (A) Tandem MS spectrum of the purified intermediate i. (B) Expected fragmentation pattern of the intermediate i.....	164
Figure S-3.4. (A) Tandem MS spectrum of the purified intermediate ii. (B) Expected fragmentation pattern of the intermediate ii.....	166
Figure 4.1. Structure of <i>N</i> -coronafacoyl-L-isoleucine (CFA-L-Ile) produced by <i>Streptomyces scabies</i>	185
Figure 4.2. Schematic outline of principle steps performed during the extraction of coronafacoyl phytotoxins from <i>S. scabies</i> culture supernatants.....	186
Figure 4.3. Extraction of <i>S. scabies</i> culture supernatants with chloroform	187

Figure 4.4. TLC analysis of the <i>S. scabiei</i> organic extract containing CFA-L-Ile	188
Figure 4.5. Preparative TLC analysis of the <i>S. scabiei</i> organic extract containing CFA-L-Ile.	189
Figure 4.6. Purification of CFA-L-Ile by semi-preparative RP-HPLC.....	190
Figure 5.1. Molecular structures of (A) Coronatine (COR); (B) CFA-L-isoleucine (CFA-Ile).....	217
Figure 5.2. The CFA and CFA-like biosynthetic gene clusters from <i>P. syringae</i> and <i>S. scabiei</i> respectively.	218
Figure 5.3. Proposed biosynthetic steps catalyzed by the Cfl enzyme during COR production in <i>P. syringae</i>	220
Figure 5.4. Partial protein alignment of highly conserved regions of the Cfl enzyme from bacteria previously shown to contain homologues to the <i>cfl</i> gene.	221
Figure 5.5. Detection of <i>cfl</i> homologues in <i>Streptomyces</i> genomes..	223
Figure 5.6. SDS-PAGE and Western blot analysis of the <i>S. scabiei</i> Cfl-His ₆ protein purified from <i>E. coli</i>	224
Figure 5.7. Schematic showing the mechanism of the molybdate/malachite green colorimetric enzyme assay used for detecting enzyme adenylation activity.	225

Figure 5.8. (A) Malachite green enzyme reaction assay for detection of <i>S. scabies</i> Cfl enzyme adenylation activity. (B) Quantification of adenylation enzyme activity by the <i>S. scabies</i> Cfl.	226
Figure 5.9. Detection of CFA-Ile produced <i>in vitro</i> by the <i>S. scabies</i> Cfl enzyme using LC-LRESIMS analysis. The LC chromatograms shown are for the CFA-Ile standard (A) and the Cfl enzyme reaction extract (B).....	228
Figure 6.1. Production of thaxtomin A by plant pathogenic <i>Streptomyces</i> spp. isolated in this study.	257
Figure 6.2. Phylogenetic analysis of plant pathogenic <i>Streptomyces</i> spp. isolated in this study.	258
Figure 6.3. RFLP analysis of the 16S-23S rDNA ITS sequence in the thaxtomin A-producing <i>Streptomyces</i> spp. isolated in this study. (A) Diagram of the genomic 16S-23S rDNA ITS region in <i>S. scabies</i> 87-22. (B) Agarose gel electrophoresis of the PCR-amplified 16S-23S rDNA ITS region following digestion with <i>Hpy99I</i>	260
Figure 6.4. Rep-PCR analysis of the thaxtomin A-producing <i>Streptomyces</i> spp. isolated in this study.	262
Figure 6.5. Plant pathogenic phenotype of <i>Streptomyces</i> sp. strain 11-1-2 on different plant hosts.	264
Figure 6.6. Analysis of concanamycin A and borrelidin production by <i>Streptomyces</i> spp.	266

List of Tables

Table 2.1. Bacterial strains, cosmids and plasmids used in the study of the Sdr and Oxr enzymes from <i>S. scabies</i>	96
Table 2.2. 1-dimensional (^1H , ^{13}C) NMR spectral data (in ppm) for purified CFA-Ile and the Δsdr metabolites 1 and 2 in CD_3OD with 0.1% TFA-d.....	99
Table S-2.1: Accession numbers of proteins used to construct the Oxr and Sdr phylogenetic trees.....	115
Table S-2.2. Oligonucleotides used in the study of the <i>oxr</i> and <i>sdr</i> genes from <i>S. scabies</i>	117
Table 3.1. Bacterial strains, cosmids and plasmids used in the study of the CYP107AK1 enzyme from <i>S. scabies</i>	159
Table 5.1. Bacterial strains, cosmids and plasmids used in the study of the Cfl enzyme from <i>S. scabies</i>	229
Table S-5.1. Oligonucleotides used in the study of the Cfl enzyme.....	230
Table 6.1: Primers used for PCR and sequence analysis of the Newfoundland pathogenic <i>Streptomyces</i> isolates.....	268
Table 6.2: Phenotypic and genotypic characterization of the Newfoundland pathogenic <i>Streptomyces</i> isolates.....	269

List of Symbols, Abbreviations and Nomenclature

Δ – deletion

ABC – ATP-binding cassette

ACN – acetonitrile

amp^r – ampicillin resistance

AMP – adenosine monophosphate

ANOVA – analysis of variance

apra^r – apramycin resistance

AS – acid scab

AT – acyl transferase

ATP – adenosine triphosphate

BGC – biosynthetic gene cluster

BLASTP – basic local alignment search tool proteins

BSA – bovine serum albumin

cam^r – chloramphenicol resistance

CCR - crotonyl-CoA reductase

CFA – coronafacic acid

CFA-*a*Ile – coronafacoyl-L-*allo*-isoleucine

CFA-Ile – coronafacoyl-L-isoleucine

CFA-Val – *N*-coronafacoyl-L-valine

Cfl – coronafacate ligase

Cfl-HIS₆ – Histidine tagged Cfl protein
CMA – coronamic acid
CoA – coenzyme A
coi1 – coronatine insensitive 1
COR – coronatine
COSY – correlated spectroscopy
CPC – 2-carboxy-2-cyclopentenone
CPE – 2-[1-oxo-2-cyclopente-2-yl-methyl] butanoic acid
CS – common scab
cv – cultivar
CYP – cytochrome P450
CYP107AK1 – cytochrome P450 monooxygenase

DH – dehydratase
DMSO – dimethyl sulfoxide
DNA – deoxyribonucleic acid

ER – enoyl reductase
ESI – electrospray ionization

FMN – flavin mononucleotide
FPLC – fast protein liquid chromatography

HGAP – Hierarchical Genome Assembly Process
HGT – horizontal gene transfer
HIS₆ – Histidine x 6

HMBC – heteronuclear multiple bond correlation
HPLC – high performance liquid chromatography
HRESIMS – high resolution electrospray ionization mass spectra
HRESIMS/MS – tandem high-resolution electrospray ionization mass spectra
HSQC – heteronuclear single quantum coherence
hyg^r – hygromycin B resistance

IPTG – Isopropyl β -D-thiogalactopyranoside
ISP-4 – International *Streptomyces* Project Medium 4
ISP-9 – International *Streptomyces* Project Medium 9
ISR – induced systemic resistance
ITS – internally transcribed spacer

JA – jasmonic acid
JA-Ile – jasmonoyl-L-isoleucine
JAZ – jasmonate ZIM-domain

kan^r – kanamycin resistance
KHCO₃ – potassium bicarbonate
KR – ketoreductase
KS – ketosynthase

LB – lysogeny broth
LC – liquid chromatography
LC-MS – liquid chromatography-mass spectrometry

LC-HRESIMS – liquid chromatography-high resolution electrospray ionization mass spectrometry

LC-LRESIMS – liquid chromatography-low resolution electrospray ionization mass spectrometry

MWCO – molecular weight cut-off

NA – nutrient agar

NAD – nicotinamide adenine dinucleotide

NADP – nicotinamide adenine dinucleotide phosphate

NCBI – National Center for Biotechnology Information

NINJA – novel interactor of JAZ

Ni-NTA – nickel charged affinity resin

NMR – nuclear magnetic resonance

NOESY – nuclear Overhauser effect spectroscopy

NRPS – non-ribosomal peptide synthetase

NS – netted scab

OBA – oat bran agar

OD – optical density

OMPG – methyl- α -D-galactopyranoside

oriT – origin of transfer

Oxr – oxidoreductase

PAI – pathogenicity island

PCR – polymerase chain reaction

Pi – inorganic phosphate

PKS – polyketide synthase

PMA – potato mash agar

PP – phosphopanthoate

PPi – inorganic pyrophosphate

pv – pathovar

rDNA – ribosomal deoxyribonucleic acid

rif^r – rifampin resistance

RP-HPLC – reverse phase-high performance liquid chromatography

rpm – revolutions per minute

rRNA – ribosomal ribonucleic acid

SA – salicylic acid

SCF – Skp1-Cullin-F-box

Sdr – short chain dehydrogenase/reductase

SDS-PAGE – sodium dodecyl sulfate polyacrylamide gel electrophoresis

SFMB – soy flour mannitol broth

SMRT – single-molecule real-time

SIS – systemic induced susceptibility

SOB – super optimal broth

SOC – super optimal broth with catabolite repression

spp. – species

TBE – tris/borate/EDTA

TE – thioesterase

tet^r – tetracycline resistance

TFA-d – deuterated trifluoroacetic acid

TIC – total ion current

thio^r – thiostrepton resistance

TLC – thin layer chromatography

TOF – time-of-flight

TPL – TOPLESS repressor

t_R – retention time

TSB – trypticase soy broth

txt – thaxtomin

UV – ultraviolet

v/v – volume/volume

w/v – weight/volume

Chapter 1: Introduction and Overview

1.1 Background

Streptomyces is a genus of Actinobacteria that is mainly composed of terrestrial soil dwelling species, although examples of species isolated from marine sources such as fish, sponges, seaweeds, molluscs and sediment samples have been documented (Dharmaraj 2010; Pathom-aree et al. 2006). There are, at present, roughly 550 described species of *Streptomyces*, members of which are Gram-positive, obligate aerobes that utilize a saprophytic lifestyle and have linear chromosomes with a high guanine-cytosine (GC) content relative to other species. The first *Streptomyces* genome to be sequenced was that of *Streptomyces coelicolor* A(2), and it possesses a GC content of 72.12% with a chromosome size of 8.7 Mbp (Bentley et al. 2002). The genome size for these organisms is also large in comparison to other bacteria and can vary considerably within the genus as seen with *Streptomyces albus* J1074 and *Streptomyces bingchenggensis* BCW-1 which have genome sizes of 6.4 and 11.9 Mbp respectively (Zaburannyi et al. 2014; Wang et al. 2010). In comparison, the genome of the well-studied organism *Escherichia coli* K-12 has a GC content of 50.8% and a size of 4.6 Mbp (Riley et al. 2006).

1.2 Lifestyle and Reproduction

The *Streptomyces* have a complex and distinctive lifestyle compared to other bacterial species (Fig. 1.1). Unlike other bacteria that reproduce through binary fission, *Streptomyces* spp. reproduce through sporulation in a manner very similar to that of

filamentous fungi. The life-cycle begins with the germination of a spore in response to a source of soluble nutrients (Chater 2006), and growth occurs as a mass of branching vegetative hyphae that form a substrate mycelium. The multigenomic and non-septate hyphae grow through tip extension and the introduction of branching segments thus cell wall synthesis only occurs at the hyphal tips (Flärdh and Buttner 2009; Flärdh et al. 2012). After the supply of soluble nutrients has been exhausted, the cells of the mycelium begin to synthesize and excrete extracellular enzymes that break down insoluble organic material, such as chitin or cellulose for use as nutrient sources (Chater 2006; Chater et al. 2010; Bertram et al. 2004). As nutrients in the environment surrounding the substrate mycelium are exhausted, the *Streptomyces* begin to produce hydrophobic aerial hyphae that break the surface of the medium and extend upward into the air (Flärdh and Buttner 2009; Chater 2006). The nutrients necessary for this growth are at least partially provided by the autolysis of the substrate mycelium (Wildermuth 1970; Chater 2006). Growth into the aerial environment necessitates the production of a protective, hydrophobic coating produced by at least three distinct proteins, SapB, the chaplins, and the rodmins (McCormick and Flärdh 2012). When the newly emerged aerial hyphae have acquired adequate biomass through cell elongation they synchronously differentiate into a segmented chain of compartments, and at the same time a single copy of the chromosome is deposited through a process of active segregation into each of the pre-spore compartments (Hamedi et al. 2017; McCormick and Flärdh 2012; Flärdh and Buttner 2009). Following maturation, the resulting spores can then be dispersed into the environment and will germinate into a new mycelial network when they encounter a suitable environment. However, this classically defined version of the *Streptomyces* lifestyle has recently been expanded upon by the

discovery that under specific conditions involving co-culturing with yeast cells, several *Streptomyces* spp. have demonstrated a previously uncharacterized form of growth termed “exploratory growth” (Jones et al. 2017). This growth is related to glucose starvation, is dependant on the elevation of local pH by the release of a volatile organic compound, and results in rapid outgrowth of hydrophilic, unbranching hyphae. The rate of expansion for these exploratory hyphae has been determined to be $10 \times$ that of normal vegetative growth and they have demonstrated the ability to rapidly expand beyond the confines of the original *Streptomyces* colony by growing over significant obstacles such as rocks or the dividers of a petri dish (Jones et al. 2017). However, it is currently unknown if this new form of development represents a means of replication that will result in a new *Streptomyces* colony or if it is a means of nutrient acquisition for the original colony.

1.3 Secondary Metabolite Production

Perhaps the most well documented and notable characteristic of the *Streptomyces* is their propensity to produce natural products and secondary metabolites in particular. Natural products are composed of primary metabolites that are essential for the growth and development of a cell, and secondary metabolites which are considered to be non-essential for growth under laboratory conditions. While the exact physiological role of secondary metabolites is not understood in many cases, they are thought to confer some advantage in the producing organisms’ environment due to the metabolic cost associated with their biosynthesis.

Secondary metabolites can encompass a multitude of different classes of compounds including polyketides, peptides, steroids, alkaloids, carbohydrates, lipids and terpenoids among others (O'Brien and Wright 2011). These products are not only differentiated based on their chemical structure but on their different bioactivities such as chelators, pigments and anti-microbial agents, which has led to numerous ideas about why organisms expend the energy to synthesize these products. Some secondary metabolites have a known function such as siderophores which are chelating agents that have a high affinity and selectivity for iron (III) and are secreted into the environment to bind this usually essential mineral and bring it into the cell. Bacteria, fungi and some plants have been shown to produce siderophores as a means of acquiring iron (III) under low-iron stress conditions (Neilands 1995; Crowley 2000). Pigments are suspected of functioning in the protection of spores against UV radiation or predation and many compounds produced by *Streptomyces* spp. have been observed to have an antibiotic effect on other types of microorganisms found in the surrounding environment and may therefore function in intermicrobial competition, though these functions are predicted based on laboratory observations and may not be representative of natural conditions (Chater et al. 2010). It is notable that some secondary metabolites with antibiotic activity have been shown to stimulate specific intracellular responses in other microbes at sub-inhibitory concentrations, leading to the suggestion that these compounds may function in intercellular communication rather than as agents of intercellular warfare in nature (Fajardo and Martínez 2008; Yim et al. 2007; Linares et al. 2006). While many compounds that have an observed antibiotic effect at high concentrations may be produced at sub-inhibitory concentrations in the environment, the coproduction of compounds such as β -lactams and

β -lactamase inhibitors as well as the presence of resistance genes to the produced antibiotics in other environmental microorganisms suggest that at least some of the secondary metabolites demonstrating these effects have evolved for use specifically as antibiotics (Challis and Hopwood 2003; O'Brien and Wright 2011).

In the case of the *Streptomyces*, the implications of secondary metabolite biosynthesis have been far-reaching and numerous in their applications. As of 2005, roughly one-third of all bioactive metabolites isolated from microbial (including fungal) sources originated from *Streptomyces* spp. (Bérdy 2005). These compounds display a myriad of bioactivities including anti-bacterial, anti-fungal, anti-parasitic, anti-helminthic, herbicidal, insecticidal, anti-tumor, growth promotion and enzyme inhibition to name some (Bérdy 2005). While it has been theorized that not all compounds that display antibacterial effects in a laboratory setting may actually be utilized as such in the environment, observations about the relationship between secondary metabolite biosynthesis and the *Streptomyces* lifestyle suggest that many are in fact produced for this purpose. In *Streptomyces* spp., the production of antibiotic compounds occurs at the same time as the depletion of nutrients in the surrounding environment and the lysis of the substrate mycelium. The concurrence of this production with the lysis of the substrate mycelium for the release of nutrients is suspected to be a means of eliminating microbial competitors in the surrounding environment that may benefit from the sudden increase of available nutrients and prevent the loss of those nutrients before the aerial hyphae can utilize them (Chater 2006; McCormick and Flärdh 2012; Chater and Dyson 2011). Mathematical models have been used to calculate the number of potential antibiotic compounds produced

by *Streptomyces* spp. and have estimated that the number of compounds currently isolated may be only a fraction of those which are actually produced, and that the decline in the number of recently discovered antibiotics may be related to the screening methods used (Watave et al. 2001).

There is also evidence that through these secondary metabolites *Streptomyces* spp. can interact, not just with other microorganisms in their environment, but with more complex multicellular organisms as well. For example, *Streptomyces philanti* has been shown to be cultivated through vertical transmission in specialized antennal glands of solitary digger wasps (genera *Philanthus*, *Trachypus* and *Philanthinus*). The organism is passed to the insect larvae and produces at least nine separate antibiotic compounds that are used to protect the larvae from pathogenic fungi that can occur in the underground cocoon (Kaltenpoth et al. 2012). *Streptomyces* have also been shown to have complex symbiotic relationships with various species of plants and fungi, where secreted growth factors can increase growth rates or the production of antibiotic compounds can reduce the number of potential pathogens (Berg 2009). The development of mycorrhizal fungi on plant roots will increase water and nutrient uptake by the plants while providing the fungi with a source of carbohydrates. *Streptomyces* sp. AcH 505 has been demonstrated to increase the growth rate of the mycelia and the development of the ectomycorrhiza for the fungus *Amanita muscaria*, which is associated with spruce trees (*Picea abies*). At the same time, this *Streptomyces* suppresses the mycelial growth of the plant pathogenic fungal species *Armillaria obscura* and *Heterobasidion annosum* (Schrey et al. 2005).

1.4 Pathogenic *Streptomyces*

Not all symbiotic relationships involving *Streptomyces* spp. are beneficial to other organisms. A small number of *Streptomyces* spp. can act as plant pathogens and cause the development of diseases in plants, and this ability is due in part to the production of secondary metabolites that aid in the colonization and infection of plant hosts (Loria et al. 1997). The lesions on the potato tubers produced by scab diseases reduce the marketability of the crop and result in significant economic losses for potato growers (Hill and Lazarovits 2005). Due to the ubiquitous nature of *Streptomyces* in soil environments, the distribution of pathogenic strains is worldwide (Wanner 2009; Zhao 2010; Dees et al. 2012; Bouček-Micheche et al. 1998; Park et al. 2003; Leiminger et al. 2013).

The pathogenic *Streptomyces* spp. causing scab diseases are not tissue specific and have a broad host range that includes root crops such as potato, carrot, radish, beet, peanut and other tap root species. However, due to the economic importance of potato crops, the majority of current studies have focused on potato infection (Goyer and Beaulieu 1998; Loria et al. 2006; Kritzman et al. 1996; Dees and Wanner 2012). The first reported and most extensively studied of the *Streptomyces* plant pathogens is *Streptomyces scabies* (syn. *S. scabiei*), although there are other pathogenic species such as *Streptomyces acidiscabies*, *Streptomyces turgidiscabies*, *Streptomyces europaeiscabiei* and *Streptomyces stelliscabiei* (Loria et al. 2006). Phylogenetic analysis has shown that the scab-causing species are polyphyletic, which indicates that development of the pathogenic phenotype may be due to horizontal gene transfer (HGT) of a pathogenicity island (PAI) containing the genes necessary for the biosynthesis of virulence factors (Bukhalid et al. 2002; Kers et al. 2005).

These pathogenic species produce similar though distinctive disease characteristics in their potato plant hosts that can be distinguished either by physical appearance or by the conditions present in the environment where the disease developed. Acid scab (AS) is characterized by superficial, raised or pitted lesions on the potato tuber surface and occurs in soils with acidic conditions as low as pH 4.5 (Loria et al. 1997). Netted scab (NS) produces superficial lesions with a net-like appearance over the tuber surface as well as necrosis of the fibrous plant roots, and it mainly occurs in Europe (Scholte and Labruière 1985; Loria et al. 1997; Bouček-Mechiche et al. 1998). Common scab (CS) is considered to be the most important of the scab-based diseases and is caused by *S. scabies* as well as other species (Fig. 1.2) (Loria et al. 1997; Bignell et al. 2014b). CS displays similar symptomology as AS except that it does not occur in low pH soils (Lambert and Loria 1989; Loria et al. 1997; Waterer 2002). Infection by *S. scabies* and CS development has also been shown to delay the emergence of tubers while decreasing the overall yield and increasing the number of small tubers (Hiltunen et al. 2005).

The process of plant infection by *Streptomyces* spp. is not well understood, which when combined with the ubiquitous nature of *Streptomyces* in the soil, has made the development of treatment and prevention methods difficult. Traditional control methods that have been attempted with mixed results include field irrigation during tuber formation, reducing the pH of the soil, crop rotation, biological control agents, disease-free seed tubers, seed treatment with fungicide, and chemical fumigation (Dees and Wanner 2012). These control methods have either failed altogether, or can limit crop rotation due to altering the soil conditions, can have mixed results between various locations, can work

well under controlled conditions but not under environmental conditions, can fail due to *Streptomyces* being ubiquitous in the soil, or can be prohibitively expensive and environmentally unfriendly (Dees and Wanner 2012; Liu et al. 1995; Wilson et al. 1999; Peters et al. 2004; Lazarovits 2010; Larkin et al. 2010; Larkin et al. 2011).

It has been shown that the severity of the infection process is dependent on elements such as environmental conditions, inoculum density and pathogen virulence factors (Ryan and Kinkel 1997; Bukhalid et al. 2002; Bouchek-Mechiche et al. 2000; Lazarovits et al. 2007). Not all tissues of the host plant are equally susceptible to development of CS symptoms since underground portions such as the stems, stolons and developing tubers can develop them, but the fibrous roots do not. Above-ground portions of the infected plant appear healthy unless the scab-like lesions develop to the point where they restrict the transfer of water or nutrients between plant roots and stems (Dees and Wanner 2012). *S. scabies* has been shown to only infect potato tubers that are undergoing rapid growth expansion and CS symptoms occur in conjunction with this expansion of the tuber tissue. Once growth of the tuber has completed and expansion has ceased, CS symptoms do not develop further and there is no expansion of the size of lesions already present (Loria et al. 2006).

1.5 Virulence Factors

Infection of the plant host is mediated by a number of virulence factors produced by *S. scabies* and other pathogenic species. The exact function of these virulence factors

is not known, although several of them have been shown to be essential for the colonization and infection process.

1.5.1 *Nec1*

The *nec1* gene encodes a virulence factor that produces a necrogenic phenotype in the species expressing it. In *S. turgidiscabies* this gene is found on a large 660 kb mobile PAI in other pathogenic *Streptomyces* spp. this PAI is split into two distinct segments, and a large region of the PAI between these segments is missing. The PAI in *S. scabies* also contains a large flanking region that is absent from other pathogenic species (Zhang et al. 2016). Despite these structural differences, the virulence genes found on the PAI display nearly identical nucleotide sequence across strains of *S. scabies*, *S. acidiscabies* and *S. turgidiscabies*, suggesting that the genes were introduced onto the PAI prior to dissemination (Kers et al. 2005; Bukhalid et al. 2002; Joshi et al. 2007). The *nec1* gene has a GC content of 54% which is atypically low for a *Streptomyces* species and could indicate that it was introduced through HGT from another genus of bacteria (Bukhalid and Loria 1997; Bukhalid et al. 1998). Introduction of *nec1* into *Streptomyces lividans* allowed this previously non-pathogenic species to begin to necrotize potato tuber tissue through the production of the secreted Nec1 protein (Bukhalid and Loria 1997; Joshi et al. 2007). The Nec1 protein does not appear to be essential for plant pathogenicity as it is missing from a number of pathogenic strains isolated from Western Europe and North America (Flores-González et al. 2008; Wanner 2009). However, it is necessary for the organism to display full virulence as demonstrated by a constructed Δ *nec1* strain of *S. turgidiscabies* (Joshi et al. 2007). In plant bioassays, the Δ *nec1* strain caused some root necrosis and slowed growth

of radish seedlings relative to the control plants, but the majority of seedlings survived. In contrast, the wild-type *S. turgidiscabies* strain produced severe root necrosis on all plants and the majority of seedlings died during the experiment (Joshi et al. 2007). The exact function that the Nec1 protein plays in the plant infection process is not currently understood, although experimental results suggest that it may be involved in suppression of the host defense response. This is due to the apparent lack of an effective plant defence response in wild-type inoculated plants and the success of the plant defence response in the absence of Nec1 (Joshi et al. 2007).

1.5.2 *TomA*

The *tomA* gene encodes a functional tomatinase and is located on the same mobile PAI as *nec1* (Kers et al. 2005; Seipke and Loria 2008). Tomatinase enzymes function to inactivate a class of saponin antibiotic compounds called α -tomatins which are active against fungal microorganisms. These antibiotics are thought to work by interacting with 3β -hydroxy sterols within fungal cell membranes leading to increased membrane permeability and cell death (Keukens et al. 1992). In *S. scabies* TomA has been shown to be active against α -tomatin and a $\Delta tomA$ gene disruption mutant was seen to be more sensitive to α -tomatin than the wild-type strain in disc diffusion assays. However, there was no appreciable difference between the wild-type and gene disruption mutant in terms of disease severity on tomato (*Solanum lycopersicum*) seedlings (Seipke and Loria 2008). The fact that the *tomA* gene has been maintained on the mobile PAI and is present in *S. scabies*, *S. acidiscabies* and *S. turgidiscabies* but is absent from non-pathogenic

Streptomyces spp. suggests that it plays a role in virulence and plant infection, but this role is currently not understood (Kers et al. 2005).

1.5.3 Thaxtomin A

The predominant virulence factor produced by CS and AS-causing *Streptomyces* spp. is a family of phytotoxic metabolites called the thaxtomins, which are cyclic dipeptides (2,5-diketopiperazines) derived from 4-nitro-L-tryptophan and L-phenylalanine (King et al. 1989; King and Calhoun 2009). There are eleven different thaxtomin family members although thaxtomin A (Fig. 1.3) is the primary member produced by *S. scabies*, *S. acidiscabies* and *S. turgidiscabies* (King and Calhoun 2009). The thaxtomin (*txt*) biosynthetic genes are clustered together on the mobile PAI, accounting for the high conservation of the genes among the different scab-causing species (Kers et al. 2005; Zhang et al. 2016). Production of thaxtomin A is essential for strain pathogenicity and the development of disease symptoms, and a positive correlation has been demonstrated between the levels of thaxtomin A produced and the overall virulence of the producing bacterial strains (King et al. 1989; Goyer et al. 1998; Kinkel et al. 1998; Healy et al. 2000; Kers et al. 2005; Loria et al. 1995).

Thaxtomin A induces multiple effects in both monocot and dicot plants at nanomolar concentrations, including hypertrophy which is the enlargement of individual cells in plants, root and shoot stunting, tissue necrosis, as well as inhibiting the incorporation of ^{14}C -glucose into the acid-insoluble cell wall fraction. In addition, studies have shown that thaxtomin A can cause the induction of programmed cell death, can stimulate Ca^{2+} signalling in plant cells and can also stimulate the biosynthesis of pectin,

hemicellulose and scopoletin (Leiner et al. 1996; Fry and Loria 2002; Duval et al. 2005; Bischoff et al. 2009; Lerat et al. 2009; Scheible et al. 2003). Although the exact function of thaxtomin A is not known, there is convincing evidence that it contributes to the plant infection and colonization process by inhibiting cellulose biosynthesis in the plant cell wall (Loria et al. 2008). The superficial similarities between known cellulose synthesis inhibitors and the effects produced by thaxtomin have been previously noted (Bischoff et al. 2009; King and Lawrence 2001).

Thaxtomin biosynthesis is stimulated by the presence of cellobiose, and other short $\beta(1-4)$ linked glucose polymers, which are released from the expanding plant cell walls in rapidly growing and expanding plant tissues (Johnson et al. 2007; Loria et al. 2008). This could explain why infection and disease symptoms only occur on rapidly expanding tubers and not on mature plants due to the location of cellulose biosynthesis in meristematic tissues. The induction of tissue hypertrophy may then allow the filamentous *Streptomyces* to invade the expanding plant tissue (Loria et al. 2008; Bischoff et al. 2009).

1.6 Coronafacoyl Phytotoxins

The genome of *S. scabies* also contains a biosynthetic gene cluster (BGC) that produces a potential virulence factor called *N*-coronafacoyl-L-isoleucine (CFA-Ile). This BGC is referred to as the CFA-like BGC due to its resemblance to the CFA BGC in the well-studied plant pathogen *Pseudomonas syringae* pv. *tomato* DC3000 (Fig. 1.4). CFA-Ile is a member of the coronafacoyl family of phytotoxins, which are composed of

the bicyclic hydrindane ring-containing polyketide coronafacic acid (CFA) linked via an amide bond to an amino acid or amino acid derivative (Fig. 1.5; Bender et al. 1999a). The best characterized coronafacoyl phytotoxin is coronatine (COR), which is produced by different *Pseudomonas* spp. and contains the ethylcyclopropyl amino acid, coronamic acid (CMA) (Fig. 1.5-A), which is derived from L-*allo*-isoleucine and is synthesized through the action of the CMA BGC (Mitchell and Young 1985; Bender et al. 1999a). Other coronafacoyl compounds such as CFA-Ile, N-coronafacoyl-L-*allo*-isoleucine (CFA-*alle*) and N-coronafacoyl-L-valine (CFA-Val) have been detected in minor amounts in culture extracts of COR-producing *Pseudomonas* spp. (Bender et al. 1999a). *S. scabies* is unable to produce COR as it lacks the CMA BGC, and instead it produces CFA-Ile as the primary coronafacoyl phytotoxin as well as other minor related compounds (Fig. 1.5-B) (Fyans et al. 2015).

The majority of studies conducted on the virulence, bioactivity and biosynthesis of coronafacoyl (or COR-like) phytotoxins have focused on COR. This phytotoxin is produced by several *P. syringae* pathovars as well as pathovars of *Pseudomonas coronafaciens*, *Pseudomonas amygdali* and *Pseudomonas savastanoi* which are known to infect ryegrass (*Lolium* spp.), soybean (*Glycine max*), crucifers, multiple tree species of the *Prunus* genus, and tomato (Bender et al. 1996; Bender et al. 1999a; Qi et al. 2011). COR and other coronafacoyl phytotoxins are also produced by *Xanthomonas campestris* pv. *phormiicola* which infects flax (*Phormium tenax*) crops in New Zealand, and the genes necessary to produce coronafacoyl phytotoxins are present in plant pathogenic

Pectobacterium spp. that are responsible for diseases such as potato soft rot and black leg (Mitchell 1991; Bell et al. 2004).

COR is a non-host-specific phytotoxin that is highly bioactive against plant tissues and induces a number of effects in the plant host. In tomato plants it induces chlorosis in the leaves, thickening of epidermal cell walls, accumulation of serine proteinase inhibitor in vacuoles, inhibition of seedling root growth, accumulation of anthocyanins, and modification of the chloroplast structure so that they were smaller, stained more intensely and were clustered near the bottom of palisade mesophyll cells (Uppalapati et al. 2005). COR has also induces localized chlorosis in leaf infiltration areas of soy bean and systemic development of chlorosis in subsequently developed trifoliate leaves, and it causes stunting of plant growth (Gnanamanick et al. 1982). Intense chlorosis was demonstrated in the leaves of French bean (*Phaseolus vulgaris*), tobacco (*Nicotiana tabacum*), potato, tomato, pepper (*Capsicum annuum*), cabbage (*Brassica oleracea*) and corn (*Zea mays*) after a period of 24-48 hours, however infiltration of COR into the leaves of marigold (*Tagetes erecta*) plants resulted in very mild chlorosis only after a period of 7-10 days (Gnanamanick et al. 1982). The development of hypertrophy of potato tuber tissue has also been demonstrated after a period of 3-4 days (Gnanamanick et al. 1982). The related coronafacoyl phytotoxins CFA-Ile and CFA-Val are also biologically active against plant tissues, though not to the same degree as COR. They can induce leaf chlorosis and root stunting in radish (*Raphanus raphanistrum*) and tomato plants, as well as potato tuber tissue hypertrophy (Fyans et al. 2015; Uppalapati et al. 2005). In contrast, CFA alone displays

very little bioactivity against plant tissues, indicating that the attached amino acid is critical for the phytotoxic effects of the metabolites (Shiraishi et al. 1979; Uppalapati et al. 2005).

As a virulence factor, COR allows the pathogen to overcome initial stomatal defences that act to close the stoma present on the surface of the plant and prevent bacterial entry into the host. In addition, COR promotes pathogen replication and persistence within the host apoplast, it contributes to disease symptom development, and it induces systemic induced susceptibility (SIS) in previously uninfected tissues of the plant host (Xin and He 2013). Transposon mutants of *P. syringae* pv. *tomato*, which were defective in COR production and demonstrated little to no production of chlorosis on plant leaves, induced the development of necrotic lesions that were smaller than those induced by the wild-type strain (Bender et al. 1987). In addition, the population size of the COR-deficient mutants was lower *in planta* as compared to the wild-type strain. Together, these results suggested that the COR-deficient strains exhibit decreased fitness during infection of the plant host (Bender et al. 1987).

The physiological role of COR as a virulence factor may be directly related to its chemical structure as it bears a high degree of structural similarity to the plant hormone jasmonic acid (JA), particularly the jasmonoyl-L-isoleucine conjugate (JA-Ile) (Fig. 1.5-C), which is the most active form of JA (Fonseca et al. 2009; Krumm et al. 1995; Katsir et al. 2008a). It has been shown that a mutant strain of *Arabidopsis*, *coi1* (*coronatine insensitive 1*), is resistant to the effects of both COR and JA, suggesting that the metabolites share a similar mode of action (Feys et al. 1994). This idea is supported by the fact that COR

induces several effects that are also induced by JA-Ile such as induction of protease inhibitors and regulation of JA-responsive genes (Uppalapati et al. 2005; Xin and He 2013).

In eukaryotes, diverse cell functions such as the cell cycle and gene transcription are regulated through the ubiquitin/26S proteasome pathway by linking extracellular signals to the proteolysis of regulatory proteins (Moon et al. 2004). These proteins are recognized by the attachment of polymeric ubiquitin chains involving the action of three enzyme families, one of the most well characterized of which are the Skp1-Cullin-F-box (SCF) ligase complexes. These complexes are composed of the core Skp1 and Cullin subunits, and the variable F-box subunit (Moon et al. 2004). The F-box protein connects the Skp1-Cullin subunits to the target protein. In *Arabidopsis*, the COI1 protein is the F-box portion of the SCF^{COI1} complex (Yan et al. 2013; Petroski and Deshaies 2005). In *Arabidopsis*, COI1 is stabilized through its association with the SCF^{COI1} complex while disassociated COI1 is degraded through the 26S proteasome pathway (Yan et al. 2013).

COI1 also interacts with the jasmonate ZIM-domain (JAZ) family of repressor proteins. This physical interaction requires the presence of JA-Ile, but the effect can be replicated with COR in yeast cells (Thines et al. 2007; Melotto et al. 2008). This may indicate that it is the physical interaction between the COI1 protein and the ZIM domain of the JAZ repressors which is the virulence target of COR. This idea is supported by studies showing that COR will preferentially bind to the JAZ complex in place of JA-Ile (Katsir et al. 2008b). The JAZ proteins are believed to block gene expression by binding the co-repressors TOPLESS (TPL) and TPL-related proteins through association with the novel interactor of JAZ (NINJA) in the G-box region of the target promoter (Fig. 1.6). This

repression is removed by JA-Ile - induced SCF^{COI1} degradation of the JAZ proteins utilizing the 26S proteasome pathway (Santino et al. 2013; Pauwels et al. 2010).

Activation of the JA signalling pathway normally occurs as a response to tissue wounding and insect feeding, among other stimuli (Glazebrook 2005). The activation of the JA signalling pathway is known to be antagonistic to the salicylic acid (SA) signalling pathway and will act to repress it (Niki et al. 1998; Pieterse and van Loon 1999; Glazebrook 2005). The SA pathway is involved primarily in the plant immune response to infection by biotrophic and hemibiotrophic pathogens, and its suppression is believed to be a means of evading the host immune response by COR-producing *Pseudomonas* spp., which are hemibiotrophic (Bender et al. 1999b; Glazebrook 2005).

Despite the structural similarities between COR and the COR-like metabolites, it is currently not known if any of the coronafacoyl phytotoxins other than COR are involved in a similar means of host immune response evasion. A *S. scabies* mutant unable to produce CFA-Ile showed reduced virulence with regards to root disease symptoms on host tobacco plants, but it still caused extensive root and shoot stunting, as well as the development of chlorosis and eventual host death (Bignell et al. 2010). Recently, a *S. scabies* strain engineered to produce high levels of CFA-Ile caused greater necrosis and pitting of potato tuber tissue as compared to the control strains (L. Cheng, unpublished results). Thus, while CFA-Ile is not required for the pathogenicity of *S. scabies*, there is evidence that it contributes to the virulence phenotype of the organism. Given the similarities in molecular structure between COR, CFA-Ile and JA-Ile, the possibility of similar modes of action for these phytotoxins remains plausible.

1.7 Coronafacoyl Phytotoxin Biosynthesis

As previously mentioned, CFA-Ile in *S. scabies* is synthesized through the action of the CFA-like BGC which is similar in structure and organization to the CFA BGC from *P. syringae*. The CFA and CFA-like BGCs are responsible for synthesizing the CFA polyketide moiety, which is then ligated through an amide bond to an amino acid or amino acid derivative. The core genes of the BGC are composed of the *cfaI*-8 and *cfl* genes which are conserved in both *S. scabies* and *P. syringae* (Fig. 1.4) (Bignell et al. 2010). The exact mechanism of CFA biosynthesis is currently unknown, but a pathway has been proposed based on studies conducted in *Pseudomonas* spp. (Fig. 1.7) (Rangaswamy et al. 1998a; Bender et al. 1999a).

In *P. syringae* the CFA BGC is composed of nine biosynthetic genes, *cfaI*-9, and a gene encoding a coronafacate ligase, *cfl*, which is predicted to catalyse the ligation of the CMA and CFA moieties (Bender et al. 1999a; Bender et al. 1999b). Precursor feeding studies have indicated that CFA is synthesized from a single unit of pyruvate, a unit of butyrate and three residues of acetate (Parry et al. 1994). The *cfaI*-3 gene products show sequence similarity to acyl carrier proteins, fatty acid dehydratases and β -ketoacyl synthetases of type II polyketide synthases (PKS), respectively (Penfold et al. 1996). The function of the *cfa4* gene product is currently unknown since database searches do not reveal any homologous proteins with a predicted or known function (Bender et al. 1999a; Bender et al. 1999b). However, *cfa4* is thought to encode a cyclase enzyme since no other enzyme encoded by the *cfaI*-5 region displays a cyclase motif (Rangaswamy et al. 1998a).

The predicted protein product of the *cfa5* gene shows similarity to an acyl-CoA ligase (Penfold et al. 1996). *cfa6* and *cfa7* are large open reading frames at 8.0 kb and 6.2 kb respectively, and the corresponding proteins (284 and 221 kDa respectively) are predicted to be multifunctional modular type I PKSs (Rangaswamy et al. 1998a). The *cfa8* gene product shows similarity to crotonyl-CoA reductase/carboxylase (CCR) enzymes and is believed to be involved in the reductive carboxylation of crotonyl-CoA to form (2*S*)-ethylmalonyl-CoA, which serves as an extender unit for polyketide synthesis (Fig. 1.7) (Rangaswamy et al. 1998b; Chan et al. 2009; Bignell et al. 2010; Wilson and Moore 2012). The final gene in the CFA BGC is *cfa9* which is predicted to encode a thioesterase enzyme that is non-essential for CFA or COR production (Rangaswamy et al. 1998b).

The theorized precursor molecule for initial CFA biosynthesis in *Pseudomonas* spp. is α -ketoglutarate that has been produced from pyruvate via the citric acid cycle (Parry et al. 1996). It is currently believed that α -ketoglutarate is decarboxylated to form succinic semialdehyde, which the Cfa1-5 enzymes use to create enzyme-bound 2-carboxy-2-cyclopentenone (CPC) (Fig. 1.7) (Mitchell et al. 1995). The creation of this precursor requires a cyclization step, and as there are no identified cyclase enzymes encoded in the CFA BGC, it has been postulated that this function may be performed by the Cfa4 enzyme whose function is currently unknown (Rangaswamy et al. 1998a). The CPC intermediate is then thought to be passed to the Cfa6 type I PKS enzyme, which catalyzes the extension of CPC by a butyrate unit and the complete reduction of the β -keto ester to form enzyme-bound 2-[1-oxo-2-cyclopenten-2-yl-methyl] butanoic acid (CPE) (Fig. 1.7) (Gross & Loper 2009). Then, CPE is predicted to be transferred to the Cfa7 type

I PKS, which extends CPE by a malonate unit. A reactive β -keto thioester is then formed that rapidly undergoes a cascade reaction to produce a controlled *6-endo-trig* cyclization of the structure (Fig. 1.7) (Strieter et al. 2009; Gross & Loper 2009). The now bicyclic structure then undergoes a ketoreduction and dehydration reaction while still attached to the Cfa7 PKS to complete the CFA moiety (Strieter et al. 2009). The CFA polyketide is then released from the Cfa7 PKS through the action of the internal thioesterase domain present in the Cfa7, and/or through the Cfa9 thioesterase, although the latter is not required for COR biosynthesis (Rangaswamy et al. 1999b). The final step in COR biosynthesis is the ligation of the CFA and CMA moieties, which is predicted to be catalyzed by the Cfl enzyme (Bender et al. 1999b). The Cfl enzyme has sequence homology with a number of adenylate-forming enzymes, suggesting that it needs to bind and then hydrolyze ATP in order to facilitate the ligation reaction (Liyange et al. 1995). To date, this adenylation reaction has not been shown experimentally.

A comparison of the BGCs involved in CFA biosynthesis in *S. scabies* and *P. syringae* has revealed some notable differences. The predicted thioesterase-encoding *cfa9* gene found in *P. syringae* BGC is absent from the *S. scabies* gene cluster (Fig. 1.4). There is an enoyl reductase domain present in the Cfa7 protein of *S. scabies* that is absent from the corresponding proteins of *P. syringae* and *Pectobacterium atrosepticum* (Bignell et al. 2010). Within the *S. scabies* gene cluster, there are two regulatory and four biosynthetic genes present that are absent from the *P. syringae* gene cluster (Fig. 1.4) (Bignell et al. 2010). The two regulatory genes have been shown to be divergently co-transcribed (Bignell et al. 2010; Cheng et al. 2015). The four unique biosynthetic genes

(*scab79681*, *scab79691*, *scab79711* and *scab79721*) are co-expressed with the conserved core biosynthetic genes (*cfa1-8*, *cfl*), suggesting that they are involved in the biosynthesis of the CFA moiety in *S. scabies* (Bignell et al. 2010). The *scab79721* gene (herein referred to as *sdr*) is predicted to encode a short chain dehydrogenase reductase enzyme, *scab79691* (herein referred to as *CYP107AK1*) is predicted to encode a P450 monooxygenase and *scab79681* (herein referred to as *oxr*) is predicted to encode a F₄₂₀-dependant oxidoreductase (Bignell et al. 2010). The *scab79711* gene is predicted to encode a 3-hydroxybutyryl-CoA dehydrogenase that may be involved in the reduction of acetoacetyl-CoA to 3-hydroxybutyryl-CoA, which is an intermediate molecule involved in crotonyl-CoA biosynthesis (Chan et al. 2009; Bignell et al. 2010). This may indicate that the SCAB79711 enzyme is involved along with Cfa8 in biosynthesis of the (2*S*)-ethylmalonyl-CoA precursor used for CFA polyketide biosynthesis.

Given the presence of the additional biosynthetic genes in the *S. scabies* CFA-like BGC, it was previously proposed that *S. scabies* may produce novel coronafacoyl phytotoxins and that the additional biosynthetic genes may function as tailoring enzymes that contribute to metabolite structural diversity (Bignell et al. 2010). However, the identification of CFA-Ile as the primary coronafacoyl phytotoxin produced by *S. scabies* suggests that hypothesis is not correct, and thus the role of these genes requires further investigation (Fyans et al. 2015).

1.8 Thesis Objectives

The coronafacoyl phytotoxins are an important family of phytotoxic secondary metabolites that contribute to the virulence phenotype of different plant pathogenic bacteria. To date, most studies have focused on COR, which functions as a molecular mimic of the plant hormone JA-Ile. Recently, *S. scabies* was shown to be able to produce the coronafacoyl compound CFA-Ile, and there is some evidence that this metabolite enhances the virulence of the organism. The biosynthetic pathway for coronafacoyl phytotoxin production in plant pathogenic bacteria is largely hypothetical, and the role of most genes involved is primarily based on sequence analysis of the corresponding protein products. Furthermore, the CFA-like BGC in *S. scabies* contains four additional putative biosynthetic genes that are absent from the CFA BGC in *P. syringae*, and it is possible that some of these genes are required for CFA-Ile production in *S. scabies*. Thus, one of the objectives of this thesis was to further investigate the biosynthetic pathway for coronafacoyl phytotoxin production in *S. scabies*.

In Chapters 2 and 3, the role of the *oxr*, *sdr* and *CYP107AK1* genes in the biosynthesis of the *S. scabies* CFA-Ile phytotoxin was examined by constructing mutant strains defective in each gene and examining the effects of the mutations on metabolite production. Intermediates that accumulated in the Δsdr and $\Delta CYP107AK1$ mutant cultures were purified and structurally characterized, and the bioactivity of each intermediate relative to CFA-Ile was examined using a plant bioassay. In addition, investigations into the distribution of coronafacoyl phytotoxin BGCs among different bacterial genera and the differences that exist between the gene clusters were conducted in order to gain insights

into the evolution of coronafacoyl phytotoxin biosynthesis in bacteria. Chapter 4 describes in detail the protocol that was developed for the large-scale purification of CFA-Ile and its biosynthetic intermediates from *S. scabies* cultures.

Chapter 5 investigated the conserved Cfl enzyme that is predicted to catalyze the final step in coronafacoyl phytotoxin production. The *S. scabies* Cfl protein was purified from *E. coli* and was used in enzyme assays to determine whether it can produce CFA-Ile *in vitro* and whether it activates CFA by adenylation prior to the ligation step. In addition, an amino acid alignment of Cfl homologues from different bacteria was generated in order to identify conserved amino acid residues that may be important for enzyme function. Finally, oligonucleotide primers were designed to allow for PCR screening of *Streptomyces* spp. that harbour a *cfl* gene homologue, and thus may produce coronafacoyl phytotoxins.

Although *S. scabies* is the best characterized CS-causing pathogen, there are at least nine other *Streptomyces* spp. that have the ability to cause the disease (Bignell et al. 2014b). While studies on the types and distribution of scab-causing *Streptomyces* spp. in North America have been conducted, to date there has been no comprehensive study on the pathogenic species that are associated with CS disease on the island of Newfoundland. An in-depth analysis of the pathogens that exist in Newfoundland and the virulence factors they possess would enhance our knowledge of the distribution and prevalence of pathogenic *Streptomyces* spp. in Canada as well as increase our understanding of the pathogenicity of CS-causing organisms. The second objective of this thesis, therefore, was to further investigate the pathogenic *Streptomyces* spp. associated with CS disease in Newfoundland.

Chapter 6 describes the identification and characterization of several *Streptomyces* strains isolated from CS-infected potato tubers harvested in Newfoundland. The isolates were tested in various plant bioassays to determine the virulence of each strain relative to that of *S. scabies* 87-22, and PCR was performed to detect the thaxtomin biosynthesis genes as well as *nec1* and *tomA*. Phylogenetic characterisation of the isolates was also conducted, and culture extracts for each strain were analyzed by reverse phase-high performance liquid chromatography (RP-HPLC) to detect and quantify the production of CS-associated thaxtomin A phytotoxin. In addition, the production of other phytotoxic secondary metabolites known to be produced by CS-associated *Streptomyces* spp. was examined. Chapter 7 describes the genome sequence and putative identification of one novel *Streptomyces* isolate that displayed a highly pathogenic phenotype against plants but did not produce thaxtomin A or other known phytotoxins in liquid culture.

CS is an important disease of potato and other root crops, and currently there are no control strategies that can effectively and consistently manage the disease. By deepening our understanding of the CS-causing pathogens and their interactions with plant hosts, it is anticipated that the knowledge gained can be applied to the development of new control strategies that better manage this disease in order to reduce the economic impact on growers.

1.9 References

- Bell K.S., Sebaihia M., Pritchard L., Holden M.T., Hyman L.J., Holeva M.C., Thomson N.R., Bentley S.D., et al. (2004). Genome sequence of the enterobacterial phytopathogen *Erwinia carotovora* subsp. *atroseptica* and characterization of virulence factors. *Proc Natl Acad Sci USA*, 101: 11105-11110.
- Bender C., Palmer D. (1996). Biosynthesis of coronatine, a thermoregulated phytotoxin produced by the phytopathogen *Pseudomonas syringae*. *Arch Microbiol*, 166: 71-75.
- Bender C., Rangaswamy V., Loper J. (1999a). Polyketide production by plant-associated pseudomonads. *Annu Rev Phytopathol*, 37: 175-196.
- Bender C.L., Alarcon-Chaidez F., Gross D.C. (1999b). *Pseudomonas syringae* phytotoxins: mode of action, regulation, and biosynthesis by peptide and polyketide synthetases. *Microbiol Mol Biol Rev*, 63: 266-292.
- Bender C.L., Stone H.E., Sims J.J., Cooksey D.A. (1987). Reduced pathogen fitness of *Pseudomonas syringae* pv. *tomato* Tn5 mutants defective in coronatine production. *Physiol Mol Plant Pathol*, 30:273-283.
- Bentley S.D., Chater K.F., Cerdeño-Tárraga A.-M., Challis G.L., Thomson N.R., James K.D., Harris D.E., Quail M.A., et al. (2002). Complete genome sequence of the model actinomycete *Streptomyces coelicolor* A3(2). *Nature*, 417: 141-147.
- Bérdy J. Bioactive microbial metabolites. *J Antibiot (Tokyo)*, 2005; 58: 1-26.

- Berg G. (2009). Plant-microbe interactions promoting plant growth and health: perspectives for controlled use of microorganisms in agriculture. *Appl Microbiol Biotechnol*, 84: 11-18.
- Bertram R., Schlicht M., Mahr K., Nothaft H., Saier, Jr. M.H., Titgemeyer F. (2004). In silico and transcriptional analysis of carbohydrate uptake systems of *Streptomyces coelicolor* A3(2). *J Bacteriol*, 186(5): 1362-1373.
- Bignell D.R., Francis I.M., Fyans J.K., Loria R. (2014a). Thaxtomin A production and virulence are controlled by several *bld* gene global regulators in *Streptomyces scabies*. *Mol Plant Microbe Interact*, 27: 875-885.
- Bignell D.R., Fyans J.K., Cheng Z. (2014b). Phytotoxins produced by plant pathogenic *Streptomyces* species. *J Appl Microbiol*, 116: 223-235.
- Bignell D.R.D., Seipke R.F., Huguet-Tapia J.C., Chambers A.H., Parry R., Loria R. (2010). *Streptomyces scabies* 87-22 contains a coronafacic acid-like biosynthetic cluster that contributes to plant-microbe interactions. *Mol Plant Microbe Interact*, 23: 161-175.
- Bischoff V., Cookson S.J., Wu S., Scheible W.R. (2009). Thaxtomin A affects CESA-complex density, expression of cell wall genes, cell wall composition, and causes ectopic lignification in *Arabidopsis thaliana* seedlings. *J Exp Bot*, 60: 955-965.
- Bouchek-Mechiche K., Gardan L., Normand P., Jouan B. (2000). DNA relatedness among strains of *Streptomyces* pathogenic to potato in France: description of three new species, *S. europaeiscabiei* sp. nov. and *S. stelliscabiei* sp. nov. associated with

- common scab, and *S. reticuliscabiei* sp. nov. associated with netted scab. *Int J Syst Evol Microbiol*, 50(1): 91-99.
- Bouček-Mechiche K., Guérin C., Jouan B., Gardan L. (1998). *Streptomyces* species isolated from potato scabs in France: numerical analysis of “Biotype-100” carbon source assimilation data. *Res Microbiol*, 149: 653-663.
- Bukhalid R.A., Chung S.Y., Loria R. (1998). *necI*, a gene conferring a necrogenic phenotype, is conserved in plant-pathogenic *Streptomyces* spp. and linked to a transposase pseudogene. *Mol Plant Microbe Interact*, 11: 960-967.
- Bukhalid R.A., Loria R. (1997). Cloning and expression of a gene from *Streptomyces scabies* encoding a putative pathogenicity factor. *J Bacteriol*, 179(24): 7776-7783.
- Bukhalid R.A., Takeuchi T., Labeda D., Loria R. (2002). Horizontal transfer of the plant virulence gene, *necI*, and flanking sequences among genetically distinct *Streptomyces* strains in the diastatochromogenes cluster. *Appl Environ Microbiol*, 68(2): 738-744.
- Challis G.L., Hopwood D.A. (2003). Synergy and contingency as driving forces for the evolution of multiple secondary metabolite production by *Streptomyces* species. *Proc Natl Acad Sci USA*, 100(2): 14555-14561.
- Chan Y.A., Podevels A.M., Kevany B.M., Thomas M.G. (2009). Biosynthesis of polyketide synthase extender units. *Nat Prod Rep*, 26:90-114.

- Chater K.F., Dyson P. (2011). Differentiation in *Streptomyces*: the properties and programming of diverse cell-types. In Dyson P. (Ed.) *Streptomyces: Molecular biology and biotechnology*, (pp.43-86). Norfolk, UK: Caister Academic Press.
- Chater K.F. (2006). *Streptomyces* inside-out: a new perspective on the bacteria that provide us with antibiotics. *Philos Trans R Soc Lond B Biol Sci*, 361: 761-768.
- Chater K.F., Biró S., Lee K.J., Palmer T., Schrempf H. (2010). The complex extracellular biology of *Streptomyces*. *FEMS Microbiol Rev*, 34: 171-198.
- Cheng Z., Bown L., Tahlan K., Bignell D.R.D. (2015). Regulation of coronafacoyl phytotoxin production by the PAS-LuxR family regulator CfaR in the common scab pathogen *Streptomyces scabies*. *PLoS one*, 10:e0122450.
- Crowley D. (2000). Function of siderophores in the plant rhizosphere. In Varanini Z., Joseph N., Nannipieri P. (Eds.), *The Rhizosphere* (pp. 239-278). CRC Press.
- Dees M.W., Somervuo P., Lysoe E., Aittamaa M., Valkonen J.P. (2012). Species' identification and microarray-based comparative genome analysis of *Streptomyces* species isolated from potato scab lesions in Norway. *Mol Plant Pathol*, 13: 174-186.
- Dees M.W., Wanner L.A. (2012). In search of better management of potato common scab. *Potato Res*, 55: 249-268.
- Dharmaraj S. (2010). Marine *Streptomyces* as a novel source of bioactive substances. *World J Microbiol Biotechnol*, 26: 2123-2139.

- Duval I., Brochu V., Simard M., Beaulieu C., Beaudoin N. (2005). Thaxtomin A induces programmed cell death in *Arabidopsis thaliana* suspension-cultured cells. *Planta*, 222: 820-831.
- Fajardo A., Martínez J.L. (2008). Antibiotics as signals that trigger specific bacterial responses. *Curr Opin Microbiol*, 11: 161-167.
- Feys B.J.F., Benedetti C.E., Penfold C.N., Turner J.G. (1994). *Arabidopsis* mutants selected for resistance to the phytotoxin coronatine are male sterile, insensitive to methyl jasmonate and resistant to a bacterial pathogen. *Plant Cell*, 8: 751-759.
- Flärdh K., Buttner M.J. (2009). *Streptomyces* morphogenetics: dissecting differentiation in a filamentous bacterium. *Nature Rev Microbiol*, 7: 36-49.
- Flärdh K., Richards D.M., Hempel A.M., Howard M., Buttner M.J., (2012). Regulation of apical growth and hyphal branching in *Streptomyces*. *Curr Opin Microbiol*, 15: 737-743.
- Flores-González R., Velasco I., Montes F. (2008). Detection and characterization of *Streptomyces* causing potato common scab in Western Europe. *Plant Pathol*, 57: 162-169.
- Fonseca S., Chini A., Hamberg M., Adie B., Porzel A., Kramell R., Miersch O., Wasternack C., Solano R. (2009). (+)-7-*iso*-jasmonoyl-L-isoleucine is the endogenous bioactive jasmonate. *Nat Chem Biol*, 5(5): 344.
- Fry B.A., Loria R. (2002). Thaxtomin A: evidence for a plant cell wall target. *Physiol Mol Plant Pathol*, 60: 1-8.

- Fyans J.K., Altowairish M.S., Li Y., Bignell D.R.D. (2015). Characterization of the coronatine-like phytotoxins produced by the common scab pathogen *Streptomyces scabies*. *Mol Plant Microbe Interact*, 28:443-454.
- Glazebrook J. (2005). Contrasting mechanisms of defense against biotrophic and necrotrophic pathogens. *Annu Rev Phytopathol*, 43:205-27.
- Gnanamanickam S.S., Starratt A.N., Ward E.W.B. (1982). Coronatine production *in vitro* and *in vivo* and its relation to symptom development in bacterial blight of soybean. *Can J Bot*, 60: 645-650.
- Goyer C., Vachon J., Beaulieu C. (1998). Pathogenicity of *Streptomyces scabies* mutants altered in thaxtomin A production. *Phytopathology*, 88: 442-445.
- Gross H., Loper J.E. (2009). Genomics of secondary metabolite production by *Pseudomonas* spp. *Nat Prod Rep*, 26: 1408-1446.
- Hamed J., Poorinmohammad N., Papiran R. (2017). Growth and life cycle of actinobacteria. In Wink J., Mohammadipanah F., Hamed J. (Eds.), *Biology and biotechnology of actinobacteria* (pp. 29-50). Springer: DOI 10.1007/978-3-319-60339-1.
- Healy F.G., Wach M., Krasnoff S.B., Gibson D.M., Loria R. (2000). The *txtAB* genes of the plant pathogen *Streptomyces acidiscabies* encode a peptide synthetase required for phytotoxin thaxtomin A production and pathogenicity. *Mol Microbiol*, 38: 794-804.
- Hill J., Lazarovits G. (2005). A mail survey of growers to estimate potato common scab prevalence and economic loss in Canada. *Can J Plant Pathol*, 27: 46-52.

- Hiltunen L.H., Weckman A., Ylhainen A., Rita H., Richter E., Valkonen J.P.T. (2005). Responses of potato cultivars to the common scab pathogens, *Streptomyces scabies* and *S. turgidiscabies*. *Ann Appl Biol*, 146: 395-403.
- Jiralerspong S., Rangaswamy V., Bender C.L., Parry R.J. (2001). Analysis of the enzymatic domains in the modular portion of the coronafacic acid polyketide synthase. *Gene*, 270: 191-200.
- Johnson E.G., Joshi M.V., Gibson D.M., Loria R. (2007). Cello-oligosaccharides released from host plants induce pathogenicity in scab-causing *Streptomyces* species. *Physiol Mol Plant Pathol*, 71: 18-25.
- Jones S.E., Ho L., Rees C.A., Hill J.E., Nodwell J. R., Elliot M.A. (2017). *Streptomyces* exploration is triggered by fungal interactions and volatile signals. *Elife*, 6, e21738.
- Joshi M., Rong X., Moll S., Kers J., Franco C., Loria R. (2007). *Streptomyces turgidiscabies* secretes a novel virulence protein, Nec1, which facilitates infection. *Mol Plant Microbe Interact*, 20: 599-608.
- Kaltenpoth M., Yildirim E., Gürbüz M.F., Herzner G., Strohm E. (2012). Regining the roots of the Beewolf-*Streptomyces* symbiosis: Antennal symbionts in the rare genus *Philanthinus* (Hymenopter, Crabronidae). *Appl Environ Microbiol*, 78(3): 822-827.
- Katsir L., Chung H.S., Koo A.J.K., Howe G.A. (2008a). Jasmonate signaling: a conserved mechanism of hormone sensing. *Curr Opin Plant Biol*, 11: 428-435.

- Katsir L., Schilmiller A.L., Staswick P.E., He S.Y., Howe G.A. (2008b). COI1 is a critical component of a receptor for jasmonate and the bacterial virulence factor coronatine. *Proc Natl Acad Sci USA*, 105: 7100-7105.
- Kers J.A., Cameron K.D., Joshi M.V., Bukhalid R.A., Morello J.E., Wach M.J., Gibson D.M., Loria R. (2005). A large, mobile pathogenicity island confers plant pathogenicity on *Streptomyces* species. *Mol Microbiol*, 55: 1025-1033.
- Keukens E.A., de Vrije T., Fabrie C.H., Demel R.A., Jongen W.M., de Kruijff B. (1992). Dual specificity of sterol-mediated glycoalkaloid induced membrane disruption. *Biochim Biophys Acta, Biomembr*, 1110(2): 127-136.
- King R.R., Calhoun L.A. (2009). The thaxtomin phytotoxins: sources, synthesis, biosynthesis, biotransformation and biological activity. *Phytochemistry*, 70: 833-841.
- King R.R., Lawrence C.H. (2001). Herbicidal properties of the thextomin group of phytotoxins. *J Agri Food Chem*, 49: 2298-2301.
- King R.R., Lawrence C.H., Clark M.C., Calhoun L.A. (1989). Isolation and characterization of phytotoxins associated with *Streptomyces scabies*. *J Chem Soc, Chem Commun*, 13: 849-850.
- Kinkel L.L., Bowers J.H., Shimizu K., Neeno-Eckwall E.C., Schottel J.L. (1998). Quantitative relationships among thaxtomin A production, potato scab severity, and fatty acid composition in *Streptomyces*. *Can J Microbiol*, 44: 768-776.
- Kritzman G., Shani-Cahani A., Kirshner B., Riven Y., Bar Z., Katan J., Grinstein A. (1996). Pod ward disease of peanuts. *Phytoparasitica*, 24(4): 293-304.

- Krumm T., Bandemer K., Boland W. 1995). Induction of volatile biosynthesis in the Lima bean (*Phaseolus lunatus*) by leucine and isoleucine conjugates of 1-oxo- and 1-hydroxyindan-4-carboxylic acid: evidence for amino acid conjugates of jasmonic acid as intermediates in the octadecanoid signalling pathway. *FEMS Lett*, 377: 523-529.
- Lambert D.H., Loria R. (1989). *Streptomyces scabies* sp. nov., nom. rev. *Int J Syst Bacteriol*, 39: 387-392.
- Larkin R.P., Griffin T.S., Honeycutt C.W. (2010). Rotation and cover crop effects on soilborne potato diseases, tuber yield and soil microbial communities. *Plant Dis*, 94(12): 1491-1502.
- Larkin R.P., Honeycutt C.W., Griffin T.S., Olanya O.M., Halloran J.M., He Z. (2011). Effects of different potato cropping system approaches and water management on soilborne diseases and soil microbial communities. *Phytopathology*, 101(1): 58-67.
- Lazarovits G. (2010). Managing soilborne disease of potatoes using ecologically based approaches. *Am J Pot Res*, 87: 401-411.
- Lazarovits G., Hill J., Patterson G., Conn K.L., Crump N.S. (2007). Edaphic soil levels of mineral nutrients, pH, organic matter, and cationic exchange capacity in the geocaulosphere associated with potato common scab. *Phytopathology*, 97(9): 1071-1082.
- Leiminger J., Frank M., Wenk C., Poschenrieder G., Kellermann A., Schwarfischer A. (2013). Distribution and characterization of *Streptomyces* species causing potato common scab in Germany. *Plant Pathol*, 62: 611-623.

- Leiner R.H., Fry B.A., Carling D.E., Loria R. (1996). Probable involvement of thaxtomin A in pathogenicity of *Streptomyces scabies* on seedlings. *Phytopathology*, 86(7): 709-713.
- Lerat S., Babana A.H., Oirdi M.E., Hadrami A.E., Daayf F., Beaudoin N., Bouarab K., Beaulieu C. (2009). *Streptomyces scabiei* and its toxin thaxtomin A induce scopoletin biosynthesis in tobacco and *Arabidopsis thaliana*. *Plant Cell Rep*, 28: 1895-1903.
- Linares J.F., Gustafsson I., Baquero F., Martinez J.L. (2006). Antibiotics as intermicrobial signaling agents instead of weapons. *Proc Natl Acad Sci USA*, 103(51): 19484-19489.
- Liu D., Anderson N.A., Kinkel L.L. (1995). Biological control of potato scab in the field with antagonistic *Streptomyces scabies*. *Phytopathology*, 85(7): 827-831.
- Liyanage H., Palmer D.A., Ullrich M., Bender C.L. (1995). Characterization and transcriptional analysis of the gene cluster for coronafacic acid, the polyketide component of the phytotoxin coronatine. *Appl Environ Microbiol*, 61: 3843-3848.
- Loria R., Bignell D.R., Moll S., Huguet-Tapia J.C., Joshi M.V., Johnson E.G., Seipke R.F., Gibson D.M. (2008). Thaxtomin biosynthesis: the path to plant pathogenicity in the genus *Streptomyces*. *Antonie Van Leeuwenhoek*, 94: 3-10.
- Loria R., Bukhalid R.A., Creath R.A., Leiner R.H., Olivier M., Steffens J.C. (1995). Differential production of thaxtomins by pathogenic *Streptomyces* species *in vitro*. *Phytopathology*, 85: 537-541.

- Loria R., Bukhalid R.A., Fry B.A., King R.R. (1997). Plant pathogenicity in the genus *Streptomyces*. *Plant Dis*, 81: 836-846.
- Loria R., Kers J., Joshi M. (2006). Evolution of plant pathogenicity in *Streptomyces*. *Annu Rev Phytopathol*, 44: 469-487.
- McCormick J.R., Flärdh K. (2012). Signals and regulators that govern *Streptomyces* development. *FEMS Microbiol Rev*, 36(1): 206-231.
- Melotto M., Mecey C., Niu Y., Chung H.S., Katsir L., Yao J., Zeng W., Thines B., Staswick P., Browse J., Howe G.A., He S.Y. (2008). A critical role of two positively charged amino acids in the Jas motif of Arabidopsis JAZ proteins in mediating coronatine- and jasmonoyl isoleucine-dependent interactions with the COI1 F-box protein. *Plant J*, 55: 979-988.
- Mitchell R., Young H., Liddell M. (1995). Isolation and structural characterization of 2-[1-oxo-2-cyclopenten-2-ylmethyl]-butanoic acid, a polyketide product of coronatine-producing *Pseudomonas* spp. *Tetrahedron Lett*, 36: 3237-3240.
- Mitchell R.E. (1991). Implications of toxins in the ecology and evolution of plant pathogenic microorganisms bacteria. *Experientia*, 47: 791-803.
- Mitchell R.E., Young H. (1985). *N*-Coronafacoyl-L-isoleucine and *N*-coronafacoyl-L-alloisoleucine, potential biosynthetic intermediates of the phytotoxin coronatine. *Phytochemistry*, 24: 2716-2717.
- Moon J., Parry G., Estelle M. (2004). The ubiquitin-proteasome pathway and plant development. *The Plant Cell*, 16(12), 3181-3195.

- Niki T., Mitsuhashi I., Seo S., Ohtsubo N., Ohashi Y. (1998). Antagonistic effect of salicylic acid and jasmonic acid on the expression of pathogenesis-related (PR) protein genes in wounded mature tobacco leaves. *Plant Cell Physiol*, 39(5): 500-507.
- Neilands J.B. (1995). Siderophores: structure and function of microbial iron transport compounds. *J Biol Chem*, 270 (45): 26723-26726.
- O'Brien J., Wright G.D. (2011). An ecological perspective of microbial secondary metabolism. *Curr Opin Biotechnol*, 22: 552-558.
- Park D.H., Kim J.S., Kwon S.W., Wilson C., Yu Y.M., Hur J.H., Lim C.K. (2003). *Streptomyces luridiscabiei* sp. nov., *Streptomyces puniscabiei* sp. nov. and *Streptomyces niveiscabiei* sp. nov., which cause potato common scab disease in Korea. *Int J Syst Evol Microbiol*, 53: 2049-2054.
- Parry R.J., Jiralerspong S., Mhaskar S., Alemany L., Willcott R. (1996). Investigations of coronatine biosynthesis. Elucidation of the mode of incorporation of pyruvate into coronafacic acid. *J Am Chem Soc*, 118: 703-704.
- Pathom-aree W., Stach J.E.M., Ward A.C., Horikoshi K., Bull A.T., Goodfellow M. (2006). Diversity of actinomycetes isolated from Challenger Deep sediment (10,898 m) from the Mariana Trench. *Extremophiles*, 10: 181-189.
- Pauwels L., Barbero G.F., Geerinck J., Tilleman S., Grunewald W., Perez A.C., Chico J.M., Bossche R.V., Sewell J., Gil E., Garcia-Casado G., Witters E., Inze D., Long J.A., De Jaeger G., Solano R., Goossens A. (2010) NINJA connects the co-repressor TOPLESS to jasmonate signalling. *Nature*, 464:788–791.

- Penfold C.N., Bender C.L., Turner J.G. (1996). Characterisation of genes involved in biosynthesis of coronafacic acid, the polyketide component of the phytotoxin coronatine. *Gene*, 183: 167-173.
- Peters R.D., Sturz A.V., Carter M.R., Sanderson J.B. (2004). Influence of crop rotation and conservation tillage practices on the severity of soil-borne potato diseases temperate humid agriculture. *Can J Soil Sci*, 84(4): 397-402.
- Petroski M.D., Deshaies R.J. (2005). Function and regulation of cullin-ring ubiquitin ligases. *Nat Rev Mol Cell Biol*, 6: 9-20.
- Piterse C.M.J., van Loon L.C. (1999). Salicylic acid-independent plant defence pathways. *Trends Plant Sci Rev*, 4(2): 52-58.
- Qi M., Wang D., Bradley C.A., Zhao Y. (2011). Genome sequence analyses of *Pseudomonas savastanoi* pv. *glycinea* and subtractive hybridization-based comparative genomics with nine pseudomonads. *PLoS one*, 6:e16451.
- Rangaswamy V., Jiralerspong S., Parry R., Bender C.L. (1998a). Biosynthesis of the *Pseudomonas* polyketide coronafacic acid requires monofunctional and multifunctional polyketide synthase proteins. *Proc Natl Acad Sci USA*, 95: 15469-15474.
- Rangaswamy V., Mitchell R., Ullrich M., Bender C. (1998b). Analysis of genes involved in biosynthesis of coronafacic acid, the polyketide component of the phytotoxin coronatine. *J Bacteriol*, 180(13): 3330-3338.

- Riley M., Abe T., Arnaud M.B., Berlyn M.K.B., Blattner F.R., Chaudhuri R.R., Glasner J.D., Horiuchi T., et al. (2006). *Escherichia coli* K-12: a cooperatively developed annotation snapshot-2005. *Nucleic Acids Res*, 34(1): 1-9.
- Ryan A.D., Kinkel L.L. (1997). Inoculum density and population dynamics of suppressive and pathogenic *Streptomyces* strains and their relationship to biological control of potato scab. *Biol Control*, 10: 180-186.
- Santino A., Taurino M., De Domenico S., Bonsegna S., Poltronieri P., Pastor V., Flors V. (2013). Jasmonate signaling in plant development and defense response to multiple (a)biotic stresses. *Plant Cell Rep*, 32: 1085-1098.
- Scheible W.R., Fry B., Kochevenko A., Schindelasch D., Zimmerli L., Somerville S., et al. (2003). An Arabidopsis mutant resistant to thaxtomin A, a cellulose synthesis inhibitor from *Streptomyces* species. *Plant Cell*, 15: 1781-1794.
- Scholte K., Labruyère R.E. (1985). Netted scab: a new name for an old disease in Europe. *Pot Res*, 28: 443-448.
- Schrey S.D., Schelhammer M., Ecke M., Hampp R., Tarkka M.T. (2005). Mycorrhiza helper bacterium *Streptomyces* AcH 505 induces differential gene expression in the ectomycorrhizal fungus *Amanita muscaria*. *New Phytol*, 168: 205-216.
- Seipke R.F., Loria R. (2008). *Streptomyces scabies* 87-22 possesses a functional tomatinase. *J Bacteriol*, 190: 7684-7692.

- Shiraishi K., Konoma K., Sato H., Ichihara A., Sakamura S., Nishiyama K., Sakai R. (1979). The structure-activity relationships in coronatine analogs and amino compounds derived from (+)-coronafacic acid. *Agric Biol Chem*, 43(8): 1753-1757.
- Strieter E.R., Koglin A., Aron Z.D., Walsh C.T. (2009). Cascade reactions during coronafacic acid biosynthesis: elongation, cyclization, and functionalization during Cfa7-catalyzed condensation. *J Am Chem Soc*, 131: 2113-2115.
- Thines B., Katsir L., Melotto M., Niu Y., Mandaokar A., Liu G., Nomura K., He S.Y., Howe G.A., Browse J. (2007). JAZ repressor proteins are targets of the SCF(COI1) complex during jasmonate signalling. *Nature*, 448: 661-665.
- Uppalapati S.R., Ayoubi P., Weng H., Palmer D.A., Mitchell R.E., Jones W., Bender C.L. (2005). The phytotoxin coronatine and methyl jasmonate impact multiple phytohormone pathways in tomato. *Plant J*, 42: 201-217.
- Wang X.-J., Yan Y.-J., Zhang B., An J., Wang J.-J., Tian J., Jiang L., Chen Y.-H., et al. (2010). Genome sequence of the milbemycin-producing bacterium *Streptomyces bingchenggensis*. *J Bacteriol*, 192(17): 4526-4527.
- Wanner L.A. (2009). A patchwork of *Streptomyces* species isolated from potato common scab lesions in North America. *Am J Pot Res*, 86: 247-264.
- Waterer D. (2002). Impact of high soil pH on potato yeilds and grade losses to common scab. *Can J Plant Sci*, 82(3): 583-586.
- Watve M.G., Tickoo R., Jog M.M., Bhole B.D. (2001). How many antibiotics are produced by the genus *Streptomyces*? *Arch Microbiol*, 176: 386-390.

- Wildermuth H. (1970). Development and organization of the aerial mycelium in *Streptomyces coelicolor*. *J Gen Microbiol*, 60: 43-50.
- Wilson C.R., Ransom L.M., Pemberton B.M. (1999). The relative importance of seed-borne inoculum to common scab disease of potato and the efficacy of seed tuber and soil treatments for disease control. *J Phytopathology*, 147: 13-18.
- Wilson M.C., Moore B.S. (2012). Beyond ethylmalonyl-CoA: the functional role of crotonyl-CoA carboxylase/reductase homologs in expanding polyketide diversity. *Nat Prod Rep*, 29: 72-86.
- Xin X.F., He S.Y. (2013). *Pseudomonas syringae* pv. *tomato* DC3000: a model pathogen for probing disease susceptibility and hormone signaling in plants. *Annu Rev Phytopathology*, 51: 473-498.
- Yan J., Li H., Li S., Yao R., Deng H., Xie Q., Xie D. (2013). The *Arabidopsis* F-box protein Coronatine Insensitive1 is stabilized by SCF^{COI1} and degraded via the 26S proteasome pathway. *Plant Cell*, 25: 486-498.
- Yim G., Wang, H.H., Davies J. (2007). Antibiotics as signalling molecules. *Phil Trans R Soc B Biol Sci*, 362: 1195-1200.
- Zaburanyi N., Rabyk M., Ostash B., Fedorenko V., Luzhetskyy A. (2014). Insights into naturally minimised *Streptomyces albus* J1074 genome. *BMC Genomics*, 15: 97.
- Zhang Y., Bignell D.R.D., Zuo R., Fan Q., Huguet-Tapia J.C., Ding Y., Loria R. (2016). Promiscuous pathogenicity islands and phylogeny of pathogenic *Streptomyces* spp. *Mol Plant Microbe Interact*, 29(8): 640-650.

Zhao W.Q., Yu X.M., Liu D.Q. (2010). First report of *Streptomyces acidiscabies* causing potato scab in China. *Plant Pathol*, 59: 405.

1.10 Figures

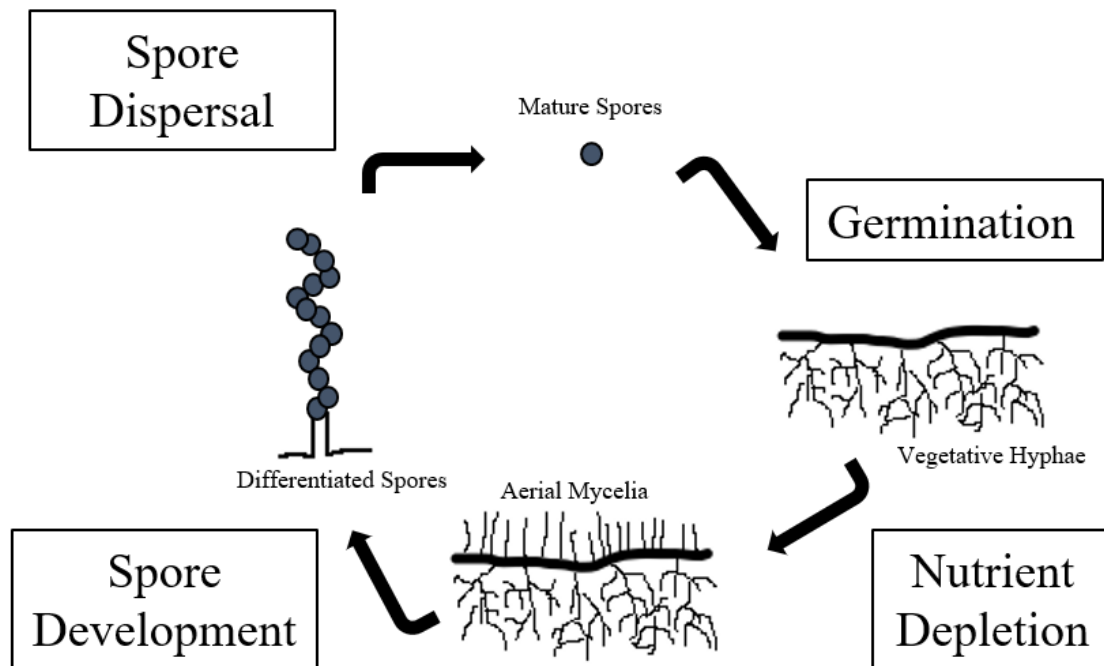


Figure 1.1. Life cycle of organisms from the *Streptomyces* genus.



Figure 1.2. Common scab disease symptoms on a potato tuber. Image courtesy of D. Bignell.

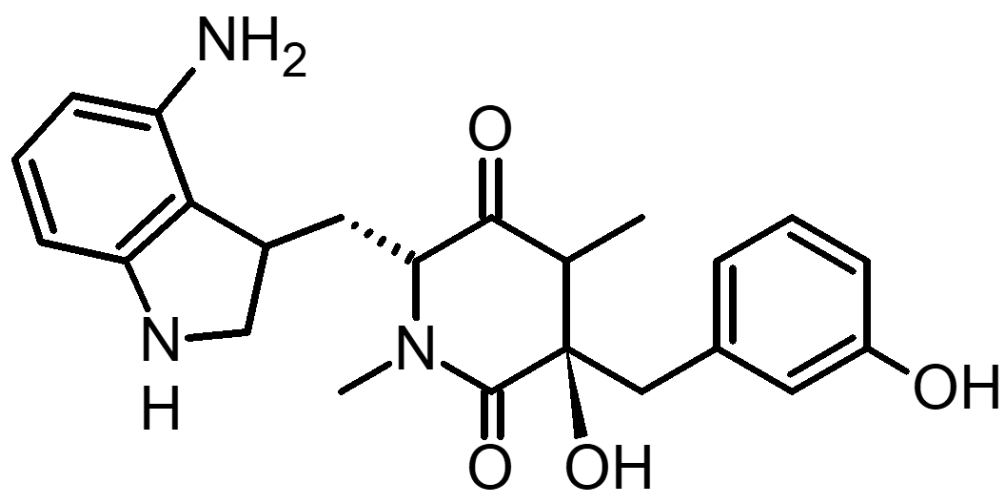


Figure 1.3. Molecular structure of the thaxtomin A phytotoxin.

P. syringae

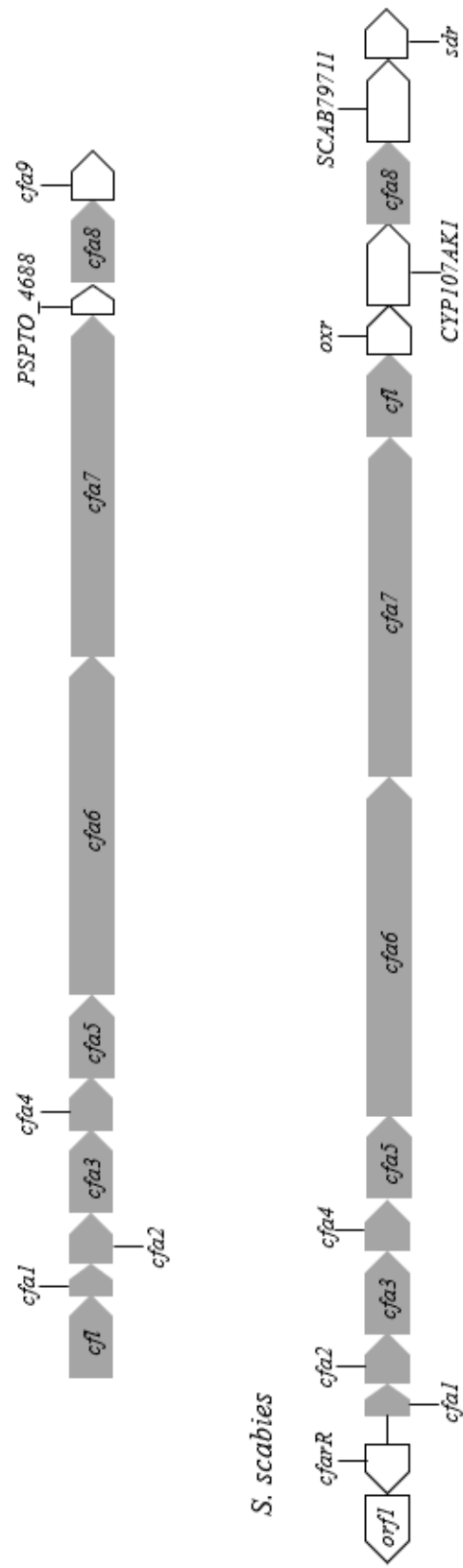


Figure 1.4. The CFA and CFA-like biosynthetic gene clusters from *P. syringae* and *S. scabies* respectively. Genes which are indicated in gray are homologous between the gene clusters, and genes which are outlined in black are unique to each respective gene cluster. The four unique biosynthetic genes found in the *S. scabies* gene cluster are *scab79681* (*oxr*), *scab79691* (*CYP107AK1*), *scab79711* and *scab79721* (*sdr*).

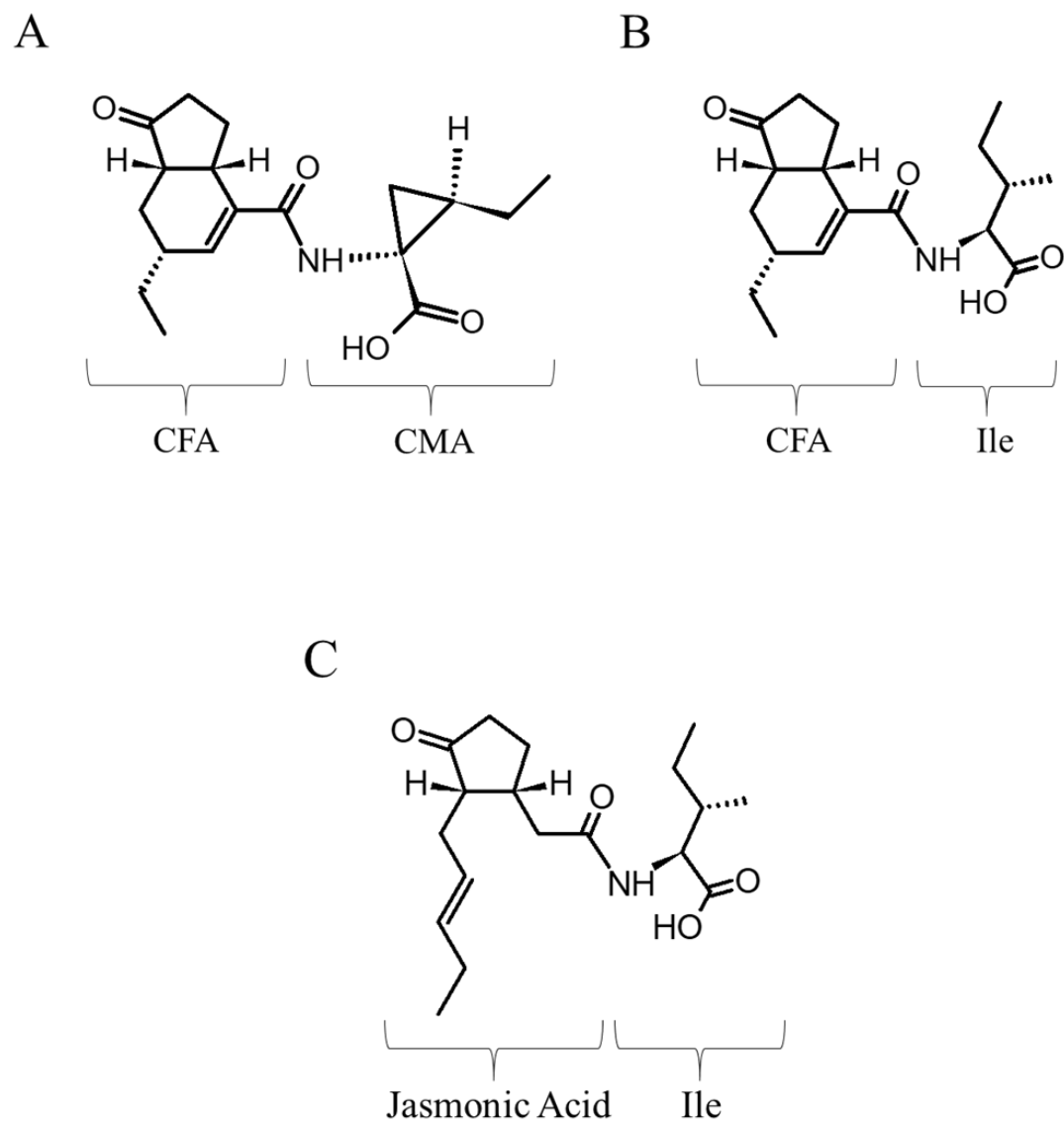


Figure 1.5. Molecular structures of (A) coronatine (COR); (B) coronafacoyl-L-isoleucine (CFA-Ile); (C) jasmonoyl-L-isoleucine (JA-Ile).

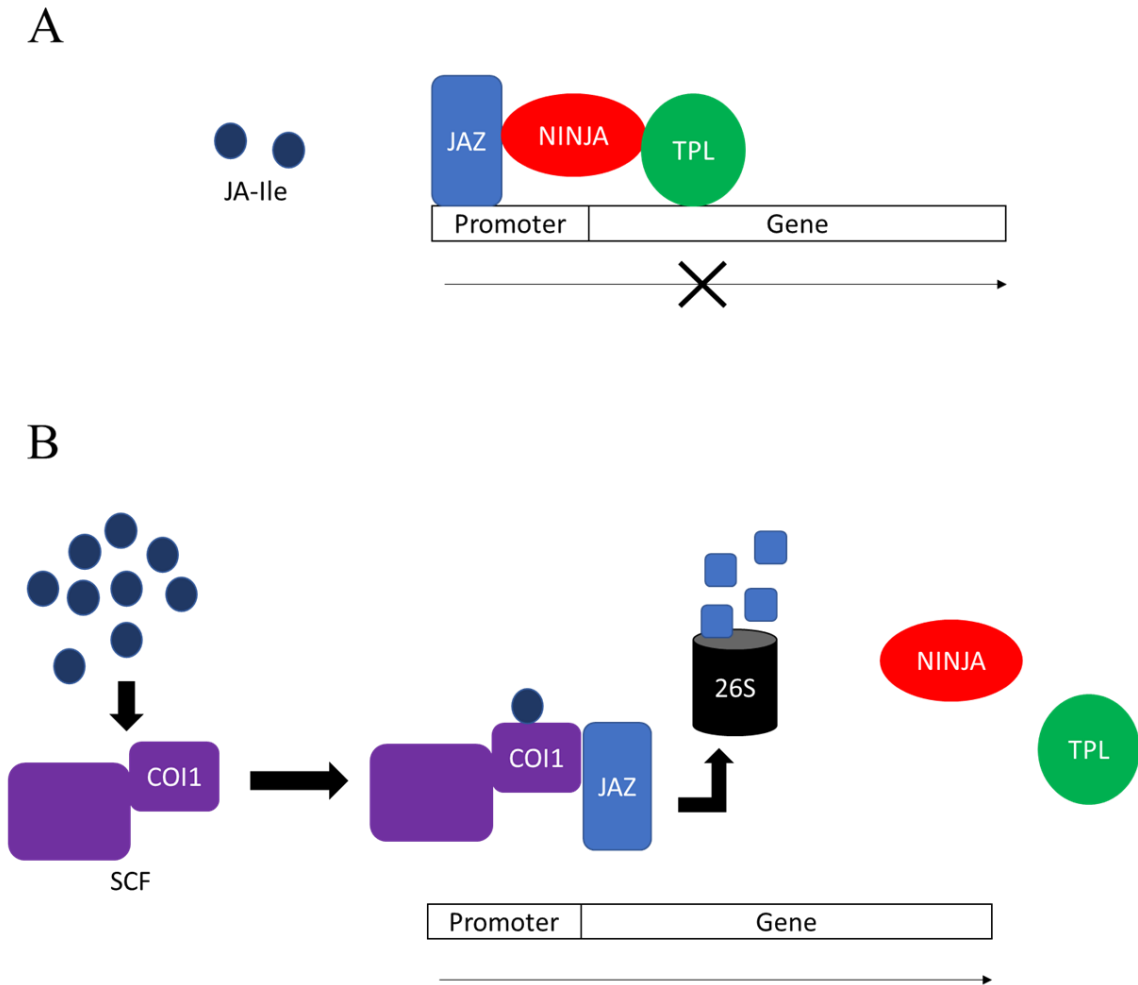


Figure 1.6. The JA-Ile regulatory pathway. (A) In the presence of low levels of JA-Ile members of the JAZ family of proteins bind to the G-box region of the target promoter along with the TPL repressor protein via association with the NINJA adaptor protein. This repressor complex prevents transcription of the involved genes. (B) High levels of JA-Ile will result in JA-Ile association with the COI1 F-box component of the SCF^{COI1} complex. This association will stimulate interaction of COI1 with the JAZ proteins, which results in

disassociation of the NINJA and TPL proteins and degradation of the JAZ proteins via the 26S proteasome pathway. Removal of the repressor complex allows for transcription and gene expression to occur.

Figure 1.7. Proposed pathway for the biosynthesis of COR in *P. syringae*. AT: acyl transferase; ACP: acyl carrier protein; KS: keto synthase; DH: dehydrogenase; ER: enoyl reductase; KR: keto reductase; TE: thioesterase. Steps of this pathway are explained in detail within the text of section 1.7.

Statement of Co-Authorship

Chapter 2 is a version of a manuscript published in Molecular Microbiology [Bown L., Altowairish M.S., Fyans J.K., Bignell D.R.D. (2016) Production of the *Streptomyces scabies* coronafacoyl phytotoxins involves a novel biosynthetic pathway with an F₄₂₀-dependent oxidoreductase and a short-chain dehydrogenase/reductase. *Mol Microbiol*, 101(1): 122-135]. The study concept was designed by D. Bignell, and the methodology was designed by D. Bignell, L. Bown and M. Altowairish. M. Altowairish constructed the Δoxr and Δsdr mutants, performed initial mutant culture extract bioassays and performed the mutant complementation experiments, and J. Fyans assisted with the initial RP-HPLC and LC-LRESIMS analysis of the Δoxr and Δsdr mutant extracts. L. Bown conducted the bioinformatics and phylogenetic analysis of the Oxr and Sdr protein sequences, the large-scale extraction and purification of biosynthetic intermediates, and the bioactivity characterization of the pure intermediates. Structural characterization of the pure intermediates was conducted by Dr. Celine Schneider of the Memorial University Centre for Chemical Analysis, Research and Training (C-CART) facility and at the McMaster Regional Centre for Mass Spectrometry (MRCMS) of McMaster University. The manuscript was drafted and prepared by L. Bown and D. Bignell, and editorial input was provided by the co-authors.

Chapter 3 is a version of a manuscript published in Applied and Environmental Microbiology [Bown L., Li Y., Berru   F., Verhoeven J.T.P., Dufour S.C., Bignell D.R.D. (2017). Coronafacoyl phytotoxin biosynthesis and evolution in the common scab pathogen

Streptomyces scabiei. *Appl Environ Microbiol*, 83: e01169-01117]. The study concept was designed by D. Bignell and L. Bown, and the methodology was designed by D. Bignell, L. Bown and Y. Li. Y. Li constructed the $\Delta CYP107AK1$ mutant strain and performed the mutant culture extract bioassays. J. Verhoeven constructed the concatenated phylogenetic tree for the core CFA biosynthetic genes. L. Bown performed the RP-HPLC and LC-LRESIMS analysis of the $\Delta CYP107AK1$ culture extracts, the extraction and purification of the accumulated biosynthetic intermediates, the bioactivity analysis of the purified intermediates, and the bioinformatics analysis of the phytotoxin BGCs from different organisms. Structural analysis of the biosynthetic intermediates was performed by F. Berru   and at the MUN C-CART facility by Dr. Celine Schneider and Dave Davidson. The initial manuscript was drafted and prepared by L. Bown and D. Bignell and editorial input was provided by the co-authors.

Chapter 4 is a version of a manuscript published in Bio-Protocol [Bown L., Bignell D.R. (2017) Purification of *N*-coronafacoyl phytotoxins from *Streptomyces scabies*, *Bio-Protocol* 7(7): e2214]. The study concept was designed by L. Bown and D. Bignell, and the methodology design and experimental work were conducted by L. Bown. The manuscript was drafted and prepared by L. Bown with editorial input by D. Bignell.

Chapter 5 is a manuscript in preparation for submission. The study concept and experimental methodology were designed by L. Bown with intellectual input from D. Bignell. T. Kiene generated the Cfl protein alignment, and the remaining experimental work and data analysis were conducted by L. Bown. Z. Cheng assisted with the FPLC

purification of the Cfl protein. The manuscript was written by L. Bown with editorial input by D. Bignell.

Chapter 6 is a version of a manuscript published in *Phytopathology* [Fyans J.K., Bown L., Bignell D.R.D. (2016) Isolation and characterization of plant-pathogenic *Streptomyces* species associated with common scab-infected potato tubers in Newfoundland. *Phytopathology* 106(2) 123-131]. The study concept was designed by D. Bignell and the experimental methodology was designed by D. Bignell, J. Fyans and L. Bown. J. Fyans performed the initial isolations of the pathogenic *Streptomyces* spp., the pathogenicity testing, the PCR detection of virulence genes, and the RP-HPLC detection of borrelidin and concanamycin production. L. Bown performed the morphological and physiological characterization of the isolates, the quantification of thaxtomin A production by the isolates, the RFLP and rep-PCR analyses and the phylogenetic analysis. The manuscript was written by J. Fyans and L. Bown with editorial input by D. Bignell. This manuscript was equally contributed to by L. Bown and J. Fyans.

Chapter 7 is a version of a manuscript published in *Genome Announcements* [Bown L., Bignell D.R.D. (2017) Draft genome sequence of the plant pathogen *Streptomyces* sp. strain 11-1-2. *Genome Announcements*, 5(37): e00968-17]. The study concept was designed by D. Bignell and the experimental methodology was designed by D. Bignell and L. Bown. All experimental procedures and data analysis were carried out by L. Bown. The manuscript was drafted and prepared by L. Bown with editorial assistance by D. Bignell.

Appendix 1 contains a manuscript published in *PLOS One* [Cheng Z., Bown L., Tahlan K., Bignell D.R.D. (2015) Regulation of coronafacoyl phytotoxin production by the

PAS-LuxR family regulator CfaR in the common scab pathogen *Streptomyces scabies*. *PLOS One*, 10(3), e0122450] and a version of a review published in Antoine van Leeuwenhoek [Bignell D.R.D., Cheng Z., Bown L. (2018) The coronafacoyl phytotoxins: structure, biosynthesis, regulation and biological activities. *Antoine van Leeuwenhoek*, 111:649-666]. This appendix is meant to demonstrate contributions to research on coronafacoyl phytotoxin production outside of the topics presented in this thesis.

Appendix 2 contains a version of a manuscript published in The Journal of Membrane Biology [Bown L., Srivastava S.K., Piercey B.M., McIssac C.K., Tahlan K. (2018) Mycobacterial membrane proteins QcrB and AtpE: roles in energetics, antibiotic targets, and associated mechanisms of resistance. *J Membrane Biol*, 251: 105-117]. This appendix is meant to demonstrate contributions to research outside of the topic of coronafacoyl phytotoxin production.

Chapter 2: Production of the *Streptomyces scabies* coronafacoyl phytotoxins involves a novel biosynthetic pathway with an F₄₂₀-dependent oxidoreductase and a short-chain dehydrogenase/reductase

Luke Bown[†], Mead S. Altowairish [†], Joanna K. Fyans[‡] and Dawn R. D. Bignell

Department of Biology, Memorial University of Newfoundland, St. John's, NL A1B 3X9, Canada

[†] These authors contributed equally to this work

[‡] Present address: School of Chemistry, The University of Manchester, Oxford Road, Manchester, M13 9PL, UK

For correspondence. Email: dbignell@mun.ca; Phone: (+1) 709-864-4573; Fax: (+1) 709-864-3018.

© 2016 John Wiley & Sons Ltd, *Molecular microbiology*, 101(1), 122-135.

2.1 Abstract

Coronafacoyl phytotoxins are secondary metabolites that are produced by various phytopathogenic bacteria, including several pathovars of the Gram-negative bacterium *Pseudomonas syringae* as well as the Gram-positive potato scab pathogen *Streptomyces scabies*. The phytotoxins are composed of the polyketide coronafacic acid (CFA) linked via an amide bond to amino acids or amino acid derivatives, and their biosynthesis involves the *cfa* and *cfa*-like gene clusters that are found in *P. syringae* and *S. scabies*, respectively. The *S. scabies* *cfa*-like gene cluster was previously reported to contain several genes that are absent from the *P. syringae* *cfa* gene cluster, including one (*oxr*) encoding a putative F₄₂₀—dependent oxidoreductase, and another (*sdr*) encoding a predicted short-chain dehydrogenase/reductase. Using gene deletion analysis, we demonstrated that both *oxr* and *sdr* are required for normal production of the *S. scabies* coronafacoyl phytotoxins, and structural analysis of metabolites that accumulated in the Δsdr mutant cultures revealed that Sdr is directly involved in the biosynthesis of the CFA moiety. Our results suggest that *S. scabies* and *P. syringae* use distinct biosynthetic pathways for producing coronafacoyl phytotoxins, which are important mediators of host-pathogen interactions in various plant pathosystems.

2.2 Introduction

The ability to produce a wide array of bioactive secondary metabolites (also known as natural products) is a hallmark of Gram-positive bacteria belonging to the genus

Streptomyces. The metabolites that are produced by these organisms include many medically-important compounds with antibacterial, antifungal, antiviral, antiparasitic, anticancer and immunosuppressive, activities (Bérdy 2005). Although nonessential for growth and survival under laboratory conditions, secondary metabolites are widely believed to play a significant role for the producing organism within its natural habit. For example, siderophores function in the scavenging of limited amounts of iron from the environment (Wandersman and Delepelaire 2004), and metabolites with antimicrobial activity are thought to allow the producer to compete with other microorganisms for a limited nutrient supply (O'Brien and Wright 2011; Wietz et al. 2013). Secondary metabolites have also been implicated in promoting symbiotic relationships between *Streptomyces* spp. and plants, fungi and animals (Seipke et al. 2012). In some instances, these relationships are mutualistic in nature, but in others they can be parasitic and result in the development of disease in the eukaryotic host. An example of such a relationship is the interaction between plant pathogenic *Streptomyces* spp. and potato (*Solanum tuberosum*) leading to the development of the economically important crop disease potato scab.

To date, at least 11 different *Streptomyces* spp. are known to cause potato scab disease, which is characterized by the formation of raised, pitted or superficial cork-like lesions on the surface of the tuber (Dees and Wanner 2012). The best characterized scab-causing pathogen is *Streptomyces scabies* (syn. *scabiei*), which was first described in 1890 and has a world-wide distribution (Loria et al. 2006; Thaxter 1891). *S. scabies* and other scab-causing pathogens produce a family of phytotoxic secondary metabolites called the thaxtomins, of which thaxtomin A is predominant (King and Calhoun 2009). Currently, it

is believed that thaxtomin A functions primarily as a cellulose synthesis inhibitor (Bignell et al. 2014), and it may contribute to the ability of *S. scabies* and other plant pathogenic *Streptomyces* spp. to penetrate expanding plant tissue during host colonization (Loria et al. 2008).

Recently, *S. scabies* was reported to synthesize an additional family of phytotoxic secondary metabolites called the coronafacoyl phytotoxins (also known as the coronatine-like phytotoxins), which consist of the polyketide compound coronafacic acid (CFA; Fig. 2.1-A) linked via an amide bond to different amino acids or amino acid derivatives (Bender et al. 1999b; Fyans et al. 2015). The best characterized coronafacoyl phytotoxin is coronatine (COR), which is composed of CFA linked to an ethylcyclopropyl amino acid called coronamic acid (CMA; Fig. 2.1-A) and is the primary coronafacoyl phytotoxin produced by several pathovars (pv) of the Gram-negative plant pathogenic bacterium *Pseudomonas syringae*, including *alisalensis*, *atropurpurea*, *glycinea*, *maculicola*, *morsprunorum*, *porri* and *tomato* (Geng et al. 2014). COR is a non-host specific toxin that is required for the full virulence of *P. syringae* as it contributes to the invasion and persistence of the pathogen within the plant host as well as to disease symptom development (reviewed in Xin and He 2013). The primary coronafacoyl phytotoxin produced by *S. scabies* is *N*-coronafacoyl-L-isoleucine (CFA-Ile; Fig. 2.1-A), which is also produced by *P. syringae* in minor amounts, and it has been shown to exhibit similar biological activities as COR, though it is not as toxic (Fyans et al. 2015; Mitchell and Young 1985). In addition, *S. scabies* produces other minor coronafacoyl phytotoxins, including CFA-valine, which is also produced by *P. syringae* (Bender et al. 1989; Fyans et al. 2015; Mitchell 1985).

In *P. syringae*, the biosynthesis of COR involves the *cfa* (Fig. 2.1-B) and *cma* biosynthetic gene clusters that are responsible for producing the CFA and CMA moieties, respectively (Bender et al. 1999b). Once produced, the two moieties are thought to be linked together by the coronafacate ligase (Cfl) enzyme encoded within the *cfa* biosynthetic gene cluster (Fig. 2.1-A) (Liyanage et al. 1995; Rangaswamy et al. 1997). Most of the CFA biosynthetic genes, including the Cfl-encoding gene, are conserved in a similar gene cluster (called the *cfa*-like gene cluster) in *S. scabies* 87-22 (Fig. 2.1-B), whereas the CMA biosynthetic genes are notably absent (Bignell et al. 2010). Interestingly, the *S. scabies* *cfa*-like gene cluster contains an additional six genes that are absent from the *P. syringae* *cfa* gene cluster (Fig. 2.1-B). Two of these genes, *cfaR* and *SCAB79581* (also known as *orf1*), are expressed as a polycistronic transcript and are involved in the regulation of CFA-Ile production (Bignell et al. 2010; Cheng et al. 2015), whereas the remaining four genes encode predicted biosynthetic enzymes (Bignell et al. 2010). All four latter genes are co-expressed with the other genes in the *cfa*-like gene cluster (Bignell et al. 2010), suggesting that they are somehow involved in the biosynthesis of coronafacoyl phytotoxins in *S. scabies*.

In this study, we set out to characterize the role of two genes, *SCAB79681* (referred to herein as *oxr*) and *SCAB79721* (referred to herein as *sdr*), in the biosynthesis of the *S. scabies* coronafacoyl phytotoxins. We show that both genes are required for normal production of the CFA-Ile phytotoxin, and we provide evidence that the Sdr protein is directly involved in the biosynthetic pathway for CFA production in *S. scabies*.

2.3 Results

2.3.1 Bioinformatics analyses indicate that *oxr* and *sdr* encode a predicted F_{420} -dependent oxidoreductase and a short chain dehydrogenase/reductase, respectively

Using the BLASTP algorithm, the predicted Oxr amino acid sequence was determined to be most similar to luciferase-like monooxygenase (LLM) class F_{420} -dependent oxidoreductases from different bacteria, with the most closely related homolog (SsS58_02710, displays 97% identity and 98% similarity to Oxr) originating from a recently sequenced *S. scabiei* isolate from Japan (Fig. 2.2-A). A search of the Pfam database revealed the presence of a luciferase-like monooxygenase domain (PF00296.15), a finding that is consistent with the fact that several luciferase-like monooxygenase family proteins are known to be F_{420} -dependent enzymes (Aufhammer et al. 2004; Bashiri et al. 2008). The enzyme cofactor F_{420} is a deazaflavin derivative of flavin mononucleotide (FMN) and is produced mainly by archaeal methanogens and actinomycetes such as *Streptomyces* spp. and *Mycobacterium* spp. (Taylor et al. 2013). In *Streptomyces* spp., F_{420} -dependent oxidoreductases are known or predicted to be involved in the biosynthesis of secondary metabolites such as chlortetracycline (Nakano et al. 2004), oxytetracycline (Wang et al. 2013) and tomaymycin (Li et al. 2009). Chemical reactions that have been attributed to these enzymes include the redox transformation of alcohols, imines and carbon-carbon double bonds (Taylor et al. 2013).

The Sdr amino acid sequence was found to be most similar to predicted oxidoreductases from actinobacteria and other bacteria, including one (SsS58_08718, displays 93% identity and 97% similarity with Sdr) from the same Japanese isolate of

S. scabiei containing the Oxr homologue (Fig. 2.2-B). BLASTP analysis revealed the presence of other proteins in the Japanese *S. scabiei* isolate that are homologous to enzymes encoded in the *S. scabies* 87-22 *cfa*-like gene cluster, suggesting that the Japanese isolate can also produce coronafacoyl phytotoxins. A domain search of Sdr revealed the presence of a short chain dehydrogenase domain (PF00106.20) within the first 164 amino acids of the protein sequence. Short chain dehydrogenases/reductases (SDRs) are NAD- or NADP-dependent oxidoreductases that catalyze carbonyl-hydroxyl oxidoreductions, decarboxylations, epimerizations, dehalogenations, and C=C and C=N reduction reactions (Kavanagh et al. 2008). The Sdr amino acid sequence was found to contain a TGxxxGxG cofactor binding motif and a YxxxK active site motif, which along with the total polypeptide chain length (260 amino acids) places the protein into the ‘classical’ subfamily of SDRs (Kavanagh et al. 2008). Such enzymes are most often involved in the NAD(P)(H)-dependent oxidoreduction of hydroxyl/keto groups in many different small molecules, including secondary metabolites (Kavanagh et al. 2008).

2.3.2 *Deletion of oxr and sdr leads to a significant reduction in CFA-Ile production in S. scabies*

The role of the *oxr* and *sdr* genes in the biosynthesis of the coronafacoyl phytotoxins was investigated by constructing *S. scabies* deletion mutants using the Redirect PCR targeting system (Gust et al. 2003a; Gust et al. 2003b) and then assessing the effect of each gene deletion on phytotoxin production levels. The mutants were constructed in the $\Delta txtA$ /pRLDB51-1 background (Table 2.1), which produces high levels of the coronafacoyl phytotoxins due to overexpression of the *cfaR* regulatory gene (Cheng et al. 2015; Fyans et

al. 2015), and is also unable to produce the thaxtomin A phytotoxin due to deletion of the *txtA* gene (Johnson et al. 2009). RP-HPLC analysis of the culture extracts from six independently generated Δoxr mutants indicated that production of the primary CFA-Ile phytotoxin as well as the minor coronafacoyl phytotoxins was significantly reduced in the mutants compared to the $\Delta txtA$ /pRLDB51-1 strain, though some production of CFA-Ile was still detectable (Fig. 2.3-A and 2.3-B; data not shown). Relative quantification of the CFA-Ile production levels revealed that the mutants produced an average of 14-26% of the metabolite levels observed in the $\Delta txtA$ /pRLDB51-1 strain (Fig. S-2.1; data not shown), and no additional peaks were detected in the mutant extracts by RP-HPLC (Fig. 2.3-B), indicating that there were no detectable biosynthetic intermediates that accumulated in the mutant extracts. When the *oxr* gene was re-introduced into the Δoxr mutant #3 on an integrative plasmid, production of the CFA-Ile metabolite was restored to levels exceeding that in the $\Delta txtA$ /pRLDB51-1 strain whereas introduction of the integrative plasmid alone had no effect, indicating that the observed decrease in metabolite production in the mutant was due to the corresponding gene deletion (Fig. S-2.1).

The Δsdr mutant isolates (six in total) were also determined to be severely reduced in production of CFA-Ile and other minor coronafacoyl phytotoxins (Fig. 2.3-C and 2.3-D; data not shown), with CFA-Ile levels reaching only 6-12% of that in the $\Delta txtA$ /pRLDB51-1 strain (Fig. S-2.1; data not shown). Within the mutant RP-HPLC chromatogram, three new peaks were observed with retention times (t_R) of 1.6, 2.3, and 2.6 min (Fig. 2.1-D). Analysis of the peaks at $t_R = 2.3$ and 2.6 min using liquid chromatography-low resolution electrospray ionization mass spectrometric analysis (LC-LRESIMS) revealed

pseudomolecular $[M-H]^-$ ions in negative ion mode at m/z 322, indicating the presence of a compound with a molecular mass of 323 Da in both instances. Analysis of the peak at $t_R = 1.6$ min revealed a pseudomolecular $[M-H]^-$ ion at m/z 308, which indicates the presence of a compound with a molecular mass of 309 Da. The three metabolites were no longer detectable upon complementation of the Δsdr mutant #1 with the *sdr* gene (data not shown), and the CFA-Ile production level in the complemented Δsdr mutant was restored to near $\Delta txtA/pRLDB51-1$ levels (Fig. S-2.1), confirming that the observed effects on metabolite production were due to the corresponding gene deletion.

The effect of each gene deletion on the bioactivity of the culture extracts was also assessed using a potato tuber disk bioassay, which detects the tissue hypertrophy-inducing activity of CFA-Ile and other coronafacoyl phytotoxins (Fyans et al. 2015). As shown in Fig. 2.4-A, extract from two of the Δoxr mutant isolates exhibited some tissue hypertrophy-inducing activity, but it was not as bioactive as the $\Delta txtA/pRLDB51-1$ extract, a result that is consistent with the observed reduction in CFA-Ile production in the mutant (Fig. 2.3-B). On the other hand, extract from two of the Δsdr mutant isolates was found to exhibit the same degree of hypertrophy-inducing activity on the tuber tissue as the $\Delta txtA/pRLDB51-1$ organic acid extract (Fig. 2.4-B), suggesting that one or more of the accumulated intermediates exhibits the same or similar bioactivity as the CFA-Ile end product.

2.3.3 *Structural elucidation of the accumulated metabolites in the Δsdr mutant indicates a role for Sdr in coronafacic acid biosynthesis.*

To further investigate the role of Sdr in the biosynthesis of the CFA-Ile phytotoxin, large-scale cultures of the Δsdr mutant were grown and extracted with organic solvent, and the accumulated metabolites 1 ($t_R = 2.3$ min) and 2 ($t_R = 2.6$ min) (Fig. 2.3-D) were purified using a combination of preparative thin-layer chromatography (TLC) and RP-HPLC (Fig. S-2.2; See Experimental Procedures). Purification of metabolite 3 ($t_R = 1.6$ min) (Fig. 2.3-D) was also attempted; however, we were unable to obtain a sufficient amount of this compound in pure form for structural analyses. High resolution electrospray ionization mass spectra (HRESIMS) of the pure metabolites indicated the presence of a pseudomolecular $[M+H]^+$ ion in positive ion mode at m/z 324.2183 for metabolite 1, and a pseudomolecular $[M+H]^+$ ion at m/z 324.2172 for metabolite 2. These results are consistent with a molecular formula of $C_{18}H_{30}NO_4$ (theoretical $[M+H]^+ = 324.2175$) for both metabolites. Tandem MS (HRESIMS/MS) analysis revealed the presence of a prominent fragment ion at m/z 193.1230 for metabolite 1 and 193.1232 for metabolite 2 (Fig. S-2.3), indicating that the metabolites may be isomers of the same molecule. It is noteworthy that the observed fragment ion is similar to the reported prominent fragment ion (m/z 191) for *N*-coronafacoyl-substituted amino acid compounds (Mitchell 1984; Mitchell and Young 1985). Analysis using 1-dimensional and 2-dimensional NMR (1H , ^{13}C , COSY, HSQC, HMBC and NOESY) (Fig. S-2.4, S-2.5) revealed the structure of each compound as shown in Figure 2.5. The key difference between the two metabolites and the CFA-Ile end-product (Fig. 2.1-A) is the presence of a hydroxyl group in place of the keto group at position 2 in the cyclopentane ring, and in both compounds, the NOESY results indicated that the hydroxyl group is oriented downwards (Table 2.2, Fig. 2.5, Fig. S-2.4, S-2.5). Given that

the HRESIMS and HRESIMS/MS results strongly suggested that the metabolites are isomers of one another, we suspect that they differ in the Ile isomer attached to the hydroxyl-containing coronafacoyl polyketide, though the NMR results were not able to distinguish between the different possible isomers. Although we previously showed using RP-HPLC co-injection experiments that the primary coronafacoyl - amino acid end product produced by *S. scabies* contains the L-Ile isomer (Fyans et al. 2015), 1-dimensional and 2-dimensional NMR analysis of CFA-Ile purified from large-scale *S. scabies* cultures revealed the presence of a mixture of two different Ile isomers attached to CFA in a ratio of approximately 2:1 (Table 2.2; Fig. S-2.2, S-2.5, S-2.6), indicating that multiple Ile isomers can be incorporated into the coronafacoyl phytotoxins in *S. scabies*.

2.3.4 *The accumulated metabolites in the Δ sdr mutant exhibit varying degrees of potato tuber tissue hypertrophy - inducing activity*

The purified metabolites 1 and 2 were tested in the potato tuber disk bioassay in order to examine their relative bioactivity as compared to the CFA-Ile end product. As shown in Figure 2.6, both compounds were able to induce potato tuber tissue hypertrophy, confirming that they retain the activity of the coronafacoyl phytotoxins. However, the two metabolites differed in their relative bioactivity in the assay, with metabolite 1 causing a reduced level of hypertrophy as compared to CFA-Ile, and metabolite 2 causing a similar amount of tissue hypertrophy as CFA-Ile. This suggests that the attached amino acid isomer affects the tissue hypertrophy-inducing activity of the resulting metabolite, a result that is consistent with previous studies of coronafacoyl phytotoxin bioactivity (Shiraishi et al. 1979).

2.4 Discussion

In this study, we have shown that the production of coronafacoyl phytotoxins by the potato scab pathogen *S. scabies* involves a predicted F₄₂₀-dependent oxidoreductase and a short chain dehydrogenase/reductase. This is the first report of such enzymes being involved in the biosynthesis of this family of phytotoxins, which function as important virulence factors in a variety of different plant pathogenic bacteria (Bell et al. 2004; Bignell et al. 2010; Geng et al. 2014). The corresponding *oxr* and *sdr* genes are situated within the *cfa*-like biosynthetic gene cluster in *S. scabies* and are co-transcribed with genes that are homologous to ones found within the *cfa* biosynthetic gene cluster in various pathovars of the Gram-negative plant pathogen *P. syringae* (Fig. 2.1-B; Bignell et al. 2010). Deletion of *oxr* and *sdr* led to a significant reduction in CFA-Ile production (up to 86% and 94%, respectively), and production was restored upon re-introduction of each gene into the corresponding mutant, indicating that the observed mutant phenotypes were due to deletion of the target genes. The fact that a small amount of CFA-Ile production could still be detected in both the Δoxr and Δsdr mutants may be explained by the presence of genes elsewhere on the chromosome that can partially complement the loss of *oxr* and *sdr*. An analysis of the *S. scabies* 87-22 genome sequence revealed the presence of at least one Oxr homologue (SCAB52161, shows 33% identity/51% similarity) and two Sdr homologues (SCAB2261 and SCAB12071, 39% identity/55% similarity and 42% identity/57% similarity, respectively) that may be able to partially compensate for the loss of Oxr or Sdr. Interestingly, *oxr* and *sdr* are among several genes that are unique to the *S. scabies* *cfa*-like

gene cluster and are not found in the corresponding *cfa* gene clusters in *P. syringae* pathovars and in *Pectobacterium atrosepticum* (syn. *Erwinia carotovora* subsp. *atroseptica*), another predicted COR-like metabolite-producing plant pathogen (Bell et al. 2004; Bender et al. 1999a; Bignell et al. 2010). Previously, it was predicted that *oxr*, *sdr* and other novel genes in the *S. scabies* *cfa*-like gene cluster may function as tailoring enzymes involved in producing novel COR-like metabolites (Bignell et al. 2010). Evidence presented here, however, suggests that Sdr, and possibly Oxr, is directly involved in the biosynthesis of the CFA polyketide in *S. scabies*.

Analysis of the Sdr protein sequence indicated that it is most similar to members of the ‘classical’ subfamily of the SDR superfamily, which consists of NAD(P)(H)-dependent oxidoreductases that are found in all domains of life. Classical SDRs are typically 250 amino acids in length and contain a TGxxxGxG cofactor binding motif and a YxxxK active site, and are most often associated with the oxidoreduction of hydroxyl/keto groups in a variety of small molecules such as steroids, growth factors, alcohols, polyols, xenobiotics and secondary metabolites (Kavanagh et al. 2008). Purification and structural analysis of two metabolites that accumulated in the Δsdr mutant cultures revealed the presence of a hydroxyl group in place of the keto group that is normally found on the cyclopentane ring in CFA (Fig. 2.1-A and Fig. 2.5). This is consistent with the predicted function of Sdr and suggests that introduction of the keto group occurs in the later stages of CFA biosynthesis in *S. scabies*. Interestingly, the hydroxyl-containing CFA intermediate was determined to be linked to different isomers of Ile, and accumulation of the polyketide intermediate alone did not occur in the Δsdr cultures. This suggests that the Cfl enzyme, which catalyzes the

ligation of CFA to Ile or other amino acids (Fig. 2.1-A), is able to efficiently utilize the intermediate as a substrate in the ligation reaction. Although we were unable to purify sufficient amounts of a third metabolite that accumulated in the Δsdr mutant cultures for structural analysis, LC-MS analysis indicated that the metabolite has a molecular mass of 309 Da, which is consistent with the hydroxyl-containing CFA intermediate linked to the amino acid valine (theoretical mass = 309.1940 Da). Given that valine is a known substrate for the Cfl enzyme in *S. scabies* and *P. syringae* (Bender et al. 1999b; Fyans et al. 2015), the accumulation of a valine-containing intermediate in the Δsdr mutant is not surprising.

Precursor feeding studies using ^{13}C -labeled substrates demonstrated that CFA in *P. syringae* is synthesized from one unit of pyruvate (which is first converted to α -ketoglutarate) and from three units of acetate and one unit of butyrate (Parry et al. 1994). Based on the feeding studies and on the isolation of a potential biosynthetic intermediate, 2-[1-oxo-2-cyclopenten-2-ylmethyl]-butanoic acid (CPE), a hypothetical biosynthetic pathway was proposed in which α -ketoglutarate is converted to 2-carboxy-2-cyclopentenone (CPC) by the Cfa1-5 proteins encoded within the CFA biosynthetic gene cluster (Fig. 2.7-A; Rangaswamy et al. 1998). Cfa1, Cfa2 and Cfa3 resemble acyl carrier proteins, dehydratases and ketotransferases, respectively, that synthesize bacterial type II polyketide secondary metabolites (Penfold et al. 1996), while Cfa4 was predicted to function as a cyclase and Cfa5 as a CoA ligase (Rangaswamy et al. 1998). CPC was then proposed to serve as a novel starter unit for synthesis of CFA by the large, multi-domain, type I polyketide synthase enzymes Cfa6 and Cfa7. It was postulated that CPE may be synthesized by Cfa6 through extension of CPC by an ethyl malonate unit followed by

complete reduction of the β -keto ester, and this was supported by the presence of trace amounts of CPE in *P. syringae* pv *glycinea* cultures (Mitchell et al. 1995). Finally, completion of CFA biosynthesis was proposed to occur from the transfer of CPE to Cfa7 followed by extension with a malonate unit, intramolecular cyclization, and reduction and dehydration of the β -keto ester (Fig. 2.7-A; Rangaswamy et al. 1998).

The requirement of both Oxr and Sdr for CFA-Ile production in *S. scabies* suggests that the biosynthesis of the coronafacoyl phytotoxins involves a novel pathway in this organism as compared to *P. syringae*. The hypothetical biosynthetic pathway proposed by Rangaswamy and colleagues suggests that in *P. syringae*, the ketone group on the cyclopentanone ring originates from the α -ketoglutarate precursor and is thus incorporated early in pathway. In contrast, we propose that in *S. scabies*, it is the Sdr enzyme that is responsible for introducing the ketone group through reduction of a hydroxyl group on the cyclopentane ring following polyketide biosynthesis (Fig. 2.7-B). In turn, the hydroxyl group could conceivably be introduced onto the cyclopentane ring by a predicted P450 monooxygenase enzyme that is encoded by the *SCAB79691* gene located within the *S. scabies* *cfa*-like gene cluster (Bignell et al. 2010). Mutational analysis has confirmed that this gene is also required for production of the coronafacoyl phytotoxins in *S. scabies* (Li 2015). The role of Oxr in phytotoxin biosynthesis is currently unclear given that the Δ *oxr* mutant did not accumulate any detectable biosynthetic intermediates in the culture supernatants. However, as Oxr is predicted to be an F₄₂₀-dependent oxidoreductase, we speculate that it could be responsible for introducing the carbon-carbon double bond that is present within the cyclohexene ring of CFA (Fig. 3.1-7B). In *P. syringae*, this double bond

is formed as a result of the incomplete reduction of the β -keto ester by Cfa7 due to the absence of an enoyl reductase domain in the polyketide synthase (Rangaswamy et al. 1998). Interestingly, it was previously reported that the *S. scabiei* Cfa7 polyketide synthase does contain an enoyl reductase (ER) domain that is predicted to be active and would allow for the complete reduction of the β -keto ester (Bignell et al. 2010). Although we cannot rule out the possibility that the Cfa7 ER domain is skipped over during polyketide biosynthesis, it is conceivable that the polyketide product released from Cfa7 may be missing the carbon-carbon double bond and that this double bond is later re-introduced by Oxr. It is noteworthy that although BLASTP analysis did reveal the presence of weakly similar homologues of Sdr encoded in the *P. syringae* pv *tomato* DC3000 genome (top hit showing 36% identity and 52% similarity to Sdr), there are no close homologues of either Oxr or SCAB79691, providing further evidence that the biosynthetic pathway for producing coronafacoyl phytotoxins is different in *S. scabiei* and *P. syringae*.

Plant pathogenic bacteria that are known or predicted to produce coronafacoyl phytotoxins span multiple genera and are collectively responsible for causing significant diseases of flax, ryegrass, soybean, crucifers, cherry, plum, leeks, tomato and potato (Bell et al. 2004; Fyans et al. 2015; Geng et al. 2014; Tamura et al. 1992). Studies of COR, the best characterized coronafacoyl phytotoxin, have shown that it stimulates jasmonic acid (JA) signaling pathways in higher plants by functioning as a molecular mimic of jasmonyl-L-isoleucine (JA-Ile), the most bioactive form of JA, and interacting directly with the JA-Ile co-receptor COI1-JAZ (Geng et al. 2014). This, in turn, leads to suppression of salicylic acid (SA)-mediated plant defence responses as a result of antagonistic crosstalk between

the JA and SA signaling pathways. Recently, it was demonstrated that COR can also disrupt cell wall-associated pathogen defense in a manner independent of its interaction with the COI1-JAZ co-receptor, suggesting that COR may have multiple targets within the plant cell (Geng et al. 2012). Thus, the production of COR and other coronafacoyl phytotoxins may represent a general strategy for allowing plant pathogenic bacteria to overcome plant defense responses in order to promote infection and colonization of the plant host. Here, we have presented evidence suggesting that the production of coronafacoyl phytotoxins involves different biosynthetic pathways in different organisms. Future work will focus on further elucidating the biosynthetic pathway in *S. scabies* as well as exploring the evolution of coronafacoyl phytotoxin biosynthesis in plant pathogenic bacteria.

2.5 Experimental Procedures

2.5.1 Bacterial strains, growth conditions and maintenance

Escherichia coli strains used in this study are listed in Table 2.1. Strains were routinely grown at 37°C unless otherwise indicated. Liquid cultures were grown with shaking (200 rpm) in Difco™ LB Lennox broth (BD Biosciences), low salt LB broth (1% w/v tryptone; 0.5% w/v yeast extract; 0.25% w/v NaCl), SOB (Sambrook and Russell 2001) or SOC (New England Biolabs Canada), while solid cultures were grown on LB (Lennox or low salt) medium containing 1.5% w/v agar (BD Biosciences). When necessary, the solid or liquid growth medium was supplemented with the following antibiotics at the indicated final concentrations: ampicillin (100 µg ml⁻¹; Sigma Aldrich Canada), kanamycin (50 µg

ml⁻¹; Millipore Canada Ltd.), hygromycin B (100 µg ml⁻¹; Millipore Canada Ltd.), chloramphenicol (25 µg ml⁻¹; MP Biomedicals North America). For hygromycin B selection, low salt LB medium was utilized at all times. All strains were maintained at -80°C as frozen stocks in 20% v/v glycerol (Sambrook and Russell 2001).

Streptomyces scabies strains used in this study are listed in Table 2.1. Strains were routinely grown at 28°C with shaking (200 rpm) in trypticase soy broth (TSB; BD Biosciences) or soy flour mannitol broth (SFMB; Kieser et al. 2000) liquid media, or on the International *Streptomyces* Project Medium 4 (ISP-4; BD Biosciences), oat bran agar (OBA; Johnson et al. 2007), soy flour mannitol agar (SFMA; Kieser et al. 2000), or Difco nutrient agar (NA; BD Biosciences) solid media. When necessary, the growth medium was supplemented with the following antibiotics at the indicated final concentrations: hygromycin B (50 µg ml⁻¹), apramycin (50 µg ml⁻¹; Sigma Aldrich Canada), nalidixic acid (50 µg ml⁻¹; Fisher Scientific), kanamycin (50 µg ml⁻¹), thiostrepton (25 µg ml⁻¹; Sigma Life Science). Strains were maintained at - 80°C as spore suspensions in 20% v/v glycerol (Kieser et al. 2000) or as mycelial suspensions in TSB containing 5% v/v DMSO (Butler et al. 2001).

2.5.2 Plasmids, cosmids, primers and DNA manipulations

Plasmids and cosmids used in this study are listed in Table 2.1. Standard procedures were used for all manipulations of plasmid or cosmid DNA (Sambrook and Russell 2001). Sequencing of DNA was performed by The Centre for Applied Genomics (Toronto, Canada). Polymerase chain reactions (PCR) were routinely performed using the Finnzymes Phusion DNA polymerase (New England Biolabs Canada) or the Fermentas

Taq DNA polymerase (Fisher Scientific Canada) according to the manufacturer's instructions, except that DMSO (5% v/v final concentration) was included in the reaction mixtures. When necessary, PCR products were cloned into the pGEM®-T Easy vector according to the manufacturer's instructions. Oligonucleotide primers used for PCR and for DNA sequencing are listed in Table S-2.2. Chromosomal DNA was extracted from TSB cultures of *S. scabiei* strains using the One-Tube Bacterial Genomic DNA Kit (Bio Basic Inc.) according to the manufacturer's instructions.

2.5.3 Construction of the *S. scabiei* Δoxr and Δsdr gene deletion mutants

The *oxr* and *sdr* coding sequences were deleted from the chromosome of *S. scabiei* $\Delta txtA/pRLDB51-1$ using the Redirect PCR targeting system (Gust et al. 2003a,b). A [*hyg+oriT*] cassette was PCR-amplified from pIJ10700 using the primers DRB653 and DRB654 (for *oxr*) and DRB655 and DRB656 (for *sdr*). The resulting products were gel purified and then introduced by electroporation into the arabinose-induced *E. coli* BW25113 strain containing pIJ790 and Cosmid 1770, which harbours the coronafacoyl phytotoxin biosynthetic gene cluster (Table 3.1-1). Mutant cosmids in which the *oxr* or *sdr* gene was replaced with the [*hyg+oriT*] cassette, were subsequently isolated and verified by PCR. A single clone of the *oxr* mutant cosmid (1770/ Δoxr) and of the *sdr* mutant cosmid (1770/ Δsdr) was then introduced into *E. coli* ET12567/pUZ8002 prior to transfer into *S. scabiei* $\Delta txtA/pRLDB51-1$ by intergeneric conjugation (Kieser et al. 2000). Exconjugants displaying resistance to hygromycin B were subsequently screened for kanamycin sensitivity to confirm that a double crossover event had taken place. Verification of each gene deletion in the hygromycin B resistant exconjugants was by PCR,

after which spore and mycelial stocks of the mutant isolates were prepared and were stored at -80°C.

2.5.4 Complementation of the Δoxr and Δsdr deletion mutants

Complementation plasmids harbouring the *oxr* or *sdr* genes were constructed by PCR-amplifying each coding sequence from Cosmid 1770 and then cloning the resulting products into pGEM®-T Easy. The cloned inserts were sequenced to confirm that no mutations were present, after which they were released by digestion with NdeI and XhoI and then ligated into similarly digested pMSAK13. The resulting pMSAK13/*oxr* and pMSAK13/*sdr* plasmids were transformed into *E. coli* ET12567/pUZ8002 and then conjugated into the corresponding *S. scabiei* gene deletion mutant (Kieser et al. 2000). As a control, the pMSAK13 plasmid without any cloned insert was also introduced into each of the *S. scabiei* mutants.

2.5.5 Analysis of *N*-coronafacoyl phytotoxin production

S. scabiei strains were cultured in duplicate or triplicate in 5 ml of SFMB for 7 days at 25°C, after which the culture supernatants were extracted with chloroform and were analyzed for coronafacoyl phytotoxin production by RP-HPLC as described previously (Fyans et al. 2015). LC-LRESIMS analysis of *S. scabiei* culture extracts was performed at the Centre for Chemical Analysis, Research and Training (C-CART, Department of Chemistry, Memorial University) using an Agilent 1100 series HPLC system (Agilent Technologies Inc.) interfaced to a Waters G1946A single quadrupole mass spectrometer (Waters Corporation). Separation was achieved using an Agilent Technologies ZORBAX SB-C18 column (4.6 × 150 mm, 5 µm particle size) held at a constant temperature of 40°C.

The solvent system consisted of 100% H₂O as mobile phase A and 100% acetonitrile as mobile phase B, both containing 0.1% v/v formic acid. The initial solvent conditions consisted of 30% B and were held for 4.5 min, after which a linear gradient of 30% B to 50% B over 12 min was applied at a constant flow rate of 1 ml min⁻¹. The system was held at 50% B for 3 min and was then returned to the initial conditions in 4.5 min. Metabolites were monitored by UV absorbance at 230 nm and by electrospray ionization MS in negative ion mode.

2.5.6 *Potato tuber slice bioassay*

An *in vitro* potato tuber slice bioassay was performed using *S. scabies* organic culture extracts (25 µl) or purified *S. scabies* metabolites (CFA-Ile, Δ sdr metabolite 1, Δ sdr metabolite 2; 100 nmol) as described previously (Fyans et al. 2015). Where indicated, pure COR (8 nmol; Sigma Aldrich Canada) was included as a positive control.

2.5.7 *Purification of N-coronafacoyl compounds*

S. scabies strains were grown by inoculating 25 ml of TSB medium with 1 ml of a DMSO mycelial stock and then incubating at 28°C for 48hr with shaking. Once dense growth was obtained, 10 ml of the seed culture was transferred into 4L flasks containing 1L of SFMB medium, and the flasks were incubated at 25°C for 10 days with shaking. Supernatants were obtained following centrifugation of the cultures and were stored at -20°C until needed. Carboxylic acid residues were isolated from the supernatants as previously described (Mitchell and Frey 1986) with some modifications. Briefly, the culture supernatants were adjusted to pH 11-12 and extracted 3× with 0.5 volumes of chloroform (Sigma Aldrich Canada). The organic extracts were discarded and the aqueous

portion was adjusted to pH 1-2 and extracted 3× with 0.5 volumes of chloroform. The resulting organic extracts were dried with anhydrous Na₂SO₄ (Fisher Scientific Canada) and then combined and concentrated to 100 ml, after which the extract was shaken 3× with 0.5 volumes of 0.5 M KHCO₃ (Sigma Aldrich Canada). The KHCO₃ extracts were combined, washed 2× with 0.5 volumes of chloroform, then adjusted to pH 1-2 and extracted 3× with 0.5 volumes of chloroform. Finally, the combined chloroform extracts were evaporated to dryness, and the resulting material was re-dissolved in 100% HPLC-grade methanol containing 0.1% v/v formic acid (Sigma Aldrich Canada) and was filtered using a 0.2 µm syringe filter (VWR International). The *N*-coronafacoyl compounds were purified from the crude carboxylic acid preparation by preparative TLC and semi-preparative HPLC as described previously (Fyans et al. 2015), and each purified compound was re-dissolved in 100% HPLC-grade methanol containing 0.1% v/v formic acid.

2.5.8 Structural elucidation of *N*-coronafacoyl compounds from *S. scabies*

HRESIMS and HRESIMS/MS analysis of the purified biosynthetic intermediates was performed at the McMaster Regional Centre for Mass Spectrometry (McMaster University, Hamilton, ON). Spectra were acquired on a Micromass Q-TOF Ultima Global mass spectrometer in positive ion mode. Structural determination of CFA-Ile and of the intermediates was by 1-dimensional (¹H and ¹³C) and 2-dimensional (COSY, HSQC, HMBC and NOESY) NMR. Spectral assignments and structural identification was carried out using a Bruker AVANCE II 600 spectrometer (Bruker BioSpin GmbH, Rheinstetten, Germany) operating at 600.33 MHz for proton and 150.96 MHz for carbon and equipped with a 5-mm inverse triple-resonance probe (TXI). The samples were dissolved in CD₃OD

with 0.1% v/v TFA-d. Chemical shifts were referenced to trimethylsilane for both ^1H and ^{13}C .

2.5.9 Bioinformatics analyses

DNA sequences and gene annotations were visualized using Geneious Pro software version 6.1.2 (Biomatters Ltd.). Protein similarity searches were conducted using the National Center for Biotechnology Information (NCBI) Basic Local Alignment Search Tool for proteins (BLASTP) (<http://blast.ncbi.nlm.nih.gov/Blast.cgi>). The Pfam program (<http://pfam.sanger.ac.uk/>) was used to detect the presence of functional domains within *S. scabiei* Cfl, Oxr and Sdr protein sequences (Finn et al. 2014). Amino acid sequence alignments were generated using ClustalW within the Geneious version 6.1.2 software. The accession numbers for the protein sequences used in the alignments are listed in Table S-2.1. Phylogenetic trees were constructed using the maximum likelihood method in the MEGA 5.2.1 program (Tamura et al. 2011). The significance of the branch order in each tree was tested using the bootstrapping method with 1000 repetitions.

2.6 Acknowledgements

The authors would like to thank Dr. Celine Schneider (Memorial University Centre for Chemical Analysis, Research and Training) for assistance with the NMR structural analyses, and the anonymous reviewers for their helpful comments and suggestions. This work was supported by a Natural Sciences and Engineering Research Council of Canada Discovery Grant No. 386696-2010 to D. R. D. Bignell. M. Altowairish was supported by

a King Abdullah Scholarship, and J. Fyans was supported by a Government of Canada Postdoctoral Research Fellowship.

2.7 References

- Aufhammer S.W., Warkentin E., Berk H., Shima S., Thauer R.K., Ermiler U. (2004). Coenzyme binding in F₄₂₀-dependent secondary alcohol dehydrogenase, a member of the bacterial luciferase family. *Structure*, 12: 361-370.
- Bashiri G., Squire C.J., Moreland N.J., Baker E.N. (2008). Crystal structures of F₄₂₀-dependent glucose-6-phosphate dehydrogenase FGD1 involved in the activation of the anti-tuberculosis drug candidate PA-824 reveal the basis of coenzyme and substrate binding. *J Biol Chem*, 283: 17531-17541.
- Bell K.S., Sebaihia M., Pritchard L., Holden M.T., Hyman L.J., Holeva M.C., *et al.* (2004). Genome sequence of the enterobacterial phytopathogen *Erwinia carotovora* subsp. *atroseptica* and characterization of virulence factors. *Proc Natl Acad Sci USA*, 101: 11105-11110.
- Bender C.L., Malvick D.K., Mitchell R.E. (1989). Plasmid-mediated production of the phytotoxin coronatine in *Pseudomonas syringae* pv. *tomato*. *J Bacteriol*, 171(2): 807-812.
- Bender C., Rangaswamy V., Loper J. (1999a). Polyketide production by plant-associated pseudomonads. *Annu Rev Phytopathol*, 37: 175-196.

- Bender C.L., Alarcon-Chaidez F., Gross D.C. (1999b). *Pseudomonas syringae* phytotoxins: mode of action, regulation, and biosynthesis by peptide and polyketide synthetases. *Microbiol Mol Biol Rev*, 63: 266-292.
- Bérdy J. (2005). Bioactive microbial metabolites. *J Antibiot (Tokyo)*, 58: 1-26.
- Bignell D.R., Fyans J.K., Cheng Z. (2014). Phytotoxins produced by plant pathogenic *Streptomyces* species. *J Appl Microbiol*, 116: 223-235.
- Bignell D.R., Seipke R.F., Huguet-Tapia J.C., Chambers A.H., Parry R., Loria R. (2010). *Streptomyces scabies* 87-22 contains a coronafacic acid-like biosynthetic cluster that contributes to plant-microbe interactions. *Mol Plant Microbe Interact*, 23: 161-175.
- Butler A.R., Flint S.A., Cundliffe E. (2001). Feedback control of polyketide metabolism during tylosin production. *Microbiology*, 147: 795-801.
- Cheng Z., Bown L., Tahlan K., Bignell D.R. (2015). Regulation of coronafacoyl phytotoxin production by the PAS-LuxR family regulator CfaR in the common scab pathogen *Streptomyces scabies*. *PLoS one*, 10: e0122450.
- Dees M.W., Wanner L.A. (2012). In search of better management of potato common scab. *Potato Res*, 55: 249-268.
- Finn R.D., Bateman A., Clements J., Coghill P., Eberhardt R.Y., Eddy S.R., *et al.* (2014). Pfam: the protein families database. *Nucleic Acids Res*, 42: D222-230.
- Fyans J.K., Altowairish M.S., Li Y., Bignell D.R. (2015). Characterization of the coronatine-like phytotoxins produced by the common scab pathogen *Streptomyces scabies*. *Mol Plant Microbe Interact*, 28: 443-454.

- Geng X., Cheng J., Gangadharan A., Mackey D. (2012). The coronatine toxin of *Pseudomonas syringae* is a multifunctional suppressor of Arabidopsis defense. *Plant Cell*, 24: 4763-4774.
- Geng X., Jin L., Shimada M., Kim M.G., Mackey D. (2014). The phytotoxin coronatine is a multifunctional component of the virulence armament of *Pseudomonas syringae*. *Planta*, 240: 1149-1165.
- Gust B., Challis G.L., Fowler K., Kieser T., Chater K.F. (2003a). PCR-targeted *Streptomyces* gene replacement identifies a protein domain needed for biosynthesis of the sesquiterpene soil odor geosmin. *Proc Natl Acad Sci USA*, 100: 1541-1546.
- Gust B., O'Rourke S., Bird N., Kieser T., Chater K.F. (2003b). *Recombineering in Streptomyces coelicolor*. The John Innes Foundation, Norwich, UK.
- Healy F.G., Wach M., Krasnoff S.B., Gibson D.M., Loria R. (2000). The *txtAB* genes of the plant pathogen *Streptomyces acidiscabies* encode a peptide synthetase required for phytotoxin thaxtomin A production and pathogenicity. *Mol Microbiol*, 38: 794-804.
- Johnson E.G., Krasnoff S.B., Bignell D.R., Chung W.C., Tao T., Parry R.J., *et al.* (2009). 4-Nitrotryptophan is a substrate for the non-ribosomal peptide synthetase TxtB in the thaxtomin A biosynthetic pathway. *Mol Microbiol*, 73: 409-418.
- Kavanagh K.L., Jornvall H., Persson B., Oppermann U. (2008). Medium- and short-chain dehydrogenase/reductase gene and protein families: the SDR superfamily: functional and structural diversity within a family of metabolic and regulatory enzymes. *Cell Mol Life Sci*, 65: 3895-3906.

- Kieser T., Bibb M.J., Buttner M.J., Chater K.F., Hopwood D.A. (2000). *Practical Streptomyces Genetics*. The John Innes Foundation, Norwich, UK.
- King R.R., Calhoun L.A. (2009). The thaxtomin phytotoxins: sources, synthesis, biosynthesis, biotransformation and biological activity. *Phytochemistry*, 70: 833-841.
- Li W., Chou S., Khullar A., Gerratana B. (2009). Cloning and characterization of the biosynthetic gene cluster for tomaymycin, an SJG-136 monomeric analog. *Appl Environ Microbiol*, 75: 2958-2963.
- Li Y. (2015). Biosynthesis and functional analysis of the COR-like metabolites produced by the common scab pathogen *Streptomyces scabies*. M.Sc. Thesis, Memorial University of Newfoundland, St. John's, NL.
- Liyanage H., Palmer D.A., Ullrich M., Bender C.L. (1995). Characterization and transcriptional analysis of the gene cluster for coronafacic acid, the polyketide component of the phytotoxin coronatine. *Appl Environ Microbiol*, 61: 3843-3848.
- Loria R., Bignell D.R., Moll S., Huguet-Tapia J.C., Joshi M.V., Johnson E.G., *et al.* (2008). Thaxtomin biosynthesis: the path to plant pathogenicity in the genus *Streptomyces*. *Antonie Van Leeuwenhoek*, 94: 3-10.
- Loria R., Kers J., Joshi M. (2006). Evolution of plant pathogenicity in *Streptomyces*. *Annu Rev Phytopathol*, 44: 469-487.
- MacNeil D.J., Gewain K.M., Ruby C.L., Dezeny G., Gibbons P.H., MacNeil T. (1992). Analysis of *Streptomyces avermitilis* genes required for avermectin biosynthesis utilizing a novel integrative vector. *Gene*, 111: 61-68.

- Mitchell R., Young H., Liddell M. (1995). Isolation and structural characterization of 2-[1-oxo-2-cyclopenten-2-ylmethyl]-butanoic acid, a polyketide product of coronatine-producing *Pseudomonas* spp. *Tetrahedron Lett*, 36: 3237-3240.
- Mitchell R.E. (1984). A naturally-occurring structural analogue of the phytotoxin coronatine. *Phytochemistry*, 23: 791-793.
- Mitchell R.E., Frey E.J. (1986). Production of *N*-coronafacoyl-L-amino acid analogues of coronatine by *Pseudomonas syringae* pv. *atropurpurea* in liquid cultures supplemented with L-amino acids. *J Gen Microbiol*, 132: 1503-1507.
- Mitchell R.E., Young H. (1985). *N*-Coronafacoyl-L-isoleucine and *N*-coronafacoyl-L-alloisoleucine, potential biosynthetic intermediates of the phytotoxin coronatine. *Phytochemistry*, 24: 2716-2717.
- Nakano T., Miyake K., Endo H., Dairi T., Mizukami T., Katsumata R. (2004). Identification and cloning of the gene involved in the final step of chlortetracycline biosynthesis in *Streptomyces aureofaciens*. *Biosci Biotechnol Biochem*, 68: 1345-1352.
- O'Brien J., Wright G.D. (2011). An ecological perspective of microbial secondary metabolism. *Curr Opin Biotechnol*, 22: 552-558.
- Parry R.J., Mhaskar S.V., Lin M.-T., Walker A.E., Mafoti R. (1994). Investigations of the biosynthesis of the phytotoxin coronatine. *Can J Chem*, 72: 86-99.
- Penfold C.N., Bender C.L., Turner J.G. (1996). Characterisation of genes involved in biosynthesis of coronafacic acid, the polyketide component of the phytotoxin coronatine. *Gene*, 183: 167-173.

- Rangaswamy V., Jiralerspong S., Parry R., Bender C.L. (1998). Biosynthesis of the *Pseudomonas* polyketide coronafacic acid requires monofunctional and multifunctional polyketide synthase proteins. *Proc Natl Acad Sci USA*, 95: 15469-15474.
- Rangaswamy V., Ullrich M., Jones W., Mitchell R., Parry R., Reynolds P., *et al.* (1997). Expression and analysis of coronafacate ligase, a thermoregulated gene required for production of the phytotoxin coronatine in *Pseudomonas syringae*. *FEMS Microbiol Lett*, 154: 65-72.
- Sambrook J., Russell D.W. (2001). *Molecular cloning: a laboratory manual*. Cold Spring Harbor Laboratory Press, Cold Spring Harbor, NY.
- Seipke R.F., Kaltenpoth M., Hutchings M.I. (2012). *Streptomyces* as symbionts: an emerging and widespread theme? *FEMS Microbiol Rev*, 36: 862-876.
- Shiraishi K., Konoma K., Sato H., Ichihara A., Sakamura S., Nishiyama K., *et al.* (1979). The structure-activity relationships in coronatine analogs and amino compounds derived from (+)-coronafacic acid. *Agric Biol Chem*, 43: 1753-1757.
- Tamura K., Peterson D., Peterson N., Stecher G., Nei M., Kumar S. (2011). MEGA5: molecular evolutionary genetics analysis using maximum likelihood, evolutionary distance, and maximum parsimony methods. *Mol Biol Evol*, 28: 2731-2739.
- Tamura K., Takikawa Y., Tsuyumu S., Goto M., Watanabe M. (1992). Coronatine production by *Xanthomonas campestris* pv. *phormiicola*. *Ann Phytopath Soc Japan*, 58: 276-281.
- Taylor M., Scott C., Grogan G. (2013). F₄₂₀-dependent enzymes - potential for applications in biotechnology. *Trends Biotechnol*, 31: 63-64.

- Thaxter R. (1891). The potato scab. *Conn Agric Expt Sta Rept*, 1890: 81-95.
- Wandersman C., Delepelaire P. (2004). Bacterial iron sources: from siderophores to hemophores. *Annu Rev Microbiol*, 58: 611-647.
- Wang P., Bashiri G., Gao X., Sawaya M.R., Tang Y. (2013). Uncovering the enzymes that catalyze the final steps in oxytetracycline biosynthesis. *J Am Chem Soc*, 135: 7138–7141.
- Wietz M., Duncan K., Patin N.V., Jensen P.R. (2013). Antagonistic interactions mediated by marine bacteria: the role of small molecules. *J Chem Ecol*, 39: 879-891.
- Xin X.F., He S.Y. (2013). *Pseudomonas syringae* pv. *tomato* DC3000: a model pathogen for probing disease susceptibility and hormone signaling in plants. *Annu Rev Phytopathol*, 51: 473-498.

2.8 Figures and Tables

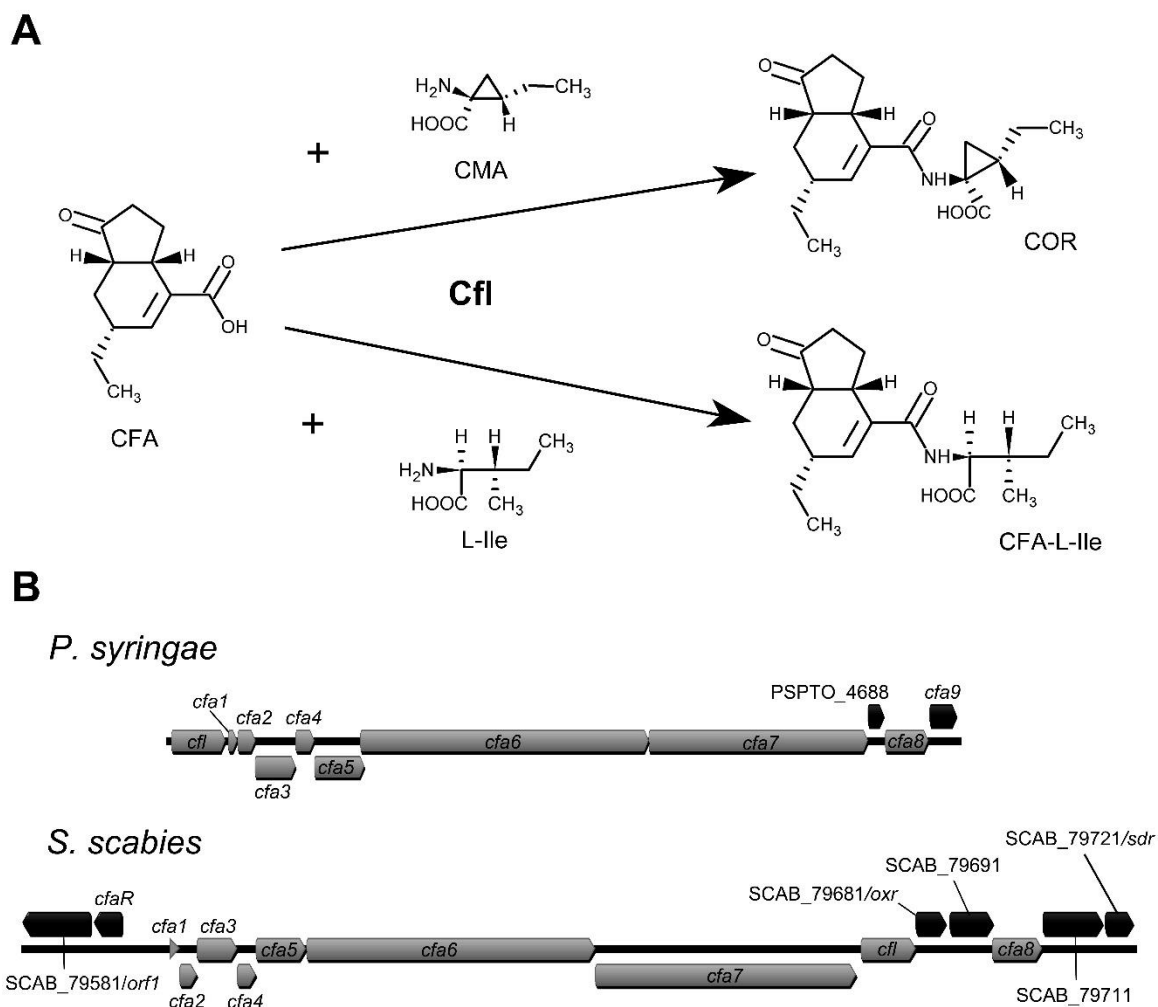


Figure 2.1. (A) Biosynthesis of coronafacoyl phytotoxins in *Pseudomonas syringae* and *Streptomyces scabies*. Coronafacic acid (CFA) is linked to coronamic acid (CMA) or L-isoleucine (L-Ile) to produce coronatine (COR) in *P. syringae* or coronafacoyl-L-isoleucine (CFA-Ile) in *S. scabies*. The linkage reaction is catalyzed by the coronafacate ligase (Cfl) enzyme encoded within the *cfa* or *cfa*-like biosynthetic gene cluster in each organism. Note that *P. syringae* can also produce CFA-Ile in minor amounts. (B)

Organization of the *cfa* biosynthetic gene cluster in *P. syringae* pv *tomato* DC3000 and the *cfa*-like biosynthetic gene cluster in *S. scabies* 87-22. Genes that are conserved in both clusters are indicated by the gray arrows whereas genes that are unique to each cluster are indicated by the black arrows.

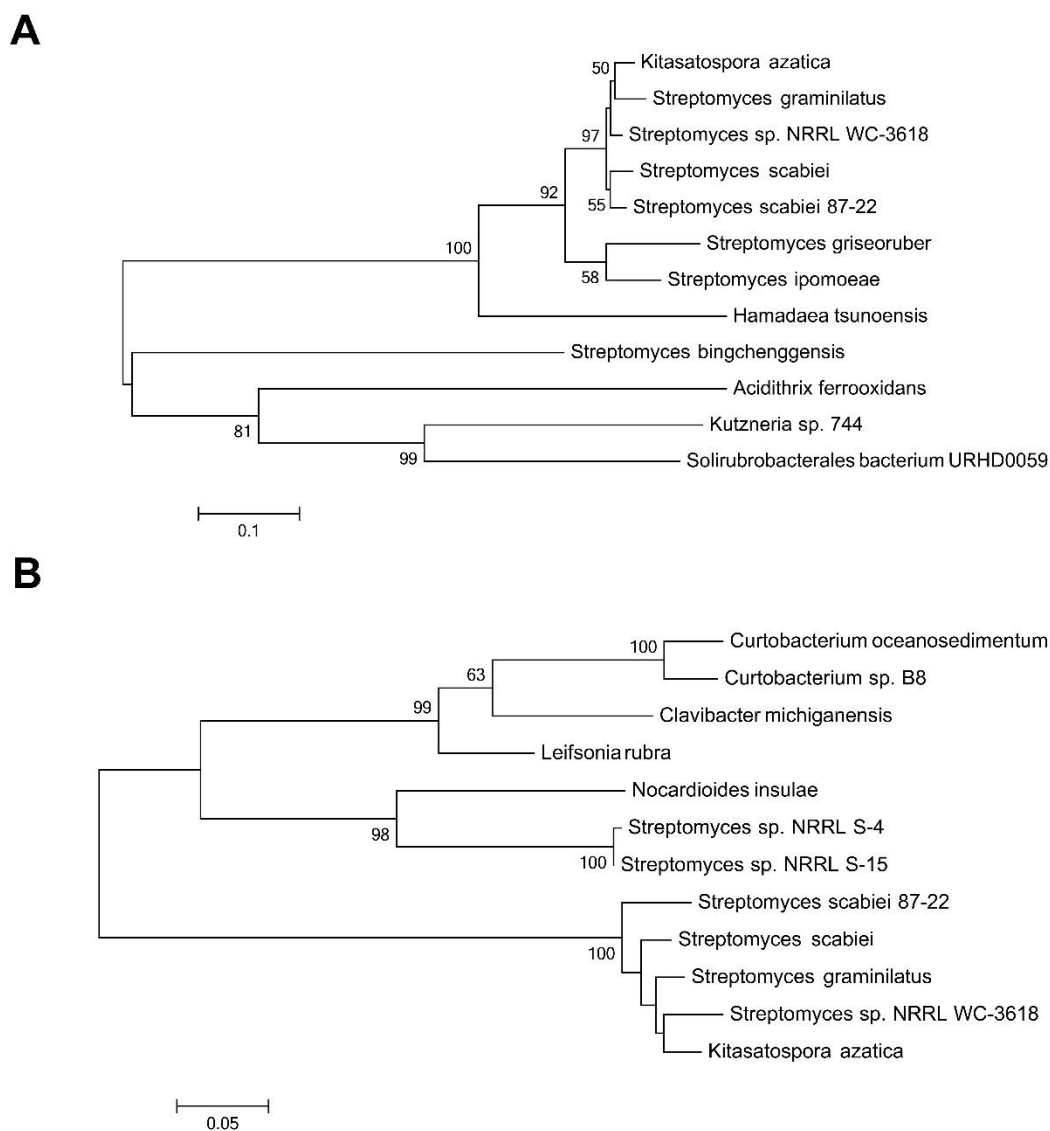


Figure 2.2. Phylogenetic relationships among homologues of Oxr (A) and Sdr (B) from the database. Bootstrap values are shown for the branch points supported $\geq 50\%$ out of 1000 repetitions. The scale bar indicates the number of amino acid substitutions per site. Accession numbers for the sequences used are listed in Table S-2.1.

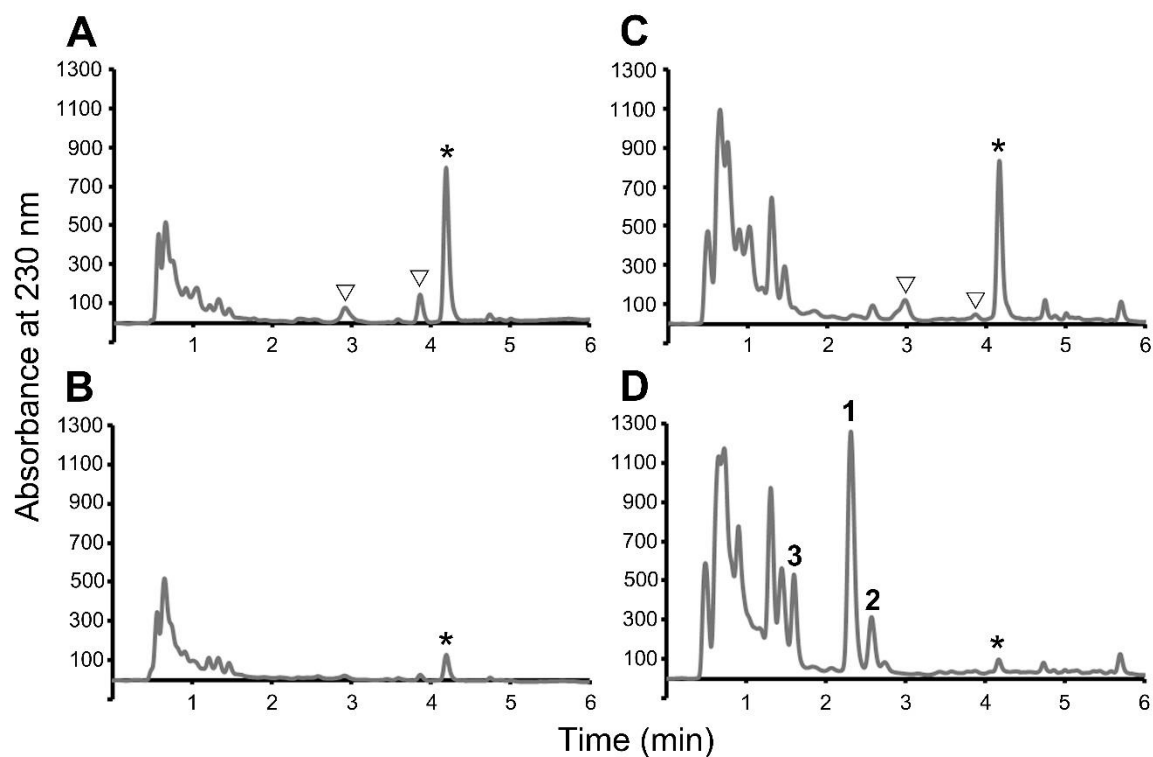


Figure 2.3. RP-HPLC analysis of coronafacoyl phytotoxin production by *Streptomyces scabies* strain $\Delta txtA$ /pRLDB51-1 (A, C), Δoxr (isolate 3) (B) and Δsdr (isolate 1) (D). The CFA-Ile peak is indicated with (*), and the minor coronafacoyl phytotoxins produced by strain $\Delta txtA$ /pRLDB51-1 are indicated with (∇). The peaks corresponding to the accumulated metabolites in the Δsdr mutant are numbered 1 ($t_R = 2.3$ min), 2 ($t_R = 2.6$ min) and 3 ($t_R = 1.6$ min).

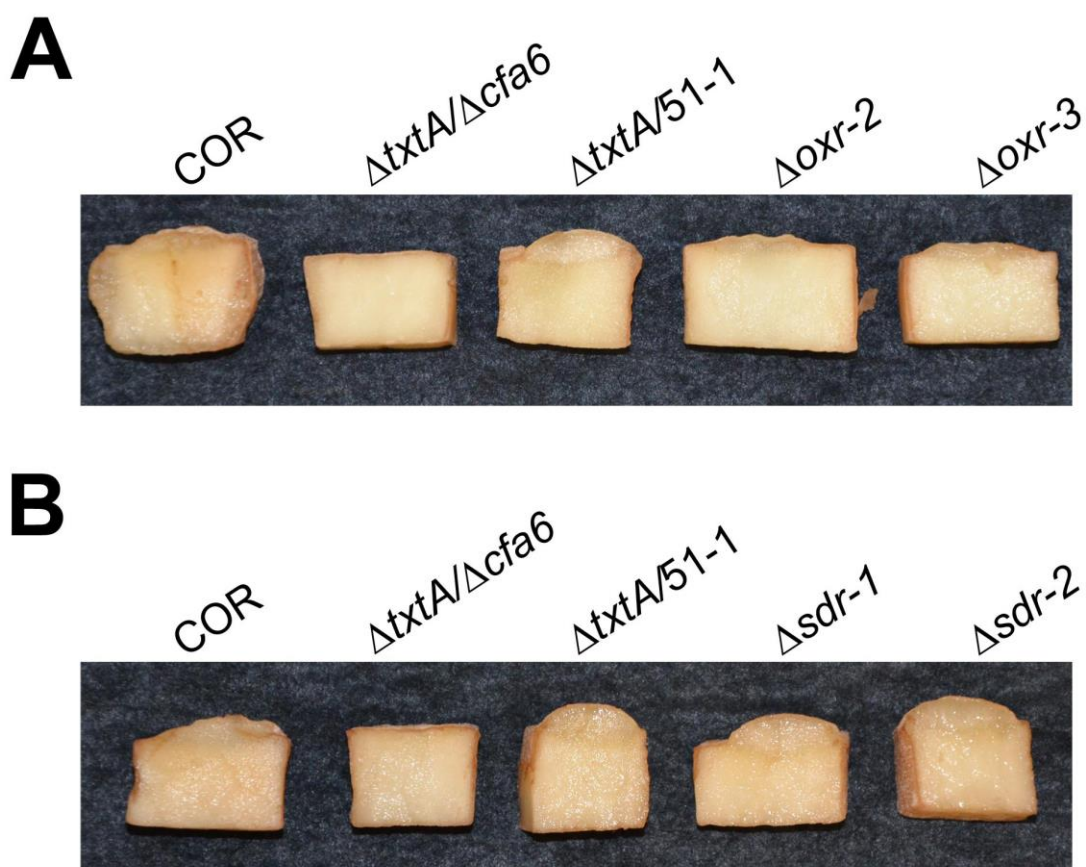


Figure 2.4. Hypertrophy-inducing activity of organic culture extracts from *Streptomyces scabies* Δoxr (isolates 2 and 3) (A) and Δsdr (isolates 1 and 2) (B) on potato tuber tissue. Pure, authentic COR (8 nmol) and extract from the $\Delta txtA/pRLDB51-1$ strain served as positive controls, whereas extract from a coronafacoyl phytotoxin non-producing strain ($\Delta txtA/\Delta cfa6$) served as a negative control.

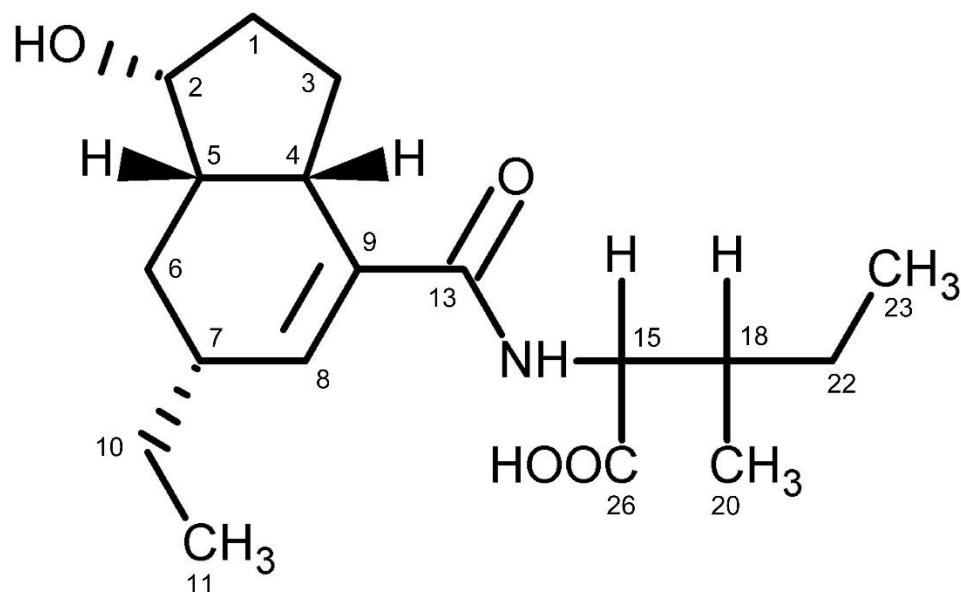


Figure 2.5. Structure of the metabolites 1 and 2 that accumulated in *Δsdr* culture supernatants. The two metabolites share the same coronafacoyl polyketide structure and differ in the attached isoleucine isomer. The carbon atoms are numbered according to the numbering scheme used for the raw data analysis (see Fig. S-2.4 and S-2.5).

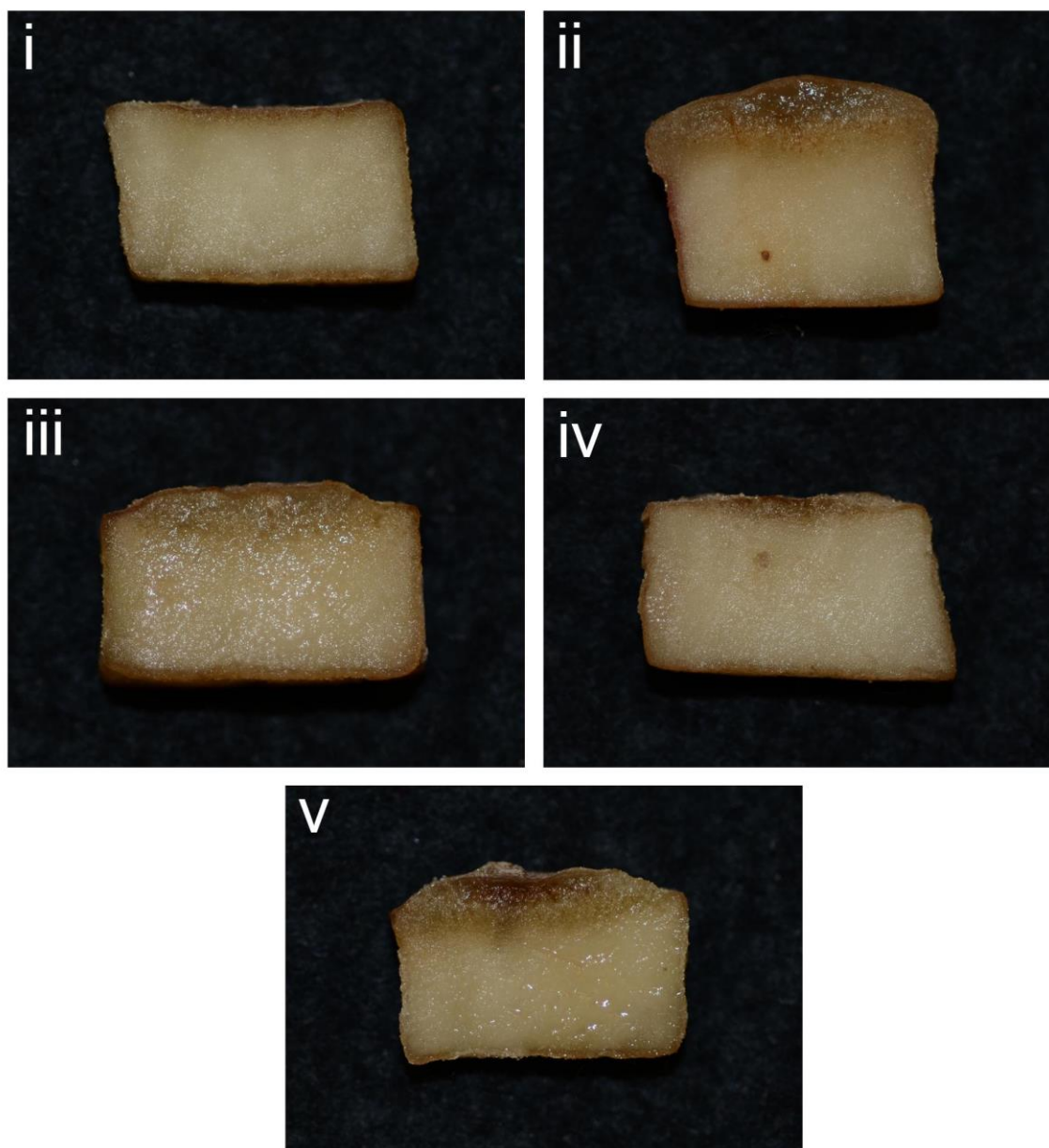


Figure 2.6. Hypertrophy-inducing activity of the purified Δsdr metabolites 1 (iv) and 2 (v) (100 nmol each) on potato tuber tissue. Pure COR (1 nmol) (ii) and CFA-Ile (100 nmol) (iii) served as positive controls while the solvent (MeOH + 0.1% formic acid) (i) served as a negative control.

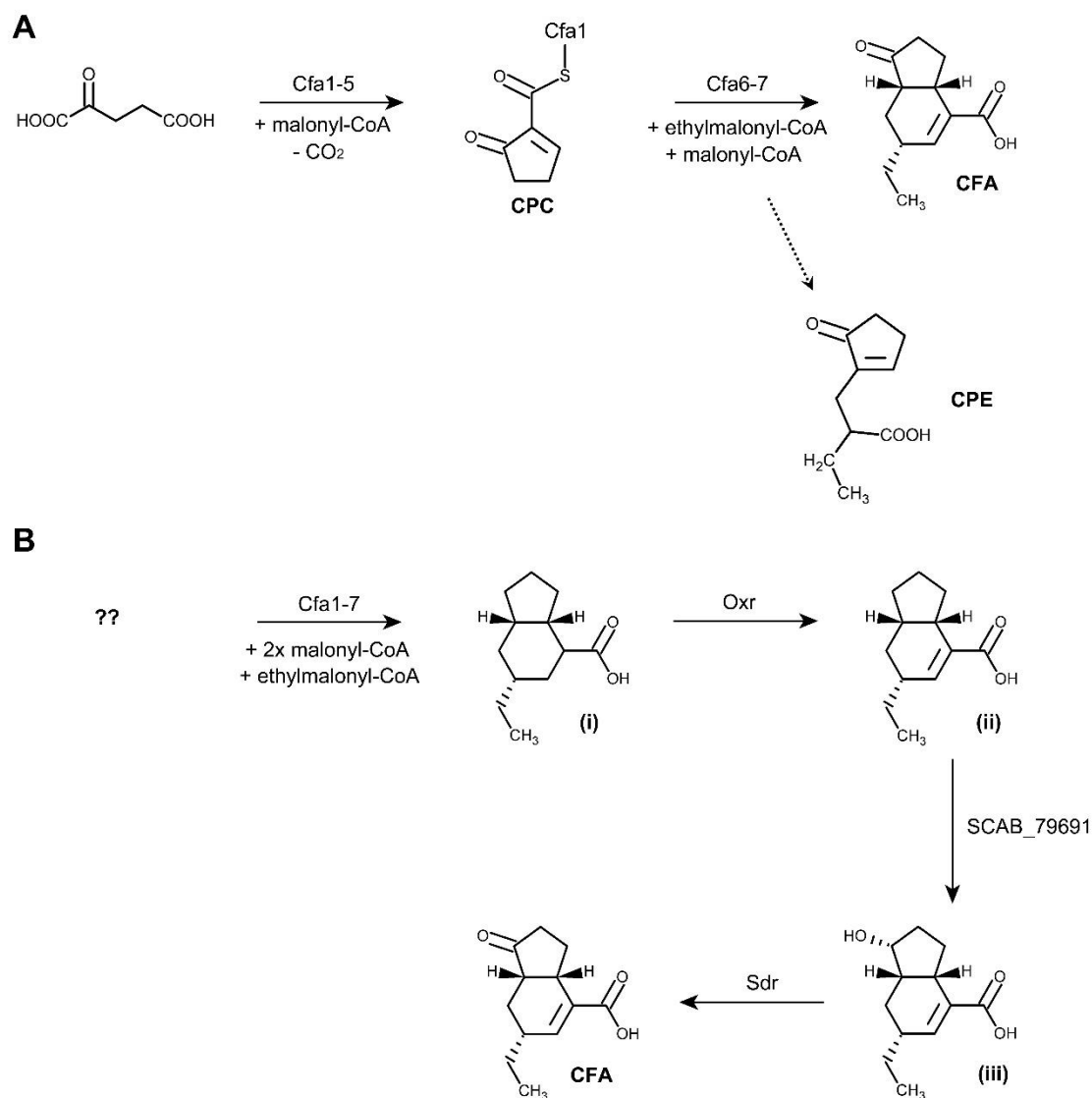


Figure 2.7. Hypothetical pathway for the biosynthesis of CFA in *Pseudomonas syringae* (A) and *Streptomyces scabies* (B). Proposed intermediates in the *P. syringae* pathway include 2-carboxy-2-cyclopentenone (CPC), which is produced by the action of the Cfa1-5 proteins, and 2-[1-oxo-2-cyclopenten-2-ylmethyl]-butanoic acid (CPE), which is produced by the Cfa6 polyketide synthase and has been detected in trace amounts in *P. syringae*

cultures. The proposed intermediates in the *S. scabies* pathway are indicted with (i)-(iii), of which (iii) was detected as an isoleucine conjugant in the Δsdr mutant cultures. It is not known whether or not the *S. scabies* pathway also starts with α -ketoglutarate, and therefore the starting metabolite is indicated with (??).

Table 2.1. Bacterial strains, cosmids and plasmids used in this study.

Strain, Plasmid or Cosmid	Description	Antibiotic Resistance†	Reference or Source
<i>Escherichia coli</i> strains			
DH5α	General cloning host	none	Gibco-BRL
NEB 5-alpha	DH5α derivative; high efficiency competent cells used for transformation	none	New England Biolabs, Canada
BW25113/pIJ790	Host for Redirect PCR targeting system	cam ^r	Gust et al. 2003a,b
ET12567/pUZ8002	Non-methylating host (<i>dam</i> ⁻ <i>dcm</i> ⁻ <i>hsdM</i> ⁻); carries the pUZ8002 plasmid that encodes the machinery for the conjugal transfer of DNA into <i>Streptomyces</i>	cam ^r , tet ^r , kan ^r	MacNeil et al. 1992; Kieser et al. 2000
<i>Streptomyces scabies</i> strains			
Δ <i>txtA</i> /pRLDB51-1	<i>S. scabies</i> strain containing a deletion of the <i>txtA</i> gene and carrying the <i>scab79591</i> overexpression plasmid pRLDB51-1	thio ^r , apra ^r	Bignell et al. 2010
Δ <i>txtA</i> /Δ <i>cfa6</i>	<i>S. scabies</i> strain containing a deletion of the <i>txtA</i> and <i>cfa6</i> genes	apra ^r ; hyg ^r	Bignell et al. 2010
Δ <i>oxr</i>	Δ <i>txtA</i> /pRLDB51-1 derivative containing a deletion of the <i>oxr</i> (<i>scab79681</i>) gene	thio ^r , apra ^r , hyg ^r	This study
Δ <i>sdr</i>	Δ <i>txtA</i> /pRLDB51-1 derivative containing a deletion of the <i>sdr</i> (<i>scab79721</i>) gene	thio ^r , apra ^r , hyg ^r	This study
Plasmid or cosmid			

pIJ10700	Template for PCR amplification of the [<i>hyg+oriT</i>] cassette used for PCR targeting	hyg ^r	Gust et al. 2003b
pMSAK13	Integrates into Φ BT1 <i>attB</i> site in <i>Streptomyces</i> chromosomes; contains the strong, constitutive promoter <i>ermEp</i> * for expression of cloned genes in <i>Streptomyces</i>	hyg ^r , kan ^r	Fyans et al. 2015
pGEM [®] - T Easy	Cloning vector for PCR products	kan ^r	Promega, Canada
pMSAK13/ <i>oxr</i>	pMSAK13 derivative containing the <i>oxr</i> gene cloned into the NdeI and XhoI sites	hyg ^r , kan ^r	This study
pMSAK13/ <i>sdr</i>	pMSAK13 derivative containing the <i>sdr</i> gene cloned into the NdeI and XhoI sites	hyg ^r , kan ^r	This study
Cosmid 1770	SuperCosI derivative containing the <i>S. scabies</i> CFA-like gene cluster	amp ^r , kan ^r	Bignell et al. 2010
1770/ Δ <i>oxr</i>	Cosmid 1770 derivative in which the <i>oxr</i> gene was replaced with the [<i>hyg+oriT</i>] disruption cassette	amp ^r , kan ^r , hyg ^r	This study
1770/ Δ <i>sdr</i>	Cosmid 1770 derivative in which the <i>sdr</i> gene was replaced with the [<i>hyg+oriT</i>] disruption cassette	amp ^r , kan ^r , hyg ^r	This study

† cam^R, tet^R, kan^R, thio^R, apra^R, hyg^R and amp^R = chloramphenicol, tetracycline, kanamycin, thiostrepton, apramycin, hygromycin B and ampicillin resistance, respectively.

Table 2.2. 1-dimensional (^1H , ^{13}C) NMR spectral data (in ppm) for purified CFA-Ile and the Δsdr metabolites 1 and 2 in CD_3OD with 0.1% TFA-d.

	CFA-Ile			1			2		
C No.	$\delta\text{ C}$	C Type	$\delta\text{ H (J, Hz)}$	$\delta\text{ C}$	C Type	$\delta\text{ H (J, Hz)}$	$\delta\text{ C}$	C Type	$\delta\text{ H (J, Hz)}$
1	37.35	CH_2	2.34 m	33.35	CH_2	H', 2.16 m H'', 1.57 q (12.8, 12.1)	32.20	CH_2	H', 2.18 m H'', 1.56 m
2	221.45	C=O	-	76.10	C-OH	3.81 dtd (14.5, 8.9, 6.0)	74.87	C-OH	3.80 q (8.3)
3	27.35	CH_2	H', 2.40 s H'', 1.57 m	27.01	CH_2	H', 2.04 qd (11.5, 7.5) H'', 1.32 qd (11.5, 7.5)	28.17	CH_2	H', 2.00 t (10) H'', 1.43 m
4	35.93	CH	3.19 s	41.63	CH	2.21 dt (12.7, 7)	40.38	CH	2.18 m
5	46.40	CH	2.39 m	48.28	CH	1.44 m	47.10	CH	1.43 m
6	25.72	CH_2	H', 1.81 dt (13.1, 4.9) H'', 1.13 dt (13.0, 10.7)	29.42	CH_2	H', 1.99 d (9.4) H'', 1.44 dp (14.6, 7.3)	25.96	CH_2	H', 2.00 t (10) H'', 1.37 m
7	37.22	CH	2.17 s	39.34	CH	2.32 s	38.10	CH	2.32 m
8	136.51	CH	6.47 s	137.46	CH	6.27 t (3.5)	137.26	CH	6.28 t (3.5)
9	†	-		†	-		†	-	
10	27.69	CH_2	H', 1.54 dt (14.0, 7.3) H'', 1.42 dt	29.16	CH_2	H', 1.57 m H'', 1.38 dd (15.4, 7.6)	27.88	CH_2	H', 1.56 m H'', 1.43 m
11	10.17	CH_3	1.01 m	12.69	CH_3	1.03 t (7.4)	11.35	CH_3	1.03 t (7.4)
13	169.43	C=O	-	170.53	C=O	-	170.42	C=O	-
15	37.23	CH	4.60 s, 4.45 s ‡	56.82	CH	4.57 d (5.4)	56.69	CH	4.39 d (6.2)

18	37.49	CH	2.01 s, 1.94 s ‡	38.16	CH	2.00 tp (14.6, 6.9, 5.4)	36.77	CH	1.95 q (9.7, 6.7)
20	10.41, 13.90 ‡	CH ₃	0.94 d (5.4)	15.04	CH ₃	0.94 d (6.9)	14.57	CH ₃	0.97 d (6.9)
22	26.21	CH ₂	H', 1.42 m H'', 1.22 m	27.16	CH ₂	H', 1.44 dp (14.6, 7.3) H'', 1.22 dp (14.6, 7.3)	25.13	CH ₂	H', 1.56 m H'', 1.26 dd (15, 7.3)
23	10.78, 14.63 ‡	CH ₃	0.97 d (7.3)	11.92	CH ₃	0.96 t (7.5)	10.17	CH ₃	0.94 t (7.5)
26	†	-	-	173.66	C=O	-	173.62	C=O	-

Conducted at 600 MHz for ¹H and 150 MHz for ¹³C in CD₃OD with 0.1% TFA-d.

Assignments are based on correlation spectroscopy (COSY), heteronuclear single-quantum correlation (HSQC), heteronuclear multiple-bond correlation (HMBC) and nuclear overhauser effect spectroscopy (NOESY). Chemical shifts are referenced to trimethylsilane (TMS).

† No signal detected

‡ Multiple shifts detected due to a mixture of different isomers in the sample

2.9 Supplemental Information

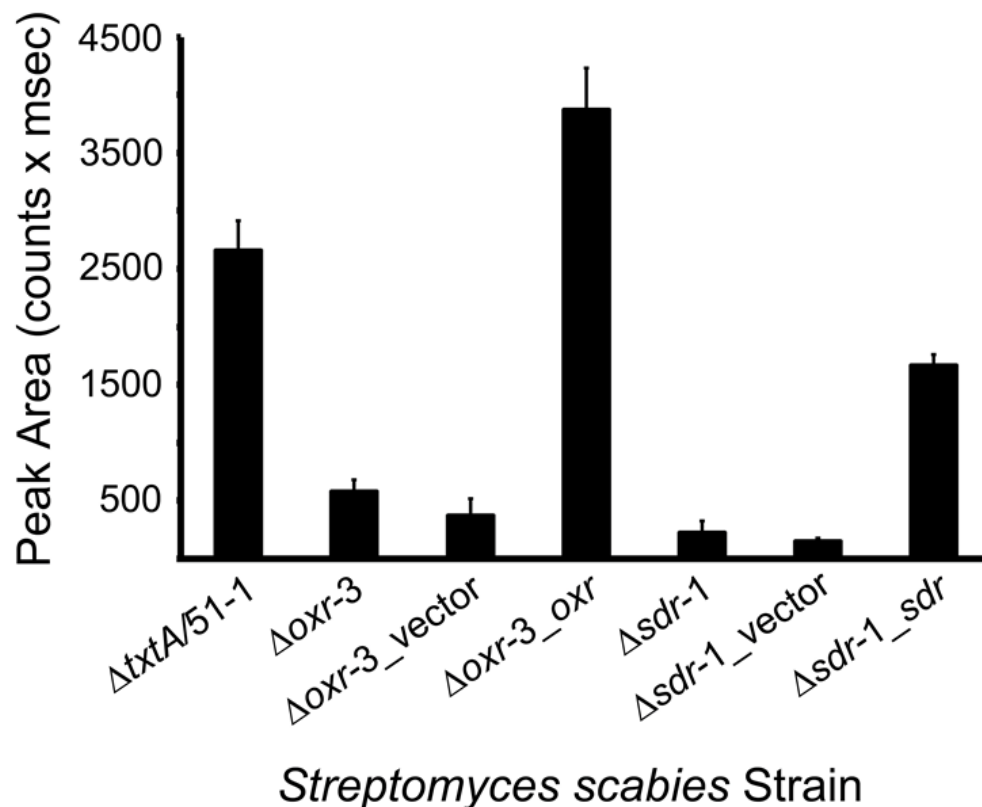


Figure S-2.1. Genetic complementation of CFA-Ile production in the Δoxr and Δsdr mutants. Extracts were prepared from cultures of the Δoxr (isolate 3) and Δsdr (isolate 1) mutant strains and of the corresponding complemented strains (Δoxr_oxr and Δsdr_sdr) and were analyzed by RP-HPLC. Extract from the $\Delta txtA/pRLDB51-1$ strain served as a positive control whereas extracts from the Δoxr and Δsdr mutants harbouring only the complementation vector (Δoxr_vector and Δsdr_vector) served as negative controls. The

bars indicate the average area of the CFA-Ile peak from triplicate cultures for each strain, and the error bars represent the standard deviation from the mean.

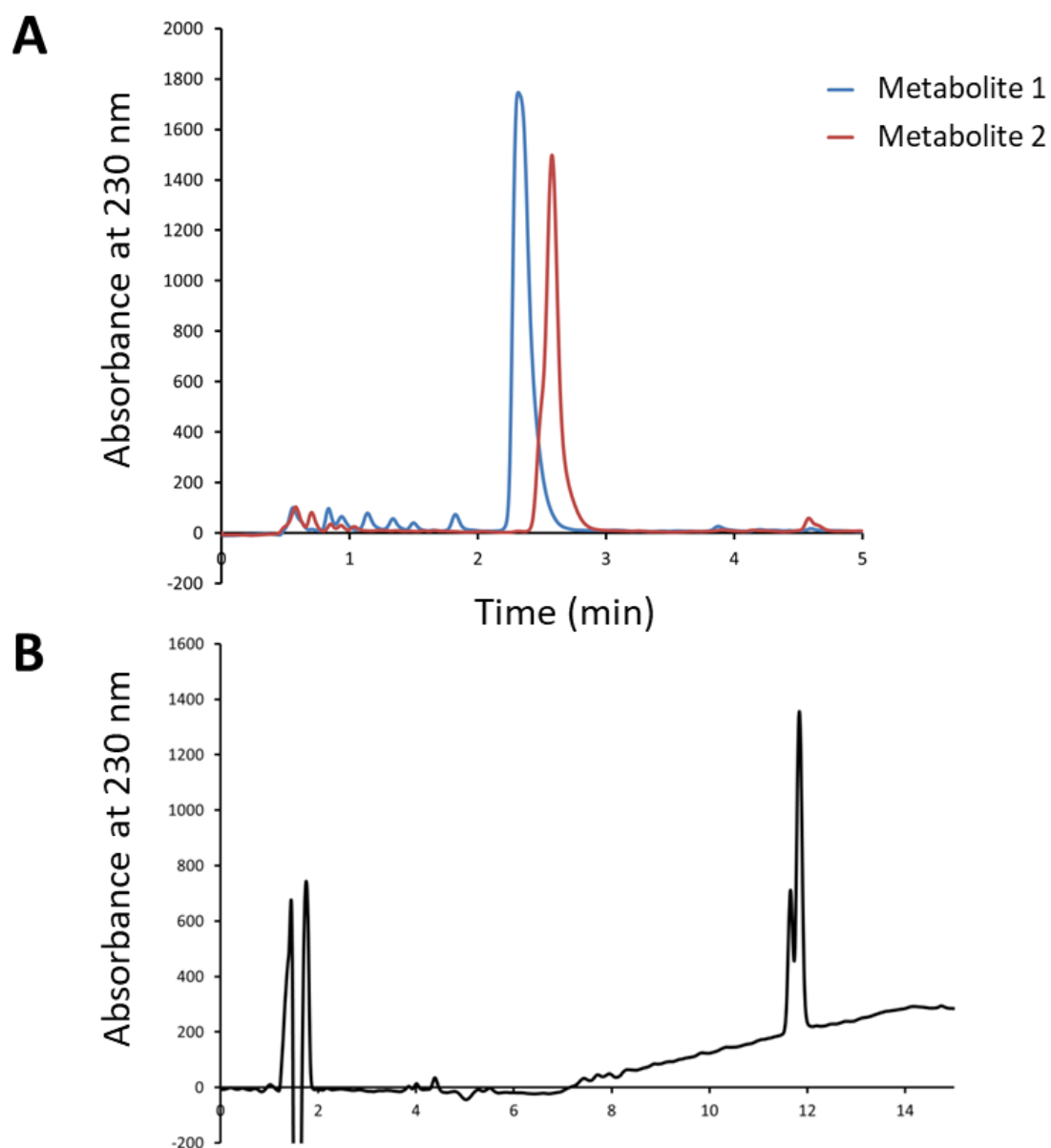


Figure S-2.2. (A) RP-HPLC analysis of the purified metabolites 1 and 2 from the Δsdr mutant. Each sample was analyzed using a Poroshell 120 EC-C18 column (4.6×50 mm) as described previously (Fyans *et al.*, 2015). (B) RP-HPLC analysis of the purified CFA-Ile

end product from the $\Delta txtA$ /pRLDB51-1 strain. Sample analysis was performed using a ZORBAX SB-C18 column (4.6×50 mm) as described in the experimental procedures. The presence of two peaks is due to the conjugation of CFA to different isomers of isoleucine as determined by 1-dimensional and 2-dimensional NMR.

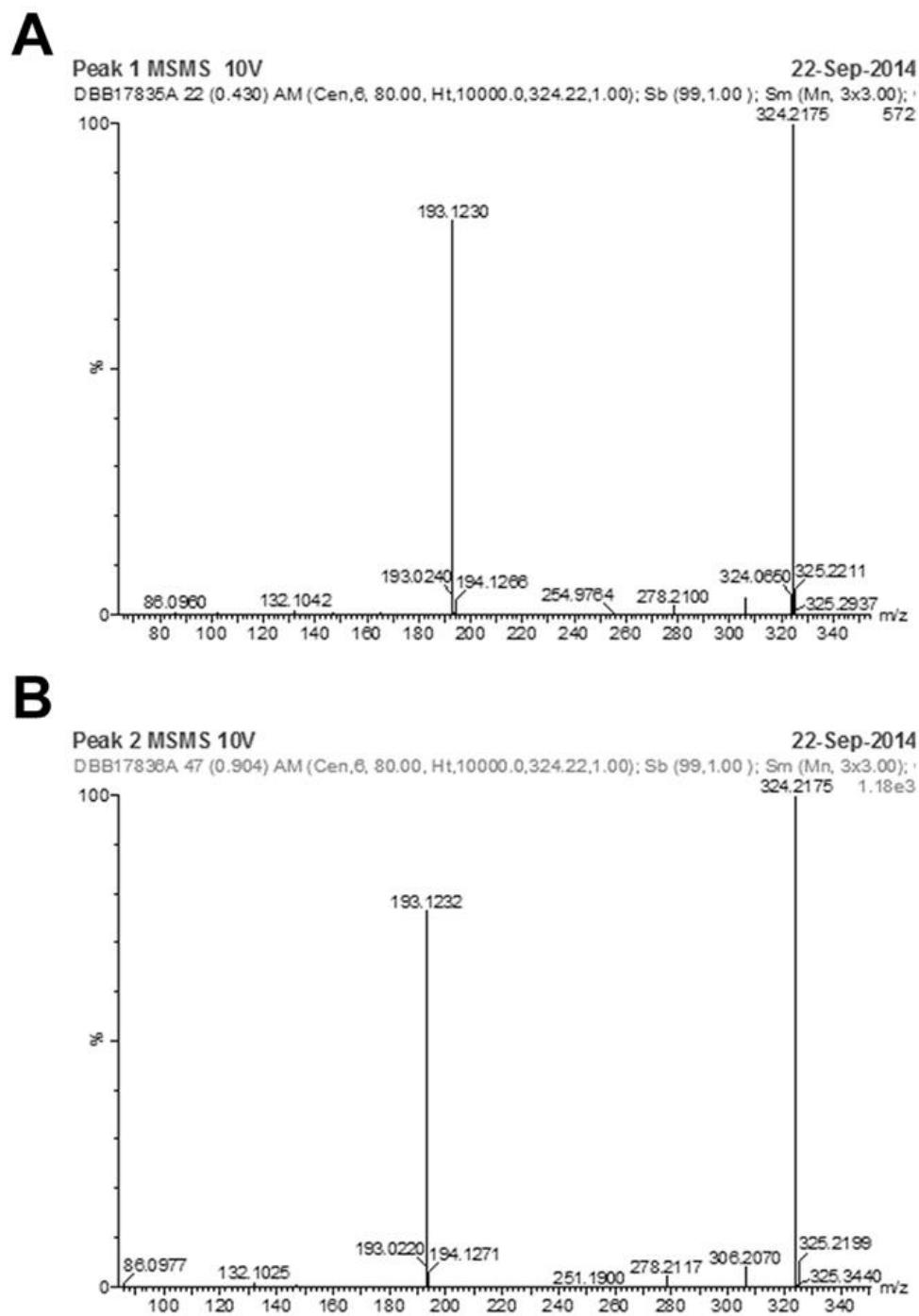
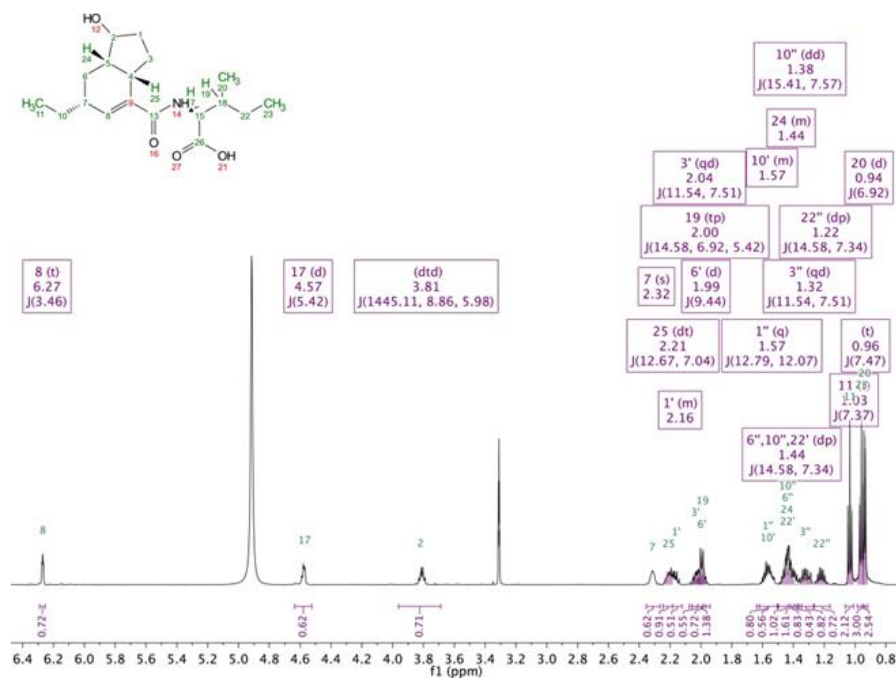
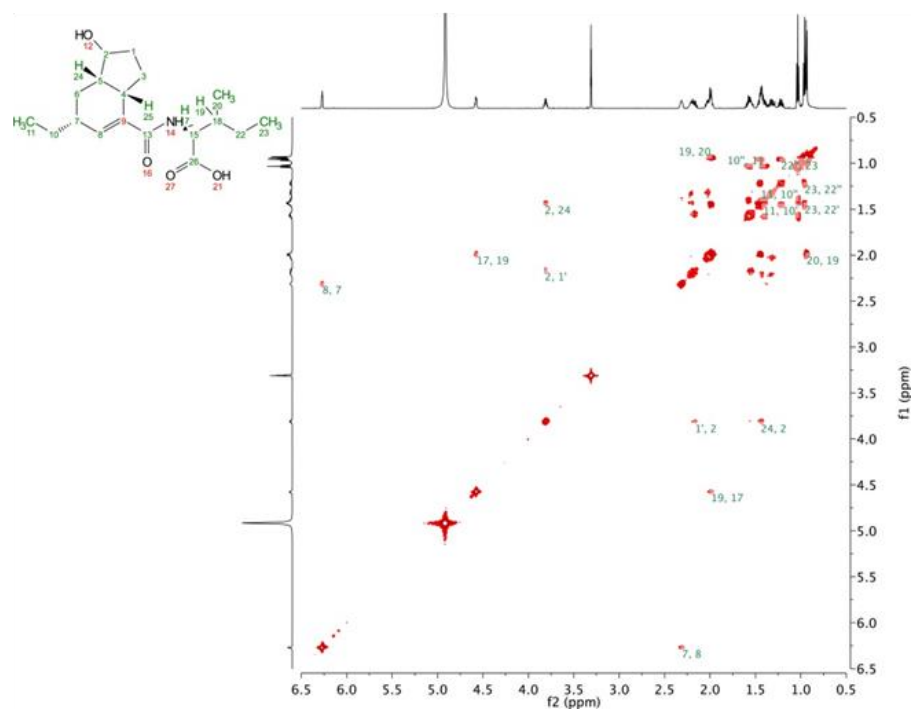


Figure S-2.3. HRESIMS/MS analysis of the purified metabolites 1 (A) and 2 (B) from the Δsdr mutant.

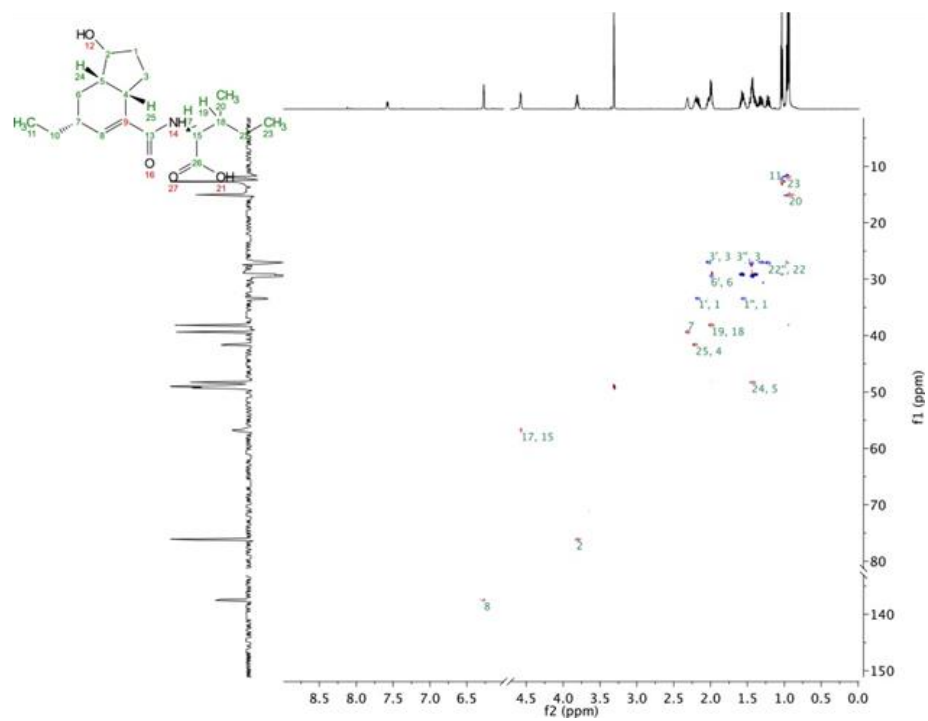
A



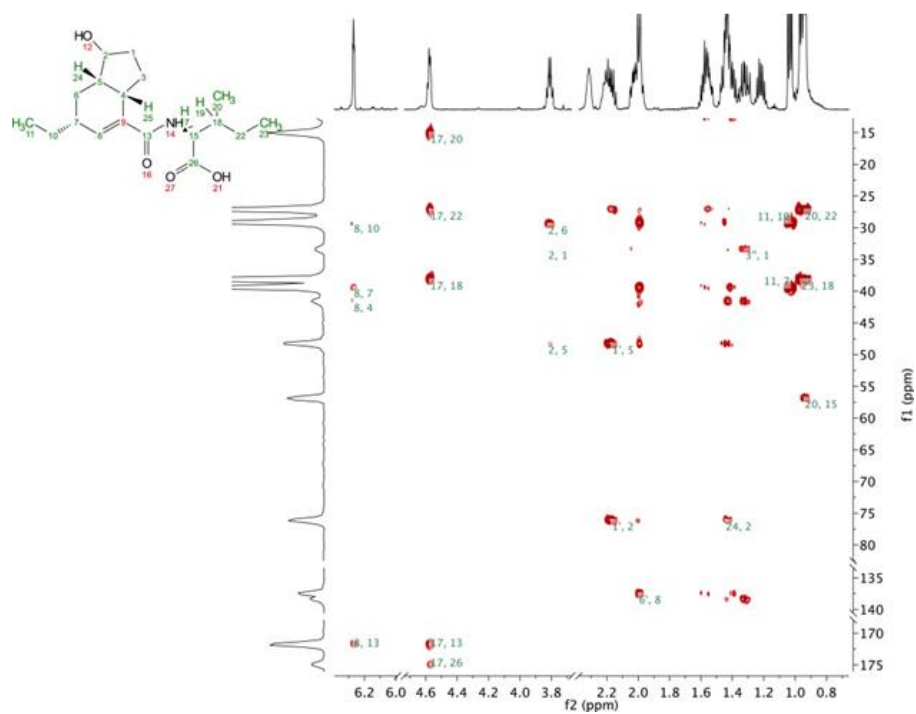
B



C



D



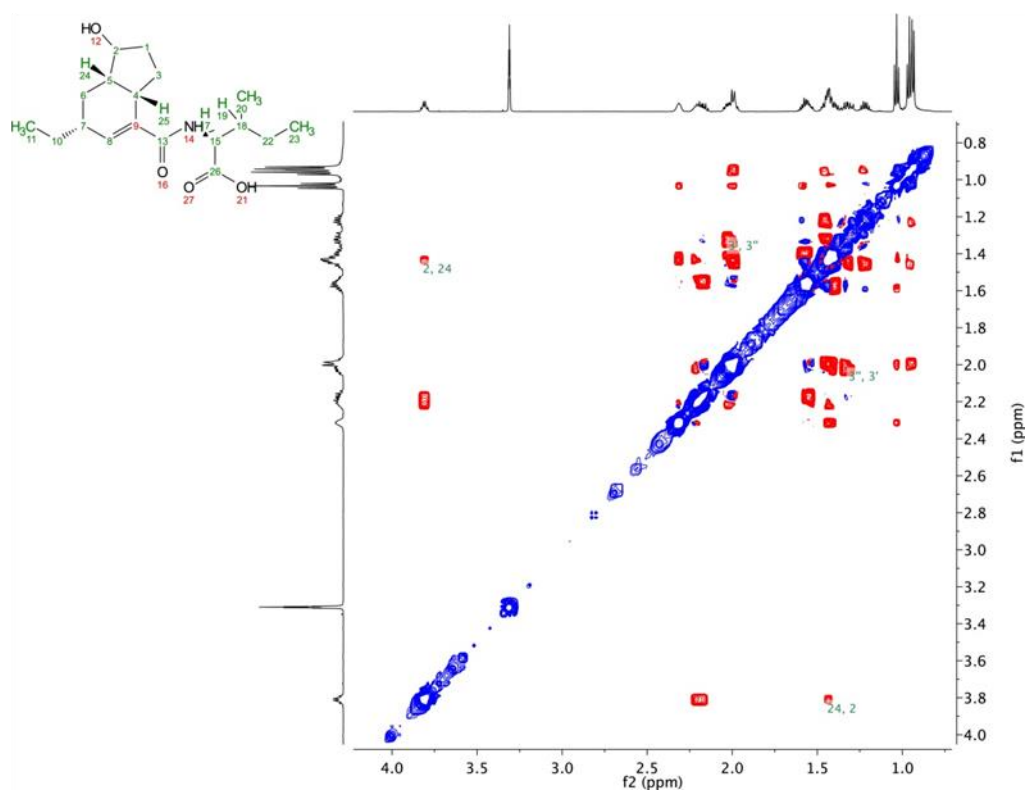
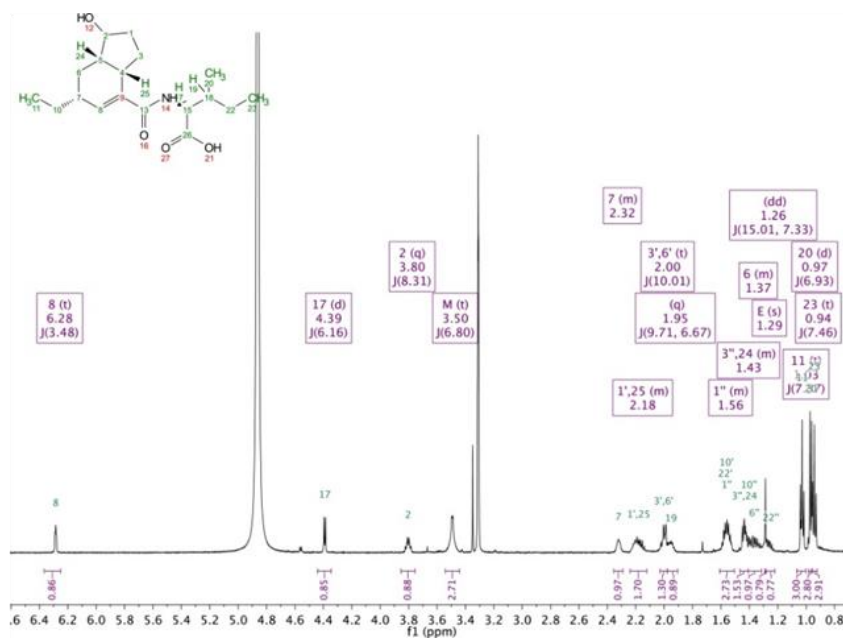
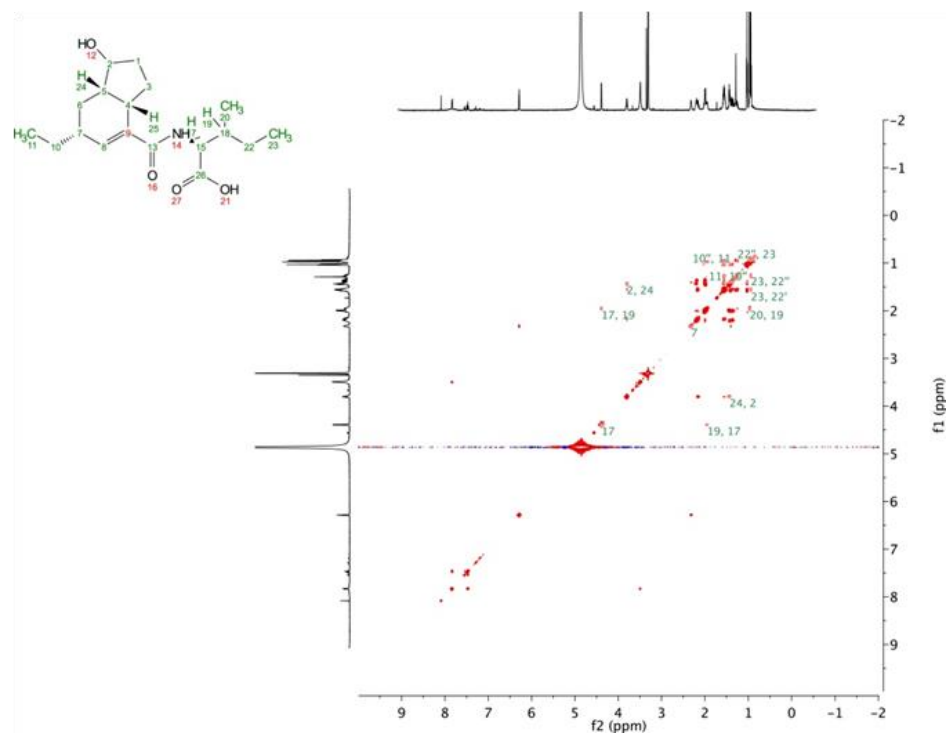
E

Figure S-2.4, related to Table 2.2 and Figure 2.5. NMR spectra of the purified Δsdr metabolite 1. Spectra were acquired at 600 MHz using CD_3OD with 0.1% TFA-d as the sample solvent. (A) ^1H -NMR spectrum. (B) COSY spectrum. (C) HSQC spectrum. (D) HMBC Spectrum. (E) NOESY spectrum.

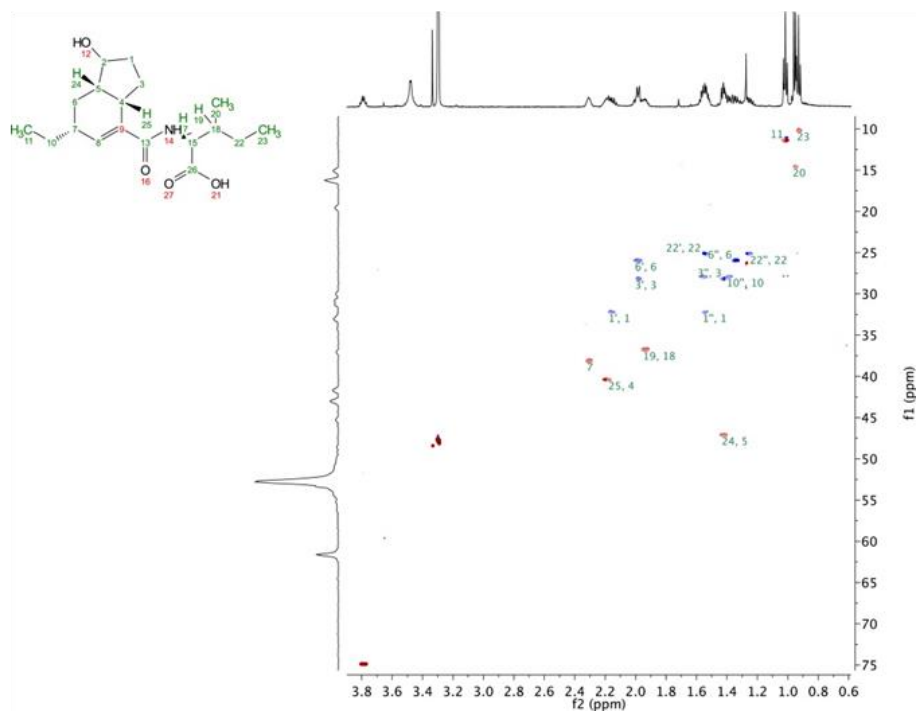
A



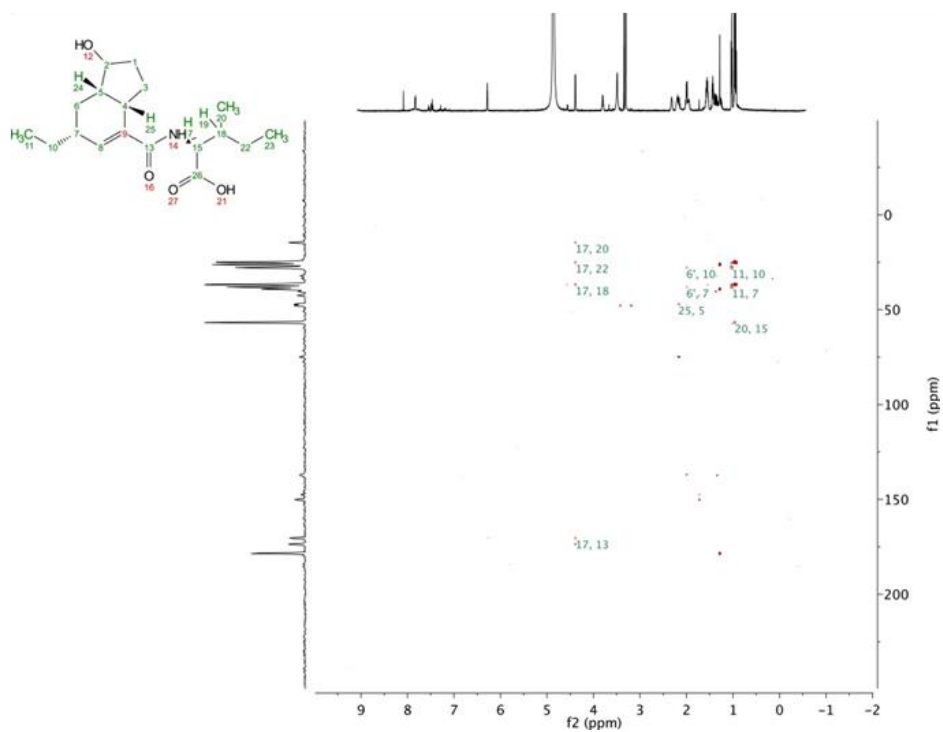
B



C



D



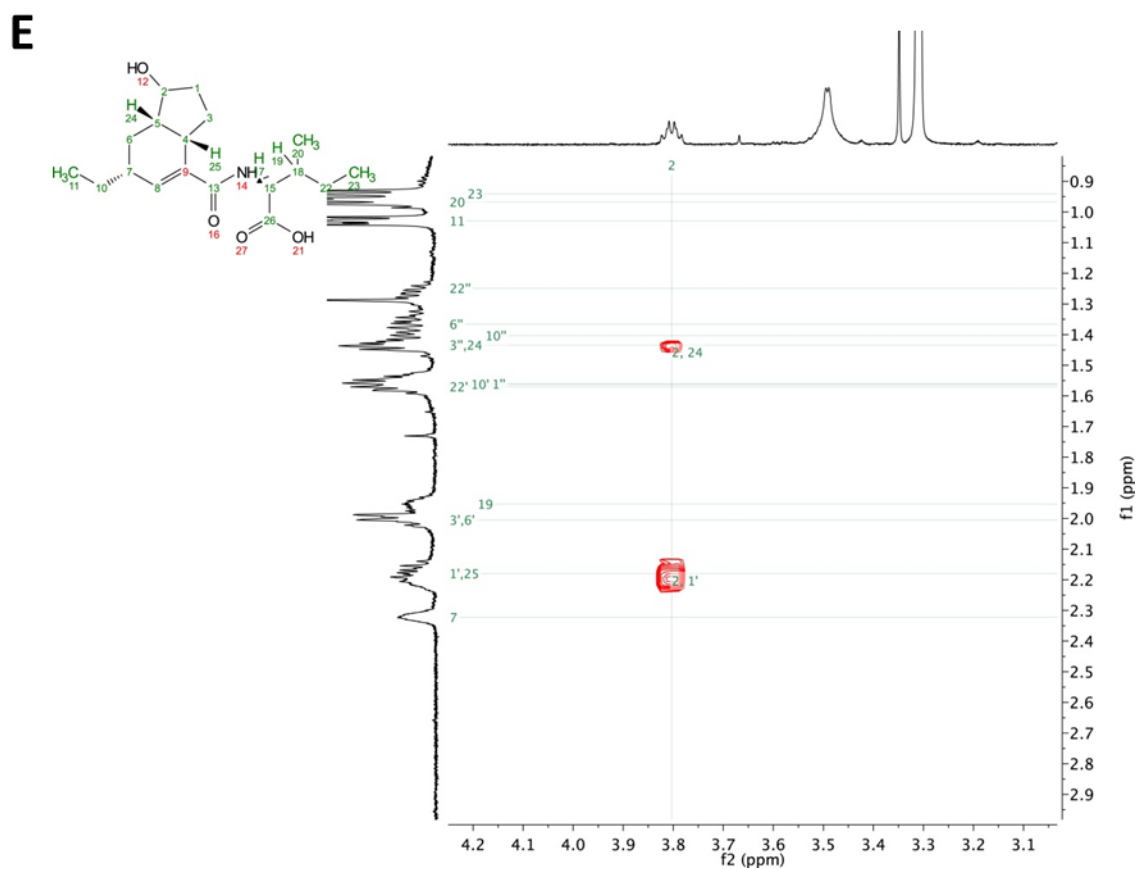
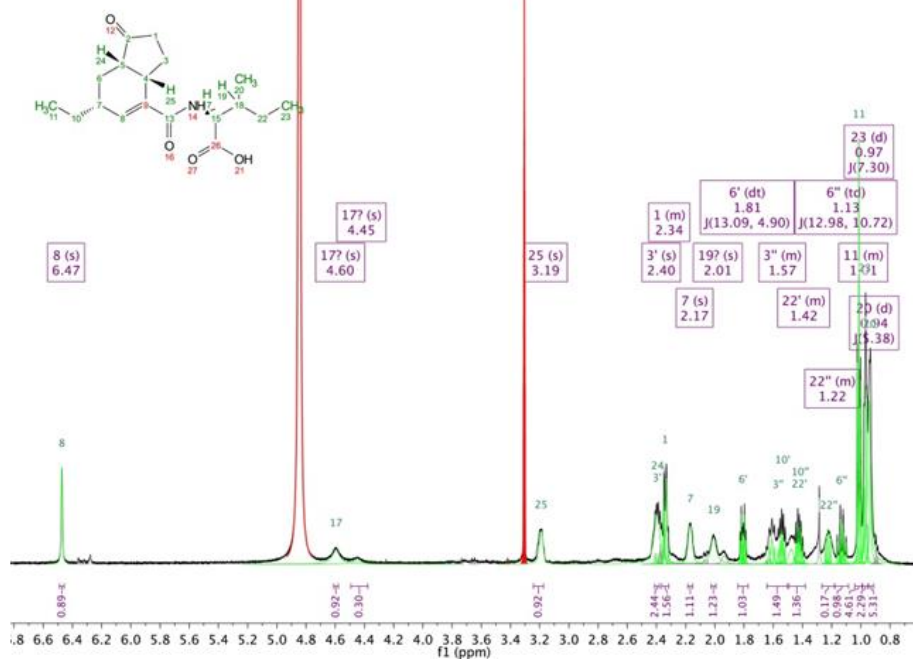


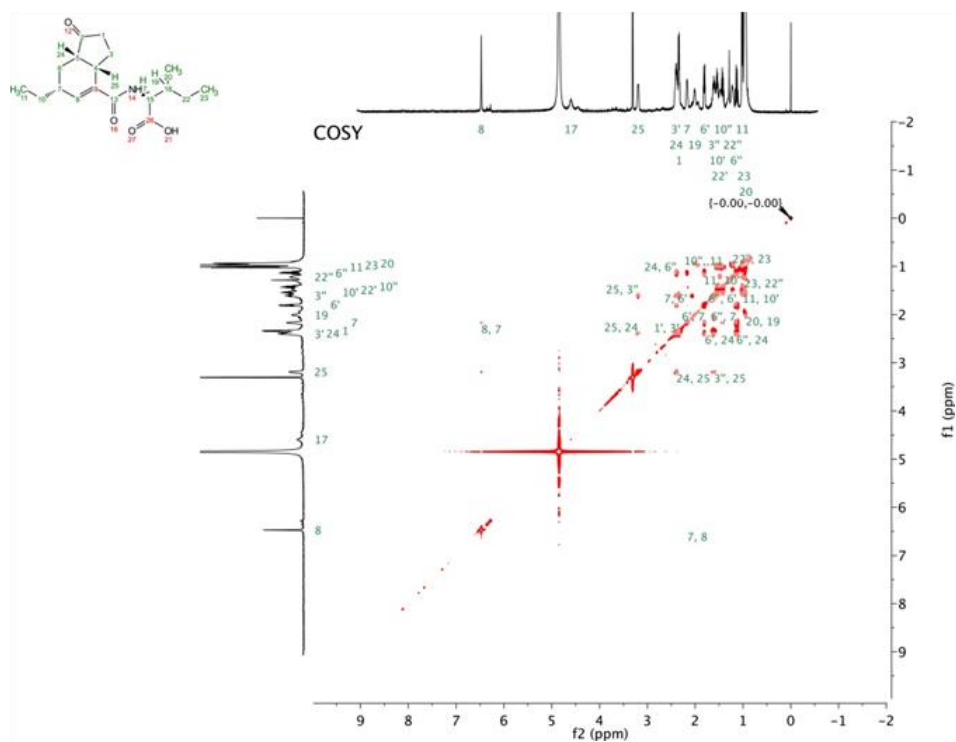
Figure S-2.5, related to Table 2.2 and Figure 2.5. NMR spectra of the purified Δsdr metabolite 2. Spectra were acquired at 600 MHz using CD_3OD with 0.1% TFA-d as the sample solvent. (A) ^1H -NMR spectrum. (B) COSY spectrum. (C) HSQC spectrum. (D) HMBC Spectrum. (E) NOESY spectrum.

A

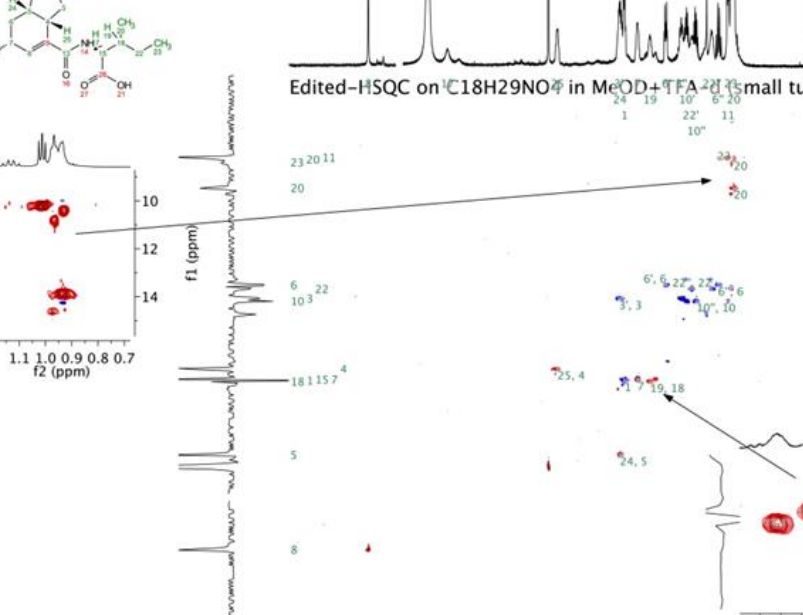
1D ¹H 30 pulse on C18H29NO4 in MeOD+TFA-d (small tube)



B



c



Chemical structure of compound 1 is shown in the top left. The NMR spectra are recorded in MeOD- d_4 .

The top spectrum is the ^1H NMR spectrum, showing peaks at 7.0, 6.5, 5.0, 4.5, 4.0, 3.5, 3.0, 2.5, 2.0, 1.5, 1.0, 0.5, and 0.0 ppm.

The bottom left spectrum is the 2D COSY spectrum, showing correlations between peaks at 1.1, 1.0, 0.9, 0.8, and 0.7 ppm.

The bottom right spectrum is the 2D HSQC spectrum, showing correlations between ^1H and ^{13}C peaks. The ^1H peaks are labeled at 7.0, 6.5, 5.0, 4.5, 4.0, 3.5, 3.0, 2.5, 2.0, 1.5, 1.0, 0.5, and 0.0 ppm. The ^{13}C peaks are labeled at 23, 20, 11, 6, 22, 10, 3, 18, 11, 5, 8, 25, 4, 19, 18, 24, 5, 1, 2, 3, 4, 5, 6, 7, 8, 9, 10, 11, 12, 13, 14, 15, 16, 17, 18, 19, 20, 21, 22, 23, 24, 25, 26, 27, 28, 29, 30, 31, 32, 33, 34, 35, 36, 37, 38, 39, 40, 41, 42, 43, 44, 45, 46, 47, 48, 49, 50, 51, 52, 53, 54, 55, 56, 57, 58, 59, 60, 61, 62, 63, 64, 65, 66, 67, 68, 69, 70, 71, 72, 73, 74, 75, 76, 77, 78, 79, 80, 81, 82, 83, 84, 85, 86, 87, 88, 89, 90, 91, 92, 93, 94, 95, 96, 97, 98, 99, 100 ppm.

D

Figure S-2.6, related to Table 2.2. NMR spectra of the purified CFA-Ile. Spectra were acquired at 600 MHz using CD₃OD with 0.1% TFA-d as the sample solvent. (A) ¹H-NMR spectrum. (B) COSY spectrum. (C) HSQC spectrum. (D) HMBC spectrum.

Table S-2.1: Accession numbers of proteins used to construct the Oxr and Sdr phylogenetic trees

Source Organism	Accession Number
Oxr Phylogeny	
<i>Streptomyces scabies</i> 87-22	CBG74928.1
<i>Streptomyces</i> sp. NRRL WC-3618	WP_053745363.1
<i>Streptomyces scabiei</i>	GAQ62345.1
<i>Kitasatospora azatica</i>	WP_035840047.1
<i>Streptomyces graminilatus</i>	WP_055529804.1
<i>Streptomyces ipomoeae</i>	WP_009328786.1
<i>Streptomyces griseoruber</i>	WP_055634212.1
<i>Hamadaea tsunoensis</i>	WP_027345034.1
<i>Streptomyces bingchengensis</i>	WP_014181183.1
<i>Acidithrix ferrooxidans</i>	WP_052606897.1
<i>Solirubrobacterales bacterium</i> URHD0059	WP_028075542.1
<i>Kutzneria</i> sp. 744	WP_043727268.1

Sdr Phylogeny	
<i>Streptomyces scabies</i> 87-22	CBG74932.1
<i>Streptomyces scabiei</i>	GAQ68259.1
<i>Streptomyces graminilatus</i>	WP_055532281.1
<i>Kitasatospora azatica</i>	WP_035840039.1
<i>Streptomyces</i> sp. NRRL WC-3618	WP_053746114.1
<i>Nocardioides insulae</i>	WP_028659072.1
<i>Leifsonia rubra</i>	WP_021810222.1
<i>Streptomyces</i> sp. NRRL S-15	WP_031093146.1
<i>Streptomyces</i> sp. NRRL S-4	WP_053930576.1
<i>Curtobacterium</i> sp. B8	WP_022904672.1
<i>Clavibacter michiganensis</i> LMG 26808	KDP89681.1
<i>Curtobacterium oceanosedimentum</i>	WP_058727374.1

Table S-2.2. Oligonucleotides used in this study.

Primer Name	Sequence* (5' – 3')	Use
DRB653	<u>GTGAAGTTCGGCTTCGTCATGTTCCC</u> <u>CACCCAGGACGCCATTCCGGGGATC</u> CGTCGACC	Redirect primer for Δoxr mutant cosmid construction
DRB654	<u>TCAGCGCAGGCGGTCGCCGAGTTGC</u> <u>AGGGCGATCCGGTCTGTAGGCTGGA</u> GCTGCTTC	Redirect primer for Δoxr mutant cosmid construction
DRB655	<u>ATGCAAGACAGGTTACACGACAAGG</u> <u>TCGCCCTGATAACCATCCGGGGAT</u> CCGTCGACC	Redirect primer for Δsdr mutant cosmid construction
DRB656	<u>TCAGGCCCCGCTCGGAGCGGCCACCG</u> <u>TCGATCGTCACCACTGTAGGCTGGA</u> GCTGCTTC	Redirect primer for Δsdr mutant cosmid construction
DRB664	ATCCCCGTGGACAGGCTCCC	Verification of Δoxr mutant cosmid and strain
DRB665	CTTGCCGGTCTGCCGGTCTG	Verification of Δoxr mutant cosmid and strain
ermEp*	GCGATGCTGTTGTGGGC	Sequencing of cloned inserts in pMSAK13
MSA1	ACTTCATGCCGTCGCCCCGTG	Verification of Δsdr mutant cosmid and strain
MSA2	AGGGGCGGGTCAAGGACCTC	Verification of Δsdr mutant cosmid and strain
MSA7	<u>GCGCCATATG</u> CAAGACAGGTTCAACCG	PCR amplification of <i>sdr</i> for construction of complementation plasmid
MSA9	<u>GCGCCATATGA</u> AGTTCGGCTTCGTC	PCR amplification of <i>oxr</i> for construction of complementation plasmid
MSA14	<u>GCGCCTCGAGT</u> CAGGCCCGCTCGGAGCGG	PCR amplification of <i>sdr</i> for construction of complementation plasmid

MSA15	GCGCCT TCGAG TCAGCGCAGGCGGT CGCCG	PCR amplification of <i>oxr</i> for construction of complementation plasmid
M13F	CGCCAGGGTTTTCCCAGTCACGAC	Sequencing of pGEM®-T Easy inserts
M13R	TCACACAGGAAACAGCTATGAC	Sequencing of pGEM®-T Easy inserts

* Non-homologous extensions are underlined, while engineered restriction sites are indicated in bold.

**Chapter 3: Coronafacoyl phytotoxin biosynthesis and evolution in the common scab
pathogen *Streptomyces scabiei***

Luke Bown^a, Yuting Li^a, Fabrice Berru  ^b, Joost T. P. Verhoeven^a, Suzanne C. Dufour^a
and Dawn R. D. Bignell^a

Department of Biology, Memorial University of Newfoundland, St. John's, NL, Canada^a;
Aquatic and Crop Resource Development, National Research Council of Canada, Halifax,
NS, Canada^b

Address correspondence to Dawn R. D. Bignell: dbignell@mun.ca

Copyright   American Society for Microbiology, Applied and Environmental
Microbiology, Volume 83, 2017, e01169-17.

3.1 Abstract

Coronafacoyl phytotoxins are an important family of plant toxins that are produced by several different phytopathogenic bacteria, including the gammaproteobacterium *Pseudomonas syringae* and the actinobacterium *Streptomyces scabies*. The phytotoxins consist of coronafacic acid (CFA) linked via an amide bond to different amino acids or amino acid derivatives. Previous work suggested that *S. scabies* and *P. syringae* use distinct biosynthetic pathways for producing CFA, which is subsequently linked to its amino acid partner to form the complete phytotoxin. Here, we provide further evidence that the *S. scabies* CFA biosynthetic pathway is novel by characterizing the role of CYP107AK1, a predicted cytochrome P450 that has no homologue in *P. syringae*. Deletion analysis of the *CYP107AK1* gene abolished production of coronafacoyl-isoleucine (CFA-Ile), the primary coronafacoyl phytotoxin produced by *S. scabies*. Structural elucidation of accumulated biosynthetic intermediates in the $\Delta CYP107AK1$ mutant indicated that CYP107AK1 is required for introducing the oxygen atom that ultimately forms the carbonyl group in the CFA backbone. The *CYP107AK1* gene along with two additional genes involved in CFA-Ile biosynthesis in *S. scabies* were found associated with putative CFA biosynthetic genes in other actinobacteria but not in other organisms. Analysis of the overall genetic content and organization of known and putative CFA biosynthetic gene clusters, together with phylogenetic analysis of the core biosynthetic genes indicates that horizontal gene transfer has played an important role in the dissemination of the gene cluster, and that rearrangement, insertion and/or deletion events have likely contributed to the divergent biosynthetic evolution of coronafacoyl phytotoxins in bacteria.

3.2 Introduction

The ability of plants to protect themselves from invading microbial pathogens relies on complex signalling networks that are controlled by key hormones such as salicylic acid (SA) and jasmonic acid (JA) (Glazebrook 2005; Thaler et al. 2012). SA is primarily responsible for regulating defence against biotrophic and hemi-biotrophic pathogens, while JA is mainly responsible for mediating defence against necrotrophic pathogens as well as against chewing insects and other herbivores. SA and JA signalling pathways are generally antagonistic in that activation of SA-regulated pathways leads to suppression of JA-regulated pathways, and *vice versa* (Glazebrook 2005; Thaler et al. 2012). JA is also critical for regulating the plant response to abiotic stress, and it modulates plant growth and developmental processes and influences plant secondary metabolism (Wasternack and Hause 2013).

In order to overcome the plant immune response, many plant pathogenic microorganisms have evolved strategies that allow them to manipulate the plant hormone signalling pathways for their own benefit. One of the best-studied examples of this is the production of coronatine (COR; Fig. 3.1-A) by several pathovars (pv) of the Gram-negative hemi-biotrophic plant pathogen *Pseudomonas syringae*. COR functions as a molecular mimic of (+)-*iso*-jasmonyl-L-isoleucine (JA-Ile; Fig. 3.1-A), the most bioactive form of JA (Fonseca et al. 2009). Both JA-Ile and COR promote the binding of the F-box protein CORONATINE-INSENSITIVE 1 (COI1) to JASMONATE ZIM DOMAIN (JAZ)

repressor proteins, thereby leading to degradation of the JAZ proteins and activation of the JA signalling pathway (Browse 2009). This, in turn, causes suppression of the SA-mediated defence response, which is important for combatting *P. syringae* infections (Xin and He 2013). Intriguingly, COR is ≈ 1000 times more active than JA-Ile at promoting the formation of the COI1-JAZ complex and subsequent degradation of the JAZ proteins, suggesting that COR is a highly effective mimic of JA-Ile perception in plants (Fonseca et al. 2009; Katsir et al. 2008). Furthermore, COR suppresses callose deposition in an SA-independent manner and enables bacterial entry into the plant host by overcoming stomatal defenses (Xin and He 2013; Geng et al. 2012). Thus, the production of COR provides an adaptive advantage to *P. syringae* by serving as a multifunctional suppressor of plant defences during infection.

COR consists of the polyketide metabolite coronafacic acid (CFA) linked via an amide bond to coronamic acid (CMA), which is derived from L-isoleucine (Bender et al. 1999). In *P. syringae*, the two moieties are produced independently by the *cfa* and *cma* biosynthetic gene clusters, respectively, after which they are joined together most likely by the coronafacate ligase (Cfl) enzyme encoded within the *cfa* gene cluster [Fig. 3.2; (Bender et al. 1999)]. Although COR is the primary product synthesized by *P. syringae* and is the most toxic, other related compounds (referred to as coronatine analogs or coronatine-like compounds) can also be produced where CFA is linked to amino acids such as isoleucine or valine (Bender et al. 1999). Together, these compounds form a family of molecules called the coronafacoyl phytotoxins. COR and COR-like molecules are known or predicted to be produced by several plant pathogenic bacteria other than *P. syringae*, including

Pseudomonas savastanoi, *Pectobacterium atrosepticum*, *Pectobacterium carotovorum* subsp. *carotovorum*, *Xanthomonas campestris* pv *phormiicola* and *Streptomyces scabies* (Bender et al. 1999; Bell et al. 2004; Fyans et al. 2015; Qi et al. 2011; Slawiak and Lojkowska 2009). The conservation of this family of compounds across diverse bacterial genera suggests that the JA signalling pathway is a common target for manipulation during host-pathogen interactions.

We have been studying the production of coronafacoyl phytotoxins by *S. scabies* (syn. *S. scabiei*), which is an important causative agent of potato common scab disease worldwide. This organism produces *N*-coronafacoyl-L-isoleucine (CFA-Ile; Fig. 3.1-A) as the primary product as well as other minor coronafacoyl phytotoxins, but it does not produce COR due to the absence of the *cma* biosynthetic genes in the genome (Fyans et al. 2015; Bignell et al. 2010). *S. scabies* harbours a biosynthetic gene cluster that contains homologues of the *cfa* biosynthetic genes from *P. syringae* (Fig. 3.1-B). Interestingly, this gene cluster also contains six additional genes that are absent from the *cfa* biosynthetic gene cluster in *P. syringae*. Two of these genes, *cfaR* and *scab79581*, are found at the beginning of the *S. scabies* *cfa* biosynthetic gene cluster (Fig. 3.1-B) and are regulatory genes that activate the production of CFA-Ile (Bignell et al. 2010; Cheng et al. 2015). The four remaining unique genes are predicted to encode biosynthetic enzymes and are co-transcribed with the other biosynthetic genes in the gene cluster (Bignell et al. 2010). Recently, we reported that two of the genes, *scab79681* (also called *oxr*) and *scab79721* (also called *sdr*), are required for normal production of CFA-Ile, and that the Sdr enzyme and possibly Oxr are directly involved in the biosynthesis of the CFA moiety [Fig. 3.2;

(Bown et al. 2016)]. Given that the *P. syringae* genome does not encode an Oxr homolog and only encodes a weakly similar Sdr homolog, our results suggested that *S. scabies* utilizes a novel biosynthetic pathway for producing coronafacoyl phytotoxins (Bown et al. 2016).

In this study, we provide further evidence that the production of the coronafacoyl phytotoxins in *S. scabies* involves a novel biosynthetic pathway by characterizing the function of the *scab79691* gene (herein referred to as *CYP107AK1*). We also utilize bioinformatics and genome sequencing data to investigate the evolutionary history of coronafacoyl phytotoxin biosynthesis in different bacteria.

3.3 Results

3.3.1 CYP107AK1 encodes a predicted cytochrome P450 monooxygenase.

Protein BLAST and phylogenetic analyses revealed that the *S. scabies* CYP107AK1 amino acid sequence is most closely related to a predicted cytochrome P450 (CYP) from *Streptomyces* sp. NRRL WC-3618 (WP_053745364; 87% identity and 90% similarity to CYP107AK1) and *Kitasatospora azatica* (WP_035840040.1; 88% identity and 91% similarity to CYP107AK1) and also shows similarity to other known or predicted CYPs from various species of actinomycetes. Analysis using the Pfam database showed that CYP107AK1 contains a cytochrome P450 domain (Pfam domain accession: PF00067) within the amino acid sequence. Also identified were two signature CYP motifs, the EXXR motif found in the K-helix and the GXXXCXG motif found in the heme-binding loop and

containing the invariant cysteine residue (Nelson et al. 1996). Analysis of the Cytochrome P450 Homepage database (<http://drnelson.uthsc.edu/cytochromeP450.html>) revealed that CYP107AK1 was previously classified as a member of the CYP107A subfamily of CYPs. This subfamily includes P450 enzymes that are known to be associated with microbial secondary metabolism.

3.3.2 Gene deletion analysis confirms that CYP107AK1 plays a direct role in CFA biosynthesis in *S. scabies*.

To determine the role of CYP107AK1 in the production of the coronafacoyl phytotoxins, a *S. scabies* mutant was created where the *CYP107AK1* gene was deleted and the corresponding levels of phytotoxin production were examined. The $\Delta CYP107AK1$ mutant was created in the $\Delta txtA$ /pRLDB51-1 strain, which exhibits high production levels of coronafacoyl phytotoxins due to *cfaR* regulatory gene overexpression, and also lacks production of the virulence-associated phytotoxin thaxtomin A due to deletion of the *txtA* biosynthetic gene (Fyans et al. 2015; Cheng et al. 2015). The latter feature allows for the rapid detection of phytotoxic activity associated with coronafacoyl phytotoxins in culture extracts, and it also simplifies the purification of coronafacoyl phytotoxins from the extracts. Organic extraction of the culture supernatants followed by reverse phase RP-HPLC analysis revealed that production of CFA-Ile and of the other minor coronafacoyl phytotoxins is abolished in the $\Delta CYP107AK1$ mutant. In addition, two new metabolites (i and ii) were observed in the mutant extract with retention times (t_R) of 9.16 min and 14.02 min, respectively (Fig. 3.3-A). Liquid chromatography-low resolution mass spectrometry electrospray ionization (LC-LRMSIMS) analysis of these metabolite peaks

in negative ion mode demonstrated the presence of pseudomolecular $[M-H]^-$ ions at m/z 292 and 306, which indicated a molecular mass of 293 Da for compound i and 307 Da for compound ii. The two metabolites were subsequently purified, and analysis by liquid chromatography-high resolution mass spectrometry (LC-HRMS) in positive ion mode revealed pseudomolecular $[M+H]^+$ and $[M+Na]^+$ ions at m/z 294.2064 and 316.1884, respectively, for compound i, while $[M+H]^+$ and $[M+Na]^+$ ions at m/z 308.2219 and 330.2040, respectively, were observed for compound ii (Fig. S-3.1). This is consistent with a molecular formula of $C_{17}H_{27}NO_3$ (calc m/z 294.2069 $[M+H]^+$, $\Delta = -1.7$ ppm) and $C_{18}H_{29}NO_3$ (calc m/z 308.2226 $[M+H]^+$, $\Delta = -2.3$ ppm) for compounds i and ii, respectively.

Analysis using 1-dimensional (1H and ^{13}C ; see Table S1) and 2-dimensional (correlation spectroscopy [COSY], heteronuclear single-quantum correlation [HSQC], heteronuclear multiple-bond correlation [HMBC] and nuclear overhauser effect spectroscopy [NOESY]) NMR revealed the structure of each compound as shown in Fig. 3.3-B. Both metabolites differ from the CFA-Ile end product by the absence of the carbonyl group at position C-2 of the CFA backbone (Fig. 3.1-A). In addition, compound i was determined to contain a methyl side chain at position C-7 instead of an ethyl side chain (Fig. 3.1-A and 3.3-B). This is supported by the strong HMBC correlations between the methyl H-10 and C-6, C-7 and C-8 from the CFA backbone (Fig. S-3.2). Tandem high-resolution electrospray ionization mass spectra (HRESIMS/MS) analysis of compound i revealed two prominent fragment ions in positive ion mode at m/z 163.1190 and 135.1193, which is in agreement with the proposed structure (Fig. S-3.3). HRESIMS/MS was additionally used to confirm the proposed structure of compound ii (Fig. S-3.4).

3.3.3 *The attached oxygen at position C-2 is important for the bioactivity of CFA-Ile.*

The bioactivity of the $\Delta CYP107AK1$ intermediates was tested using a potato tuber disk bioassay, which detects the tissue hypertrophy-inducing activity of the coronafacoyl phytotoxins (Fyans et al. 2011). Assays using total organic culture extract from the $\Delta CYP107AK1$ mutant demonstrated that the extract exhibited very weak bioactivity as compared to extract from the parental ($\Delta txtA$ /pRLDB51-1) strain (Fig. 3.3-C), and neither intermediate was able to induce any tissue hypertrophy as compared to CFA-Ile when equimolar amounts (100 nmol) of the pure metabolites were used (Fig. 3D). This suggests that the enzyme activity of CYP107AK1 is critical for the hypertrophy-inducing bioactivity of the CFA-Ile end-product.

3.3.4 *The CYP107AK1 gene is conserved in a subset of bacterial CFA biosynthetic gene clusters.*

Given the requirement of CYP107AK1 for the biosynthesis of CFA-Ile in *S. scabies*, we were interested to know whether the *CYP107AK1* gene is associated with known or predicted CFA biosynthetic gene clusters in other organisms. Although it was already known that a *CYP107AK1* homologue is absent from the CFA biosynthetic gene cluster in *P. syringae* pv *tomato* DC3000 and in *P. atrosepticum* SCRI1043 (Bignell et al. 2010), the availability of a large number of bacterial genome sequences in the database presented an opportunity to look for other CFA biosynthetic gene clusters that may harbour a *CYP107AK1* homologue. To first identify potential CFA gene clusters, we performed a protein BLAST analysis using the core CFA biosynthetic gene products from *S. scabies*

(Cfa1-7, Cfl) in order to identify homologues of each protein. Using this approach, we identified the known CFA biosynthetic enzymes from different plant pathogenic *Pseudomonas* species (e.g. *P. syringae*, *P. coronafaciens*, *P. amygdali*, *P. savastanoi*) as well as the predicted CFA biosynthetic enzymes from different plant pathogenic *Pectobacterium* spp. (e.g. *P. atrosepticum*, *P. carotovorum*, *P. betavascularum*) (Fig. 3.4-A). Interestingly, we also found homologues of the CFA biosynthetic enzymes from a plant pathogenic bacterium (*Brenneria* sp. EniD312) not known to produce coronafacoyl phytotoxins as well as from organisms not known to be plant pathogens, including *Azospirillum* sp. B510, *Kitasatospora azatica*, *Pseudomonas psychrotolerans*, *Streptomyces griseoruber* and *Streptomyces* sp. NRRL WC-3618. A comparison of the amino acid sequences of each protein revealed that the *S. scabies* proteins are most similar to the corresponding homologues from *S. griseoruber*, *Streptomyces* sp. NRRL WC-3618, and *K. azatica* (Fig. 3.4-A). As expected, the corresponding *cfa1-7* and *cfl* genes were found clustered together in all of the genome sequences analyzed (Fig. 3.4-B). The *S. griseoruber*, *Streptomyces* sp. NRRL WC-3618, and *K. azatica* gene clusters were additionally found to harbour a *CYP107AK1* homologue as well as a homologue of the *oxr* gene, which encodes a predicted F₄₂₀-dependent oxidoreductase and is also involved in CFA-Ile biosynthesis in *S. scabies* [Fig. 3.2 and 3.4-B; (Bown et al. 2016)]. Although a *sdr* homologue was only detected in the *K. azatica* gene cluster, a homologue (ADL01_RS35145) was found elsewhere in the *Streptomyces* sp. NRRL WC-3618 genome. No homologues of *oxr*, *sdr* and *CYP107AK1* were detected in the genome sequences of the other organisms harbouring CFA biosynthetic genes (Fig. 3.4-B).

3.3.5 Gene content and phylogenetic analyses provide insights into the evolution of coronafacoyl phytotoxin biosynthesis in bacteria.

In our previous study (Bown et al. 2016), we proposed that *S. scabies* utilizes a novel biosynthetic pathway for producing coronafacoyl phytotoxins as compared to *P. syringae* due to the involvement of the *oxr* and *sdr* genes, and work presented here on *CYP107AK1* further supports this idea (Fig. 3.2). The conservation of *oxr*, *sdr* and/or *CYP107AK1* in known or predicted CFA biosynthetic gene clusters from some bacterial species, but not others, raises intriguing questions about the evolution of coronafacoyl phytotoxin biosynthesis in bacteria. To investigate this further, we first examined the overall gene content and architecture of the CFA biosynthetic gene clusters obtained from the database. As shown in Fig. 3.4-B, the *cfa1-3* genes encoding the type II polyketide synthase (PKS) enzymes, the *cfa4-5* genes encoding the CFA synthetase enzymes, and the *cfa6-7* genes encoding the type I PKS enzymes are found in the identical arrangement in all of the gene clusters analyzed. In contrast, the relative position of the *cfl* gene encoding the coronafacate ligase enzyme was found to vary when comparing the *Pseudomonas/Pectobacterium/Brenneria* gene clusters and the *Streptomyces/Azospirillum/Kitasatospora* gene clusters (Fig. 3.4-B). Most of the gene clusters were also determined to harbour a gene (designated *cfa8* in *P. syringae*) encoding a predicted crotonyl-CoA carboxylase/reductase (CCR), which most likely serves to provide a sufficient amount of the ethylmalonyl-CoA extender unit required for CFA polyketide biosynthesis (Chan et al. 2009). In addition, the *S. scabies* and *K. azatica* gene clusters both harbour a gene encoding a predicted 3-hydroxybutyryl-CoA dehydrogenase,

which presumably functions together with the CCR to synthesize the ethylmalonyl-CoA extender unit (Chan et al. 2009). A gene (designated *cfa9* in *P. syringae*) encoding a predicted thioesterase was found within the *Pseudomonas* and *Azospirillum* gene clusters but not in the other gene clusters analyzed. Furthermore, a small gene encoding a hypothetical protein with a predicted thioesterase domain was found upstream of the CCR-encoding gene in the *Pseudomonas*, *Pectobacterium* and *Brenneria* gene clusters. Many of the gene clusters additionally have regulatory genes that are divergently transcribed from the biosynthetic genes (Fig. 3.4-B). Homologues of both *cfaR* and *scab79581*, which are involved in activating production of CFA-Ile in *S. scabies* (Bignell et al. 2010; Cheng et al. 2015), are conserved in the other *Streptomyces* and *Kitasatospora* gene clusters, suggesting that the regulation of metabolite production in these organisms is similar.

An analysis of the enzymatic domain architecture of the Cfa7 modular PKS also revealed interesting differences among the different CFA biosynthetic gene clusters (Fig. 3.4-C). Previously, it was reported that the *S. scabies* Cfa7 protein contains an enoyl reductase (ER) domain that is absent from the corresponding Cfa7 proteins from *P. syringae* pv *tomato* DC3000 and *P. atrosepticum* SCRI1043 (Bignell et al. 2010), and results presented here show that this domain is also found in the Cfa7 amino acid sequences from *S. griseoruber*, *Streptomyces* sp. NRRL WC-3618, and *K. azatica*. All four ER domains contain an amino acid sequence that is highly similar to the conserved NADP(H) binding motif that is characteristic of these domains [HAAAGGVGMA; (Kwan et al. 2008)], suggesting that they are functional (Fig. 3.5). Intriguingly, the domain is additionally predicted to be present in the Cfa7 protein from *Azospirillum* sp. B510, though

it is not clear whether the domain is active due to differences in the NADP(H) binding motif as compared to the consensus sequence (Fig. 3.5). In contrast, none of the Cfa7 homologues from the *Pseudomonas* spp., *Pectobacterium* spp. or *Brenneria* sp. were predicted to harbour an ER domain (Fig. 3.4-C).

The evolutionary relationships among the different CFA biosynthetic gene clusters was further examined by constructing a concatenated phylogenetic tree using the *cfa1-7* and *cfl* core CFA biosynthetic genes. In the case of the *cfa6* and *cfa7* type I PKS genes, we utilized the sequences encoding the ketosynthase (KS) domains from each gene rather than the entire gene sequence as recommended for such analyses (Ziemert and Jensen 2012). As shown in Figure 3.6, the phylogeny of the core CFA biosynthetic genes is not congruent with that of the corresponding 16S rRNA genes, suggesting that horizontal gene transfer (HGT) has played a key role in the dissemination of the core biosynthetic gene cluster among the different bacteria. Notably, the CFA biosynthetic genes from the different actinobacteria (*S. scabies*, *K. azatica*, *Streptomyces* sp. WC3618, *S. griseoruber*) form a distinct clade with those from the distantly related alphaproteobacterium *Azospirillum* sp. B510 (Fig. 3.6-A). In turn, the genes from these organisms appear to share a common ancestor with those from the *Pseudomonas* spp., which are members of the Gammaproteobacteria class. In contrast, the core CFA biosynthetic genes from the other Gammaproteobacteria members (*Pectobacterium* and *Brenneria* spp.) appear to form a separate clade from the *Pseudomonas* genes (Fig. 3.6).

3.4 Discussion

This study has shown that the *CYP107AK1* gene is required for coronafacoyl phytotoxin biosynthesis in the common scab pathogen *S. scabies*. *CYP107AK1* is predicted to encode an enzyme belonging to the CYP superfamily, members of which are heme-thiolate proteins that utilize a wide variety of substrates and are ubiquitously distributed in all domains of life (Munro et al. 2013). Most CYPs are monooxygenases that catalyze the scission of molecular oxygen and the regio- and stereo-specific insertion of an oxygen atom into the substrate. Oxidation reactions attributed to CYPs include epoxidation, hydroxylation, dealkylation, *N*-oxidation, deamination, dehalogenation and decarboxylation (Munro et al. 2013). In *Streptomyces* spp., CYPs are often associated with secondary metabolite biosynthesis gene clusters, and many have been shown to play a direct role in the biosynthesis of the resulting metabolite(s). For example, CYPs are involved in the production of the antibacterial compounds pikromycin (Xue et al. 1998) and oleandomycin (Rodriguez et al. 1995), the antifungal/insecticidal compound nikkomycin (Chen et al. 2002), the antitumor compound pladienolide (Machida et al. 2008) and the phytotoxin thaxtomin (Barry et al. 2012; Healy et al. 2002).

Previous work from our lab demonstrated that two additional genes, *oxr* and *sdr*, are also involved in coronafacoyl phytotoxin production in *S. scabies*. A constructed Δsdr mutant strain was found to accumulate biosynthetic intermediates that contain a hydroxyl group at position C-2 of the CFA backbone, and it was proposed that CYP107AK1 may catalyze the hydroxylation of C-2 and that Sdr then reduces the hydroxyl group to form the C-2 carbonyl in the final CFA molecule [Fig. 3.2; (Bown et al. 2016)]. Work presented here

supports this hypothesis as the $\Delta CYP107AK1$ mutant accumulated two intermediates that were both missing the oxygen attached to C-2 (Fig. 3.3-B). Neither intermediate was able to induce potato tuber tissue hypertrophy as compared to an equimolar amount of CFA-Ile (Fig. 3.3-D), indicating that the oxygen at position C-2 is critical for the bioactivity of the phytotoxin. As previously noted with the Δsdr mutant, the CFA intermediates in the $\Delta CYP107AK1$ mutant were only isolated as Ile conjugates, indicating that the coronafacate ligase enzyme is able to efficiently utilize the CFA intermediates as a substrate for ligation to Ile. Surprisingly, one of the $\Delta CYP107AK1$ intermediates was found to contain a methyl group attached to the C-7 position of CFA instead of the ethyl group that is normally present (Fig. 3.3-B). This would presumably occur as a result of the incorporation of methylmalonyl-CoA instead of ethylmalonyl-CoA during polyketide assembly of the CFA backbone by Cfa6. The selection and incorporation of extender units during polyketide biosynthesis is controlled by the acyltransferase (AT) domains of modular PKSs, and while such domains typically exhibit a high degree of specificity for their substrate (Smith and Tsai 2007), there is precedence for some AT domains exhibiting a broader substrate specificity. For example, it has been reported that either ethylmalonyl-CoA or methylmalonyl-CoA can be incorporated at the same elongation stage during the biosynthesis of monensin and ascomycin (FK520), and the AT5 domain involved in niddamycin biosynthesis shows a preference for ethylmalonyl-CoA but is able to accept methylmalonyl-CoA (Hatanaka et al. 1988; Liu and Reynolds 1999; Stassi et al. 1998). It is noteworthy that the parental *S. scabies* $\Delta txtA$ /pRLDB50-1a strain accumulates a minor metabolite that was previously thought to be CFA conjugated to valine (Fyans et al. 2015),

and a predicted valine-containing biosynthetic intermediate was observed to accumulate in the Δsdr mutant (Bown et al. 2016). As these metabolites would have the exact same molecular formula as an Ile conjugate of a methyl-substituted CFA derivative (or intermediate in the case of the Δsdr mutant), it is possible that the production of different CFA derivatives occurs naturally in *S. scabies* depending on the availability of the ethylmalonyl-CoA and methylmalonyl-CoA substrates during polyketide biosynthesis, an idea that warrants further investigation.

The requirement of *CYP107AK1* for the production of the CFA moiety in *S. scabies* provides further evidence that the CFA biosynthetic pathway in this organism is distinct from that of *P. syringae* since the *P. syringae* genome sequence does not encode any proteins showing similarity to *CYP107AK1*. Additionally, our study revealed that other bacteria may produce coronafacoyl phytotoxins using a similar biosynthetic pathway as that observed in *S. scabies*. Protein Blast analysis resulted in the identification of putative CFA biosynthetic gene clusters in two other *Streptomyces* spp. and in the actinobacterium *K. azatica*, and these gene clusters all contain homologues of both *CYP107AK1* and *oxr* (Fig. 3.4-B). A *sdr* homologue is additionally present in the *K. azatica* gene cluster, while a homologue is located elsewhere in the genome of *Streptomyces* sp. WC-3618 (Fig. 3.4-B). Although known or putative CFA biosynthetic gene clusters were identified in different *Pseudomonas* spp., *Pectobacterium* spp., *Brenneria* sp. and in *Azospirillum* sp. B510, none of these gene clusters appear to contain homologues of *CYP107AK1*, *oxr* and *sdr*, and homologues were not identified elsewhere in the genome sequences. It appears, therefore,

that the involvement of these enzymes in CFA biosynthesis is limited to members of the actinobacteria.

This study also investigated the evolution of coronafacoyl phytotoxin biosynthesis among phylogenetically distinct bacteria. A comparison of the CFA biosynthetic gene clusters among the different members of the gammaproteobacteria, alphaproteobacteria and actinobacteria revealed that although a core set of genes (*cfa1-7*, *cfl*) are conserved among all of the gene clusters, variations exist in the organization of such genes as well as in the presence or absence of other genes (Fig. 3.4-B). The overall genetic architecture, together with the phylogenetic analysis of the core genes, suggests that the *S. scabies* gene cluster is most closely related to the gene clusters from the other actinobacteria (Fig. 3.4 and 3.6). As the *CYP107AK1*, *oxr* and *sdr* homologues were only found in a subset of gene clusters, it is possible that these genes represent a subcluster that was recently joined to an ancestral core gene cluster. Interestingly, the core CFA gene tree also suggests that the *Azospirillum* sp. 510 gene cluster shares a common ancestor with the actinobacterial gene clusters, which agrees with the observation that the Cfa7 homologue from *Azospirillum* sp. B510 is the only homologue outside of the actinobacteria that is predicted to harbour an ER domain (Fig. 3.4-C). How this ER domain arose in the Cfa7 homologues in these organisms is unclear, but it could either be due to an insertion event in a common ancestor, or a deletion event that resulted in loss of the domain in the other Cfa7 homologues. Overall, our analyses provide evidence that HGT has played a critical role in the propagation of the CFA biosynthetic genes among the different bacteria, with intragenic rearrangement, insertion and/or deletion events likely contributing to the divergence of the gene clusters within these

bacteria (Fischbach et al. 2008). It is noteworthy that the biosynthetic gene cluster for coronamic acid, which is found in the COR phytotoxin (Fig. 3.1-A), is only present in the genome sequences of a subset of known or predicted CFA producers (*Pseudomonas* spp. and *Azospirillum* sp. B510), suggesting that the acquisition of this cluster likely occurred independently from that of the CFA biosynthetic genes.

A final revelation arising from this study is the observation that predicted CFA biosynthetic genes are not only found in plant pathogenic bacteria, but they appear to be present in bacteria that are not known to be pathogenic (Fig. 3.4). This may suggest that the production of JA mimics by microbes provides an evolutionary advantage that is not always directly related to host-pathogen interactions. It is known, for example, that JA plays an important role in regulating the induced systemic resistance (ISR), an enhanced state of resistance that provides plants with broad spectrum protection against pathogens and parasites (Pieterse et al. 2014). ISR is elicited by exposure to certain non-pathogenic bacteria, and this primes the whole plant to mount a stronger and/or faster response upon pathogen challenge in order to better combat the invading pathogen. It is conceivable that the production of a JA mimic by a beneficial plant symbiont may help to protect the plant host by ensuring that the host is ready to mount an effective response when it encounters an invading pathogen. It is notable that the *Azospirillum* sp. B510 strain was originally isolated as a rice endophyte and has been shown to promote plant growth as well as resistance to the fungal and bacterial rice pathogens (Kaneko et al. 2010). Whether coronafacoyl phytotoxin production contributes to the beneficial features of this organism remains to be determined.

3.5 Experimental Procedures

3.5.1 Bacterial strains and culture conditions.

All strains, plasmids and cosmids used in this study are listed in Table 3.1. *Escherichia coli* strains were routinely cultured at 37°C with shaking (200 RPM) in Difco™ LB Lennox broth (BD Biosciences), low salt LB broth (1% w/v tryptone; 0.5% yeast extract; 0.25% w/v NaCl), SOB (Sambrook et al. 1989) or SOC (New England Biolabs), or on LB (Lennox or low salt) medium with 1.5% w/v agar (BD Biosciences). When required, the media were supplemented with the following antibiotics at the indicated final concentrations: ampicillin (100 µg ml⁻¹), kanamycin (50 µg ml⁻¹), hygromycin B (100 µg ml⁻¹), chloramphenicol (25 µg ml⁻¹). For hygromycin B, low salt LB media was always utilized. *S. scabies* strains were routinely cultured at 28°C with shaking (200 RPM) in trypticase soy broth (TSB; BD Biosciences), or at 25°C with shaking (125 RPM) in soy flour mannitol broth (SFMB; 2% defatted soy flour, 2% mannitol). Solid cultures were grown on the International *Streptomyces* Project Medium 4 (ISP-4; BD Biosciences), soy flour mannitol agar [SFMA; (Kieser et al. 2000)], Difco™ nutrient agar (NA; BD Biosciences) or potato mash agar [PMA; (Fyans et al. 2015)]. When required, the media were supplemented with the following antibiotics at the indicated final concentrations: hygromycin B (50 µg ml⁻¹), apramycin (50 µg ml⁻¹), nalidixic acid (50 µg ml⁻¹), kanamycin (50 µg ml⁻¹), thiostrepton (25 µg ml⁻¹).

3.5.2 Construction of the *S. scabiei* Δ CYP107AK1 gene deletion mutant.

Deletion of the *CYP107AK1* gene in the *S. scabiei* Δ *txtA*/pRLDB51-1 strain was accomplished using a λ RED – mediated PCR targeting system (Gust et al. 2003). A cassette [*hyg+oriT*] containing the hygromycin resistance gene and origin of transfer sequence was PCR-amplified using pIJ10700 (Table 3.1) as template and the primers JS3 (5'-GTGGTGCTGGGCGCGGAGTTCGTGCGGAATCCGCATGAGATTCCGGGGATCCGTCGACC-3') and YL7 (5'-CGCTGTGCCGTCCGGACGGGCAGGGACCGCAGCCCGTGGTGTAGGCTGGAGCTGCTTC-3'), which contain 39 nt homology extensions for targeting of the *CYP107AK1* gene. Following gel purification, the PCR product was electroporated into the *E. coli* BW25113 strain containing the λ RED expression plasmid pIJ790 and Cosmid 1770, which harbours the *S. scabiei* CFA biosynthetic gene cluster (Table 3.1). Mutant cosmids where the *CYP107AK1* gene was replaced by the [*hyg+oriT*] cassette were isolated and verified by PCR using the primers YL8 (5'-GGGACAAGGAGTGCGGAGCC-3') and YL9 (5'-CATCGGGTTTCCCCGCGCC-3') (data not shown). A single mutant cosmid (1770/ Δ CYP107AK1) was subsequently introduced into the *E. coli* ET12567 strain containing pUZ8002 (Table 3.1) before being transferred to *S. scabiei* Δ *txtA*/pRLDB51-1 via intergenic conjugation (Kieser et al. 2000). Hygromycin resistant exconjugants that arose were screened for kanamycin sensitivity, and PCR was used to confirm the resulting mutant isolates using the YL8 and YL9 primers (data not shown).

3.5.3 Analysis of *N*-coronafacoyl phytotoxin production.

Triplicate cultures of *S. scabies* strains were grown in 5 ml of SFMB for 7 days in 6-well tissue culture plates, after which the culture supernatants were harvested and extracted with organic solvent as described previously (Fyans et al. 2015). Detection of *N*-coronafacoyl phytotoxins in the extracts was by RP-HPLC as described previously (Fyans et al. 2015), except that the separation was achieved using an isocratic mobile phase consisting of 50:50 acetonitrile:water with 0.1% v/v formic acid, and the method run time was 6 minutes with no post-run extension. LC-LRESIMS analysis of the *S. scabies* culture extracts was performed using an Agilent 1100 series HPLC system (Agilent Technologies Inc.) interfaced to a Waters G1946A single quadrupole mass spectrometer (Waters Corporation). Separation and detection of *N*-coronafacoyl phytotoxins was as described previously (Bown et al. 2016) except that an isocratic mobile phase consisting of 50:50 acetonitrile:water with 0.1% v/v formic acid was used with a run time of 10 min.

3.5.4 Purification of *N*-coronafacoyl biosynthetic intermediates.

Large-scale *S. scabies* cultures (1L) were prepared, and the supernatants were subjected to chemical extraction as described in (Bown et al. 2016). Purification of the metabolites was by preparative TLC and semi-preparative RP-HPLC as described before (Fyans et al. 2015), except that an isocratic mobile phase consisting of 50:50 acetonitrile:water with 0.1% formic acid was used for the semi-preparative RP-HPLC.

3.5.5 Structural elucidation of the *N*-coronafacoyl biosynthetic intermediates.

LC-LRESIMS analysis of the purified biosynthetic intermediates structures was performed on an Accela 1250 system (Thermo Fisher Scientific) hyphenated with an ExactiveTM benchtop Orbitrap mass spectrometer (Thermo Fisher Scientific) equipped with electrospray ionization probe and an Ultimate 3000 DAD (Thermo Scientific Dionex) and ELSD 3300 (Alltech). Reversed phase separation was achieved on an hypersil C18 column (2.1 x 50 mm, 1.9 μ m, GL Sciences) with a mobile phase consisting of (A) 0.1% formic acid in water and (B) 0.1% formic acid in acetonitrile, with a linear gradient from 5% B to 100% B in 4.2 min, held for 3.3 min, flow-rate was at 500 μ L/min. The mass spectra were acquired in positive ion mode. HRMS/MS of the intermediates was conducted using a Waters Q-ToF Premier mass spectrometer equipped with a lockspray ESI source with a collision energy of 20eV. One-dimensional (¹H and ¹³C) and 2-dimensional (COSY, HSQC, HMBC and NOESY) NMR spectra of each metabolite were acquired at the Memorial University Centre for Chemical Analysis, Research and Training (C-CART) using a Bruker AVANCE II 600 spectrometer (Bruker BioSpin GmbH, Rheinstetten, Germany) operating at 600.33 MHz for proton and 150.96 MHz for carbon and equipped with a 5-mm inverse triple-resonance probe (TXI). The samples were dissolved in CD₃OD with 0.1% TFA-d. Chemical shifts were referenced to trimethylsilane for both ¹H and ¹³C.

3.5.6 Potato tuber slice bioassay.

An *in vitro* potato tuber slice bioassay was performed using *S. scabies* organic culture extracts (25 μ l) or purified *S. scabies* metabolites [CFA-Ile, Δ CYP107AK1 intermediates i and ii (100 nmol each)] as previously described (Fyans et al. 2015). Solvent alone [HPLC grade methanol (100%) with or without formic acid (0.1% final

concentration)] was used as a negative control, while pure COR (1 nmol; Sigma Aldrich Canada) dissolved in 100% methanol was used as a positive control. Each bioassay was conducted at least twice.

3.5.7 Bioinformatics analyses.

Homologues of the *S. scabiei* 87-22 CFA biosynthetic gene cluster were identified by using NCBI BLAST (online version, blastp, default settings) (Altschul et al. 1990) with the *S. scabiei* Cfa1-7 and Cfl amino acid sequences. Protein domain analyses were performed using the Pfam database (Finn et al. 2008) or the Structure Based Sequence Analysis of Polyketide Synthase website [SBSPKS; (Anand et al. 2010)] in the case of the modular PKS proteins. Alignment of the *cfa1-5*, *cfa6* (KS domain), *cfa7* (KS domain) and *cfl* nucleotide sequences from the different bacteria species was conducted using MUSCLE (alignment by codons using default parameters) within the Molecular Evolutionary Genetic Analysis (MEGA) software version 7.0.21 (Kumar et al. 2016). Alignments were subsequently concatenated for phylogenetic analysis of the CFA biosynthetic genes. A model selection was performed for each partition within the concatenated alignment using jModelTest version 2.1.9 (Santorum et al. 2014) to identify the most suited model for distance estimation, *cfa1* – TPM3+G (Santorum et al. 2014), *cfa2* – HKY+G (Hasegawa et al. 1985), *cfa3* – TPM3uf+I+G (Santorum et al. 2014), *cfa4* – HKY+I+G (Hasegawa et al. 1985), *cfa5* – TPM3uf+I+G (Santorum et al. 2014), *cfa6* (*ks*) – HKY+G (Hasegawa et al. 1985), *cfa7*(*ks*) – HKY+I+G (Hasegawa et al. 1985), *cfl* – TPM3uf+I+G (Santorum et al. 2014). Phylogeny was inferred using PhyML (version 3.3.20161110) using the concatenated gene alignments. Alignment of the 16S rRNA gene sequences was conducted

using MUSCLE (default parameters) within the MEGA software, and the 16S rRNA phylogenetic tree was constructed using MEGA with the maximum likelihood method and the Tamura-Nei substitution model (Tamura and Nei 1993). The significance of the branch order in both trees was tested using the bootstrapping method (Felsenstein 1985) with 100 replicates for the CFA gene tree and 1000 replicates for the 16S rRNA gene tree.

3.6 Acknowledgements

The authors would like to thank Dr. Celine Schneider and Dave Davidson of the Memorial University C-CART facility for assistance with the NMR structural analyses, and the anonymous reviewers for their helpful comments and suggestions.

This work was supported by a Natural Sciences and Engineering Research Council of Canada Discovery Grant No. 386696-2010 to D.R.D.B. J.T.P.V. was supported by a Natural Sciences and Engineering Research Council of Canada Discovery Grant No. 06548-2015 to S.C.D.

3.7 References

Altschul S.F., Gish W., Miller W., Myers E.W., Lipman D.J. (1990). Basic local alignment search tool. *J Mol Biol*, 215:403-10.

- Anand S., Prasad M.V., Yadav G., Kumar N., Shehara J., Ansari M.Z., Mohanty D. (2010). SBSPKS: structure based sequence analysis of polyketide synthases. *Nucleic Acids Res*, 38:W487-96.
- Barry S.M., Kers J.A., Johnson E.G., Song L., Aston P.R., Patel B., Krasnoff S.B., Crane B.R., Gibson D.M., Loria R., Challis G.L. (2012). Cytochrome P450-catalyzed L-tryptophan nitration in thaxtomin phytoxin biosynthesis. *Nat Chem Biol*, 8:814-6.
- Bell K.S., Sebaihia M., Pritchard L., Holden M.T., Hyman L.J., Holeva M.C., Thomson N.R., Bentley S.D., Churcher L.J., Mungall K., Atkin R., Bason N., Brooks K., Chillingworth T., Clark K., Doggett J., Fraser A., Hance Z., Hauser H., Jagels K., Moule S., Norbertczak H., Ormond D., Price C., Quail M.A., Sanders M., Walker D., Whitehead S., Salmond G.P., Birch P.R., Parkhill J., Toth I.K. (2004). Genome sequence of the enterobacterial phytopathogen *Erwinia carotovora* subsp. *atroseptica* and characterization of virulence factors. *Proc Natl Acad Sci USA*, 101:11105-10.
- Bender C.L., Alarcon-Chaidez F., Gross D.C. (1999). *Pseudomonas syringae* phytotoxins: mode of action, regulation, and biosynthesis by peptide and polyketide synthetases. *Microbiol Mol Biol Rev*, 63:266-92.
- Bignell D.R., Seipke R.F., Huguet-Tapia J.C., Chambers A.H., Parry R., Loria R. (2010). *Streptomyces scabies* 87-22 contains a coronafacic acid-like biosynthetic cluster

- that contributes to plant-microbe interactions. *Mol Plant Microbe Interact*, 23:161-175.
- Bown L., Altowairish M.S., Fyans J.K., Bignell D.R.D. (2016). Production of the *Streptomyces scabies* coronafacoyl phytotoxins involves a novel biosynthetic pathway with an F₄₂₀-dependent oxidoreductase and a short-chain dehydrogenase/reductase. *Mol Microbiol*, 101:122-35.
- Browse J. (2009). Jasmonate passes muster: a receptor and targets for the defense hormone. *Annu Rev Plant Biol*, 60:183-205.
- Chan Y.A., Podevels A.M., Kevany B.M., Thomas M.G. (2009). Biosynthesis of polyketide synthase extender units. *Nat Prod Rep*, 26:90-114.
- Chen H., Hubbard B.K., O'Connor S.E., Walsh C.T. (2002). Formation of beta-hydroxy histidine in the biosynthesis of nikkomycin antibiotics. *Chem Biol*, 9:103-12.
- Cheng Z., Bown L., Tahlan K., Bignell D.R.D. (2015). Regulation of coronafacoyl phytotoxin production by the PAS-LuxR family regulator CfaR in the common scab pathogen *Streptomyces scabies*. *PLoS One*, 10:e0122450.
- Felsenstein J. (1985). Confidence limits on phylogenies: an approach using the bootstrap. *Evolution*, 39:783-791.
- Finn R.D., Tate J., Mistry J., Coghill P.C., Sammut S.J., Hotz H.R., Ceric G., Forslund K., Eddy S.R., Sonnhammer E.L., Bateman A. (2008). The Pfam protein families database. *Nucleic Acids Res*, 36:D281-8.

- Fischbach M.A., Walsh C.T., Clardy J. (2008). The evolution of gene collectives: How natural selection drives chemical innovation. *Proc Natl Acad Sci USA*, 105:4601-8.
- Fonseca S., Chini A., Hamberg M., Adie B., Porzel A., Kramell R., Miersch O., Wasternack C., Solano R. (2009). (+)-7-iso-Jasmonoyl-L-isoleucine is the endogenous bioactive jasmonate. *Nat Chem Biol*, 5:344-50.
- Fyans J.K., Altowairish M.S., Li Y., Bignell D.R.D. (2015). Characterization of the coronatine-like phytotoxins produced by the common scab pathogen *Streptomyces scabies*. *Mol Plant Microbe Interact*, 28:443-454.
- Geng X., Cheng J., Gangadharan A., Mackey D. (2012). The coronatine toxin of *Pseudomonas syringae* is a multifunctional suppressor of Arabidopsis defense. *Plant Cell*, 24:4763-74.
- Glazebrook J. (2005). Contrasting mechanisms of defense against biotrophic and necrotrophic pathogens. *Annu Rev Phytopathol*, 43:205-27.
- Gust B., Challis G.L., Fowler K., Kieser T., Chater K.F. (2003). PCR-targeted *Streptomyces* gene replacement identifies a protein domain needed for biosynthesis of the sesquiterpene soil odor geosmin. *Proc Natl Acad Sci USA*, 100:1541-6.
- Gust B., Chandra G., Jakimowicz D., Yuqing T., Bruton C.J., Chater K.F. (2004). Lambda red-mediated genetic manipulation of antibiotic-producing *Streptomyces*. *Adv Appl Microbiol*, 54:107-28.

- Hasegawa M., Kishino H., Yano T. (1985). Dating of the human-ape splitting by a molecular clock of mitochondrial DNA. *J Mol Evol*, 22:160-74.
- Hatanaka H., Kino T., Miyata S., Inamura N., Kuroda A., Goto T., Tanaka H., Okuhara M. (1988). FR-900520 and FR-900523, novel immunosuppressants isolated from a *Streptomyces*. II. Fermentation, isolation and physico-chemical and biological characteristics. *J Antibiot (Tokyo)*, 41:1592-601.
- Healy F.G., Krasnoff S.B., Wach M., Gibson D.M., Loria R. (2002). Involvement of a cytochrome P450 monooxygenase in thaxtomin A biosynthesis by *Streptomyces acidiscabies*. *J Bacteriol*, 184:2019-29.
- Kaneko T., Minamisawa K., Isawa T., Nakatsukasa H., Mitsui H., Kawaharada Y., Nakamura Y., Watanabe A., Kawashima K., Ono A., Shimizu Y., Takahashi C., Minami C., Fujishiro T., Kohara M., Katoh M., Nakazaki N., Nakayama S., Yamada M., Tabata S., Sato S. (2010). Complete genomic structure of the cultivated rice endophyte *Azospirillum* sp. B510. *DNA Res*, 17:37-50.
- Katsir L., Schilmiller A.L., Staswick P.E., He S.Y., Howe G.A. (2008). COI1 is a critical component of a receptor for jasmonate and the bacterial virulence factor coronatine. *Proc Natl Acad Sci USA*, 105:7100-5.
- Kieser T., Bibb M.J., Buttner M.J., Chater K.F., Hopwood D.A. (2000). Practical *Streptomyces* Genetics. The John Innes Foundation, Norwich, UK.

- Kumar S., Stecher G., Tamura K. (2016). MEGA7: Molecular Evolutionary Genetics Analysis Version 7.0 for Bigger Datasets. *Mol Biol Evol*, 33:1870-4.
- Kwan D.H., Sun Y., Schulz F., Hong H., Popovic B., Sim-Stark J.C., Haydock S.F., Leadlay P.F. (2008). Prediction and manipulation of the stereochemistry of enoylreduction in modular polyketide synthases. *Chem Biol*, 15:1231-40.
- Liu H., Reynolds K.A. (1999). Role of crotonyl coenzyme A reductase in determining the ratio of polyketides monensin A and monensin B produced by *Streptomyces cinnamonensis*. *J Bacteriol*, 181:6806-13.
- Machida K., Arisawa A., Takeda S., Tsuchida T., Aritoku Y., Yoshida M., Ikeda H. (2008). Organization of the biosynthetic gene cluster for the polyketide antitumor macrolide, pladienolide, in *Streptomyces platensis* Mer-11107. *Biosci Biotechnol Biochem*, 72:2946-52.
- MacNeil D.J., Gewain K.M., Ruby C.L., Dezeny G., Gibbons P.H., MacNeil T. (1992). Analysis of *Streptomyces avermitilis* genes required for avermectin biosynthesis utilizing a novel integration vector. *Gene*, 111:61-68.
- Munro A.W., Girvan H.M., Mason A.E., Dunford A.J., McLean K.J. (2013). What makes a P450 tick? *Trends Biochem Sci*, 38:140-50.
- Nelson D.R., Koymans L., Kamataki T., Stegeman J.J., Feyereisen R., Waxman D.J., Waterman M.R., Gotoh O., Coon M.J., Estabrook R.W., Gunsalus I.C., Nebert

- D.W. (1996). P450 superfamily: update on new sequences, gene mapping, accession numbers and nomenclature. *Pharmacogenetics*, 6:1-42.
- Pieterse C.M., Zamioudis C., Berendsen R.L., Weller D.M., Van Wees S.C., Bakker P.A. (2014). Induced systemic resistance by beneficial microbes. *Annu Rev Phytopathol*, 52:347-75.
- Qi M., Wang D., Bradley C.A., Zhao Y. (2011). Genome sequence analyses of *Pseudomonas savastanoi* pv. *glycinea* and subtractive hybridization-based comparative genomics with nine pseudomonads. *PLoS One*, 6:e16451.
- Rodriguez A.M., Olano C., Mendez C., Hutchinson C.R., Salas J.A. (1995). A cytochrome P450-like gene possibly involved in oleandomycin biosynthesis by *Streptomyces antibioticus*. *FEMS Microbiol Lett*, 127:117-20.
- Sambrook J., Fritsch E.F., Maniatis T. (1989). Molecular cloning: a laboratory manual, 2nd ed. Cold Spring Harbor Laboratory, Cold Spring Harbor, N.Y.
- Santorum J.M., Darriba D., Taboada G.L., Posada D. (2014). jmodeltest.org: selection of nucleotide substitution models on the cloud. *Bioinformatics*, 30:1310-1.
- Slawiak M., Lojkowska E. (2009). Genes responsible for coronatine synthesis in *Pseudomonas syringae* present in the genome of soft rot bacteria. *Eur J Plant Pathol*, 124:353-361.
- Smith S., Tsai S.C. (2007). The type I fatty acid and polyketide synthases: a tale of two megasynthases. *Nat Prod Rep*, 24:1041-72.

- Stassi D.L., Kakavas S.J., Reynolds K.A., Gunawardana G., Swanson S., Zeidner D., Jackson M., Liu H., Buko A., Katz L. (1998). Ethyl-substituted erythromycin derivatives produced by directed metabolic engineering. *Proc Natl Acad Sci USA*, 95:7305-9.
- Tamura K., Nei M. (1993). Estimation of the number of nucleotide substitutions in the control region of mitochondrial DNA in humans and chimpanzees. *Mol Biol Evol*, 10:512-26.
- Thaler J.S., Humphrey P.T., Whiteman N.K. (2012). Evolution of jasmonate and salicylate signal crosstalk. *Trends Plant Sci*, 17:260-70.
- Wasternack C., Hause B. (2013). Jasmonates: biosynthesis, perception, signal transduction and action in plant stress response, growth and development. An update to the 2007 review in Annals of Botany. *Ann Bot*, 111:1021-58.
- Xin X.F., He S.Y. (2013). *Pseudomonas syringae* pv. *tomato* DC3000: a model pathogen for probing disease susceptibility and hormone signaling in plants. *Annu Rev Phytopathol*, 51:473-98.
- Xue Y., Wilson D., Zhao L., Liu H., Sherman D.H. (1998). Hydroxylation of macrolactones YC-17 and narbomycin is mediated by the *pikC* - encoded cytochrome P450 in *Streptomyces venezuelae*. *Chem Biol*, 5:661-7.
- Ziemert N., Jensen P.R. (2012). Phylogenetic approaches to natural product structure prediction. *Methods Enzymol*, 517:161-82.

3.8 Figures and Tables

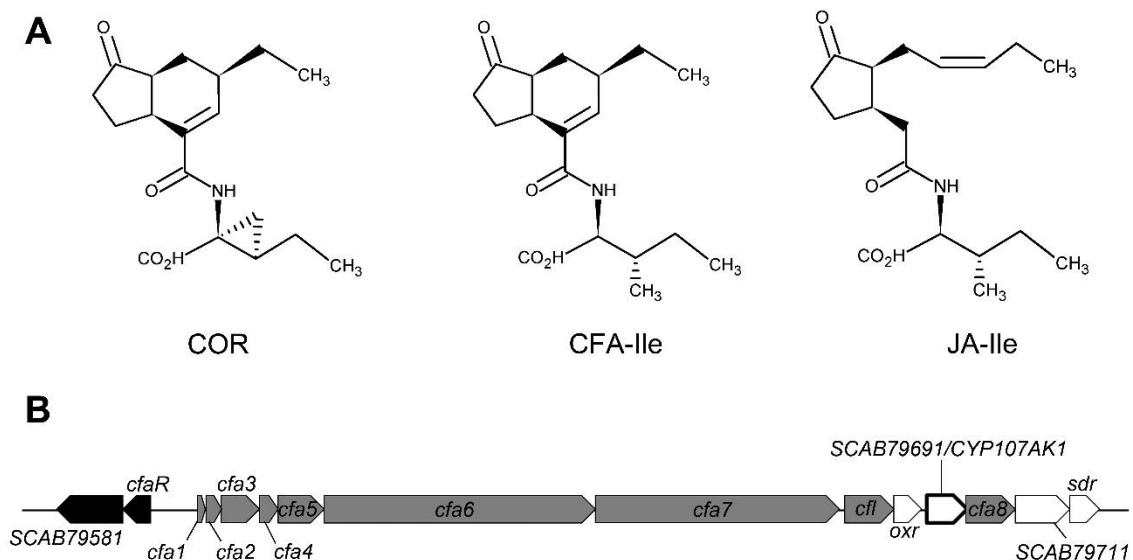


Figure 3.1. (A) Structure of the coronafacoyl phytotoxins coronatine (COR) and coronafacoyl-L-isoleucine (CFA-Ile) produced by *P. syringae* and *S. scabiei*, respectively, and of the bioactive plant hormone conjugate (+)-7-*iso*-jasmonyl-L-isoleucine (JA-Ile). (B) Organization of the CFA biosynthetic gene cluster from *S. scabiei* 87-22. Regulatory genes are indicated in black, biosynthetic genes that have homologues in the *P. syringae* CFA biosynthetic gene cluster are indicated in gray, and biosynthetic genes unique to the *S. scabiei* gene cluster are indicated in white. The *CYP107AK1* gene is highlighted in bold.

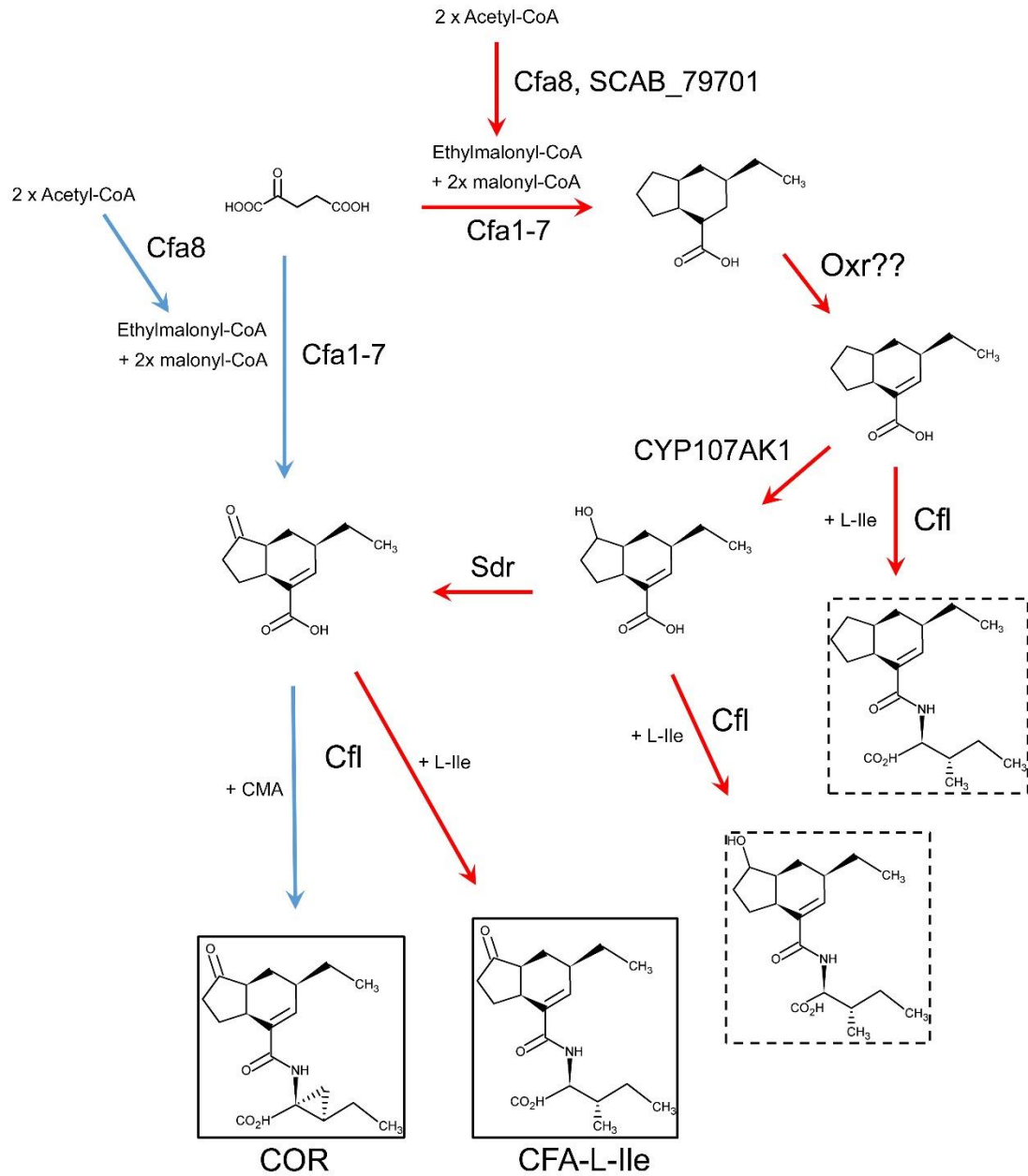


Figure 3.2. Proposed biosynthetic pathways for the production of coronafacoyl phytotoxins in *P. syringae* and *S. scabies*. The hypothetical pathway in *P. syringae* is indicated by the blue arrows, whereas the hypothetical pathway in *S. scabies* is indicated by the red arrows. Biosynthetic intermediates that have been isolated from *S. scabies* biosynthetic mutants are indicated with hatched boxes.

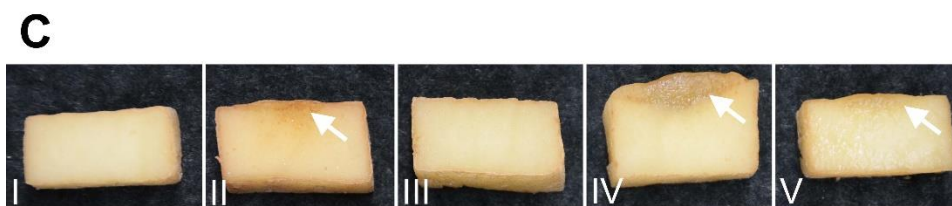
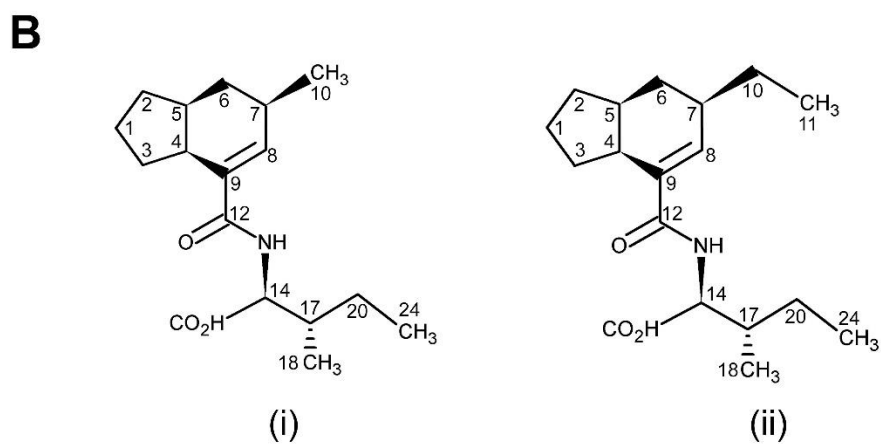
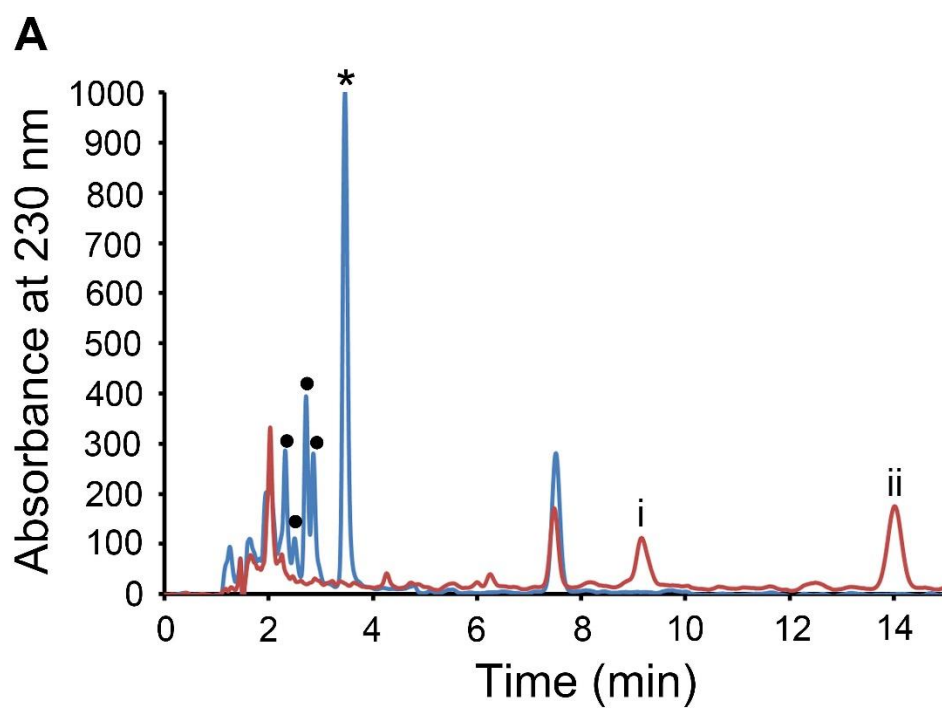


Figure 3.3. (A) RP-HPLC analysis of culture extracts from the *S. scabies* $\Delta txtA$ /pRLDB51-1 strain (blue line) and the $\Delta CYP107AK1$ mutant (red line). The peak corresponding to the CFA-Ile coronafacoyl phytotoxin is indicated with (*), and the peaks corresponding to minor coronafacoyl phytotoxins are indicated with (•). The two intermediates (i and ii) that accumulated in the $\Delta CYP107AK1$ mutant extract are also indicated. (B) Chemical structure of the purified intermediates i and ii. The carbon atoms are numbered according to the numbering scheme used for the raw data analysis (see Table S-3.1). (C) Hypertrophy-inducing activity of organic culture extracts of *S. scabies* $\Delta txtA$ /pRLDB51-1 (IV) and $\Delta CYP107AK1$ (V) on potato tuber tissue. Pure COR (1 nmol) was included as a positive control (II), while organic solvent (100% methanol; I) and culture extract from the CFA-Ile-deficient *S. scabies* strain $\Delta txtA/\Delta cfa6$ (III), were included as negative controls. The observed tissue hypertrophy is indicated by the white arrows. (D) Hypertrophy-inducing activity of purified CFA-Ile (III) and of the $\Delta CYP107AK1$ mutant intermediates i (IV) and ii (V) on potato tuber tissue. Solvent (methanol + 0.1% formic acid) served as a negative control (I) while pure COR (1 nmol) was used as a positive control (II). The observed tissue hypertrophy is indicated by the white arrows.

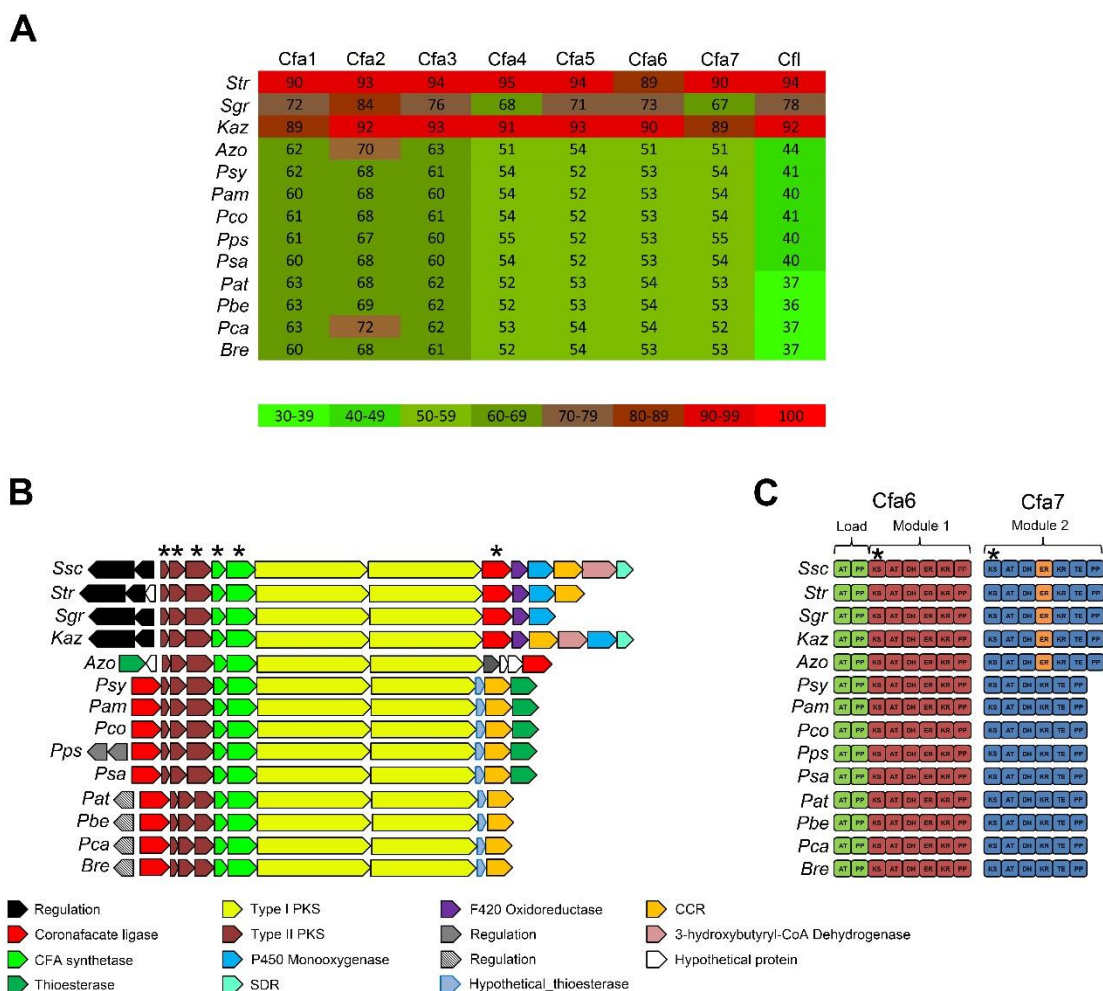


Figure 3.4. (A) Heat map showing the protein BLAST identity hits to the *S. scabies* 87-22 Cfa1-7 and Cfl proteins in different bacterial genomes. The actual % amino acid identity is indicated in each square. Abbreviations are as follows: *Str*, *Streptomyces* sp. NRRL WC-3618; *Sgr*, *Streptomyces griseoruber* DSM40281; *Kaz*, *Kitasatospora azatica* ATCC9699; *Azo*, *Azospirillum* sp. B510, *Psy*, *Pseudomonas syringae* pv *tomato* DC3000; *Pam*, *Pseudomonas amygdali* pv *morsprunorum*, *Pco*, *Pseudomonas coronafaciens* pv

porri LMG 28495; *Pps*, *Pseudomonas psychrotolerans* NS274; *Psa*, *Pseudomonas savastanoi* pv *glycinea* B076; *Pat*, *Pectobacterium atrosepticum* SCRI1043; *Pbe*, *Pectobacterium betavascularum* NCPPB 2795; *Pca*, *Pectobacterium carotovorum* subsp. *carotovorum* UGC32; *Bre*, *Brenneria* sp. EniD312. (B) Organization of known and putative CFA biosynthetic gene clusters identified in sequenced bacterial genomes. Related genes are indicated in the same colour, and the known or predicted functions are indicated below. * denotes the genes that were used for construction of the concatenated phylogenetic tree (Fig. 3.6-A). *Ssc* = *Streptomyces scabies* 87-22. (C) Domain organization of the Cfa6 and Cfa7 type I polyketide synthases encoded in the CFA biosynthetic gene clusters from different bacteria. The different modules (load, module 1 and 2) are indicated as well as the enoyl reductase (ER) domain that is only found in a subset of Cfa7 proteins (indicated in orange). * denotes the domain nucleotide sequences that were used for construction of the concatenated phylogenetic tree (Fig. 3.6-A). Abbreviations are as follows: AT, acyltransferase; PP, phosphopantetheinate; KS, ketosynthase; DH, dehydratase; KR, ketoreductase; TE, thioesterase.

<i>Azospirillum</i> sp. B510	HA GT GG T GMA
<i>Kitasatospora azatica</i>	HA G AGGVGMA
<i>Streptomyces griseoruber</i>	HAAAGGVGMA
<i>Streptomyces scabies</i>	HAAAGGVGMA
<i>Streptomyces</i> sp. NRRL WC3618	HAAAGGVGMA
Consensus binding motif	HAAAGGVGMA

Figure 3.5. NAD(P)H binding motifs from the Cfa7 ER domains of *S. scabies*, *Azospirillum* sp. B510, *K. azatica*, *S. griseoruber* and *Streptomyces* sp. WC3618. The consensus NAD(P)H cofactor binding motif is indicated in bold. Differences in motif sequences as compared to the consensus sequence are indicated in red.

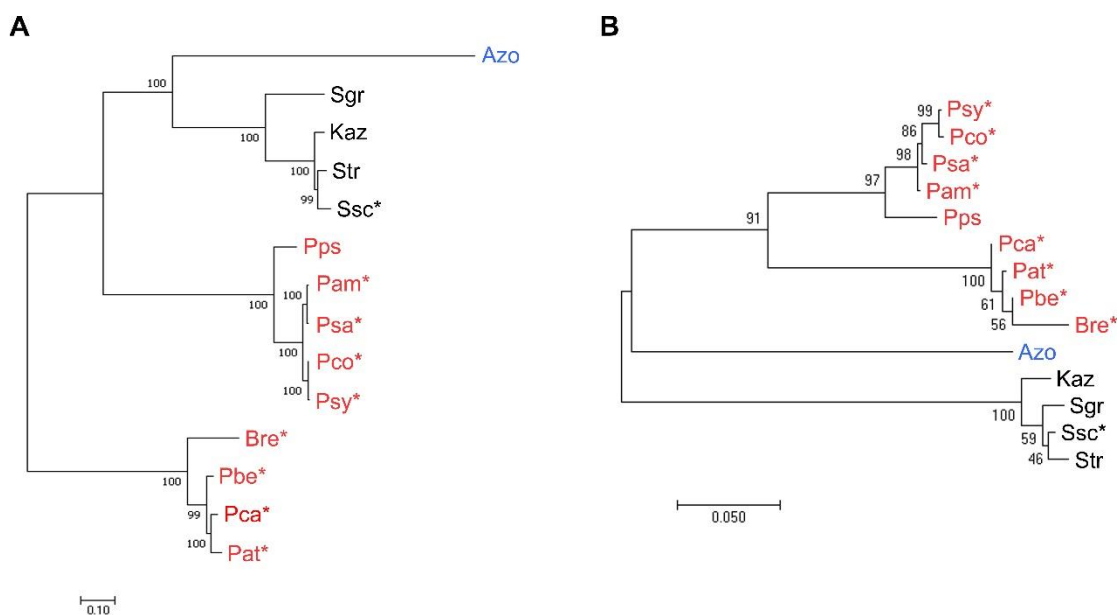


Figure 3.6. Maximum likelihood phylogeny of the core CFA biosynthetic genes (A) and the 16S rRNA gene (B) from different bacteria. The CFA biosynthetic gene cluster tree was constructed using the concatenated *cfa1-5*, *cfl*, *cfa6* (*ks*) and *cfa7* (*ks*) nucleotide sequences. Bootstrap values $\geq 50\%$ are shown at the respective branch points and are based on 100 repetitions for the CFA gene cluster tree and 1000 repetitions for the 16S rRNA gene tree. The scale bars indicate the number of nucleotide substitutions per site. Gammaproteobacteria are indicated in red, Alphaproteobacteria are indicated blue, and Actinobacteria are indicated in black. Known plant pathogenic organisms are indicated with *. Abbreviations are as described for Figure 3.4.

Table 3.1. Bacterial strains, cosmids and plasmids used in this study.

Strain, Plasmid or Cosmid	Description	Antibiotic Resistance†	Reference or Source
<i>Escherichia coli</i> strains			
BW25113/pIJ790	Host for Redirect PCR targeting system	cam ^r	Gust et al. 2003; Gust et al. 2004
ET12567/pUZ8002	Non-methylating host (<i>dam</i> ⁻ <i>dcm</i> ⁻ <i>hsdM</i> ⁻); carries the pUZ8002 plasmid that encodes the machinery for the conjugal transfer of DNA into <i>Streptomyces</i>	cam ^r , tet ^r , kan ^r	Kieser et al. 2000; MacNeil et al. 1992
<i>Streptomyces scabies</i> strains			
Δ <i>txtA</i> /pRLDB51-1	<i>S. scabies</i> strain containing a deletion of the <i>txtA</i> gene and carrying the <i>cfaR</i> (<i>scab79591</i>) overexpression plasmid pRLDB51-1	thio ^r , apra ^r	Bignell et al. 2010
Δ <i>txtA</i> /Δ <i>cfa6</i>	<i>S. scabies</i> strain containing a deletion of the <i>txtA</i> and <i>cfa6</i> genes	hyg ^r , apra ^r	Bignell et al. 2010
Δ <i>CYP107AK1</i>	Δ <i>txtA</i> /pRLDB51-1 derivative containing a deletion of the <i>CYP107AK1</i> (<i>scab79691</i>) gene	thio ^r , apra ^r , hyg ^r	This study
Plasmid or cosmid			
pIJ10700	Template for PCR amplification of the [<i>hyg+oriT</i>] cassette used for PCR targeting	hyg ^r	Gust et al. 2004
Cosmid 1770	SuperCos1 derivative containing the <i>S. scabies</i> CFA biosynthetic gene cluster	amp ^r , kan ^r	Bignell et al. 2010
1770/Δ <i>CYP107AK1</i>	Cosmid 1770 derivative in which the <i>CYP107AK1</i> gene was replaced with the [<i>hyg+oriT</i>] disruption cassette	amp ^r , kan ^r , hyg ^r	This study

† cam^r, tet^r, kan^r, thio^r, apra^r, hyg^r and amp^r = chloramphenicol, tetracycline, kanamycin, thiostrepton, apramycin, hygromycin B and ampicillin resistance, respectively.

3.9 Supplementary Information

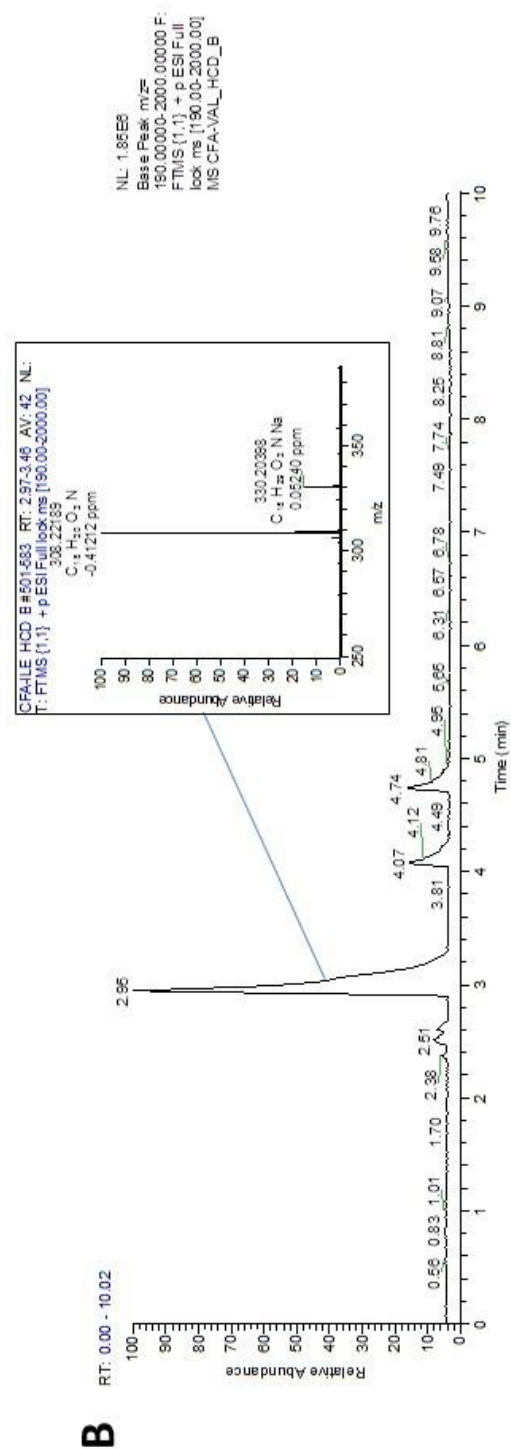
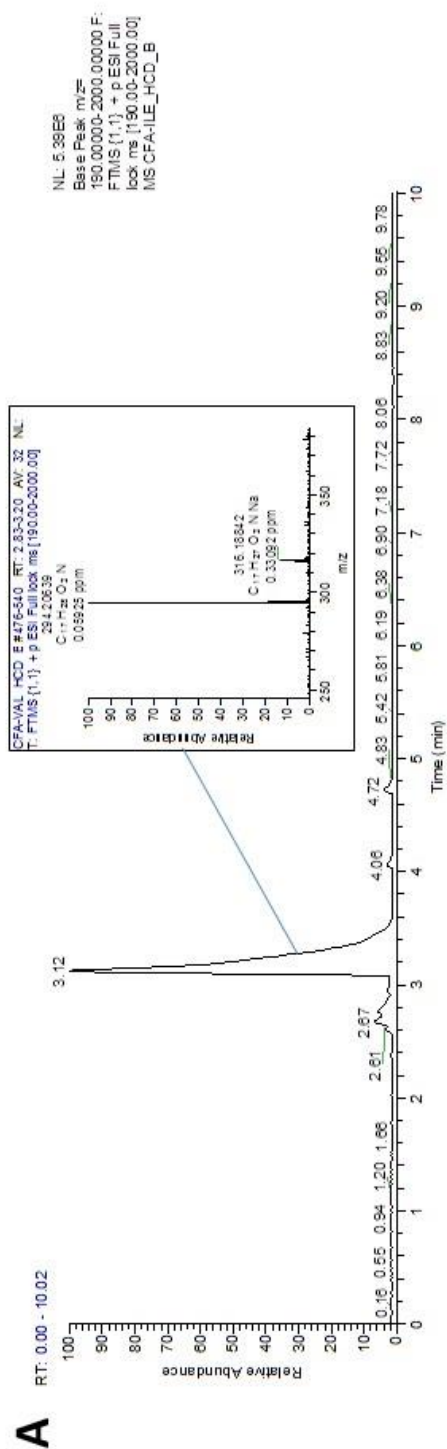


Figure S-3.1. LC-HRMS analysis of the purified intermediates i (A) and ii (B) from the *S. scabies* $\Delta CYP107AK1$ mutant.

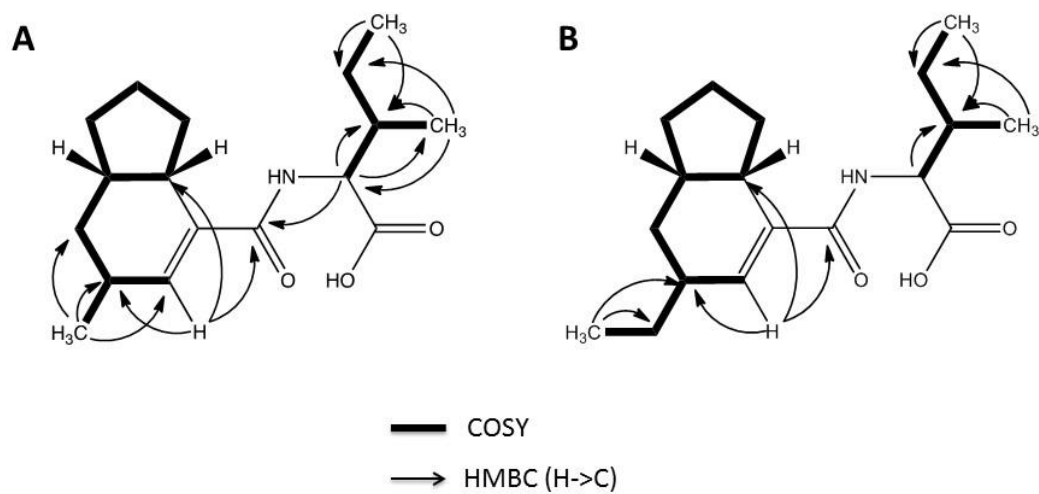


Figure S-3.2. Key COSY and HMBC correlations of the purified intermediates i (A) and ii (B) from the *S. scabiei* $\Delta CYP107AK1$ mutant.

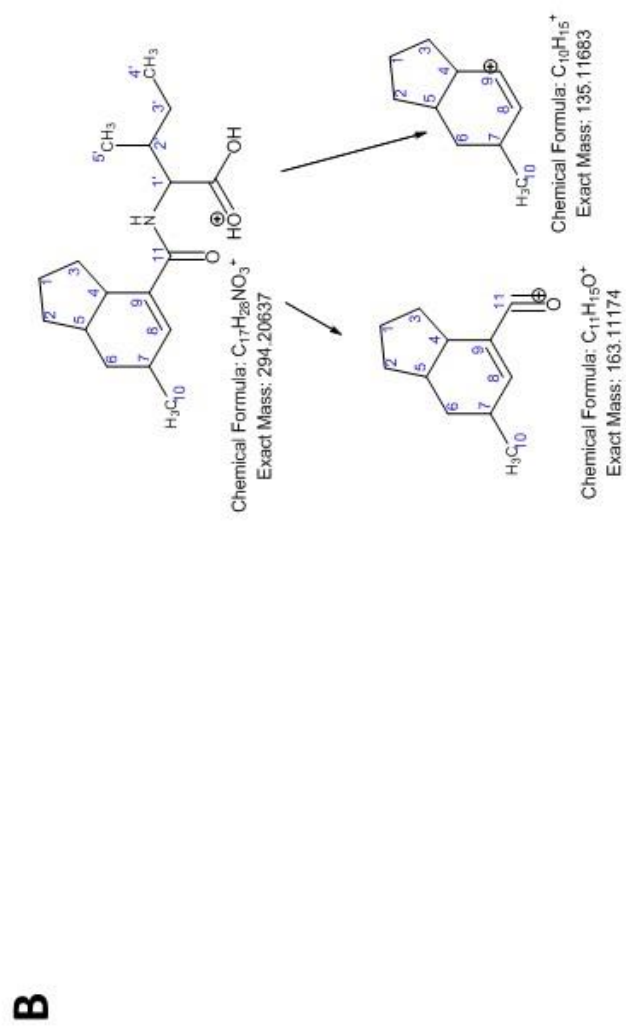
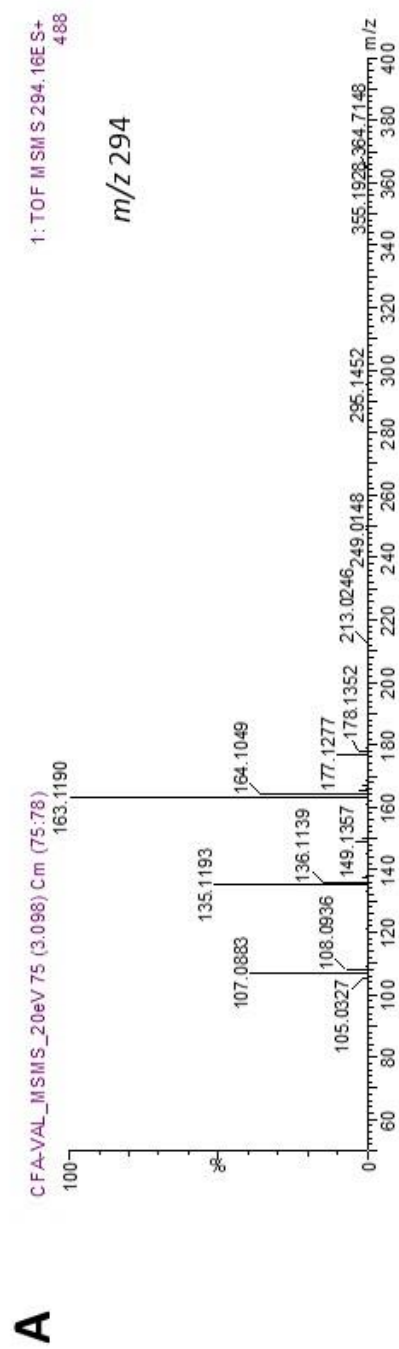


Figure S-3.3. (A) Tandem MS spectrum of the purified intermediate **i**. The presence of the ion fragments at m/z 163.1190 and 135.1193 confirm the proposed structure of **i**. (B) Expected fragmentation pattern of the intermediate **i**.

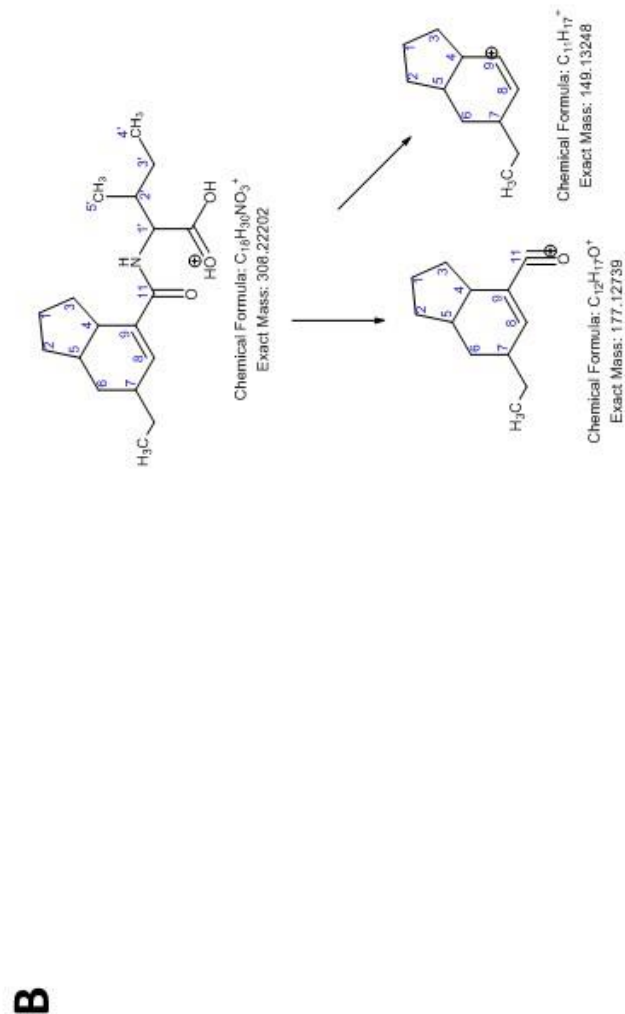
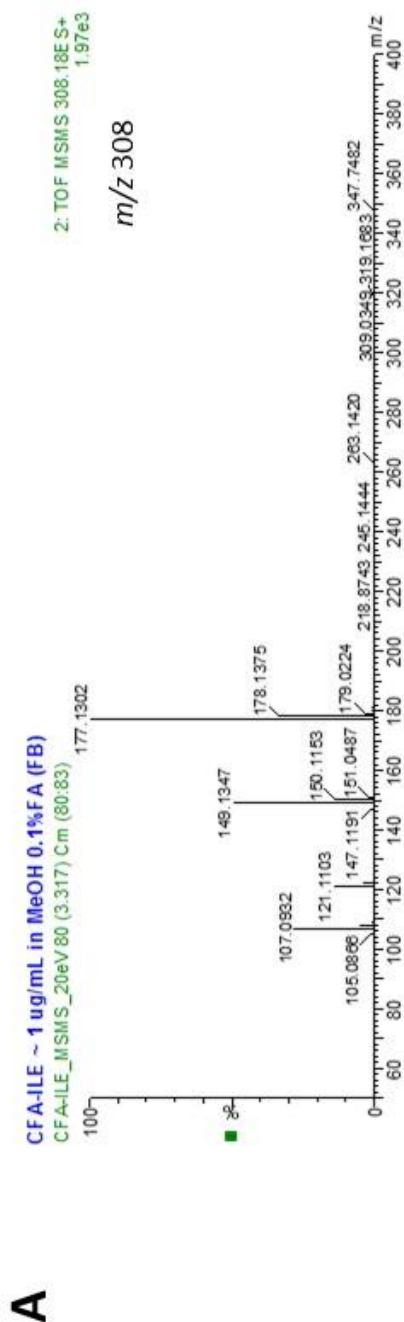


Figure S-3.4. (A) Tandem MS spectrum of the purified intermediate ii. The presence of the ion fragments at m/z 177.1302 and 149.1347 confirm the proposed structure of ii. (B) Expected fragmentation pattern of the intermediate ii.

Chapter 4: Purification of *N*-Coronafacoyl Phytotoxins from *Streptomyces scabies*

Luke Bown and Dawn R. D. Bignell

Department of Biology, Memorial University of Newfoundland, St. John's, NL, Canada

For correspondence: dbignell@mun.ca

4.1 Abstract

This procedure is used for large-scale purification of *N*-coronafacoyl phytotoxins that are produced by the potato common scab pathogen *Streptomyces scabies*. The procedure employs organic extraction of *S. scabies* culture supernatants under alternating basic and acidic conditions in order to preferentially isolate the phytotoxin-containing carboxylic acid fraction of the supernatant. Preparative thin layer chromatography and semi-preparative reverse phase - high performance liquid chromatography are then used to further purify the individual *N*-coronafacoyl phytotoxins of interest.

4.2 Introduction

Potato common scab is an economically important crop disease that is caused by Gram-positive, filamentous, soil bacteria from the genus *Streptomyces*. The first described and best characterized scab - causing *Streptomyces* spp. is *Streptomyces scabies* (syn.

S. scabiei), which has a worldwide distribution (Bignell et al. 2010). Current control practices for common scab disease management include crop rotation, irrigation and soil fumigation; however, these strategies often fail, produce inconsistent results or are environmentally unfriendly (Dees and Wanner 2012). In order to develop better control strategies for the disease, we must first understand the molecular mechanisms used by *S. scabies* to infect the plant and to induce disease symptoms. Research has shown that the ability of *S. scabies* to cause disease is due to the production of virulence factors that play different roles during the infection process. Among the known or potential virulence factors that are produced by *S. scabies* is a family of plant toxins referred to as the *N*-coronafacoyl phytotoxins (also known as the COR-like metabolites), which resemble the plant hormone jasmonic acid and may function to suppress the plant immune response during pathogen infection (Bignell et al. 2010; Fyans et al. 2015). The primary coronafacoyl phytotoxin produced by *S. scabies* is *N*-coronafacoyl-L-isoleucine (CFA-L-Ile; Fig. 4.1), which consists of the polyketide metabolite coronafacic acid linked via an amide bond to L-isoleucine. In addition, other *N*-coronafacoyl phytotoxins containing different isoleucine isomers or different amino acids (*e.g.*, valine) can be produced in minor amounts (Bown et al. 2016; Fyans et al. 2015).

The protocol described here was developed to isolate and purify *N*-coronafacoyl phytotoxins and their biosynthetic intermediates from large-scale cultures of *S. scabies* for purposes of structural and functional characterization. Previously, Fyans et al. (2015) described a protocol that was based in part on a published procedure for the isolation of the related *N*-coronafacoyl phytotoxin coronatine (COR) from cultures of the Gram-negative

plant pathogenic bacterium *Pseudomonas syringae* (Palmer and Bender 1993). As outlined by Fyans et al. (2015), strains of *S. scabies* are cultured in a soy flour mannitol broth (SFMB) medium, which promotes the production of the coronafacoyl phytotoxins, and then the culture supernatants are subjected to a two-step extraction with organic solvent under basic and acidic conditions in order to selectively isolate the phytotoxin-containing carboxylic acid fraction of the culture supernatants. The phytotoxins are then further purified using a combination of preparative thin layer chromatography (TLC) and semi-preparative reverse phase-high performance liquid chromatography (RP-HPLC). More recently, we described a modified version of this protocol in which we incorporated additional extraction steps using an aqueous solution of potassium bicarbonate (Bown et al. 2016). This modification was based on the procedure described by Mitchell and Frey (1986) for the isolation of *P. syringae* *N*-coronafacoyl phytotoxins, and we found that the incorporation of the additional extraction steps significantly improved the purity of the final *S. scabies* phytotoxin preparations. Moreover, we modified the organic solvent for the *N*-coronafacoyl phytotoxins by the addition of a small amount of acid, which significantly improved the solubility and yield of the purified phytotoxins for downstream structural and functional studies.

Here, we present the detailed step-by-step protocol for how we currently purify the *S. scabies* *N*-coronafacoyl phytotoxins in our laboratory.

4.3 Materials and Reagents

1. pH test strips (VWR, BDH[®], catalog number: [BDH35309.606](#))
2. Hydrophilic polypropylene membrane filters, 47 mm diameter, 0.45 µm pore size (Pall, catalog number: [66548](#))
3. Fisherbrand[™] class B clear glass threaded vials with closures attached, 3.7 ml (Fisher Scientific, catalog number: [03-338A](#))
4. Slip tip syringes, 1 ml (BD, catalog number: [309659](#))
5. PTFE membrane filters, 0.2 µm pore size, 6 mm diameter (VWR, catalog number: [28145-491](#))
6. Whatman[™] filter discs, 12.5 cm (Sigma-Aldrich, catalog number: [WHA1113125](#))
7. Conical centrifuge tubes, 50 ml (Corning, Falcon[®], catalog number: [352098](#))
8. Silica gel GF preparative TLC plates with pre-adsorbent zone, 20 × 20 cm, 1,000 µm (Analtech/iChromatography, catalog number: [P32013](#))
9. DMSO mycelial freezer stock of *S. scabies* (Fyans *et al.*, 2015)
10. Bacto[™] tryptic soy broth medium (BD, Bacto[™], catalog number: [211825](#))
11. Sodium hydroxide (NaOH) (Fisher Scientific, catalog number: [BP359-212](#))
12. Chloroform, ACS grade (VWR, BDH[®], catalog number: [BDH1109](#))
13. Hydrochloric acid (HCl), ACS grade (Avantor[®] Performance Materials, catalog number: [638801](#))
14. Sodium sulfate anhydrous (Na₂SO₄), ACS grade (Fisher Scientific, catalog number: [S421-500](#))
15. Ethylene glycol (VWR, BDH[®], catalog number: [BDH1125](#))

16. Potassium bicarbonate (KHCO_3), ACS grade (Sigma-Aldrich, catalog number: [237205](#))
17. Methanol (MeOH), HPLC grade (Sigma-Aldrich, catalog number: [34860](#))
18. Formic acid, reagent grade (Sigma-Aldrich, catalog number: [F0507](#))
19. HiPerSolv CHROMANORM[®] Acetonitrile (ACN) for HPLC (VWR, BDH[®], catalog number: [BDH83639.400](#))
20. Soy flour, defatted (MP Biomedicals, catalog number: [960024](#))
21. D-mannitol (AMRESCO, catalog number: [0122](#))
22. Ethyl acetate, ACS grade (Sigma-Aldrich, catalog number: [319902](#))
23. 2-propanol, HPLC grade (Fisher Scientific, catalog number: [A451SK-4](#))
24. Acetic acid, ACS grade (Sigma-Aldrich, catalog number: [695092](#))
25. Water, HPLC grade (EMD Millipore, catalog number: [WX0008-1](#))
26. Soy flour mannitol broth (SFMB) medium (see Recipes)
27. Preparative TLC mobile phase (see Recipes)

4.4 Equipment

1. Glass Erlenmeyer flask, 125 ml (Corning, Pyrex[®], catalog number: [C4980125](#))
2. Glass Erlenmeyer flask, 4 L (Corning, Pyrex[®], catalog number: [C49804L](#))
3. Glass filter holder assembly with funnel, fritted base, stopper and clamp, 47 mm (EMD Millipore, catalog number: [XX1004700](#))
4. Nalgene[™] PPCO centrifuge bottles with sealing closure, 250 ml (Thermo Fisher Scientific, Thermo Scientific[™], catalog number: [31410250](#))

5. Sorval™ ST 16R benchtop refrigerated centrifuge (Thermo Fisher Scientific, Thermo Scientific™, model: Sorval™ ST 16R, catalog number: [BCT25](#))
6. Innova® 42R refrigerated incubator shaker, orbit diameter 1.9 cm (Eppendorf, New Brunswick™, model: Innova® 42R, catalog number: [M1335-004](#))
7. 2 L plastic container
8. Nalgene™ Teflon™ FEP separatory funnel with closure, 2 L (Thermo Fisher Scientific, Thermo Scientific™, catalog number: [4301-2000](#))
9. IKA® rotary evaporator system (IKA®, model: [RV 10 digital V](#))
10. VWR® refrigerated circulating bath with programmable temperature controller (VWR, model: VWR® Refrigerated Circulating Baths, catalog number: [89202-982](#))
11. KIMAX® Squibb separatory funnel with PTFE stopcock and glass stopper, 125 ml (Kimble Chase Life Science and Research Products, catalog number: [29048F-125](#))
12. DryFast diaphragm vacuum pump (Welch Vacuum – Gardner Denver, catalog number: [2044](#))
13. Biohit mLINE® single-channel mechanical pipettor, 2-20 µl (VWR International, catalog number: [47745-545](#))
14. Aldrich® rectangular TLC developing tank (Sigma-Aldrich, model: [Z126195](#))
15. UV lamp with portable cabinet (Analtech/iChromatography, catalog number: [A93-04](#))
16. Metal spatula
17. Thermo Scientific™ dry block heater (Thermo Fisher Scientific, Thermo Scientific™, catalog number: [88-860-021](#))

18. ZORBAX StableBond 80Å C18 semi-preparative HPLC column, 9.4 x 250 mm, 5 µm (Agilent Technologies, catalog number: [880975-202](#))
19. Chemical safety hood
20. KIMAX® graduated filtering flask, 1 L (Kimble Chase Life Science and Research Products, catalog number: [27060-1000](#))
21. GeneMate vortex mixer (VWR, catalog number: [490000-094](#))
22. Agilent 1260 Infinity analytical-scale LC purification system with quaternary pump, autosampler, diode array detector and fraction collector (Agilent Technologies, model: [1260 Infinity](#))

4.5 Procedure

4.5.1 Culture growth

1. Prepare a seed culture of *S. scabiei* by inoculating 1 ml of the DMSO freezer stock into 25 ml of tryptic soy broth medium in a 125 ml Erlenmeyer flask, and incubate at 28 °C with shaking (200 RPM) for 48 hrs.
2. Subculture 10 ml of the seed culture into 1 L of SFMB medium in a 4 L Erlenmeyer flask, and incubate at 25 °C with shaking (200 RPM) for 10 days (see Notes 1 and 2).
3. Divide the culture into four 250 ml centrifuge bottles and centrifuge at $3,005 \times g$ for 15 min at 4 °C to pellet the cell material. Decant the supernatants into a 2 L plastic container and store at -20 °C until needed, discard cell pellets. Even if the

supernatant is going to be extracted immediately, it is useful to freeze it for a minimum of 24 hrs (see Note 3).

4.5.2 Organic extraction (see Fig. 7.2 and Note 4)

1. Measure the pH of the culture supernatant using a pH strip, and adjust the pH to 11-12 using a 5 N solution of NaOH (~4-5 ml).
2. Decant the supernatant into a 2 L separatory funnel and extract with 0.5 volumes (~450 ml) of chloroform. To perform the extraction, add the chloroform to the separatory funnel, close the funnel stopper, and shake the funnel to mix the contents well. Open the stopcock to release any expressed gas, then repeat the shaking until no more gas is expressed. Allow the organic (bottom) and aqueous (top) layers to separate as much as possible by gravity (~15-20 min; Figure 7.3-A), then open the stopcock and collect the organic layer. If an emulsion layer is present, this can be collected and separated by centrifugation at $3,005 \times g$ for 10 min at 4 °C, and the aqueous layer returned to the separatory funnel (Figure 4.3-B). Discard the organic layer, and repeat the extraction of the aqueous supernatant with another 0.5 volumes of fresh chloroform. Perform the extraction a total of three times, discarding the organic layer after each extraction (see Note 5).
3. Acidify the aqueous supernatant to a pH of 1-2 by adding 1 N HCl_(aq) (~5 ml).
4. Decant the supernatant back into the 2 L separatory funnel and extract with 0.5 volumes (~450 ml) of chloroform. Use the same extraction procedure as described under 2 except that now the organic layer should be collected and saved. Perform

the extraction a total of three times, after which the collected organic layers can be pooled and the aqueous layer discarded (see Note 6).

5. Remove any residual water from the organic extract by adding ~30 g of anhydrous Na_2SO_4 and gently swirling the mixture. The anhydrous Na_2SO_4 is added until it no longer forms clumps, indicating that all of the residual water has been absorbed.
6. Filter the organic extract using a 0.45 μm polypropylene membrane filter and a glass filter assembly attached to a vacuum pump. Wash the beaker that contained organic extract as well as the filter assembly with fresh chloroform to recover all of the residual extract.
7. Concentrate the organic extract to ~100 ml using a rotary evaporator. The evaporator heating bath (filled with water) should be set to 50 °C, and the condenser should be chilled with a circulating solution of 50% v/v ethylene glycol (chilled to -10 °C using a refrigerated circulating bath).
8. Transfer 50 ml of the organic concentrate into each of two 125 ml separatory funnels. Extract each concentrate with 0.5 volumes (25 ml) of a 0.5 M aqueous solution of KHCO_3 . After mixing, allow ~5 min for the phases to separate by gravity, then collect each phase separately. Repeat the extraction of the organic concentrates two more times, then pool the collected aqueous phases (to give two sets of aqueous extracts, ~75 ml each) and discard the organic extracts (see Note 7).
9. Wash the aqueous extracts twice with 0.5 volumes (35-40 ml) of chloroform. To wash, add the chloroform to a separatory funnel containing the aqueous extract, mix, then leave for 5 min to allow the phases to separate. Collect and discard the

organic layer, and repeat. After washing, combine the aqueous extracts together (total volume ~140-150 ml).

10. Adjust the pH of the aqueous extract to 1-2 using 1 N HCl_(aq) (~12-15 ml). The acid will cause a neutralization reaction with the KHCO₃ that will produce heat and a large amount of CO₂. The acid must be added slowly or the reaction can become violent and will cause the acid to splash. After each 1 ml of acid has been added, gently mix the solution until the CO₂ dissipates.
11. Pour ~40 ml of the aqueous extract into each of four 125 ml separatory funnels. Extract each aliquot three times with 0.5 volumes (20 ml) of chloroform. Collect and combine all of the organic extracts together, and discard the aqueous layers. Evaporate the organic extract to dryness overnight in an uncovered beaker in a chemical safety hood (see Note 8).

4.5.3 Preparative TLC (see Note 4)

1. Re-dissolve the dried organic extract in 2-3 ml of MeOH containing 0.1% v/v formic acid by pipetting up and down. Transfer the extract to a clean screw-capped glass vial. Rinse the beaker with an additional 1 ml of MeOH + 0.1% formic acid to recover residual amounts of the extract. Filter the extract into a new screw-capped vial using a 1 ml syringe and a 0.2 µm PTFE membrane filter.
2. Pour the TLC mobile phase (see Recipes) into a TLC developing tank and fill to a depth of ~2 cm. Saturate the air in the TLC chamber by placing two pieces of 12.5 cm filter paper into the tank and covering the tank for at least 30 min.

3. Mark a 5 × 20 cm analytical TLC plate with a pencil to indicate the submersion point of the mobile phase solution (see Note 9).
4. Apply at least ~30-50 µg of a standard of the molecule of interest (or of a comparative analogue; see Note 10) dissolved in 100% MeOH + 0.1% formic acid onto the TLC plate. Apply the standard at least 1 cm from the edge of the plate and at least 1 cm above the submersion mark on the plate.
5. Apply ~30-50 µl of the organic extract along ~2 cm of the plate width. Ensure that the applied extract is at least 1 cm from the edge of the plate, 1 cm above the submersion mark on the plate and 1 cm away from the previously applied standard (see Note 11).
6. Remove the filter paper discs from the TLC tank and place the TLC plate into the tank and cover. Allow the mobile phase to migrate to within 1 cm of the top of the plate (~20-40 min). Remove the TLC plate and allow to air dry (~15 min). Repeat the process.
7. Place the air dried TLC plate under a UV lamp and use a pencil to mark the positions of the applied standard and the *N*-coronafacoyl phytotoxin of interest in the organic extract (Figure 4.4).
8. Mark the preparative TLC plate with a pencil to indicate the area of the plate that will be submersed in the mobile phase solution.
9. Apply the organic extract along the entire width of the TLC plate, 10 µl at a time. Do not place any sample within 1 cm of either edge of the plate or within 1 cm of the marked submersed area (see Note 11).

10. Remove the filter paper discs from the TLC tank and place the TLC plate into the tank and cover. Allow the mobile phase to migrate to within 1 cm of the top of the plate (~1-1.5 hrs). Remove the plate from the tank and allow to air dry (~20-30 min). Return the plate to the tank and repeat the separation.
11. Place the air dried TLC plate under a UV lamp and use a pencil to mark the region of the plate where the *N*-coronafacoyl phytotoxin migrated to (Fig. 4.5; see Note 12).
12. Scrape the marked region using the flat edge of a metal spatula to remove the silica gel - bound metabolites. Transfer the silica gel to a Falcon conical tube and add 10 ml of MeOH + 0.1% v/v formic acid. Vortex the mixture, and then incubate at room temperature for 1 h, vortexing for 1 min every 10 min.
13. Centrifuge the mixture at $3,803 \times g$ for 5 min at room temperature to pellet the silica gel. Transfer the MeOH extract to a clean Falcon tube. Repeat the centrifugation of the silica gel mixture to recover as much of the MeOH extract as possible.
14. Filter the MeOH extract using a 1 ml syringe and a 0.2 μ m PTFE membrane filter. Concentrate the extract to a final volume of 1-1.5 ml using a dry heating block set to 60 °C (see Note 13).

4.5.4 Semi-preparative RP-HPLC

1. Begin running the HPLC mobile phase (30% ACN:70% H₂O, with 0.1% formic acid) through the C18 semi-preparative HPLC column (held at a constant

temperature of 50 °C) at a constant flow rate of 4 ml/min until the column is equilibrated.

2. Load 50 µl of the sample onto the column, and use the following mobile phase running conditions for sample separation: hold at 30% ACN:70% H₂O for 7.5 min, then increase linearly to 50% ACN:50% H₂O over a period of 12.5 min. Hold at 50% ACN:50% H₂O for 5 min, then return to initial conditions using a linear gradient over 7.5 min. Hold at the initial conditions for at least 12 min before beginning the next injection (see Note 14).
3. Monitor the separated metabolites using a detection wavelength of 230 nm, and collect fractions of the peak that corresponds to the desired *N*-coronafacoyl phytotoxin (see Note 15).
4. Repeat the sample injection, metabolite separation and fraction collection until all of the initial extract has been used.
5. Pool the collected fractions for the *N*-coronafacoyl phytotoxin of interest, and evaporate to dryness using a rotary evaporator. The evaporator heating bath (filled with water) should be set to 70 °C, and the condenser should be chilled with a circulating solution of 50% v/v ethylene glycol (chilled to -10 °C using a refrigerated circulating bath).
6. Re-dissolve the pure metabolite in 3 ml of MeOH + 0.1% v/v formic acid. Transfer the solution to a pre-weighed screw cap vial, and dry down in a heating block set to 60 °C.
7. Weigh the vial + dried sample, and calculate the weight of the purified sample. Store the dried sample at -20 °C until needed (see Notes 16 and 17).

4.6 Notes

1. We have observed variations in the production levels of the *N*-coronafacoyl phytotoxins depending on the strain of *S. scabies* that is used, and therefore the volume of culture that is grown may need to be altered depending on the production efficiency of the particular strain.
2. The large-scale cultures can be left to incubate for up to 14 days; however, the levels of metabolite present in the culture will not increase significantly after 10 days.
3. The freezing process forces proteins and any other dissolved material out of solution, which will then be removed during the first chloroform extraction. This will make the subsequent extractions cleaner and will allow for faster and more complete phase separation. Use of a plastic container to freeze/thaw the supernatant is recommended, since a glass beaker may crack during the freezing process.
4. All steps (with the exception of the centrifugation in steps B2 and C8) should be carried out in a chemical safety hood or a fume hood.
5. This step serves as a purification step since many non-carboxylic acid compounds will move into the organic phase under the basic pH conditions used. Carboxylic acids such as the *N*-coronafacoyl phytotoxins will be in the unprotonated form at the high pH and therefore will remain in the aqueous phase.
6. Under the pH conditions used, the *N*-coronafacoyl phytotoxins are in the protonated form and will therefore be more soluble in the chloroform than in the aqueous culture supernatant.

7. The pH of the KHCO_3 solution promotes deprotonation of the *N*-coronafacoyl phytotoxins and their subsequent movement into the aqueous phase.
8. This mixing stage produces a large amount of gas. Do not fill the 125 ml funnel with more than 75 ml of aqueous and organic solvent in total. If the funnel contains more than that volume, the expression of gas will force open the stopper or stopcock and the extract will be lost.
9. Steps C3-C7 are performed in order to determine the migration point of the *N*-coronafacoyl phytotoxin of interest. A pure sample of the molecule ($\sim 50 \mu\text{g}$) and a small portion of the organic extract ($\sim 30\text{-}50 \mu\text{l}$) are applied to a $5 \times 20 \text{ cm}$ analytical TLC plate, and separation is carried out using the same conditions that will be employed for the preparative TLC steps.
10. If a pure standard of the particular *N*-coronafacoyl phytotoxin of interest is not available, then the *N*-coronafacoyl phytotoxin coronatine (COR) can be used instead. This phytotoxin is available for purchase from Sigma-Aldrich Canada (catalog number: C8115).
11. For best results, make sure that the spotted extract has air dried before new extract is applied to the same area.
12. The position of the *N*-coronafacoyl phytotoxin of interest on the reference analytical TLC plate will not correspond exactly to the phytotoxin position on the preparative TLC plate (as demonstrated in Fig. 4.4 and 4.5). However, by comparing the relative position of the standard and extract bands on the reference plate, the location of the phytotoxin on the preparative TLC plate can be estimated. As the *N*-coronafacoyl phytotoxin of interest will not appear as a distinct band or fragment on the

preparative TLC plate but as a dark smear, it is recommended that an area of at least 1 cm past the edge of this smear is marked.

13. The sample should not be concentrated to a volume lower than this as otherwise the metabolites may precipitate out of solution.
14. The RP-HPLC running conditions described are suitable for separation of the CFA-L-Ile coronafacoyl phytotoxin from other metabolites in the extract. However, if minor *N*-coronafacoyl phytotoxins containing other isoleucine isomers (*e.g.*, D-isoleucine) are produced, they will not be separated from the CFA-L-Ile metabolite and will be co-purified. Also, if other *N*-coronafacoyl phytotoxins or biosynthetic intermediates are being targeted for purification, the RP-HPLC mobile phase running conditions may need to be adjusted accordingly in order to get good separation of those metabolites.
15. Using the HPLC column and running conditions described, the CFA-L-Ile coronafacoyl phytotoxin has a retention time of 18-19 min (Fig. 4.6).
16. The purified metabolite can also be re-dissolved in MeOH + 0.1% formic acid to a final concentration of 1 mg/ml, and then stored at -20 °C.
17. To confirm the purity of the metabolite, the sample can be analyzed using liquid chromatography-mass spectrometry (LC-MS) as described elsewhere (Bown et al. 2016).

4.7 Recipes

1. Soy flour mannitol broth (SFMB) medium (Kieser et al. 2000)

20 g/L soy flour

20 g/L d-mannitol

Dissolve mannitol in water

Add soy flour

Sterilize by autoclaving

2. Preparative TLC mobile phase (Fyans et al. 2015)

195 ml ethyl acetate

4 ml 2-propanol

0.5 ml acetic acid

0.5 ml water

4.8 Acknowledgments

This work was supported by grants from the Natural Sciences and Engineering Research Council of Canada (NSERC), the Canada Foundation for Innovation (CFI), and the Newfoundland and Labrador Research & Development Corporation (RDC) to D.R.D.B. L.B. was supported by a fellowship from the Memorial University School of Graduate Studies. This protocol is based on work originally reported in Bown *et al.* (2016) and Fyans *et al.* (2015).

4.9 References

- Bignell D.R., Huguet-Tapia J.C., Joshi M.V., Pettis G.S., Loria R. (2010). What does it take to be a plant pathogen: genomic insights from *Streptomyces* species. *Antoine van Leeuwenhoek*, 98(2): 179-194.
- Bown L., Altowairish M.S., Fyans J.K., Bignell D.R. (2016). Production of the *Streptomyces scabies* coronafacoyl phytotoxins involves a novel biosynthetic pathway with an F₄₂₀-dependent oxidoreductase and a short-chain dehydrogenase/reductase. *Mol Microbiol*, 101(1): 122-135.
- Dees M.W., Wanner L.A. (2012). In search of better management of potato common scab. *Potato Res*, 55: 249-268.
- Fyans J.K., Altowairish M.S., Li Y., Bignell D.R.D. (2015). Characterization of the coronatine-like phytotoxins produced by the common scab pathogen *Streptomyces scabies*. *Mol Plant Microbe Interact*, 28:443-454.
- Kieser T., Bibb M.J., Buttner M.J., Chater K.F., Hopwood D.A. (2000). Practical *Streptomyces* genetics. *The John Innes Foundation*.
- Mitchell R.E., Frey E.J. (1986). Production of *N*-coronafacoyl-L-amino acid analogues of coronatine by *Pseudomonas syringae* pv. *atropurpurea* in liquid cultures supplemented with L-amino acids. *Microbiology*, 132(6): 1503-1507.
- Palmer D.A., Bender C.L. (1993). Effects of environmental and nutritional factors on production of the polyketide phytotoxin coronatine by *Pseudomonas syringae* pv. *glycinea*. *Appl Environ Microbiol*, 59(5): 1619-1626.

4.9 Figures

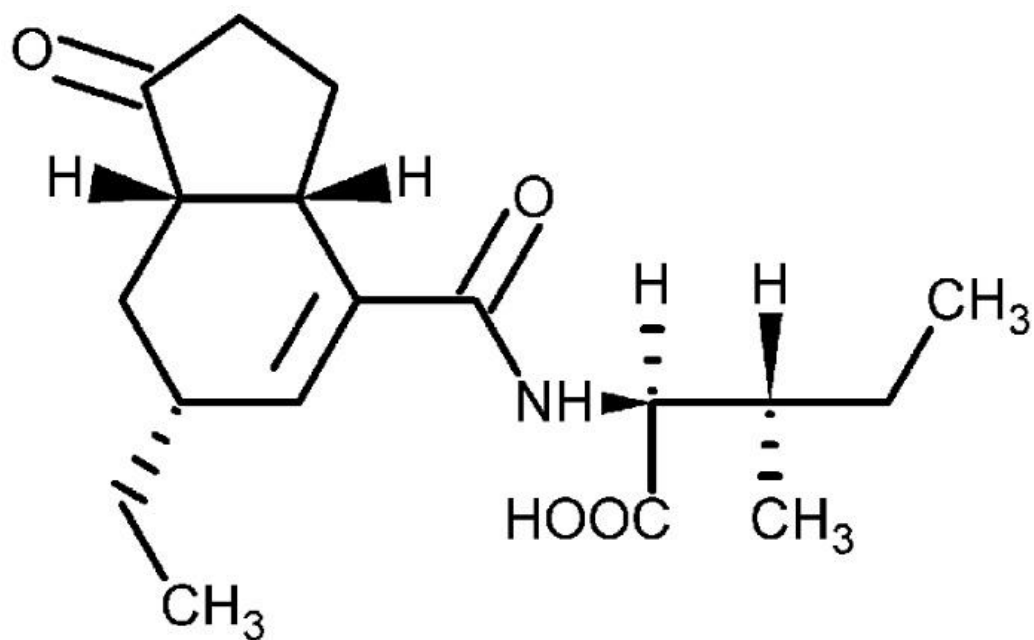


Figure 4.1. Structure of *N*-coronafacoyl-L-isoleucine (CFA-Ile) produced by *Streptomyces scabies*.

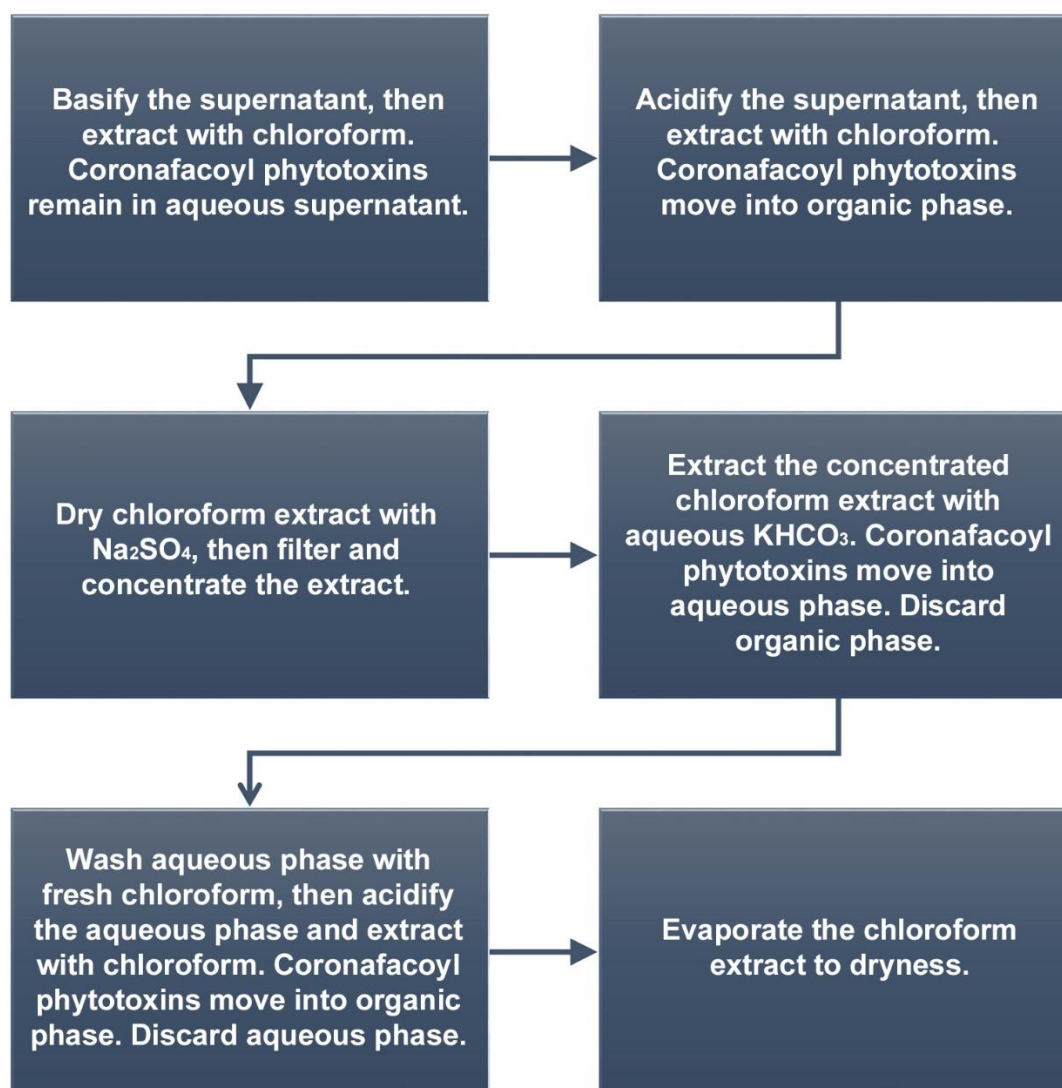


Figure 4.2. Schematic outline of principal steps performed during the extraction of coronafacoyl phytotoxins from *S. scabies* culture supernatants.

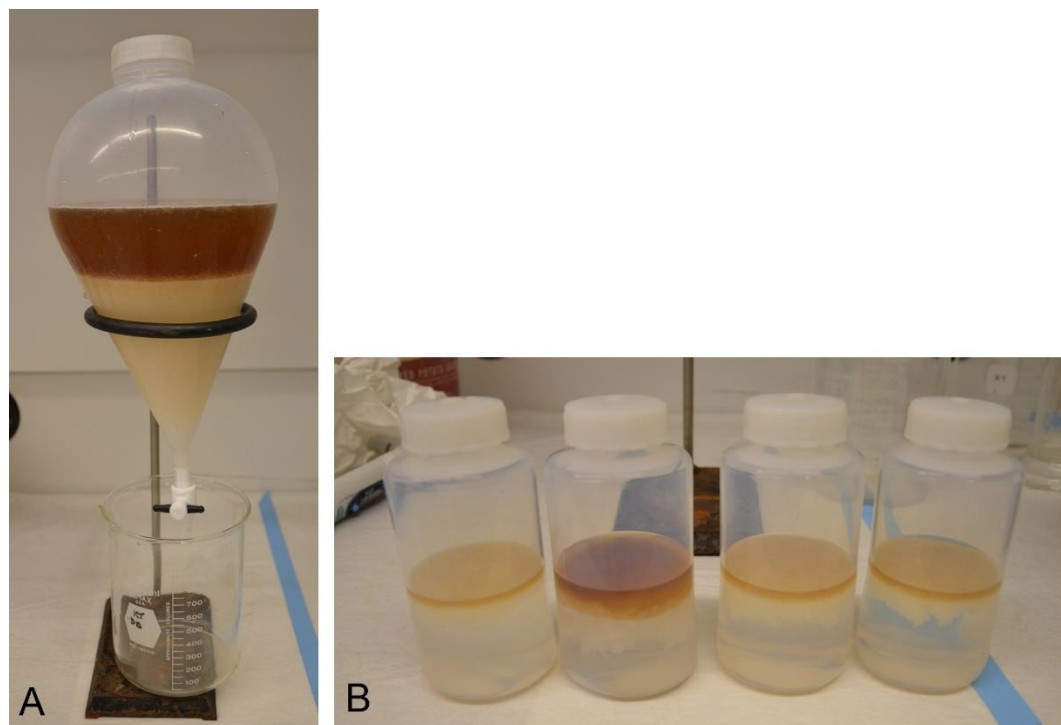


Figure 4.3. Extraction of *S. scabiei* culture supernatants with chloroform. (A). The extraction is performed using a 2 L separatory funnel. After mixing the supernatant and chloroform, the phases are allowed to separate as much as possible by gravity. The upper dark brown layer is the aqueous phase, and the lower layer is the organic phase. (B). When an emulsion layer is present, it is collected into centrifuge bottles and the phases are separated by centrifugation.



Figure 4.4. TLC analysis of the *S. scabiei* organic extract containing CFA-L-Ile. A pure sample (50 μg) of CFA-L-Ile (i) and a small portion (30-50 μl) of the organic extract (ii) containing CFA-L-Ile is spotted onto a 5×20 cm silica gel GF analytical TLC plate. Following separation, the plate is visualized under UV light, and the position of the pure standard is marked (blue circle) along with the expected position of the phytotoxin within the extract (blue rectangle). The black arrow indicates the direction of migration of the samples on the plate.

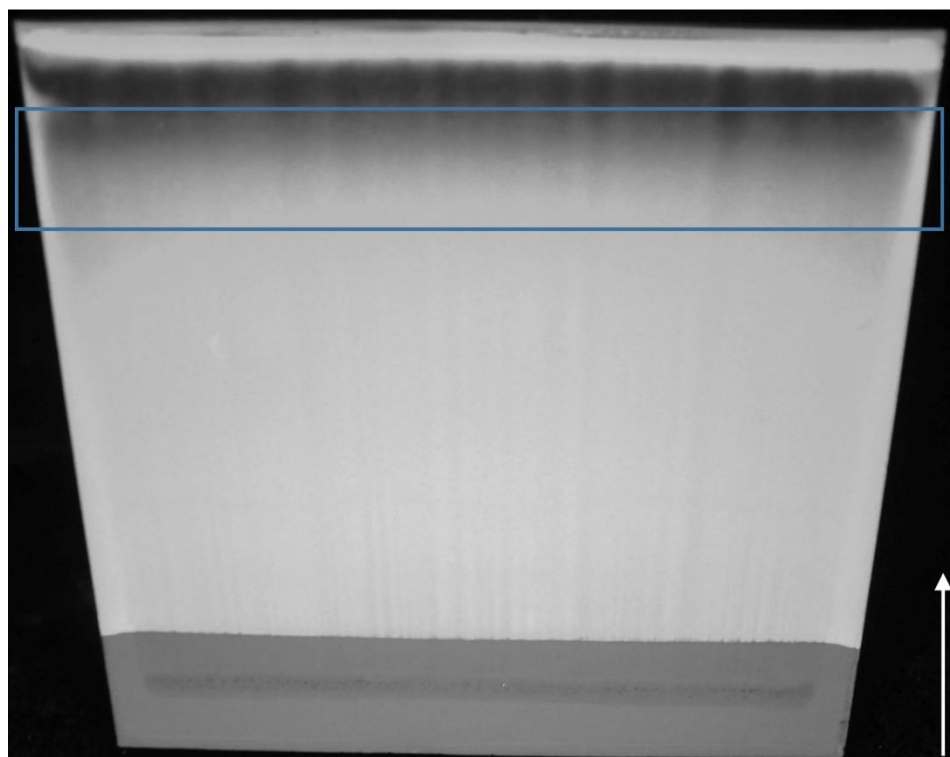


Figure 4.5. Preparative TLC analysis of the *S. scabiei* organic extract containing CFA-L-Ile. The CFA-L-Ile will be found within the dark smear as indicated by the analytical TLC reference plate (see Figure 4.4). To ensure complete recovery of the CFA-L-Ile, a large area (indicated by the blue rectangle) of the silica is scraped from the plate. The white arrow indicates the direction of migration of metabolites on the plate.

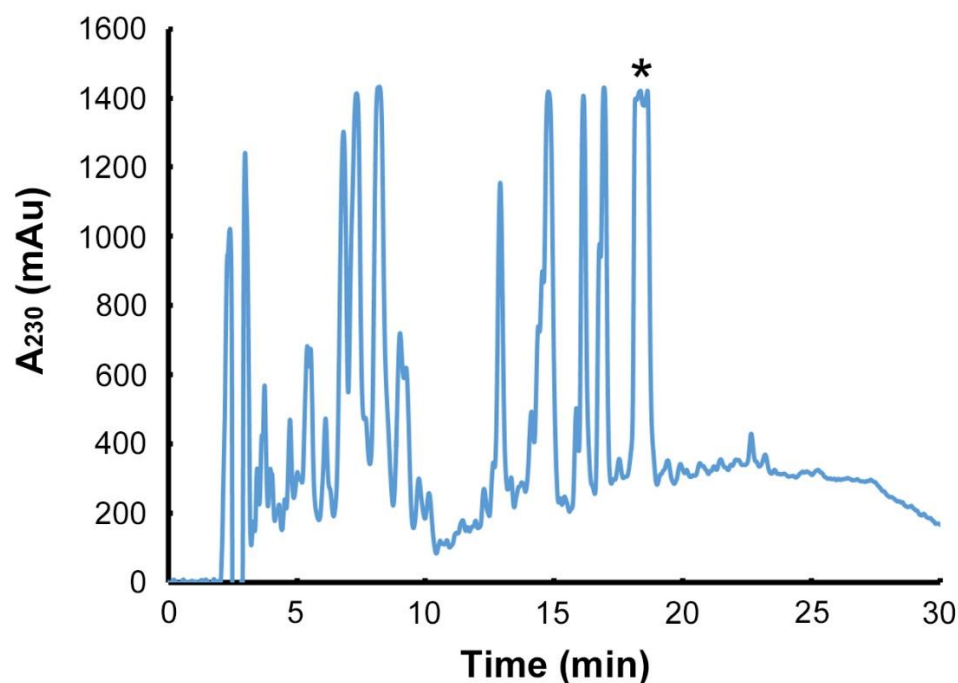


Figure 4.6. Purification of CFA-L-Ile by semi-preparative RP-HPLC. Following purification by preparative TLC, the CFA-L-Ile - containing extract is loaded onto a C18 semi-preparative HPLC column, and the metabolite is monitored by measuring the absorbance at 230 nm. The peak corresponding to CFA-L-Ile is indicated by the asterisks, and it is this peak that is targeted for collection by the HPLC fraction collector. Note that due to the high amount of CFA-L-Ile in the extract, the absorbance reading exceeds the maximum level measured by the detector, and thus the peak appears cut off in the chromatogram. Also, as *N*-coronafacoyl phytotoxins containing different isoleucine isomers can sometimes be produced by *S. scabies* in SFMB, the collected peak may contain a mixture of the different isomers since they will not separate out during the HPLC purification (Bown et al. 2016).

Chapter 5: Coronafacate ligase functions as an adenylate-forming enzyme in the biosynthesis of the coronafacoyl phytotoxin CFA-L-Ile in the plant pathogen *Streptomyces scabies*

Luke Bown, Tara Kiene, Zhenlong Cheng and Dawn R. D. Bignell*

Department of Biology, Memorial University of Newfoundland, St. John's, NL, Canada

*For correspondence. Email: dbignell@mun.ca

5.1 Abstract

Coronafacoyl phytotoxins are secondary metabolites that are synthesized as virulence factors by a variety of plant pathogenic bacteria such as *Streptomyces scabies* and *Pseudomonas syringae*. These phytotoxins are composed of a coronafacic acid (CFA) bicyclic polyketide bound via an amide linkage to an amino acid or amino acid derivative and are synthesized through the *cfa* and *cfa*-like biosynthetic gene clusters (BGCs) in *P. syringae* and *S. scabies* respectively. These gene clusters contain homologues of the *coronafacate ligase* (*cfl*) gene that encodes an enzyme believed to catalyse a reaction that utilizes the hydrolysis of ATP to create an adenylate-intermediate during the formation of the amide bond. Heterogenous hosts were used to induce production of the Cfl enzyme

from *S. scabies* and *P. syringae*. Using a malachite green phosphate detection assay we demonstrated that the Cfl enzyme forms an adenylate-intermediate complex in the formation of the amide bond between the Cfa polyketide and an isoleucine amino acid in *S. scabies*. Our results indicate that an active form of the Cfl enzyme and the Cfa polyketide are essential for the formation of the adenylate-intermediate complex but that the Cfl enzyme and amino acid substrate alone cannot form the intermediate. These results experimentally demonstrate that purified Cfl enzyme can ligate the CFA polyketide to an L-isoleucine amino acid to form CFA-L-Ile and that this ligation reaction occurs through a process of adenylation.

5.2 Introduction

One of the defining characteristics of the *Streptomyces* genus of Actinobacteria is the ability of its members to synthesize a wide variety of natural product compounds (also referred to as secondary metabolites). Many of the metabolites that are synthesized by these Gram-positive bacteria have useful applications in medicine and/or agriculture as antibacterial, antifungal, immunosuppressive, antiparasitic, and anticancer compounds (Bérdy 2005). The role that secondary metabolites play for the producing organism in its natural habitat is not always known, although the function of some has been predicted. For example, siderophores are thought to be used by saprophytic species to overcome the insolubility of ferric ions in the soil and allow them to be brought into the cell for metabolic use (Challis and Hopwood 2003). Compounds with antibacterial or antifungal properties may serve to inhibit other microorganisms competing for limited nutrients in the producing

organisms' immediate environment (O'Brian and Wright 2011). There has also been speculation that secondary metabolites may function in intercellular communication when produced at sub-inhibitory concentrations as they have been shown to produce various intracellular responses and to have an effect on gene expression (Fajardo and Martínez 2008; Yim et al. 2007; Linares et al. 2006). Some *Streptomyces* have been shown to form symbiotic relationships with eukaryotic organisms such as marine sponges, insects, fungi and plants, and it is known or suspected that secondary metabolites produced by the *Streptomyces* symbionts play an integral role in mediating these relationships (Seipke et al. 2012; Kaltenpoth et al. 2012; Schrey et al. 2005). A notable example of this is the production of phytotoxic secondary metabolites that promote the colonization and infection of plants by phytopathogenic *Streptomyces* species such as *Streptomyces scabies* (syn. *scabiei*), which causes common scab (CS) disease of potato (*Solanum tuberosum*) crops (Loria et al. 1997).

CS is an economically important disease that reduces the market value of the potato crop by producing raised, pitted or superficial corky lesions on the surface of the potato tuber (Dees and Wanner 2012). The predominant phytotoxin produced by *S. scabies* and the other scab-causing *Streptomyces* species is thaxtomin A, which is a member of a family of cyclic dipeptides (2,5-diketopiperazines) derived from 4-nitro-L-tryptophan and L-phenylalanine (King and Calhoun 2009). The production of thaxtomin A is believed to be triggered by the presence of plant-associated molecules such as cellobiose and suberin (Johnson et al. 2007; Loria et al. 2008; Lerat et al. 2010), and the phytotoxin is thought to inhibit cellulose production in the plant cell wall in order to allow for colonization of

expanding plant tissues (Loria et al. 2008). In addition, *S. scabies* was recently reported to be able to produce *N*-coronafacoyl-L-isoleucine (CFA-Ile) (Fig. 5.1-B), which is a member of the coronafacoyl family of phytotoxins synthesized by several different plant pathogenic bacteria (Fyans et al. 2015). Coronafacoyl phytotoxins are composed of the bicyclic hydrindane-ring-containing polyketide coronafacic acid (CFA) linked via an amide bond to an amino acid or amino acid derivative. The best characterized coronafacoyl phytotoxin is coronatine (COR) (Fig. 5.1-A), which is synthesized by several *Pseudomonas syringae* pathovars and consists of CFA linked to coronamic acid (CMA), an ethylcyclopropyl amino acid derived from L-*allo*-isoleucine (Mitchell and Young 1985; Bender et al. 1999). COR is required for the full virulence phenotype of *P. syringae*, and there is evidence that CFA-Ile production also contributes to the virulence phenotype of *S. scabies*, though it is not essential for *S. scabies* pathogenicity (Bignell et al. 2010; Cheng, personal communication). Although COR and CFA-Ile exhibit similar effects in plant tissues, COR is the more toxic species as it is much more active at lower concentrations (Fyans et al. 2015; Shiraishi et al. 1979). On the other hand, CFA alone causes negligible effects in plant tissues, suggesting that the amino acid moiety is required for the biological effects of coronafacoyl phytotoxins (Shiraishi et al. 1979; Uppalapati et al. 2005).

In *P. syringae* and *S. scabies*, the biosynthesis of COR and CFA-Ile involves the CFA and CFA-like biosynthetic gene clusters (BGC), respectively (Fig. 5.2), which consist of genes encoding the enzymes that synthesize the CFA moiety (Fig. 5.2) (Bender et al. 1999; Bignell et al. 2010). In addition, both gene clusters contain a gene called *cfl* which encodes the coronafacate ligase (Cfl) enzyme that is believed to catalyze the final step in

coronafacoyl phytotoxin biosynthesis by coupling CFA to its amino acid partner (Rangaswamy et al. 1998; Bignell et al. 2010). Deletion of *cfl* in *S. scabies* resulted in accumulation of CFA in the mutant culture supernatant, supporting the notion that Cfl is required for the final coupling step (Fyans et al. 2015).

The *P. syringae* Cfl protein was previously shown to have sequence homology with a group of adenylate-forming enzymes that utilize adenosine triphosphate (ATP) hydrolysis to facilitate the ligation of cyclic carboxylic acids to adenosine monophosphate (AMP) or coenzyme A (CoA) (Liyange et al. 1995). Adenylation is a process whereby a carboxylate is bound to ATP in a condensation reaction between the nucleophilic carboxylic acid and the electrophilic phosphate. This results in the production of pyrophosphate as a by-product of the reaction and the activation of the adenylated carboxylate-AMP intermediate (Fig. 5.3). This intermediate is reactive and unstable in water necessitating the adenylation enzyme to catalyze a second reaction to introduce the nucleophilic group to the intermediate in order to create the end product (Schmelz and Naismith 2009). In the case of the *P. syringae* Cfl protein, it was previously proposed that the enzyme catalyzes the condensation of the CFA carboxylic acid with an ATP molecule to form the activated CFA-AMP intermediate and liberating one molecule of pyrophosphate. Cfl would then catalyze the ligation of the activated CFA-AMP intermediate to CMA to produce COR (Liyange et al. 1995). However, no studies to date have been carried out which demonstrate that the Cfl enzyme from *P. syringae* or other coronafacoyl phytotoxin producers function in this manner.

In this study, we set out to characterize the *in vitro* activity of the Cfl enzyme from *S. scabies* in order to confirm that the enzyme catalyzes the final coupling step in CFA-Ile biosynthesis and to determine whether it does so via adenylation of the CFA moiety. We also identified amino acid residues that are conserved in Cfl homologues from different bacteria and which may be important for enzyme function.

5.3 Results

5.3.1 Analysis of the Cfl amino acid sequences from *S. scabies* 87-22 and *P. syringae* pv. tomato DC3000

Analysis of the Cfl amino acid sequences from *S. scabies* and *P. syringae* using the Pfam database (Finn et al. 2016) indicated that both enzymes contain a predicted AMP-binding enzyme domain (PF00501; <https://pfam.xfam.org/family/PF00501.27>) and an AMP-binding enzyme C-terminal domain (PF13193; <https://pfam.xfam.org/family/PF13193.5>). The AMP-binding enzyme domain is a member of the ANL superfamily that consists of luciferase, long chain fatty-acid CoA-ligase, acetyl CoA-synthetase and other related enzymes. The ANL superfamily enzymes act as catalysts for the adenylation of a carboxylate which is usually followed by the formation of a thioester (Gulick et al. 2009; Finn et al. 2016). The AMP-binding enzyme C-terminal domain is a member of a superfamily of enzymes of the same name that are found at the C-terminal of AMP-binding enzyme domains (Finn et al. 2016). Figure 5.4 shows an amino acid alignment which demonstrates some of the highly conserved regions of Cfl

homologues from a number of bacterial species. These regions include the conserved domains which have previously been identified as being important for adenylation activity (Liyanage et al. 1995), although it should be noted that these motifs are not absolutely conserved. The previously identified conserved domains are composed of SGTGXXKG and TGD amino acid residue motifs, however the *Streptomyces* and *Kitasatospora* species examined in this study contain SGTGXXKS and SGD amino acid motifs instead.

5.3.2 Identification of putative *cfl* genes in *Streptomyces* spp.

It was recently demonstrated that the genomes of several *Streptomyces* species not known to be pathogenic contain the CFA-like biosynthetic gene cluster and therefore may have the potential to synthesize coronafacoyl phytotoxins (Bown et al. 2017; see Chapter 3). In order to identify putative *cfl* genes from a variety of *Streptomyces* spp., including species that are not currently known to display a plant pathogenic phenotype, primers were designed which would amplify an internal region of the *cfl* gene (Table S-5.1). These primers were tested to determine if they could successfully differentiate species of *Streptomyces* whose genomes are known to either contain or lack a *cfl* gene homologue. As shown in Figure 5.5, a single amplicon of 499 bp was detected for *S. scabies* strains 87-22, 85-08, 84-34, 95-17, 96-04 and 87-67, all of which were previously shown to contain the *cfa6* and *cfa7* polyketide synthase genes involved in coronafacoyl phytotoxin biosynthesis (Bignell et al. 2010). In contrast, no amplicon of similar size was observed for strains LF12-3-2, LF12-2-1 and LF12-2-3A, which were isolated from scab lesions on potatoes harvested in Newfoundland and were identified as *Streptomyces europaeiscabiei* (Fyans et al. 2016; see Chapter 6), a pathogenic species not known to produce coronafacoyl

phytotoxins. Strain LF12-3-2 produced a faint band in the expected area of ~500 bp as well as another band of smaller size and several extremely faint bands of larger size in the 1-2 kb range (Fig. 5.5, Lane 7). Due to the large number of these amplified fragments and the poor amplification of the bands compared to that of the *S. scabies* strains, these may represent non-specific amplification. Strains 11-2-4, 11-1-2 and 12-5-2 were also isolated from Newfoundland potato scab lesions, however phylogenetic and sequencing analysis indicates that strains 11-2-4 and 11-1-2 are likely novel pathogenic *Streptomyces* species that are not closely related to the known pathogens (Fyans et al. 2016; see Chapter 6) while strain 12-5-2 is suspected to be a *Micromonospora* species (Bown; unpublished results). These strains produced only background amplification that is likely nonspecific, though one amplified fragment from the 12-5-2 strain is close to the anticipated amplicon size.

BLASTP analysis of the *S. sp.* 11-1-2 genome revealed that it does not contain homologues to any genes in the CFA-like BGC (Bown and Bignell 2017; see Chapter 7). The absence of potential *cfl* amplicons from the utilized environmental scab-associated isolates may indicate that production of coronafacoyl phytotoxins is not essential for the development of disease symptoms. Therefore, any study that attempts to examine coronafacoyl phytotoxin production cannot rely on the development of disease symptoms as a positive indicator for the presence of the CFA or CFA-like BGC, and that the use of internal primers should be used to detect these gene clusters.

5.3.3 Cloning, expression and purification of the *Cfl* enzyme

The *cfl* gene was PCR-amplified from wildtype cultures of *S. scabies* 87-22 and *P. syringae* pv. *tomato* DC3000, and analysis of the product by agarose gel electrophoresis

indicated the presence of an amplicon of approximately 1500 bp in both cases, which is close to the expected size of 1545 bp for *S. scabies* and 1530 bp for *P. syringae* (data not shown). The pET30b/SC_cfl and pET30b/PS_cfl plasmids were transformed into the BL21(DE3) *E. coli* expression host, which allowed for overproduction of C-terminal 6 × histidine tagged Cfl protein (Cfl-HIS₆) using the inducible T7 *lac* promoter. Small-scale protein expression experiments were performed, and it was determined that induction of *E. coli* cells at 16° C for 24 hrs resulted in the greatest amount of soluble Cfl-HIS₆ protein product (data not shown). Large-scale production and purification of the *S. scabies* Cfl-HIS₆ protein was performed using a Ni-NTA gravity elution column, and SDS-PAGE analysis of the eluted protein revealed the presence of one major protein band of ~60 kDa, which is close to the expected size of 55 kDa for the Cfl protein. Western blot analysis using anti-HIS antibodies provides evidence for this protein to be Cfl-HIS₆ (Fig. 5.6). Further experiments were conducted using only the *S. scabies* Cfl homologue due to a limitation in enzyme substrate availability.

5.3.4 *The S. scabies Cfl enzyme exhibits adenylation activity in vitro*

A modified version of a nonradioactive colorimetric assay described previously (McQuade et al. 2009; Xia et al. 2012) was employed to determine whether the *S. scabies* Cfl-HIS₆ enzyme functions as an adenylate-forming enzyme (Fig. 5.7). In order to demonstrate whether the Cfl enzyme exhibits adenylation activity, reactions were set up containing purified Cfl-HIS₆ together with the CFA and/or L-Ile substrates. As shown in Figure 5.8-A, a dark green colour indicative of adenylation activity was observed in the reaction wells containing Cfl-HIS₆ and both substrates (Fig. 5.8-Ai), whereas the wells

containing an equimolar amount of BSA in place of Cfl-HIS₆ displayed a pale green colour (Fig. 5.8-Aii). A pale green colour was also observed in the wells in which heat-inactivated Cfl-HIS₆ was used (Fig. 5.8-Aiii), confirming that active Cfl is required for the observed colour change. Reaction wells containing Cfl-HIS₆ with only the CFA substrate also showed the formation of a dark green colour (Fig. 5.8-Av), while wells containing Cfl-HIS₆ with L-Ile only remained a pale green colour (Fig. 5.8-Aiv), suggesting that CFA but not L-Ile is the substrate for adenylation by Cfl.

Enzyme activity was quantified by measuring the absorbance at 630 nm in each well, and the results are shown in Figure 5.8-B. Statistical analysis of the recorded absorbance readings was performed using a one-way ANOVA and a Tukey multiple comparison of means test. This indicated that the absorbance readings in the wells containing Cfl-HIS₆ with both CFA and Ile substrates (Fig.5.8-Bi), and those containing Cfl-HIS₆ with CFA only (Fig. 5.8-Bv) were not significantly different (p-value = 0.3473124). Similarly, the readings obtained for the wells containing BSA, the wells containing heat-inactivated Cfl-HIS₆ and the wells containing the L-Ile substrate only (Fig. 5.8-Bii-iv) were not significantly different from one another based on the statistical analysis. However, these latter readings were significantly different from the readings obtained for the reaction wells containing active Cfl-HIS₆ with both substrates. The results of the enzyme assay therefore support the hypothesis that Cfl activates the CFA carboxylic acid via adenylation during the production of CFA-Ile.

5.3.5 Confirmation of CFA-Ile production by the Cfl enzyme

The ability of the *S. scabiei* Cfl enzyme to produce CFA-Ile from the individual components was investigated using liquid chromatography-high resolution electrospray ionization mass spectrometric analysis (LC-HRESIMS) of the enzyme reaction products following extraction with organic solvent. The total ion current (TIC) chromatogram displayed in Fig. 5.9-A was obtained for the purified CFA-Ile standard, which has a retention time (t_R) of 11.913 min and produces a pseudomolecular $[M-H]^-$ ion in negative ion mode at m/z 320.1930, which is consistent with that expected for CFA-Ile (theoretical $[M-H]^- = 320.1862$). Analysis of the Cfl enzyme reaction extract using LC-HRESIMS revealed the presence of two major peaks on the LC chromatogram at $t_R = 7.224$ (compound 1) and $t_R = 11.624$ (compound 2) min (Fig. 5.9-B), and pseudomolecular $[M-H]^-$ ions at m/z 207.1067 and 320.1915 were detected for compound 1 and 2 respectively. Compound 1 can be provisionally identified as CFA (theoretical $[M-H]^- = 207.1026$) while, compound 2 is identified as CFA-Ile due to the similarities in the observed $[M-H]^-$ m/z and the t_R between the enzyme reaction product and of the CFA-Ile standard (Fig. 5.9). Thus, the results confirm that the Cfl enzyme catalyzes the final coupling reaction to form CFA-Ile in *S. scabiei*.

5.4 Discussion

In this study we have further defined the role of the Cfl enzyme in coronafacoyl phytotoxin biosynthesis. Cfl is encoded within the CFA-like BGC in the plant pathogen *S. scabiei* and is part of a set of core genes that are conserved in other bacteria that are known or suspected to produce coronafacoyl phytotoxins (Bown et al. 2017; see Chapter

3). Although it was previously reported that *cfl* disruption mutants of *P. syringae* were unable to synthesize COR, the role of Cfl in COR biosynthesis was unclear given that the mutants were also defective in CFA biosynthesis (Bender et al. 1993; Rangaswamy et al. 1997). A Δcfl deletion mutant of *S. scabies* was shown to be defective in CFA-Ile biosynthesis and accumulated CFA, and production of CFA-Ile was partially restored in the mutant by reintroduction of the *cfl* gene on an integrative plasmid, suggesting that Cfl is responsible for the final coupling reaction during coronafacoyl phytotoxin biosynthesis (Fyans et al. 2015). The results presented in this study confirm that Cfl is able to catalyze the ligation of Cfa and L-Ile to produce CFA-Ile, and that no other components of the phytotoxin biosynthetic machinery are required for this step.

Previous analysis of the Cfl amino acid sequence from *P. syringae* indicated that it bears a significant similarity to adenylate-forming enzymes such as 4-coumarate CoA-ligase, bile-acid CoA-ligase and enterobactin synthase component E, all of which catalyze the ATP-dependent linking of cyclic carboxylic acids to AMP or CoA (Liyanage et al 1995). The Pfam enzyme domain analysis conducted in this study indicates that the *S. scabies* Cfl protein contains a predicted AMP-binding enzyme domain (PF00501) and an AMP-binding enzyme C-terminal domain (PF13193), suggesting that it too may function as an adenylate-forming enzyme. Two conserved motifs were previously identified in the *P. syringae* Cfl protein that were predicted to encode a P-loop (SGTTGXXKG) and ATPase (TGD) (Liyanage et al. 1995). Protein alignment and Pfam domain analysis indicated that these motifs are conserved in Cfl homologues from multiple species of bacteria (Fig. 5.4) and that they are found in the AMP-binding enzyme domain

of the protein (data not shown). However, there are observed differences between the motifs found in *S. scabies* and those previously identified in *P. syringae*, but more research is necessary to determine the effects of these differences. It is possible that they may result in variations in substrate specificity for the Cfl enzyme, which could help to explain why Ile appears to be the preferred amino acid utilized in coronafacoyl phytotoxin production in *Streptomyces* spp. Although efforts were previously made to show adenylation activity by purified Cfl from *P. syringae*, such efforts were unsuccessful (Rangaswamy et al. 1997). In the current study, we were able to demonstrate adenylation activity for the purified *S. scabies* Cfl protein using a colorimetric enzyme assay that was originally developed for the characterization of adenylation domains involved in the activation of amino acid substrates during the biosynthesis of nonribosomal peptides (McQuade et al. 2009; Xia et al. 2012). Our results therefore support the hypothesis that Cfl activates CFA by adenylation and then ligates activated CFA-adenylate to its amino acid partner (Liyange et al. 1995).

Overall, the work presented in this study provides important insights in the mechanism of action of an enzyme that is critical for the production of coronafacoyl phytotoxins in *S. scabies*, *P. syringae* and presumably in other bacteria. Future work will consist of a comparison of the amino acid substrate specificity between the *S. scabies* and *P. syringae* Cfl enzymes to determine whether these enzymes exhibit differences in their substrate preferences. Given that *P. syringae* produces COR as the main phytotoxin whereas *S. scabies* produces CFA-Ile, an analysis of the substrate specificity of the Cfl homologues will offer insights into whether the enzymes play a key role in determining the

specific coronafacoyl phytotoxins that are produced by each organism. In addition, site-directed mutagenesis can be performed to identify residues that are essential for Cfl enzyme function. These mutagenesis studies can focus on the conserved P-loop and ATPase motifs, as well as other conserved regions of the protein identified in this study (Fig. 5.4).

5.5 Experimental Procedures

5.5.1 Bioinformatics analysis

The Cfl amino acid sequences from *S. scabies* 87-22 and *P. syringae* pv. *tomato* DC3000 were analysed for the presence of conserved domains using the Pfam database v. 31.0 (Finn et al. 2016). Amino acid sequences of other Cfl homologues were collected using the National Center for Biotechnology Information (NCBI) Basic Local Alignment Search Tool for Proteins (BLASTP) (<http://blast.ncbi.nlm.nih.gov/Blast.cgi>). Alignment of the sequences was performed using Geneious Pro software v. 6.1.2 (Biomatters).

5.5.2 Bacterial strains and growth conditions

Bacterial strains used in this study are listed in Table 5.1. *Escherichia coli* strains were grown at 37° C unless otherwise stated. Liquid cultures were grown in Difco™ LB Lennox broth (BD Biosciences) or SOC (New England Biolabs) with shaking (200 RPM). Solid cultures were grown on LB Lennox media containing 1.5 % w/v agar (BD Biosciences). When necessary, cultures were supplemented with antibiotics at the following concentrations; kanamycin (50 µg mL⁻¹; Millipore Canada Ltd.), ampicillin (100

$\mu\text{g mL}^{-1}$; Sigma Aldrich Canada). *P. syringae* was grown at 20° C. Liquid cultures were grown in Kings B media (HiMedia Laboratories) with shaking (200 RPM), solid cultures were grown on Kings B media containing 1.5 % w/v agar. Cultures were supplemented with rifampin (50 $\mu\text{g mL}^{-1}$). All strains were maintained at -80° C as frozen stocks in 20 % v/v glycerol (Sambrook and Russell 2001).

5.5.3 *Plasmid, cosmids, primers and DNA manipulation*

Plasmids and cosmids which were used in this study are listed in Table 5.1. Standard procedures were used for the manipulation of all plasmid and cosmid DNA (Sambrook and Russell 2001). All DNA sequencing was performed at The Centre for Applied Genomics (Toronto, Canada). Polymerase chain reactions (PCR) were performed using the Finnzymes Phusion DNA polymerase (New England Biolabs, Canada) or the Fermentas Taq DNA polymerase (Fisher Scientific, Canada). All PCR reactions were performed according to the manufacturers instructions except that 5 % v/v DMSO and betaine (final concentration of 80 mM) (Sigma Aldrich Canada) were included in the reactions. When necessary, PCR products were cloned into the pGEM®-T Easy vector (Promega North America, USA) as per the manufacturer's protocol. Oligonucleotide primers used in this study were purchased from Integrated DNA Technologies (Coralville, IA, USA) and are listed in Supplementary Table S-5.1.

5.5.4 *Construction of the E. coli cfl expression strains*

The *S. scabiei cfl* gene was PCR amplified from Cosmid 1770 using the oligonucleotide primers cfl_SC_R2 and cfl_SC_F2, which introduced NdeI and HindIII

restriction enzyme cut sites onto the ends of the PCR product. *P. syringae* genomic DNA was isolated using the QIAamp DNA Mini Kit (Qiagen Inc. Canada), and the *cfl* gene was PCR amplified from this template using the oligonucleotide primers *cfl*_PS_F2 and *cfl*_PS_R2, which introduced NdeI and HindIII restriction enzyme cut sites onto the ends of the PCR product. The resulting amplified DNA fragments were cloned into the pGEM[®]-T Easy vector (Table 5.1) and were sequenced to ensure that no mutations were present in the nucleotide sequences. Next, the pGEM[®]-T Easy/*cfl* plasmids were digested with NdeI and HindIII restriction enzymes (New England Biolabs, Canada) and the products were gel purified using a QIAquick gel extraction kit (Qiagen Inc. Canada) prior to ligation into similarly digested pET30b vector DNA. The resulting pET30b/SC_*cfl* and pET30b/PS_*cfl* plasmids (Table 5.1) were verified by DNA sequencing prior to being transformed into the BL21(DE3) *E. coli* expression host, which allowed for overproduction of C-terminal 6 × histidine tagged Cfl protein (Cfl-HIS₆) using the inducible T7 *lac* promoter.

5.5.5 Protein purification protocol

The *E. coli* BL21(DE3)/pET30b/SC_*cfl* strain was cultured overnight with shaking in 50 mL of LB broth with kanamycin. The overnight culture was then subcultured (1 % v/v inoculum) into 1 L of LB broth, and the large-scale culture was incubated at 30° C with shaking until the OD reached 0.6. Next, the culture was induced with IPTG (Fisher Scientific, Canada) to a final concentration of 1 mM and was incubated at 16° C with shaking for a period of 24 h. The cells were harvested by centrifugation at 4° C and 3,005 × g for 10 min, and soluble Cfl-HIS₆ protein was purified from the cells using

Ni-NTA resin (QIAGEN Inc., Canada) according to the manufacturer's instructions with the following modifications. Cell pellets were resuspended in 25 mL of binding buffer consisting of 10 mM Tris-HCl (pH 7.8) (Fisher Scientific, Canada), 0.3 M NaCl (Fisher Scientific, Canada), 5 % v/v glycerol (Sigma Aldrich Canada) and 10 mM imidazole (Sigma Aldrich Canada) prior to being lysed using a French press (SLM Instruments Inc., USA). Wash and elution buffers used to purify the Cfl-HIS₆ protein were of the same composition as the binding buffer with the exception of containing 20 mM and 250 mM of imidazole respectively. Collected fractions were analysed for the presence of protein by SDS-PAGE on a 12 % w/v gel prior to being pooled and desalted by FPLC using a HiTrap Desalting 5 mL column (GE Healthcare, Canada) with a desalting buffer of 0.3 M NaCl and 10 mM Tris-HCl (pH 7.8), or by dialysis (MWCO 3,500) at 4° C in desalting buffer consisting of 1L of 0.3 M NaCl and 10 mM Tris-HCl (pH 7.8). The desalting buffer was changed every 8 hr for 24 hr during the dialysis procedure. Protein concentration was then determined using the Bradford method (Bradford 1976).

5.5.6 Western blot analysis

Western blot analysis of the Cfl protein was performed by protein separation using SDS-PAGE and transfer to Amersham[™] Hybond[™]-ECL membranes (GE Healthcare Canada) using a Mini PROTEAN[®] Tetra Cell electrophoresis transfer cell (Bio-Rad Laboratories USA) following the manufacturers instructions. Modifications to this protocol included removal of the Ponceau S transfer verification step. Cfl was detected with a HIS₆ specific 6×-His Epitope Tag Antibody at a 1:500 dilution (Thermo Fisher Scientific Canada), followed by horseradish peroxidase-based Goat anti-Mouse Ig2b

Secondary Antibody (Thermo Fisher Scientific Canada) at a 1:400 dilution. Membrane-bound secondary antibodies were visualized through chemiluminescence using Amersham™ ECL™ Western Blotting Detection Reagents (GE Healthcare Canada).

5.5.7 Enzyme assay for the detection of adenylation activity

A non-radioactive colorimetric enzyme assay was developed based on protocols described previously (McQuade et al. 2009; Xia et al. 2012). The assay utilizes a molybdate/malachite green reagent to detect the production of pyrophosphate (PPi), which is a by-product of the reaction catalyzed by adenylate-forming enzymes (Fig. 5.7). Under acidic conditions, molybdenum (IV) salts form polymolybdate (IV) structures, which react with orthophosphate (Pi) to form a phosphomolybdate complex. This complex can then bind the malachite green dye and induce a colour change from pale yellow/green to dark green, the absorbance of which can then be measured (Cogan et al. 1999; Mok and Edwards 2005). The inclusion of a pyrophosphatase enzyme in the reaction allows for the quantitative detection of adenylation activity through the complete conversion of the PPi released to Pi (McQuade et al. 2009). The amount of dark green colour generated is directly proportional to the amount of Pi that is produced, allowing for quantification of the adenylation activity.

The assay was performed with the following modifications. The total reaction mixture of 100 µL was composed of 50 mM Tris-HCl (pH 7.5), 10 mM MgCl₂ (Fisher Scientific, Canada), 1 mM dithiothreitol (DTT) (Fisher Scientific, Canada), 0.25 mM ATP (Sigma Aldrich Canada), 0.4 U/mL inorganic pyrophosphatase (Sigma Aldrich Canada), 5% v/v glycerol, 0.5 mM CFA, 0.5 mM L-Ile and 1.0 µM Cfl-HIS₆. Enzyme reactions were

performed in duplicate in 96-well plates and were initiated with the addition of ATP. After incubation for 20 min at 20° C, the reactions were stopped with the addition of 75 µL of a molybdate/malachite green reagent (Cell Signaling Technology, Inc.) and were incubated at 37° C for 30 min to allow for colour development. The absorbance at 630 nm was measured for each reaction well using a Synergy H1 microplate reader (BioTek Instruments Canada). For heat inactivation of the Cfl-HIS₆ enzyme, the protein was incubated at 100° C for 10 min and allowed to cool on ice prior to addition to the enzyme reaction mixture. Pure CFA substrate was purchased from Dr. Carol Bender (Professor Emerita, Department of Entomology and Plant Pathology, Oklahoma State University) or was prepared through the acid hydrolysis of COR (Sigma Aldrich Canada) as described previously (Mitchell 1985). In the latter case, the CFA was then recovered from the acid hydrolysis reaction by extraction with ½ volume of chloroform (BD Lifesciences) and evaporation of the organic solvent to dryness. The CFA was then resuspended in HPLC grade methanol (Fisher Scientific, Canada) with 0.1 % v/v formic acid (Sigma Aldrich Canada) to a final concentration of 48 mM. Statistical analysis of the recorded absorbance readings for the enzyme reactions was conducted using square root transformed data in a one-way ANOVA and a Tukey multiple comparison of means test to determine the overall significance of the test and the significance between individual treatments. *P* values ≤ 0.05 were considered statistically significant.

5.5.8 Analysis of Cfl enzyme ligation products

To detect the enzyme reaction assay final products, the reaction was set up as described in the previous section except that the total reaction volume was increased 10×

to 1 mL, and the substrate concentrations were altered as follows: CFA concentration was increased to 3 mM, L-Ile concentration was increased to 1 mM, and ATP concentration was increased to 0.5 mM. The reaction was stopped by the addition of 1 N HCl (Fisher Scientific, Canada) until a pH of 1-2 was obtained. The reaction product was recovered by extraction of the reaction mix with ½ volume of chloroform and evaporation of the solvent to dryness. The remaining residue was then resuspended in 50 µl HPLC grade methanol and 0.1 % v/v formic acid. Detection of the reaction product was conducted by LC-HRESIMS using an Agilent 6200 series Accurate-Mass-Time-of-Flight (TOF) system utilizing electrospray ionization (ESI) in negative ion mode. Samples were loaded onto a Zorbax SB-C18 StableBond Analytical column (4.6 × 150 mm, 5.0 -micron particle size; Agilent Technologies Canada Inc.) with a Zorbax SB-C18 Analytical Guard Column (6 × 12.5 mm, 5-micron particle size) and were eluted using a linear gradient consisting of H₂O (A) and acetonitrile (Sigma Aldrich Canada) (B) with 0.1% (v/v) formic acid at a constant flow rate of 1.0 mL/min and a runtime of 19.5 min. The initial mobile phase consisted of A/B at 70:30 %, and this was maintained for 4.5 min, after which the ratio was increased linearly to A/B at 50:50 % for 7.5 min. This ratio was held for 3.0 min and was then returned to A/B at 70:30 % using a linear gradient over 4.5 min followed by a post-run time of 6.0 min with A/B at 70:30 %. The column temperature was held constant at 40 °C, and the metabolites were monitored using a detection wavelength of 230 nm. CFA-Ile used for a standard control was purified as previously described (Bown and Bignell 2017; see Chapter 4).

5.6 Acknowledgements

We would like to thank Linda Windsor and Dr. Stefana Egli of the Memorial University C-CART facility for assistance with the LC-HRESIMS analysis, Dr. Mark Berry (Memorial University of Newfoundland, Department of Biochemistry) for helpful comments and suggestions regarding the design of the enzyme assays, Dr. Carol Bender (Professor Emerita, Department of Entomology and Plant Pathology, Oklahoma State University) for supplying us with purified CFA substrate, Dr. Darrell Desveaux (University of Toronto) for kindly providing us with the *P. syringae* pv. *tomato* DC3000 bacterial strain and Brandon Piercey for his help with the statistical analysis. This work was supported by a Natural Sciences and Engineering Research Council of Canada Discovery Grant No. 386696-2010 to D.R.D.B.

5.7 References

- Bender C.L., Alarcón-Chaidez F., Gross D. (1999). *Pseudomonas syringae* phytotoxins: mode of action, regulation and biosynthesis by peptide and polyketide synthetases. *Microbiol Mol Biol Rev*, 63: 266-292.
- Bender C.L., Liyanage H., Palmer D., Ullrich M., Young S., Mitchell R. (1993). Characterization of the genes controlling the biosynthesis of the polyketide phytotoxin coronatine including conjugation between coronafacic and coronamic acid. *Gene*, 133(1), 31-38.
- Bérdy J. (2005). Bioactive microbial metabolites. *J Antibiot (Tokyo)*, 58: 1-26.

- Bignell D.R.D., Seipke R.F., Huguet-Tapia J.C., Chambers A.H., Parry R., Loria R.. (2010). *Streptomyces scabies* 87-22 contains a coronafacic acid-like biosynthetic cluster that contributes to plant-microbe interactions. *Mol Plant Microbe Interact*, 23: 161-175.
- Bown L., Altowairish M.S., Fyans J.K., Bignell D.R.D. (2016). Production of the *Streptomyces scabies* coronafacoyl phytotoxins involves a novel biosynthetic pathway with an F₄₂₀-dependent oxidoreductase and a short-chain dehydrogenase/reductase. *Mol Microbiol*, 101: 122-135.
- Bown L., Bignell D.R.D. (2017), Draft genome sequence of the plant pathogen *Streptomyces* sp. strain 11-1-2. *Genome Announc*, 5(37): e00968-17.
- Bown L., Li Y., Berrue F., Verhoeven J.T.P., Dufour S.C., Bignell D.R.D. (2017). Coronafacoyl phytotoxin biosynthesis and evolution in the common scab pathogen *Streptomyces scabies*. *Appl Environ Microbiol*, 83: e01169-01117.
- Bradford M.M. (1976). A rapid and sensitive method for quantitation of microgram quantities of protein utilizing the principle of protein-dye binding. *Anal Biochem*, 72: 248-254.
- Buell C.R., Joardar V., Lindeberg M., Selengut J., Paulsen I.T., Gwinn M.L., et al. (2003). The complete genome sequence of the Arabidopsis and tomato pathogen *Pseudomonas syringae* pv. *tomato* DC3000. *Proc Natl Acad Sci USA*, 100(18): 10181-10186.
- Challis G.L., Hopwood D.A. (2003). Synergy and contingency as driving forces for the evolution of multiple secondary metabolite production by *Streptomyces* species. *Proc Natl Acad Sci USA*, 100: 14555-14561.

- Cogan E.B., Birrell G.B., Griffith O.H. (1999). A robotics-based automated assay for inorganic and organic phosphates. *Anal Biochem*, 271: 29-35.
- Dees M.W., Wanner L.A. (2012). In search of better management of potato common scab. *Potato Res*, 55: 249-268.
- Fajardo A., Martínez J.L. (2008). Antibiotics as signals that trigger specific bacterial responses. *Curr Opin Microbiol*, 11: 161-167.
- Finn R.D., Cogill P., Eberhardt R.Y., Eddy S.R., Mistry J., Mitchell A.L., Potter S.C., Punta M., Qureshi M., Saanador-Vegas A., Salazar G.A., Tate J., Bateman A. (2016). The Pfam protein families database: towards a more sustainable future. *Nucleic Acids Res*, 44: D279-D285.
- Fyans J.K., Altowairish M.S., Li Y., Bignell D.R.D. (2015). Characterization of the coronatine-like phytotoxins produced by the common scab pathogen *Streptomyces scabies*. *Mol Plant Microbe Interact*, 28(4): 443-454.
- Fyans J.K., Bown L., Bignell D.R.D. (2016). Isolation and characterization of plant-pathogenic *Streptomyces* species associated with common scab-infected potato tubers in Newfoundland. *Phytopathology*, 106(2): 123-131.
- Gulick A.M. (2009). Conformational dynamics in the Acyl-CoA synthetases, adenylation domains of non-ribosomal peptide synthetases, and firefly luciferase. *ACS Chem Biol*, 4: 811-827.

- Johnson E.G., Joshi M.V., Gibson D.M., Loria R. (2007). Cello-oligosaccharides released from host plants induce pathogenicity in scab-causing *Streptomyces* species. *Physiol Mol Plant Pathol*, 71: 18-25.
- Kaltenpoth M., Yildirim E., Gürbüz M.F., Herzner G., Strohm E. (2012). Refining the roots of the Beewolf-*Streptomyces* symbiosis: antennal symbionts in the rare genus *Philanthus* (Hymenoptera, Crabronidae). *Appl Environ Microbiol*, 78(3): 822-827.
- King R.R., Calhoun L.A. (2009). The thaxtomin phytotoxins: sources, synthesis, biosynthesis, biotransformation and biological activity. *Phytochemistry*, 70: 833-841.
- Lerat S., Simao-Beaunoir A.-M., Wu R., Beaudoin N. Beaulieu C. (2010). Involvement of the plant polymer suberin and the diasaccharide cellobiose in triggering thaxtomin A biosynthesis, a phytotoxin produced by the pathogenic agent *Streptomyces scabies*. *Phytopathology*, 100(1): 91-96.
- Linares J.F., Gustafsson I., Baquero F., Martinez J.L. (2006). Antibiotics as intermicrobial signaling agents instead of weapons. *Proc Natl Acad Sci USA*, 103(51): 19484-19489.
- Liyanage H., Palmer D.A., Ullrich M., Bender C.L. (1995). Characterization and transcriptional analysis of the gene cluster for coronafacic acid, the polyketide component of the phytotoxin coronatine. *Appl Environ Microbiol*, 61: 3843-3848.
- Loria R., Bignell D.R., Moll S., Huguet-Tapia J.C., Joshi M.V., Johnson E.G., Seipke R.F., Gibson D.M. (2008). Thaxtomin biosynthesis: the path to plant pathogenicity in the genus *Streptomyces*. *Antonie Van Leeuwenhoek*, 94: 3-10.

- Loria R., Bukhalid R.A., Fry B.A., King R.R. (1997). Plant pathogenicity in the genus *Streptomyces*. *Plant Dis*, 81: 836-846.
- McQuade T.J., Shalloo A.D., Sheoran A., Del Proposto J.E., Tsodikov O.V., Garneau-Tsodikova S. (2009). A nonradioactive high-throughput assay for screening and characterization of adenylation domains for nonribosomal peptide combinatorial biosynthesis. *Anal Biochem*, 386: 244-250.
- Mitchell R.E. (1985). Norcoronatine and *N*-coronafacoyl-L-valine, phytotoxic analogues of coronatine produced by a strain of *Pseudomonas syringae* pv. *glycinea*. *Phytochemistry*, 24(7): 1485-1487.
- Mitchell R.E., Young H. (1985). *N*-coronafacoyl-L-isoleucine and *N*-coronafacoyl-L-alloisoleucine, potential biosynthetic intermediates of the phytotoxin coronatine. *Phytochemistry*, 24: 2716-2717.
- Mok M.T.S., Edwards M.R. (2005). Critical sources of error in colorimetric assay for UDP-*N*-acetylglucosamine pyrophosphorylase. *Anal Biochem*, 343: 341-343.
- O'Brien J., Wright G.D. (2011). An ecological perspective of microbial secondary metabolism. *Curr Opin Biotechnol*, 22: 552-558.
- Rangaswamy V., Mitchell R., Ullrich M., Bender C. (1998). Analysis of genes involved in biosynthesis of coronafacic acid, the polyketide component of the phytotoxin coronatine. *J Bacteriol*, 180: 3330-3338.
- Rangaswamy V., Ullrich M., Jones W., Mitchell R., Parry R., Reynolds P., Bender C.L. (1997). Expression and analysis of coronafacate ligase, a thermoregulated gene

- required for production of the phytotoxin coronatine in *Pseudomonas syringae*. *FEMS Microbiol Lett*, 154: 65-72.
- Sambrook J., Russell D.W. (2001). *Molecular cloning: a laboratory manual*. Cold Spring Harbor Laboratory Press, Cold Spring Harbor, NY.
- Schmelz S., Naismith J.H. (2009). Adenylate-forming enzymes. *Curr Opin Struct Biol*, 19(6): 666-671.
- Schrey S.D. Schellhammer M., Ecke M., Hampp R., Tarkka M.T. (2005). Mycorrhiza helper bacterium *Streptomyces* AcH 505 induces differential gene expression in the ectomycorrhizal fungus *Amantia muscaria*. *New Phytol*, 168: 205-216.
- Seipke R.F., Kaltenpoth M., Hutchings M.I. (2012). *Streptomyces* as symbionts: an emerging and widespread theme? *FEMS Microbiol Rev*, 36: 862-876.
- Shiraishi K., Konomi K., Sato H., Ichihara A., Sakamura S., Nishiyama K., Sakai R. (1979). The structure-activity relationships in coronatine analogs and amino compounds derived from (+)-coronafacic acid. *Agric Biol Chem*, 43(8): 1753-1757.
- Uppalapati S.R., Ayoubi P., Weng H., Palmer D.A., Mitchell R.E., Jones W., Bender C.L. (2005). The phytotoxin coronatine and methyl jasmonate impact multiple phytohormone pathways in tomato. *Plant J*, 42: 201-217.
- Yim G., Wang, H.H., Davies J. (2007). Antibiotics as signalling molecules. *Phil Trans R Soc Lond B Biol Sci*, 362: 1195-1200.
- Xia S., Ma Y., Zhang W., Yang Y., Wu S., Zhu M., Deng L., Li B., Liu Z., Qi C. (2012). Identification of Sare0718 as an alanine-activating adenylation domain in marine actinomycete *Salinispora arenicola* CNS-205. *PLoS One*, 7(5): e37487.

5.8 Tables and Figures

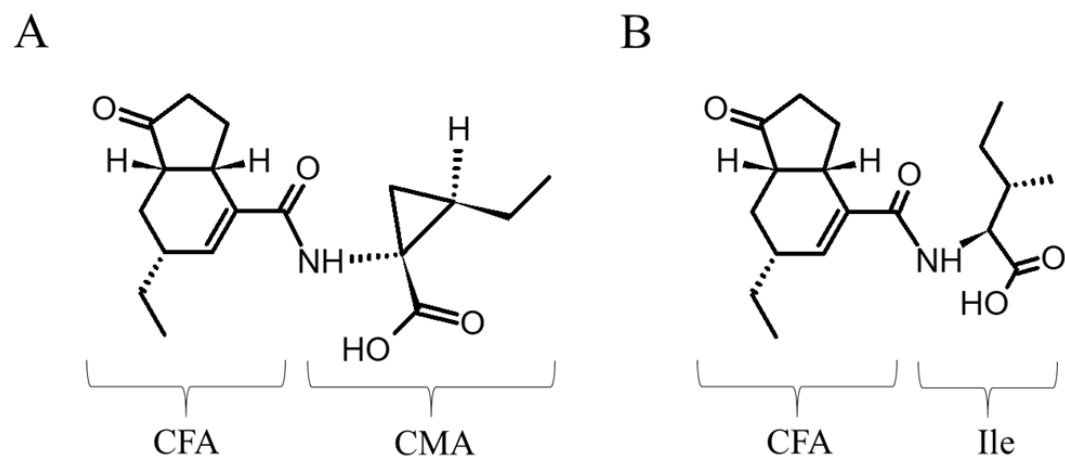
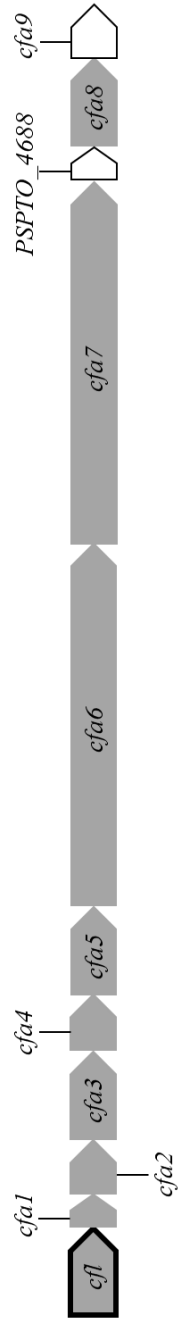


Figure 5.1. Molecular structures of (A) Coronatine (COR); (B) CFA-L-isoleucine (CFA-Ile).

P. syringae



S. scabies

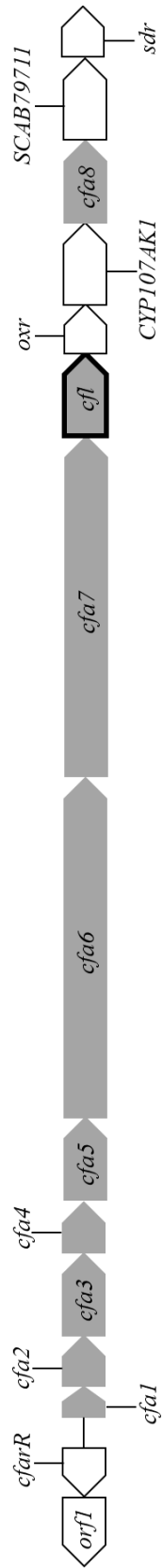


Figure 5.2. The CFA and CFA-like biosynthetic gene clusters from *P. syringae* and *S. scabies* respectively. Genes which are indicated in gray are homologous between the gene clusters and genes which are indicated in white are unique to each respective gene cluster. *cfl* genes are indicated with a black outline.

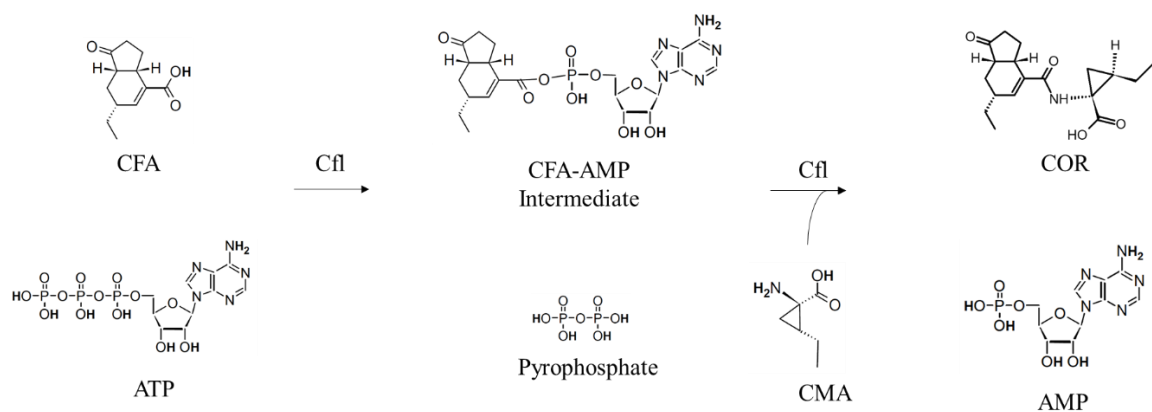


Figure 5.3. Proposed biosynthetic steps catalyzed by the Cfl enzyme during COR production in *P. syringae*. Cfl catalyzes the adenylation of CFA using ATP as a substrate. This results in the formation of a CFA-AMP intermediate complex and the release of pyrophosphate. Cfl is then thought to catalyze a second reaction in which the CFA moiety is ligated to CMA via an amide bond, resulting in the release of COR and AMP.

Consensus	70	170	350	400	400
<i>P. bet</i>	XELXXXXXXACGLXXGX	XXXJAXXIFYYTSGTTGXXKXXV	XXSIGWPLPGVXXX	XWJAXXGDJXXXX	JXXXXXZ
<i>P. car sp. act</i>	FEIATYYACGLKKGVI	DDIASIFYYTSGTTGHPKGIIV	EP SIGWPLPDVEIK	RWLTGDTGDLVRLC	LAHYKHPSE
<i>P. atro</i>	FEIATYYACGLKIGA	DEIASIFYYTSGTTGHPKGIIV	EP SIGWPLPGVEIQ	RWLTGDTGDLVRLC	LAHYKHPSE
<i>P. car sp. car</i>	FEIATYYACGLKIGA	DEIASIFYYTSGTTGHPKGIIV	EP SIGWPLPGVEIK	RWLTGDTGDLVRLC	LAHYKHPSE
<i>P. car sp. bra</i>	FEIATYYACGLKIGA	DEIASIFYYTSGTTGHPKGIIV	EP SIGWPLPGVEIK	RWLTGDTGDLVRLC	LAHYKHPSE
<i>P. psy</i>	LELVALYYACLDIGA	EWLAAIFYYTSGTTGIARKGVF	QSSIGWPLPGVEIQ	RWLTGDTGDLVRLC	LAHYKHPSE
<i>P. pyr</i>	LELVALYYACLEHGA	DSLAAIFYYTSGTTGITKGIIVF	QSSIGWPLPGVALQ	RWLTGDTGDLVRLC	LAHYKHPSE
<i>P. cor</i>	LELVALYYACLEHGA	DSLAAIFYYTSGTTGITKGIIVF	QSSIGWPLPGVALQ	RWLTGDTGDLVRLC	LAHYKHPSE
<i>P. arv</i>	LELVALYYACLEHGA	DSLAAIFYYTSGTTGITKGIIVF	QSSIGWPLPGVALQ	RWLTGDTGDLVRLC	LAHYKHPSE
<i>P. amy</i>	LELVALYYACLEHGA	DSLAAIFYYTSGTTGITKGIIVF	QSSIGWPLPGVALQ	RWLTGDTGDLVRLC	LAHYKHPSE
<i>A-to</i>	VELVPTMLACLOVGI	DDIASIFHTSGTTGRACKVVI	VPSIGWPMPCQVVR	RWLTGDTGDLVRLC	LAHYKHPSE
<i>S. gri</i>	VELVSVYYACLRVGA	DDLAAIFYYTSGTTGRPKSLVI	VPSIGWPLPGVEVR	RWLTGDTGDLVRLC	LAHYKHPSE
<i>Xlr</i>	VELVAVYYACLRVGA	DDLAAIFYYTSGTTGRPKSLVI	EP SIGWPLPGVEIR	RWLTGDTGDLVRLC	LAHYKHPSE
<i>S. sp.</i>	VELVAVYYACLRVGA	DDLAAIFYYTSGTTGRPKSLVI	EP SIGWPLPGVEIR	RWLTGDTGDLVRLC	LAHYKHPSE
<i>S. scab 87-22</i>	VELVAVYYACLRVGA	DDLAAIFYYTSGTTGRPKSLVI	EP SIGWPLPGVEIR	RWLTGDTGDLVRLC	LAHYKHPSE
<i>S. scab NRRL</i>	VELVAVYYACLRVGA	DDLAAIFYYTSGTTGRPKSLVI	EP SIGWPLPGVEIR	RWLTGDTGDLVRLC	LAHYKHPSE
<i>S. scab S58</i>	VELVAVYYACLRVGA	DDLAAIFYYTSGTTGRPKSLVI	EP SIGWPLPGVEIR	RWLTGDTGDLVRLC	LAHYKHPSE

Figure 5.4. Partial alignment of highly conserved regions of the Cfl enzyme from bacteria previously shown to contain homologues to the *cfl* gene. Black indicates 100 % amino acid identity, dark grey indicates 80-99 % amino acid identity and white indicates <60 % amino acid identity. The % identity of each amino acid was determined using the Blosum62 score matrix. The conserved SGTGXXKG and TGD motifs are outlined in red. *P. bet*: *Pectobacterium betavascularum* NCPPB2795; *P. car sp. act*: *Pectobacterium carotovorum* sp. *actinidae* KKH3; *P. atro*: *Pectobacterium atrosepticum* SCRI1043; *P. car sp. car*: *Pectobacterium carotovorum* sp. *carotovorum* UGC32; *P. car sp. bra*: *Pectobacterium carotovorum* sp. *brasiliense* NZEC1; *P. psy*: *Pseudomonas psychrotolerans* NS274; *P. syr*: *Pseudomonas syringae* pv. *tomato* DC3000; *P. cor*: *Pseudomonas coronafaciens* pv. *porri* LMG 28495; *P. sav*: *Pseudomonas savastanoi* pv. *glycinea* B076; *P. amy*: *Pseudomonas amygdali* pv. *morsrunorum* HRI--W5269; *Azo*: *Azospirillum* sp. B510; *S. gri*: *Streptomyces griseoruber* DSM40281; *Kit*: *Kitasatospora azatica* KCTC 9699; *S. sp.*: *Streptomyces* sp. NRRL WC-3618; *S. scab 87-22*: *Streptomyces scabies* 87-22; *S. scab NRRL*: *Streptomyces scabies* NRRL B-16523; *S. scab S58*: *Streptomyces scabies* S58

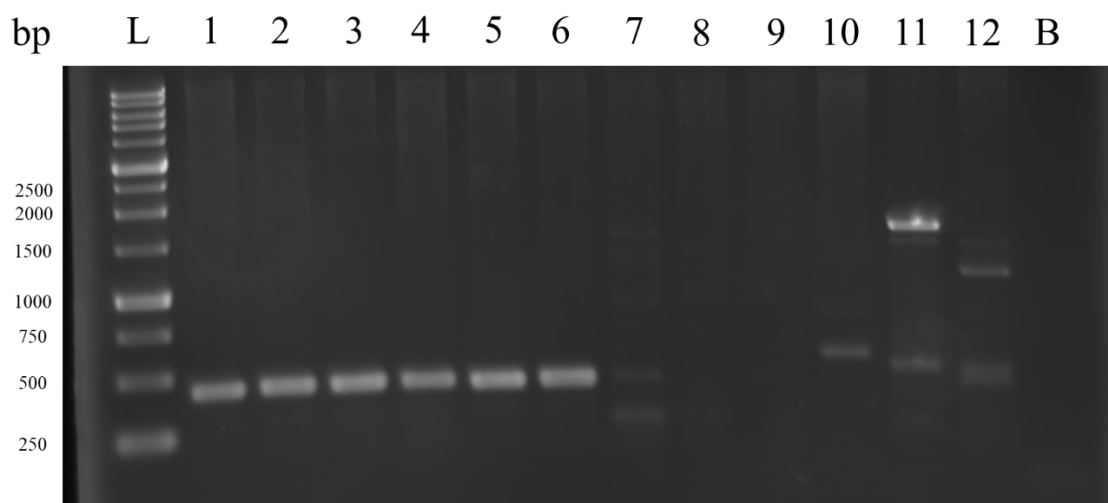


Figure 5.5. Detection of *cfl* homologues in *Streptomyces* genomes. PCR was performed using the *cfl*-specific LB_cfl_6 internal primers, and the resulting products were examined by agarose gel electrophoresis on a 1% w/v agarose TBE gel. Sample lanes are as indicated with lanes 1-5 containing strains of *S. scabies*, lanes 6-8 containing provisional strains of *S. europaeiscabiei*, lanes 9-11 containing unidentified environmental isolated species of *Streptomyces*, lane 12 containing an unidentified environmental isolated species of *Micromonospora*. Lanes (L) 1 kb DNA ladder RTU (FroggaBio Canada); (1) strain 85-08; (2) strain 84-34; (3) strain 95-17; (4) strain 96-04; (5) strain 87-67; (6) strain 87-22; (7) strain LF12-3-2; (8) strain LF12-2-1; (9) strain LF12-2-3A; (10) strain 11-2-4; (11) strain 11-1-2; (12) strain 12-5-2; (B) reaction blank containing no template DNA.

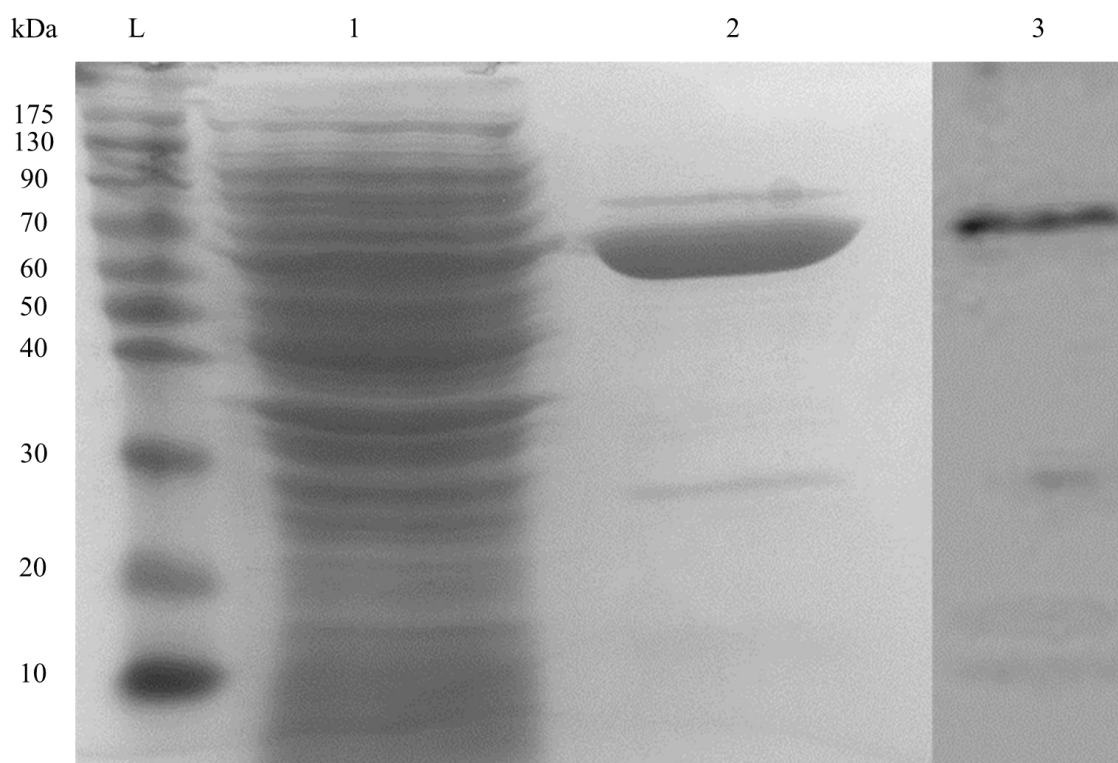


Figure 5.6. SDS-PAGE and Western blot analysis of the *S. scabiei* Cfl-His₆ protein purified from *E. coli*. Lanes (L) PiNK Plus Prestained Protein Ladder; (1) SDS-PAGE of total insoluble protein sample taken from cell pellet; (2) SDS-PAGE of purified Cfl-HIS₆ protein; (3) Western blot analysis of purified Cfl-HIS₆ protein using to anti-HIS antibodies.

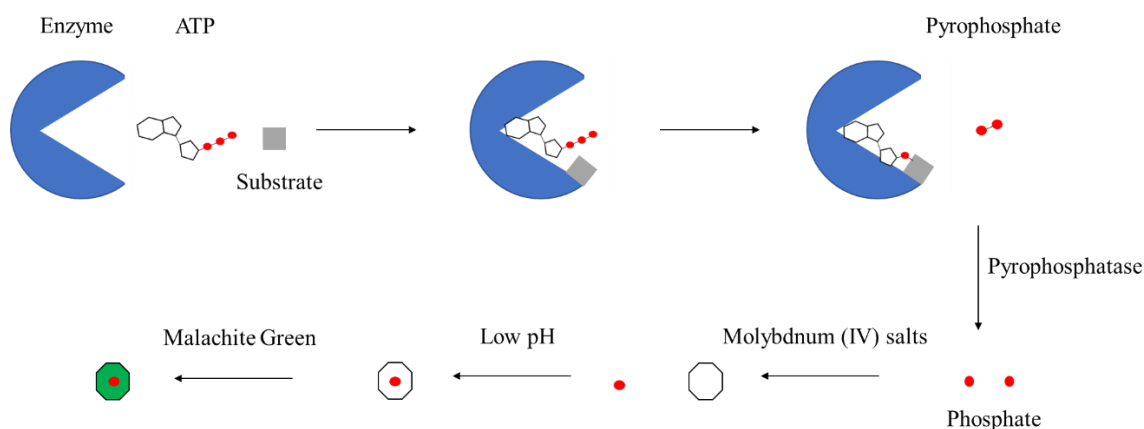


Figure 5.7. Schematic showing the mechanism of the molybdate/malachite green colorimetric enzyme assay used for detecting enzyme adenylation activity. The enzyme catalyzes the production of AMP from ATP and the formation of a substrate-AMP adenylate complex, with PPi being released as a by-product. A pyrophosphatase enzyme in the reaction mixture then converts the PPi to Pi molecules. The molybdate/malachite green reagent, which contains molybdenum (IV) salts, sulfuric acid and malachite green stain is added to stop the reaction and to allow for the formation of polymolybdate complexes in which a phosphate group is surrounded by an octahedral molybdate structure. This complex will absorb the malachite green stain and produces a colour change from light yellow-green to dark green.

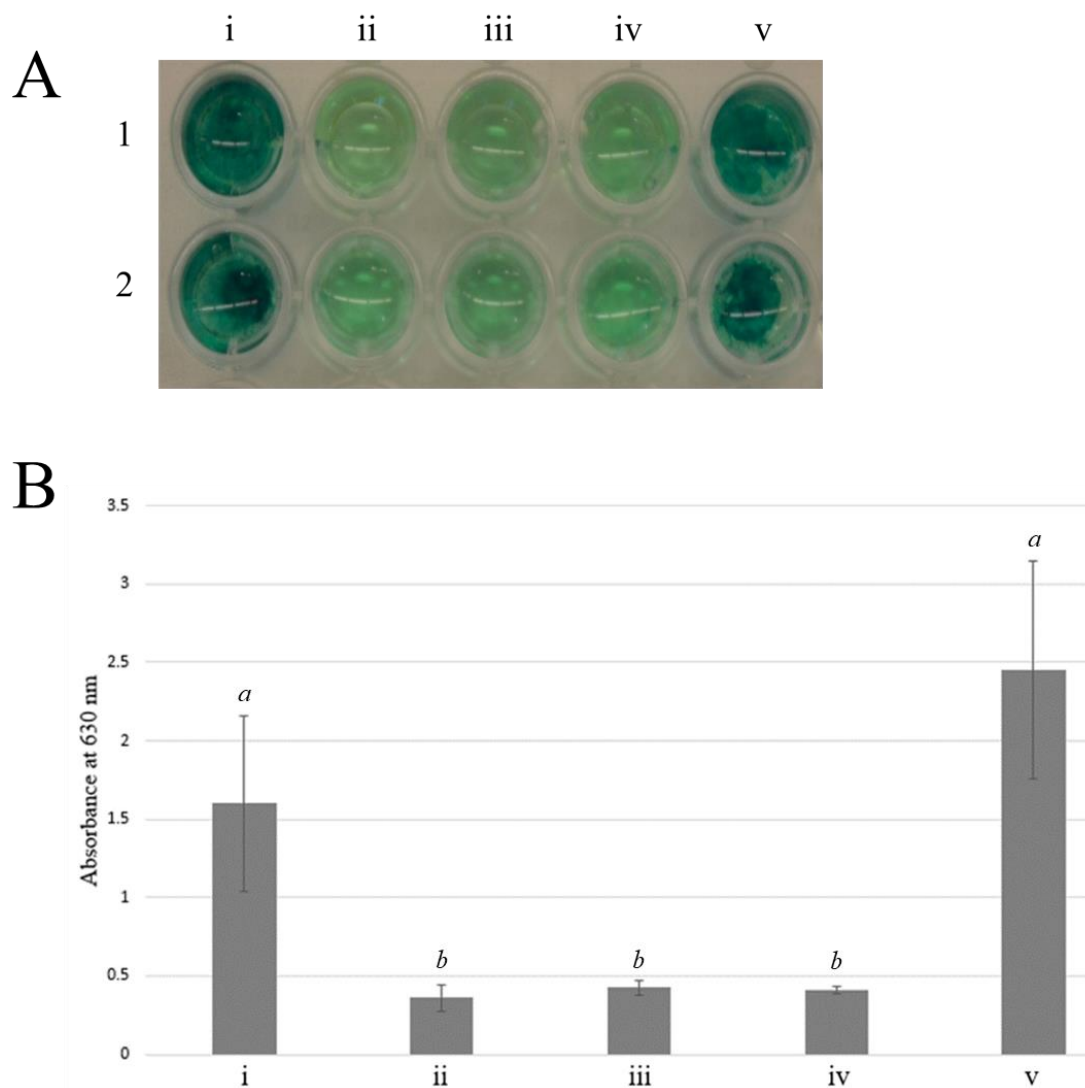


Figure 5.8. (A) Malachite green enzyme reaction assay for detection of *S. scabiei* Cfl enzyme adenylation activity. Rows 1 and 2 are duplicate reaction sets. Reaction wells (i) contain all enzyme reaction ingredients including Cfl-HIS₆, CFA and, L-Ile; (ii) lack the Cfl-HIS₆ enzyme and contain an equimolar amount of BSA; (iii) contain heat inactivated Cfl-HIS₆ enzyme; (iv) lack the CFA substrate; (v) lack the L-Ile substrate. (B)

Quantification of adenylation enzyme activity by the *S. scabies* Cfl. The reactions performed were as described in Fig. 5.7-A, and the absorbance readings at 630 nm were measured for each well using a microplate reader. The columns represent the mean absorbance reading from duplicate wells for each reaction, and the error bars represent the standard deviation from the mean. The column labels (x-axis) correspond to the assay wells shown in Fig. 5.7-A. Mean values designated with identical letters were not significantly different based on the statistical test performed ($P > 0.05$). The overall significance of the test was determined by one-way ANOVA to have a p-value of 0.00341.

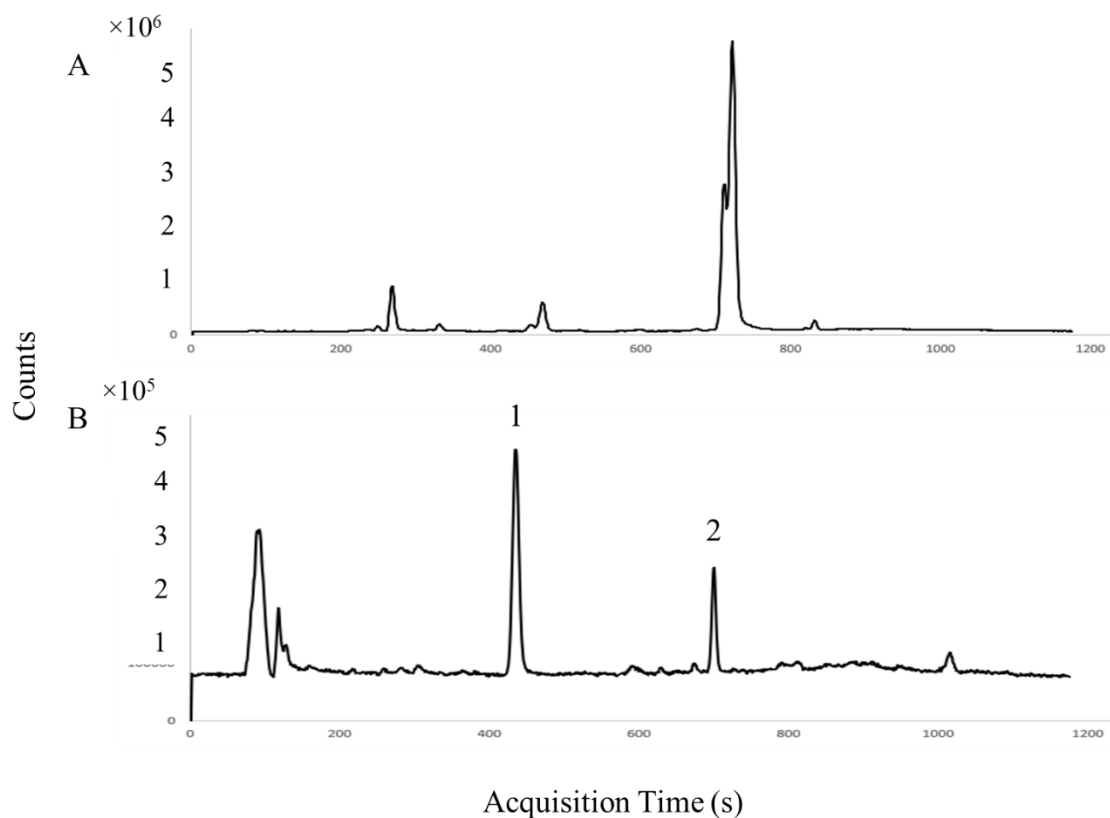


Figure 5.9. Detection of CFA-Ile produced *in vitro* by the *S. scabies* Cfl enzyme using LC-HRESIMS analysis. The TIC chromatograms shown are for the CFA-Ile standard (A) and the Cfl enzyme reaction extract (B). Compound 1 was identified as CFA and compound 2 was identified as CFA-Ile based on the detection of pseudomolecular $[M-H]^-$ ions by HRESIMS.

Table 5.1. Bacterial strains, cosmids and plasmids used in this study.

Strain, Plasmid or Cosmid	Description	Antibiotic Resistance [†]	Reference or Source
<i>Escherichia coli</i> strains			
NEB 5-alpha	DH5 α derivative; high efficiency competent cells used for transformation	none	New England Biolabs, Canada
BL21(DE3)	Host strain for protein expression	none	New England Biolabs, Canada
<i>Pseudomonas syringae</i> pv. <i>tomato</i> strains			
DC3000	COR-producing strain	rif ^r	Buell et al. 2003
<i>Cosmids</i>			
Cosmid 1770	SuperCos1 derivative containing the <i>S. scabies</i> 87-22 CFA-like gene cluster	amp ^r , kan ^r	Bignell et al. 2010
<i>Plasmid</i>			
pGEM [®] - T Easy	Cloning vector for PCR products	amp ^r	Promega North America
pET30b	N- or C- terminal 6 \times histidine (HIS ₆) – tagged protein expression vector with T7 <i>lac</i> promoter	kan ^r	Novagen Inc.
pET30b/PS_ <i>cfl</i>	pET30b derivative containing the <i>P. syringae cfl</i> gene cloned into the NdeI and HindIII restriction sites	kan ^r	This study
pET30b/SC_ <i>cfl</i>	pET30b derivative containing the <i>S. scabies cfl</i> gene cloned into the NdeI and HindIII restriction sites	kan ^r	This study

[†] kan^r, amp^r, and rif^r = kanamycin, ampicillin and rifampin resistance, respectively.

5.9 Supplementary Information

Table S-5.1. Oligonucleotides used in this study.

Primer Name	Sequence* (5' → 3')	Use
LB_cfl_6F	GGCCATCTTCTACACCTCGG	Internal detection of the <i>S. scabies cfl</i> gene by PCR
LB_cfl_6R	GATCATCAGCTCACCGGCTT	Internal detection of the <i>S. scabies cfl</i> gene by PCR
M13F	CGCCAGGGTTTTCCCAGTCACGAC	Sequencing of pGEM®-T Easy inserts
M13R	TCACACAGGAAACAGCTATGAC	Sequencing of pGEM®-T Easy inserts
cfl_SC_F2	<u>GCGCCATATG</u> TCCGTCTTCTCGG TCTT	PCR amplification of <i>S. scabies cfl</i> gene with NdeI restriction site added
cfl_SC_R2	<u>GCGCAAGCTT</u> CGACGCGCTCTC CTCGGCCG	PCR amplification of <i>S. scabies cfl</i> gene with HindIII restriction site added
cfl_PS_F2	<u>GCGCCATATG</u> AGTCTGATTTCT GAGTT	PCR amplification of <i>P. syringae cfl</i> gene with NdeI restriction site added
cfl_PS_R2	<u>GCGCAAGCTT</u> GGTCGATGGGGC GGCGCCGA	PCR amplification of <i>P. syringae cfl</i> gene with HindIII restriction site added

* Non-homologous extensions are underlined; engineered restriction sites are indicated in bold.

**Chapter 6: Isolation and characterization of plant pathogenic *Streptomyces* species
associated with common scab-infected potato tubers in Newfoundland**

Joanna K. Fyans^{†‡}, Luke Bown^{†*} and Dawn R. D. Bignell^{*}

[†] These authors contributed equally to this study

[‡] Present address: School of Chemistry, The University of Manchester, Oxford Road,
Manchester, M13 9PL, UK

^{*} Department of Biology, Memorial University of Newfoundland, St. John's, Canada

For correspondence. Email dbignell@mun.ca

Fyans, J.K., Bown, L., and Bignell, D.R.D. 2016. Isolation and characterization of plant-pathogenic *Streptomyces* species associated with common scab-infected tubers in Newfoundland. *Phytopathology* 106: 123-131. Reproduced by permission - © APS.

6.1 Abstract

Potato common scab (CS) is an economically important crop disease that is caused by several members of the genus *Streptomyces*. In this study, we characterized the plant pathogenic *Streptomyces* spp. associated with CS-infected potato tubers harvested in Newfoundland, Canada. A total of 17 pathogenic *Streptomyces* isolates were recovered from potato scab lesions, of which eight were determined to be most similar to the known CS pathogen *Streptomyces europaescabiei*. All eight *S. europaescabiei* isolates were found to produce the thaxtomin A phytotoxin and to harbour the *nec1* virulence gene, and most also carry the putative virulence gene *tomA*. The remaining isolates appear to be novel pathogenic species that do not produce thaxtomin A, and only two of these isolates were determined to harbour the *nec1* or *tomA* genes. Of the non - thaxtomin - producing isolates, strain 11-1-2 was shown to exhibit a severe pathogenic phenotype against different plant hosts and to produce a novel, secreted phytotoxic substance. This is the first report documenting the plant pathogenic *Streptomyces* spp. associated with CS disease in Newfoundland. Furthermore, our findings provide further evidence that phytotoxins other than thaxtomin A may also contribute to the development of CS by *Streptomyces* spp.

6.2 Introduction

Common scab (CS) is an economically important disease of potato (*Solanum tuberosum*) and is characterized by the presence of necrotic lesions with a corky texture on the potato tuber surface. The lesions can be superficial, erumpent (raised) or deep pitted,

and while they can be small and round, they can also coalesce to cover significant areas of the tuber surface (Loria et al. 2006). The incidence and severity of CS disease varies from field to field and within the same field, and from year to year in the same location. There are currently no commercial potato cultivars that are completely resistant to CS disease, and once established in fields the disease is extremely difficult to eradicate or control (Dees and Wanner 2012). CS causes economic losses to growers as the lesions affect the quality and market value of the potato crop. In Canada, it has been estimated that the economic losses from CS during the 2002 growing season were between 15.3-17.3 million Canadian dollars (Hill and Lazarovits 2005). There is also evidence that CS can reduce the overall yield of a potato crop and increase the number of smaller tubers in the yield (Hiltunen et al. 2005).

CS is caused by soil-borne, filamentous, saprophytic *Streptomyces* bacteria that have acquired the additional ability to cause plant disease. The best characterized CS-causing pathogen is *Streptomyces scabies* (syn. *scabiei*), which is found worldwide and is the predominant CS - causing pathogen in North America (Wanner 2009). A closely related pathogen, *Streptomyces europaeiscabiei*, is frequently found in Europe and has also been isolated in the USA and Canada (Bouček-Mechiche et al. 2000; Dees et al. 2012, 2013; Flores-González et al. 2008; Wanner 2009). *Streptomyces turgidiscabies* was first isolated from the Japanese island of Hokkaido and is associated with the formation of distinctly erumpent scab lesions on potato tubers (Miyajima et al. 1998). It has since been found in Finland, China, Korea, USA, Norway, Sweden and the UK (Dees et al. 2012, 2013; Kim et al. 1999; Kreuze et al. 1999; Lehtonen et al. 2004; Thwaites et al. 2010; Wanner 2009; Zhao et al. 2008). *Streptomyces acidiscabies*, which causes acid scab (AS)

disease, was first isolated from the northeastern USA and has now been found in China, Japan, Korea, Canada and the UK (Faucher et al. 1992; Lambert and Loria 1989a; Song et al. 2004; St-Onge et al. 2008; Thwaites et al. 2010; Tóth et al. 2001; Zhao et al. 2010). AS is essentially the same disease as CS except that it can occur in acidic pH soils where CS is suppressed (Loria et al. 1997). Other CS-causing pathogens that have been described include *Streptomyces stelliscabiei* (Bouchek-Mechiche et al. 2000), *Streptomyces luridiscabiei*, *Streptomyces puniscabiei*, *Streptomyces niveiscabiei* (Park et al. 2003), *Streptomyces* sp. IdahoX (Wanner 2007), *Streptomyces* sp. DS3024 (Hao et al. 2009) and *Streptomyces* sp. GK18 (Cao et al. 2012). In addition, some pathogenic strains of *Streptomyces bottropensis* were recently reported (Wanner 2009).

The ability of *Streptomyces* spp. to cause CS or AS disease is mainly associated with the production of a family of phytotoxic secondary metabolites called the thaxtomins, which are cyclic dipeptides (2,5-diketopiperazines) derived from L-phenylalanine and L-4-nitrotryptophan (Bignell et al. 2014; King and Calhoun 2009). Thaxtomin A, the predominant family member produced by *S. scabies*, *S. turgidiscabies* and *S. acidiscabies*, functions as an inhibitor of cellulose biosynthesis and may allow penetration of expanding plant tissues during host colonization (Loria et al. 2008). Mutants of *S. scabies* and *S. acidiscabies* that are reduced or defective in thaxtomin A biosynthesis show a corresponding reduction or loss of pathogenicity (Goyer et al., 1998; Healy et al. 2000; Joshi et al. 2007b), indicating that thaxtomin A is an essential virulence factor in these organisms. In addition, *S. scabies*, *S. acidiscabies* and *S. turgidiscabies* are known to produce a secreted necrogenic protein called Nec1, which has no homologues in the database or any characterized motifs (Loria et al. 2006). Though not essential for scab

disease development, the production of Nec1 appears to contribute to host tissue colonization and may play a role in overcoming the host defense response (Joshi et al. 2007a). The *tomA* gene, which encodes a secreted tomatinase enzyme, is also conserved in *S. scabies*, *S. acidiscabies* and *S. turgidiscabies* (Kers et al. 2005; Seipke and Loria 2008). Tomatinases belong to a group of enzymes called saponinases, which hydrolyze and detoxify plant-derived antimicrobial compounds called phytoanticipins (VanEtten et al. 1994). Genes encoding saponinases are found in fungal plant pathogens as well as in the tomato bacterial wilt and canker pathogen *Clavibacter michiganensis* subsp. *michiganensis* (Loria et al. 2006), and in addition to their role in detoxifying antimicrobial compounds, there is evidence that saponinases can play an indirect role in suppressing the induced plant defense responses (Bouarab et al. 2002; Ito et al. 2004). Although the conservation of *tomA* in several plant pathogenic *Streptomyces* spp. suggests a role in host-pathogen interactions, the precise role remains unclear given that a $\Delta tomA$ deletion mutant of *S. scabies* was indistinguishable from the wild-type strain in plant bioassays (Seipke and Loria 2008).

Several previous studies have described the pathogenic *Streptomyces* spp. associated with CS disease in eastern Canada (Faucher et al. 1992; St-Onge et al. 2008; Wanner 2009); however, to our knowledge, there is no information regarding the *Streptomyces* spp. that are responsible for the disease on the island of Newfoundland. The objective of this study was therefore to isolate and characterize the plant pathogenic *Streptomyces* spp. that are associated with potato CS disease in Newfoundland.

6.3 Results and Discussion

Potato tubers harvested in Newfoundland in 2011 and 2012 and displaying typical CS disease symptoms were used to isolate pathogenic *Streptomyces* spp. as described in the Materials and Methods. A total of 52 bacterial strains resembling *Streptomyces* spp. in appearance were recovered from scab lesions, of which 17 (33%) were determined to have a plant pathogenic phenotype when tested in a radish seedling bioassay (Table 6.2). The degree of pathogenicity varied among the different isolates, with several isolates causing severe stunting of radish seedlings in a similar manner as the known pathogenic strains *S. scabies* 87-22, *S. acidiscabies* 84.104 and *S. turgidiscabies* Car8 (Table 6.2). Like *S. scabies*, most of the pathogenic isolates produced gray spores when cultured on ISP-4 agar medium, and 10 of the isolates were determined to produce the secreted brown pigment melanin in TSB (Table 6.2). Production of melanin is a characteristic that has been reported for both *S. scabies* and *S. europaeiscabiei* (Bouchek-Mechiche et al. 2000; Lambert and Loria 1989b). Interestingly, only 8 (47%) of the pathogenic isolates were determined to produce the known virulence determinant thaxtomin A under the culture conditions used (Table 6.2 and Fig. 6.1). All of the thaxtomin-producing strains were confirmed to harbour the *txtA* and *txtD* thaxtomin biosynthetic genes as well as the *necI* virulence gene, and seven of these strains were also determined to contain the putative *tomA* virulence gene (Table 6.2). In contrast, only two of the non-thaxtomin-producing strains were found to contain either the *necI* or the *tomA* gene (Table 6.2). This suggests that novel virulence factors may be contributing to the plant pathogenic phenotype of these strains.

To determine the closest relative of each of the pathogenic isolates, a portion of the *rpoB* gene from each strain was PCR-amplified and sequenced, and the resulting sequences were used to construct a phylogenetic tree. As shown in Figure 6.2, the non-thaxtomin-producing pathogenic isolates were found scattered throughout the tree and did not cluster with any of the known scab-causing pathogens, suggesting that these isolates may represent novel pathogenic species. On the other hand, the thaxtomin A-producing isolates all clustered together with *S. scabies* and *S. europaeiscabiei*, indicating that the isolates likely belong to one of these species, a result that is consistent with the observed phenotypic characteristics (Table 6.2). To further investigate the identity of the thaxtomin-producing isolates, the strains were cultured on ISP-9 medium containing betaine, trans-aconitic acid, D-(+)-trehalose and OMPG as carbon sources. It has been reported (Bouček-Mechiche et al. 2000; Flores-González et al. 2008) that in contrast to *S. scabies*, *S. europaeiscabiei* can utilize trans-aconitate, D-(+)-trehalose and OMPG but not betaine as carbon sources. However, we found that all of the thaxtomin-producing isolates as well as the *S. scabies* 87-22 reference strain could grow on all of the ISP-9 test plates as well as on the negative control plate containing no added carbon source (data not shown). In addition, the test and reference strains all grew on nutrient agar containing 10 IU/ml of penicillin G (data not shown) even though it has been reported that *S. scabies*, but not *S. europaeiscabiei*, is sensitive to penicillin G at that concentration (Bouček-Mechiche et al. 2000; Lambert and Loria 1989b). We then performed RFLP analysis of the PCR-amplified 16S-23S rDNA ITS region using the *Hpy99I* restriction enzyme, which cuts within the *S. scabies* 16S-23S rDNA ITS region and not at all within the corresponding region in *S. europaeiscabiei* (Flores-González et al. 2008). As shown in Figure 6.3, the *S. scabies* 87-22 ITS PCR

product was, as expected, restricted with *Hpy99I*, whereas none of the ITS PCR products from the thaxtomin-producing isolates were restricted with this enzyme, suggesting that the isolates most likely belong to *S. europaeiscabiei*. Further analysis using BOX- and ERIC-PCR fingerprinting confirmed that the isolates are all genetically distinct from the *S. scabies* 87-22 reference strain (Fig. 6.4). It is noteworthy that although the BOX and ERIC band patterns were very similar among the thaxtomin - producing isolates, some differences were observed (Fig. 6.4) suggesting that there is some genetic heterogeneity among the isolates.

Given that previous reports have shown that *S. scabies* is commonly associated with CS disease in eastern Canada (Faucher et al. 1992; St-Onge et al. 2008; Wanner 2009), the absence of *S. scabies* from the Newfoundland pathogenic isolates was surprising. This may be due to the limited number of sites that were used for sampling in this study, and a more extensive survey of pathogenic isolates from different regions of the island may be needed in order to detect the presence of *S. scabies*. *S. europaeiscabiei* is known to be the predominant pathogen in Europe (Dees and Wanner 2012), and a large-scale survey by Wanner (2009) demonstrated that it is also common in North America and may be the predominant pathogenic species in the Canadian provinces of Ontario and Prince Edward Island (Wanner 2009). The results of our study suggest that *S. europaeiscabiei* may also be common in Newfoundland, though further studies will be needed to confirm this.

The 11-1-2 strain was of particular interest to us as it was the only non-thaxtomin A-producing strain that exhibited a severe pathogenic phenotype in the radish seedling bioassay (Table 6.2). Further characterization of the pathogenic phenotype of this strain was performed using a potato tuber disk assay, which demonstrated that the strain could

cause significant pitting of potato tuber tissue (Fig. 6.5-A). In addition, a *Nicotiana benthamiana* leaf infiltration assay showed that strain 11-1-2 could induce severe necrosis of the leaf tissue in the region of infiltration (Fig. 6.5-D). Interestingly, this did not occur when *S. turgidiscabies* Car8 was infiltrated into the leaf tissue, and although tissue necrosis was observed when *S. scabies* 87-22 was infiltrated, the degree of necrosis was consistently lower than that observed with strain 11-1-2 (Fig. 6.5-D). To determine whether a secreted phytotoxin contributes to the plant pathogenic phenotype of strain 11-1-2, supernatants of OBB-grown 11-1-2 were harvested, filter-sterilized and tested in different plant bioassays. Figure 6.5-C shows that in the radish seedling bioassay, the 11-1-2 culture supernatant caused seedling stunting in a similar manner as the *S. scabies* 87-22 culture supernatant, and it was consistently the only supernatant that produced chlorosis and necrosis in the *N. benthamiana* leaf infiltration assay (Fig. 6.5-E). This latter observation was of particular interest as it suggests that another virulence factor besides thaxtomin A is responsible for the observed tissue necrosis caused by the *S. scabies* 87-22 strain (Fig. 6.5-D). Furthermore, when the 11-1-2 culture supernatant was subjected to extraction with ethyl acetate, the resulting extract could cause pitting and necrosis of the potato tuber tissue (Fig. 6.5-B), indicating that the secreted phytotoxic substance produced by strain 11-1-2 is soluble in organic solvent.

In addition to thaxtomin A, *S. scabies* is known to produce concanamycin A, which displays antifungal and phytotoxic activities (Kinashi et al. 1984; Natsume et al. 1996, 1998). We hypothesized that perhaps strain 11-1-2 can also produce this phytotoxin; however, analysis of the 11-1-2 organic culture extracts using RP-HPLC could not detect the presence of concanamycin A in the extracts (Fig. 6.6-A). It was also recently reported

that a *Streptomyces* strain causing deep-pitted lesions on potato tubers does not produce thaxtomins but instead produces an 18-membered macrolide called borrelidin, which in purified form could induce necrosis of potato tuber slices and inhibit the growth of roots and shoots of radish seedlings (Cao et al. 2012). We tested for the presence of borrelidin in the 11-1-2 organic culture extracts using RP-HPLC (Fig. 6.6-B), and although an absorbance peak with a similar retention time (5.097 min) as the borrelidin standard (5.013 min) was observed in the 11-1-2 chromatogram, the two peaks did not co-elute when the standard was co-injected with the culture extract (Fig. 6.6-C). Furthermore, LC-MS analysis of the 11-1-2 organic culture extract did not detect the presence of a compound with the same molecular mass as borrelidin (data not shown). Taken together, these results suggest that strain 11-1-2 does not produce borrelidin under the culture conditions used.

This is the first study describing the isolation and characterization of plant pathogenic *Streptomyces* spp. from Newfoundland. Our results show that scab lesions on potato tubers harvested on the island are associated with a variety of pathogenic *Streptomyces* spp., some of which appear to be novel. The majority of pathogenic isolates were determined to be most similar to *S. europaeiscabiei*, which is commonly associated with CS disease in other Canadian provinces. Whether *S. scabies* and *S. acidiscabies*, which have also been reported in eastern Canada (Faucher et al. 1992; St-Onge et al. 2008; Wanner 2009), are present in Newfoundland as well remains to be determined. A particularly interesting finding from this study was the isolation of a non-thaxtomin-producing *Streptomyces* sp. that displays a severe pathogenic phenotype against different plant hosts and which produces a novel, secreted phytotoxic substance that is soluble in organic solvent. Further characterization of the strain and the phytotoxic substance it

produces is currently underway in order to better understand how the organism is able to cause disease. Until recently, it was thought that all CS-causing pathogens produce thaxtomin A and that this phytotoxin is the primary virulence factor contributing to disease development; however, our findings are among a growing body of evidence suggesting that other phytotoxins can also play a role in CS disease (Bignell et al. 2014). This has important implications for the development of long term control strategies that will effectively manage the disease in potato growing regions around the world.

6.4 Experimental Procedures

6.4.1 *Streptomyces spp. used in this study*

The previously described pathogenic *Streptomyces* spp. *S. scabies* 87-22, *S. acidiscabies* 84.104 and *S. turgidiscabies* Car8 (Lambert and Loria 1989a,b; Loria et al. 1995; Miyajima et al. 1998) as well as the non-pathogenic strain *S. scabies* $\Delta txtA/\Delta cfa6$ (Bignell et al. 2010) were used as reference strains in this study.

6.4.2 *Isolation of Streptomyces spp. from potato scab lesions*

Streptomycetes were isolated from scabby potato tubers that were harvested in Newfoundland in 2011 and 2012. The potatoes were harvested on the Avalon Peninsula from a single location in 2011 and from three different locations in 2012. The isolation procedure was as described previously (Wanner 2004) with some modifications. Briefly, a small piece of tuber containing a scab lesion was excised and surface-sterilized using 1.5% v/v Chlorox bleach for 2 minutes, after which the tissue was rinsed 10 times with sterile

HPLC-grade water. Then, the tissue was homogenized in 0.5 ml of sterile water, and the homogenate was incubated at 55°C for 30 minutes to eliminate any competing rhizobacteria. Next, the homogenate was diluted 100 fold and was plated onto agar (1.5% w/v) water plates containing 25 µg/ml of nalidixic acid and 50 µg/ml of nystatin. The plates were incubated at 28°C for up to 1 month, after which the *Streptomyces*-like colonies were picked and subjected to several rounds of culturing on the International *Streptomyces* Project medium 4 (ISP-4; BD Biosciences, Mississauga, ON) agar plates containing nalidixic acid and nystatin in order to obtain pure cultures of each isolate. Finally, spore or mycelial glycerol stocks of each *Streptomyces*-like isolate were prepared from a single, well-separated colony as described previously (Kieser et al. 2000) and were stored at -80°C.

6.4.3 Morphological and physiological characterization

Streptomyces strains were cultured on ISP-4 for 14-15 days at 28°C, after which the aerial hyphae colour of each strain was recorded. Production of the brown secreted pigment melanin was assessed by culturing the isolates in trypticase soy broth (TSB; BD Biosciences) for 2-4 days at 28°C. To test for utilization of different carbon sources, spores of *Streptomyces* strains were scraped from 10 day old potato mash agar plates (Fyans et al. 2015), washed several times with sterile water, and then resuspended in water. The suspensions (25 µl) were spotted onto plates of the International *Streptomyces* project medium 9 (ISP-9; Himedia Laboratories, Mumbai, India) containing trans-aconitic acid, D-(+) trehalose, betaine and methyl- α -D-galactopyranoside (OMPG) (Sigma Aldrich Canada, Oakville, ON) as carbon sources (1% w/v final concentration). Growth was assessed on the plates following incubation at 28°C for up to 7 days. Medium containing

D-glucose as the carbon source served as a positive control while medium containing water in place of a carbon source served as a negative control. Sensitivity to penicillin G was tested by spotting *Streptomyces* spore suspensions onto nutrient agar (BD Biosciences) containing 10 IU/ml of penicillin G (Sigma Aldrich Canada). Medium lacking antibiotic served as a negative control.

6.4.4 Pathogenicity testing

The pathogenicity of the *Streptomyces* isolates was assessed using a radish seedling bioassay as described previously (Bignell et al. 2010) with some modifications. Briefly, *Streptomyces* isolates were cultured in triplicate in 5 ml of oat bran broth (OBB; Johnson et al. 2007) medium for 7 days at 25°C with shaking (125 rpm) in 6-well tissue culture plates, after which the mycelia were harvested, washed twice with sterile water, and re-suspended in 5 ml of sterile water. Radish seeds (cv ‘Cherry Belle’; Heritage Harvest Seed, Carmen, MB) were surface sterilized by treating with 70% v/v ethanol for 5 minutes followed by 15% v/v Chlorox bleach for 10 minutes. The seeds were rinsed several times with sterile water and were then germinated by incubating at room temperature (22-24°C) for 24 hours in the dark in a sealed Petri dish containing moistened filter paper. Germinated seeds were placed into wells (13 mm in diameter) in 1.5% w/v agar-water plates and were inoculated with the *Streptomyces* mycelial suspensions (200 µl). A total of 6 germinated seeds were inoculated with each mycelial suspension (for a total of 18 seeds per *Streptomyces* isolate), and control plants were inoculated with known pathogenic *Streptomyces* species (*S. scabies* 87-22, *S. acidiscabies* 84-104, and/or *S. turgidiscabies* Car8) or were treated with a non-pathogenic strain (*S. scabies* $\Delta txtA/\Delta cfa6$) or with water

(uninoculated control). The plates were wrapped with parafilm and incubated at $22 \pm 2^{\circ}\text{C}$ under a 16-h photoperiod for 7 days. The total plant size (root + shoot) was measured and averaged for each treatment, and the Student's *t*-test was used to identify statistically significant differences among the treatments as compared to the uninoculated control ($P < 0.05$).

The pathogenicity of the 11-1-2 isolate was further characterized using a potato tuber slice bioassay as described previously (Loria et al. 1995). Potato tuber disks were aseptically prepared and were placed onto moistened filter paper (Whatman 3M, 90 mm) in deep (25 mm) Petri dishes. The tuber disks (5 in total) were then inoculated with mycelia (25 μl) prepared from OBB cultures. Negative control disks were treated with water while positive control disks were treated with mycelia of the *S. turgidiscabies* Car8 strain. The Petri dishes were wrapped with Parafilm and were incubated in the dark at $22 \pm 2^{\circ}\text{C}$ for 7 days, after which the potato slices were photographed.

A leaf infiltration bioassay was also performed to assess the pathogenicity of the 11-1-2- strain. Leaves of 6 week old *N. benthamiana* plants were infiltrated with a spore suspension of the 11-1-2 strain in water. Spores of the *S. scabies* 87-22 strain as well as other *Streptomyces* strains were included in the analysis, and water served as the negative control. A total of 2-3 plants were used for each infiltration experiment, and 2-3 leaves per plant were infiltrated with each sample. Following infiltration, the plants were incubated at $22 \pm 2^{\circ}\text{C}$ under a 16 hr photoperiod for 11 days, after which the leaves were removed and photographed.

6.4.5 Bioactivity of the secreted 11-1-2 phytotoxin

Strain 11-1-2 was cultured in OBB as described above, after which the culture supernatants were harvested and filter sterilized using 0.45 µm syringe filters. Aliquots (25 µl) were then tested for bioactivity using the radish seedling bioassay and the leaf infiltration bioassay as described above, except that the *N. benthamiana* leaves used in the infiltration assay were photographed after 5 days incubation. Uninoculated OBB medium served as the negative control while filter-sterilized OBB culture supernatants of *S. scabies* 87-22 served as the positive control. To determine whether the phytotoxic substance produced by strain 11-1-2 is soluble in organic solvent, the OBB culture supernatants (1 ml) were extracted three times with 0.5 ml of ethyl acetate, and the resulting extracts were combined, dried down and re-suspended in 0.5 ml of 100% methanol. The extracts (25 µl) were then tested in the potato tuber disk assay as described above, with 100% methanol serving as the negative control and extract from OBB cultures of *S. scabies* 87-22 serving as the positive control.

6.4.6 Production of thaxtomin A

Thaxtomin A production was assessed by culturing the *Streptomyces* isolates in OBB medium as described above. The supernatants were harvested following centrifugation of the cultures, and the remaining mycelial pellets were dried for 48 hrs at 50°C and were weighed. A 1 ml aliquot of each supernatant was extracted with 0.5 ml of ethyl acetate, and the resulting extracts were dried by evaporation, re-suspended in 100 µl of 100% HPLC-grade methanol and filtered through a 0.2 µm syringe filter. Detection of thaxtomin A in the extracts was by reverse phase RP – HPLC using an Agilent 1260 Infinity

Quaternary LC system (Agilent Technologies Canada Inc., Mississauga, ON). Samples (5 µl) were loaded onto a Poroshell 120 EC-C18 column (4.6 × 50 mm, 2.7 µm particle size; Agilent Technologies Canada Inc.) and were eluted with an isocratic mobile phase consisting of 30% acetonitrile (ACN) and 70% water at a constant flow rate of 1 ml/min. Metabolites were monitored using a detection wavelength of 380 nm, and the ChemStation software version B.04.03 (Agilent Technologies Canada Inc.) was used for data acquisition and analysis. Quantification of thaxtomin A production was performed by constructing a standard curve using known amounts of a pure, authentic thaxtomin A standard (Santa Cruz Biotechnology Inc., Dallas, TX), and the results were reported as µg of thaxtomin A produced per mg of dried cells.

6.4.7 *Production of concanamycin A and borrelidin*

Detection of concanamycin A and borrelidin production was by RP-HPLC analysis of ethyl acetate culture extracts as described previously (Natsume et al. 1998; Olano et al. 2004). Briefly, samples (5 µl) were loaded onto a Poroshell 120 EC-C18 RP column held at 40°C. For detection of concanamycin A, an isocratic mobile phase consisting of 30% ACN and 70% water was used at a constant flow rate of 1 ml/min. Metabolites were monitored using a detection wavelength of 245 nm, and a pure, authentic standard of concanamycin A (Sigma Aldrich Canada, Oakville, ON) was used for phytotoxin identification in the culture extracts. For detection of borrelidin, the solvent system consisted of 100% water as mobile phase A and 100% ACN as mobile phase B, both containing 0.1% formic acid. A linear gradient from 10% B to 100% B over 5.8 min was applied at a constant flow rate of 1 ml/min. Metabolites were monitored at 257 nm, and a

pure, authentic standard of borrelidin (kindly provided by Kenji Arakawa, Hiroshima University) was used for identification of the phytotoxin in the culture extracts.

Analysis of borrelidin production was also conducted using liquid chromatography-mass spectrometry (LC-MS) with an Agilent 1100 series HPLC system (Agilent Technologies Canada Inc.) interfaced to a Waters G1946A single quadrupole mass spectrometer (Waters Canada, Mississauga, ON). Samples (15 µl) were loaded onto a Zorbax SB-C18 column (4.6 × 150 mm, 5 µm particle size; Agilent Technologies Canada Inc.) and were eluted using a linear gradient from 10 to 100% ACN over 17.4 min at a constant flow rate of 1 ml/min. Detection was by UV radiation (257 nm) and electrospray ionization MS in negative ion mode.

6.4.8 Genotypic characterization

Genomic DNA was prepared from the *Streptomyces* isolates using the DNeasy Blood & Tissue Kit as per the manufacturer's protocol (QIAgen Inc. Canada, Toronto, ON). Primers used for PCR or sequencing were purchased from Integrated DNA Technologies (IDT; Coralville, IA) and are listed in Table 4.1. Amplification of the *rpoB*, *txtA*, *txtD*, *necI* and *tomA* genes and the 16S-23S rDNA internally transcribed spacer (ITS) region was carried out using Phusion DNA polymerase (New England Biolabs Canada, Whitby, ON) or Taq DNA polymerase (Thermo Fisher Scientific Canada, Ottawa, ON) according to the manufacturer's instructions, except that DMSO (5% v/v final concentration) was included in the reactions. Sequencing of the *rpoB* PCR products was performed at The Centre for Applied Genomics (TCAG) (Toronto, ON). RFLP analysis of the amplified 16S-23S rDNA ITS region was performed using the *Hpy99I* restriction enzyme (New England Biolabs

Canada) to distinguish *S. scabiei* from *S. europaeiscabiei* as described previously (Flores-González et al. 2008). Repetitive element PCR fingerprinting (Rep-PCR) was performed using the BOXA1R primer or the ERIC2/ERIC1R primers (Table 6.1). Reactions (25 µl) contained 1× Taq Buffer with KCl (Thermo Fisher Scientific), 4 mM (for BOX-PCR) or 6 mM (for ERIC-PCR) MgCl₂, 0.75 mM dNTPs (New England Biolabs Canada), 10% v/v DMSO, 1 µM of each primer (2 µM of the BOXA1R primer), 1.25U of Taq DNA polymerase (Thermo Fisher Scientific Canada) and 50 ng of genomic DNA. The cycling conditions were as follows: an initial denaturation step at 95°C for 5 minutes followed by 35 cycles of denaturation at 95°C for 1 minute, primer annealing at 50°C for 1 minute, and extension at 72°C for 4 minutes. The resulting products were analyzed by gel electrophoresis using a 1.5% w/v agarose gel and 1× TBE buffer.

6.4.9 Phylogenetic analyses

Alignment of the *rpoB* sequences was performed using the Geneious Pro software version 6.1.2 (Biomatters Ltd., San Francisco, CA). The phylogenetic tree was generated using the MEGA 6.0.6 program (Tamura et al. 2011) with the maximum likelihood method. The significance of the branch order was assessed using the bootstrapping method with 1000 repetitions.

6.3.10 Accession numbers

The partial *rpoB* sequences generated in this study are deposited in GenBank under the accession numbers KR817679-KR817695.

6.5 Acknowledgments

This work was supported by a Canada-Newfoundland and Labrador Agriculture Research Initiative grant (ARI-1314-005) to D.R.D.B and by a Natural Sciences and Engineering Research Council of Canada Discovery Grant (386696-2010) to D.R.D.B. The authors would like to thank Ruth-Anne Blanchard (NL Department of Natural Resources) and Dr. Andrew Lang (Dept. of Biology, Memorial University of Newfoundland) for providing the potato tubers used in this study, Dr. Kenji Arakawa (Hiroshima University) for kindly providing the pure borrelidin standard, and Linda Windsor (Memorial University Centre for Chemical Analysis, Research and Training) for assistance with the LC-MS analysis. The authors would also like to thank the anonymous reviewers for their helpful comments on the manuscript.

6.6 References

- Bignell D.R.D., Fyans J.K., Cheng Z. (2014). Phytotoxins produced by plant pathogenic *Streptomyces* species. *J Appl Microbiol*, 116: 223-235.
- Bignell D.R.D., Seipke R.F., Huguet-Tapia J.C., Chambers A.H., Parry R., Loria R..(2010) *Streptomyces scabies* 87-22 contains a coronafacic acid-like biosynthetic cluster that contributes to plant-microbe interactions. *Mol Plant Microbe Interact*, 23: 161-175.
- Bouarab K., Melton R., Peart J., Baulcombe D., Osbourn A. (2002). A saponin-detoxifying enzyme mediates suppression of plant defences. *Nature*, 418: 889-892.

- Bouchek-Mechiche K., Gardan L., Normand P., Jouan B. (2000). DNA relatedness among strains of *Streptomyces* pathogenic to potato in France: description of three new species, *S. europaeiscabiei* sp. nov. and *S. stelliscabiei* sp. nov. associated with common scab, and *S. reticuliscabiei* sp. nov. associated with netted scab. *Int J Syst Evol Microbiol*, 50(1): 91-99.
- Bukhalid R.A., Chung S.Y., Loria R. (1998). *nec1*, a gene conferring a necrogenic phenotype, is conserved in plant-pathogenic *Streptomyces* spp. and linked to a transposase pseudogene. *Mol Plant Microbe Interact*, 11: 960-967.
- Cao Z., Khodakaramian G., Arakawa K., Kinashi H. (2012). Isolation of borrelidin as a phytotoxic compound from a potato pathogenic *Streptomyces* strain. *Biosci Biotechnol Biochem*, 76: 353-357.
- Clark C.A., Chen C., Ward-Rainey N., Pettis G.S. (1998). Diversity within *Streptomyces ipomoeae* based on inhibitory interactions, rep-PCR, and plasmid profiles. *Phytopathology*, 88(11): 1179-1186.
- Dees M.W., Sletten A., Hermansen A. (2013). Isolation and characterization of *Streptomyces* species from potato scab lesions in Norway. *Plant Pathol*, 62: 217-225.
- Dees M.W., Somervuo P., Lysoe E., Aittamaa M., Valkonen J.P. (2012). Species' identification and microarray-based comparative genome analysis of *Streptomyces* species isolated from potato scab lesions in Norway. *Mol Plant Pathol*, 13: 174-186.
- Dees M.W., Wanner L.A. (2012). In search of better management of potato common scab. *Potato Res*, 55: 249-268.

- Faucher E., Savard T., Beaulieu C. (1992). Characterization of actinomycetes isolated from common scab lesions on potato tubers. *Can J Plant Pathol*, 14: 197-202.
- Flores-González R., Velasco I., Montes F. (2008). Detection and characterization of *Streptomyces* causing potato common scab in Western Europe. *Plant Pathol*, 57: 162-169.
- Fyans J.K., Altowairish M.S., Li Y., Bignell D.R.D. (2015). Characterization of the coronatine-like phytotoxins produced by the common scab pathogen *Streptomyces scabies*. *Mol Plant Microbe Interact*, 28(4): 443-454.
- Goyer C., Vachon J., Beaulieu C. (1998). Pathogenicity of *Streptomyces scabies* mutants altered in thaxtomin A production. *Phytopathology*, 88: 442-445.
- Guo Y., Zheng W., Rong X., Huang Y. (2008). A multilocus phylogeny of the *Streptomyces griseus* 16S rRNA gene clade: use of multilocus sequence analysis for streptomycete systematics. *Int J Syst Evol Microbiol*, 58: 149-159.
- Hao J.J., Meng Q.X., Yin J.F., Kirk W.W. (2009). Characterization of a new *Streptomyces* strain, DS3024, that causes potato common scab. *Plant Dis*, 93: 1329-1334.
- Healy F.G., Wach M., Krasnoff S.B., Gibson D.M., Loria R. (2000). The *txtAB* genes of the plant pathogen *Streptomyces acidiscabies* encode a peptide synthetase required for phytotoxin thaxtomin A production and pathogenicity. *Mol Microbiol*, 38: 794-804.
- Hill J., Lazarovits G. (2005). A mail survey of growers to estimate potato common scab prevalence and economic loss in Canada. *Can J Plant Pathol*, 27: 46-52.

- Hiltunen L.H., Weckman A., Ylhainen A., Rita H., Richter E., Valkonen J.P.T. (2005). Responses of potato cultivars to the common scab pathogens, *Streptomyces scabies* and *S. turgidiscabies*. *Ann Appl Biol*, 146: 395-403.
- Ito S., Eto T., Tanaka S., Yamauchi N., Takahara H., Ikeda T. (2004). Tomatidine and lycotetraose, hydrolysis products of alpha-tomatine by *Fusarium oxysporum* tomatinase, suppress induced defense responses in tomato cells. *FEBS Lett*, 571: 31-34.
- Johnson E.G., Joshi M.V., Gibson D.M., Loria R. (2007). Cello-oligosaccharides released from host plants induce pathogenicity in scab-causing *Streptomyces* species. *Physiol Mol Plant Pathol*, 71: 18-25.
- Joshi M., Rong X., Moll S., Kers J., Franco C., Loria R. (2007a). *Streptomyces turgidiscabies* secretes a novel virulence protein, Nec1, which facilitates infection. *Mol Plant Microbe Interact*, 20: 599-608.
- Joshi M.V., Bignell D.R., Johnson E.G., Sparks J.P., Gibson D.M., Loria R. (2007b). The AraC/XylS regulator TxtR modulates thaxtomin biosynthesis and virulence in *Streptomyces scabies*. *Mol Microbiol*, 66: 633-642.
- Kers J.A., Cameron K.D., Joshi M.V., Bukhalid R.A., Morello J.E., Wach M.J., Gibson D.M., Loria R. (2005). A large, mobile pathogenicity island confers plant pathogenicity on *Streptomyces* species. *Mol Microbiol*, 55: 1025-1033.
- Kieser T., Bibb M.J., Buttner M.J., Chater K.F., Hopwood D.A. (2000). Practical *Streptomyces* Genetics. The John Innes Foundation, Norwich, U.K.

- Kim Y., Cho J.M., Park D., Lee H., Kim J., Seo S., Shin K., Hur J., Lim C. (1999). Production of thaxtomin A by Korean isolates of *Streptomyces turgidiscabies* and their involvement in pathogenicity. *Plant Pathol J*, 15: 168-171.
- Kinashi H., Someno K., Sakaguchi K. (1984). Isolation and characterization of concanamycins A, B and C. *J Antibiot*, 37: 1333-1343.
- King R.R., Calhoun L.A. (2009). The thaxtomin phytotoxins: sources, synthesis, biosynthesis, biotransformation and biological activity. *Phytochemistry*, 70: 833-841.
- Kreuze J.F., Suomalainen S., Paulin L., Valkonen J.P. (1999). Phylogenetic analysis of 16SrRNA genes and PCR analysis of the *nec1* gene from *Streptomyces* spp. causing common scab, pitted scab, and netted scab in Finland. *Phytopathology*, 89: 462-469.
- Lambert D.H., Loria R. (1989a). *Streptomyces acidiscabies* sp. nov. *Int J Syst Bacteriol*, 39: 393-396.
- Lambert D.H., Loria R. (1989b). *Streptomyces scabies* sp. nov., nom. rev. *Int J Syst Bacteriol*, 39: 387-392.
- Lehtonen M.J., Rantala H., Kreuze J.F., Bang H., Kuisma L., Koski P., Virtanen E., Vihlman K., Valkonen J.P.T. (2004). Occurrence and survival of potato scab pathogens (*Streptomyces* species) on tuber lesions: quick diagnosis based on a PCR-based assay. *Plant Pathol*, 53: 280-287.
- Loria R., Bignell D.R., Moll S., Huguet-Tapia J.C., Joshi M.V., Johnson E.G., Seipke R.F., Gibson D.M. (2008). Thaxtomin biosynthesis: the path to plant pathogenicity in the genus *Streptomyces*. *Antonie Van Leeuwenhoek*, 94: 3-10.

- Loria R., Bukhalid R.A., Creath R.A., Leiner R.H., Olivier M., Steffens J.C. (1995). Differential production of thaxtomins by pathogenic *Streptomyces* species *in vitro*. *Phytopathology*, 85: 537-541.
- Loria R., Bukhalid R.A., Fry B.A., King R.R. (1997). Plant pathogenicity in the genus *Streptomyces*. *Plant Dis*, 81: 836-846.
- Loria R., Kers J., Joshi M. (2006). Evolution of plant pathogenicity in *Streptomyces*. *Annu Rev Phytopathol*, 44: 469-487.
- Miyajima K., Tanaka F., Takeuchi T., Kuninaga S. (1998). *Streptomyces turgidiscabies* sp. nov. *Int J Syst Bacteriol*, 48(2): 495-502.
- Natsume M., Ryu R., Abe H. (1996). Production of phytotoxins, concanamycins A and B by *Streptomyces* spp. causing potato scab. *Ann Phytopathol Soc Jpn*, 62: 411-413.
- Natsume M., Yamada A., Tashiro N., Abe H. (1998). Differential production of the phytotoxins thaxtomin A and concanamycins A and B by potato common scab-causing *Streptomyces* spp. *Ann Phytopathol Soc Jpn*, 64: 202-204.
- Olano C., Moss S.J., Braña A.F., Sheridan R.M., Math V., Weston A.J., Méndez C., Leadlay P.F., Wilkinson B., Salas J.A. (2004). Biosynthesis of the angiogenesis inhibitor borrelidin by *Streptomyces parvulus* Tü4055: insights into nitrile formation. *Mol Microbiol*, 52(6): 1745-1756.
- Park D.H., Kim J.S., Kwon S.W., Wilson C., Yu Y.M., Hur J.H., Lim C.K. (2003). *Streptomyces luridiscabiei* sp. nov., *Streptomyces puniscabiei* sp. nov. and *Streptomyces niveiscabiei* sp. nov., which cause potato common scab disease in Korea. *Int J Syst Evol Microbiol*, 53: 2049-2054.

- Seipke R.F., Loria R. (2008). *Streptomyces scabies* 87-22 possesses a functional tomatinase. *J Bacteriol*, 190: 7684-7692.
- Song J., Lee S.C., Kang J.W., Baek H.J., Suh J.W. (2004). Phylogenetic analysis of *Streptomyces* spp. isolated from potato scab lesions in Korea on the basis of 16S rRNA gene and 16S-23S rDNA internally transcribed spacer sequences. *Int J Syst Evol Microbiol*, 54: 203-209.
- St-Onge R., Goyer C., Coffin R., Filion M. (2008). Genetic diversity of *Streptomyces* spp. causing common scab of potato in eastern Canada. *Syst Appl Microbiol*, 31: 474-484.
- Tamura K., Peterson D., Peterson N., Stecher G., Nei M., Kumar S. (2011). MEGA5: molecular evolutionary genetics analysis using maximum likelihood, evolutionary distance, and maximum parsimony methods. *Mol Biol Evol*, 28: 2731-2739.
- Thwaites R., Wale S.J., Nelson D., Munday D., Elphinstone J.G. (2010). *Streptomyces turgidiscabies* and *S. acidiscabies*: two new causal agents of common scab of potato (*Solanum tuberosum*) in the UK. *Plant Pathol*, 59: 804.
- Tóth L., Maeda M., Tanaka F., Kobayashi K. (2001). Isolation and identification of pathogenic strains of *Streptomyces acidiscabies* from netted scab lesions of potato tubers in Hokkaido (Japan). *Acta Microbiol Immunol Hung*, 48: 575-585.
- VanEtten H.D., Mansfield J.W., Bailey J.A., Farmer E.E. (1994). Two classes of plant antibiotics: phytoalexins versus "phytoanticipins". *Plant Cell*, 6: 1191-1192.
- Wanner L.A. (2004). Field isolates of *Streptomyces* differ in pathogenicity and virulence on radish. *Plant Dis*, 88: 785-796.

- Wanner L.A. (2007). A new strain of *Streptomyces* causing common scab in potato. *Plant Dis*, 91: 352-359.
- Wanner L.A. (2009). A patchwork of *Streptomyces* species isolated from potato common scab lesions in North America. *Am J Pot Res*, 86: 247-264.
- Zhao W.Q., Liu D.Q., Yu X.M. (2008). First report of potato scab caused by *Streptomyces turgidiscabies* in China. *Plant Dis*, 92: 1587.
- Zhao W.Q., Yu X.M., Liu D.Q. (2010). First report of *Streptomyces acidiscabies* causing potato scab in China. *Plant Pathol*, 59: 405.

6.7 Figures and Tables

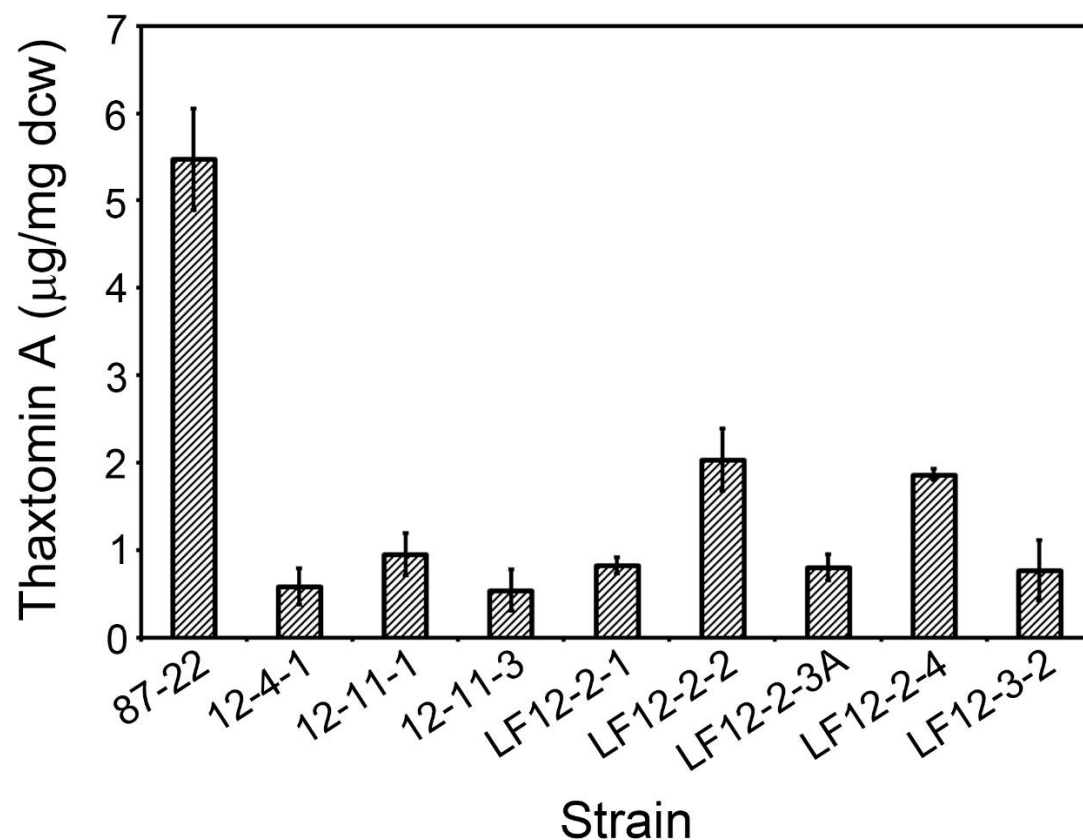


Figure 6.1. Production of thaxtomin A by plant pathogenic *Streptomyces* spp. isolated in this study. Supernatants from triplicate OBB cultures of *S. scabies* 87-22 and of the pathogenic isolates were extracted with ethyl acetate, and the resulting extracts were analyzed by RP-HPLC. The average production level (µg thaxtomin A/mg dry cell weight) for each strain is shown, and the errors bars represent the standard deviation from the mean.



Figure 6.2. Phylogenetic analysis of plant pathogenic *Streptomyces* spp. isolated in this study. The tree is based on the partial *rpoB* gene sequence from the pathogenic isolates and from *Streptomyces* spp. in the database. Bootstrap values $\geq 50\%$ for 1000 repetitions are shown. The scale bar indicates the number of nucleotide substitutions per site. Known pathogenic *Streptomyces* spp. are indicated with *, and non-pathogenic species that have been reported to have some pathogenic strains are indicated with **. The *rpoB* sequence from *Micromonospora aurantiaca* was included as an outgroup.

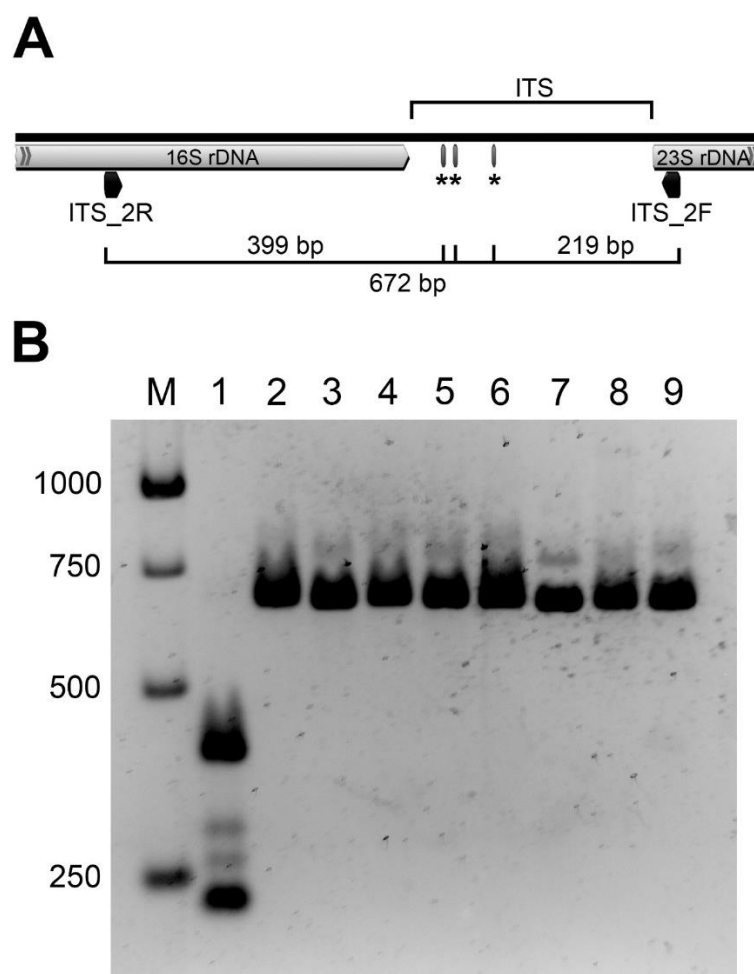


Figure 6.3. RFLP analysis of the 16S-23S rDNA ITS sequence in the thaxtomin A-producing *Streptomyces* spp. isolated in this study. (A) Diagram of the genomic 16S-23S rDNA ITS region in *S. scabies* 87-22. The primers used for PCR amplification of the ITS region are shown as well as the *Hpy*99I restriction sites (indicated by *) that are present within the amplified region. The size of the amplified PCR product as well as the main fragment sizes expected following digestion with *Hpy*99I are also indicated. (B) Agarose gel electrophoresis of the PCR-amplified 16S-23S rDNA ITS region following digestion

with *Hpy99I*. Electrophoresis was conducted using a 2% w/v agarose gel and 1× TBE buffer, and DNA bands were visualized under UV light following staining with ethidium bromide. Lane assignments are as follows: M, 1 kb DNA ladder (Frogga Bio Inc.); 1, *S. scabiei* 87-22; 2, strain LF12-2-3; 3, strain LF12-2-1; 4, strain LF12-2-3A; 5, strain LF12-2-4; 6, strain LF12-3-2; 7, strain 12-11-1; 8, strain 12-11-3; 9, strain 12-4-1. The sizes (in bp) of the DNA ladder bands are indicated.

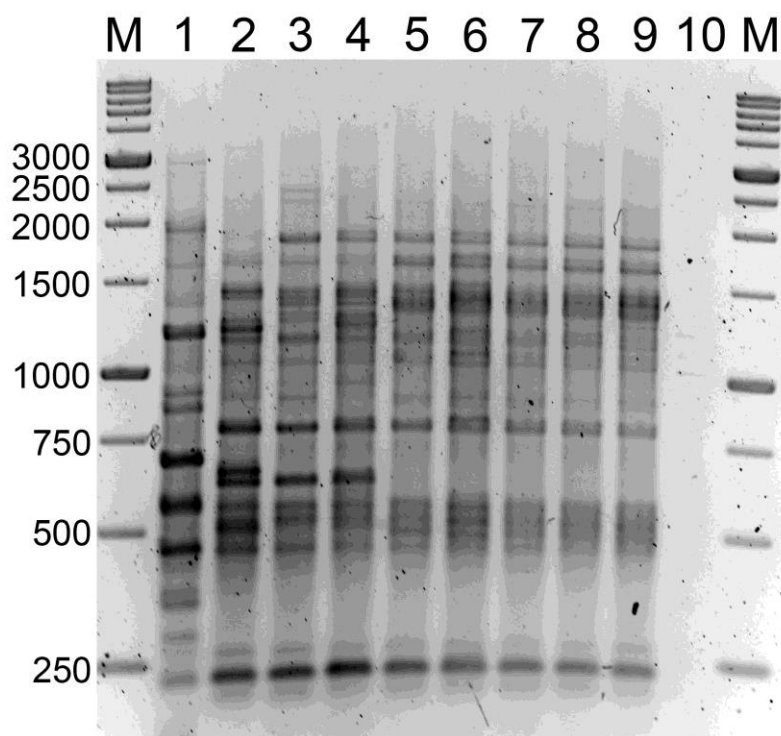
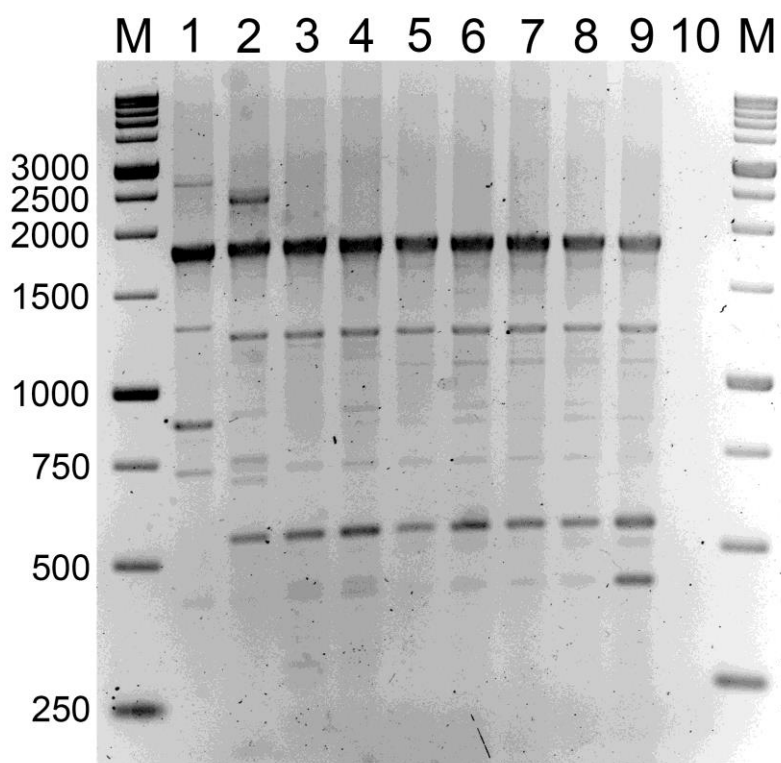
A**B**

Figure 6.4. Rep-PCR analysis of the thaxtomin A-producing *Streptomyces* spp. isolated in this study. BOX-PCR (A) and ERIC-PCR (B) fingerprints following electrophoresis on a 1.5% w/v agarose gel in 1× TBE buffer. DNA bands were visualized under UV light following staining with ethidium bromide. Lane assignments are as follows: M, 1 kb DNA ladder (Frogga Bio Inc.); 1, *S. scabies* 87-22; 2, strain 12-4-1; 3, strain 12-11-1; 4, strain 12-11-3; 5, strain LF12-2-1; 6, strain LF12-2-2; 7, strain LF2-2-3A; 8, strain LF12-2-4; 9, strain LF12-3-2; 10, water control. The sizes (in bp) of the DNA ladder bands are indicated.

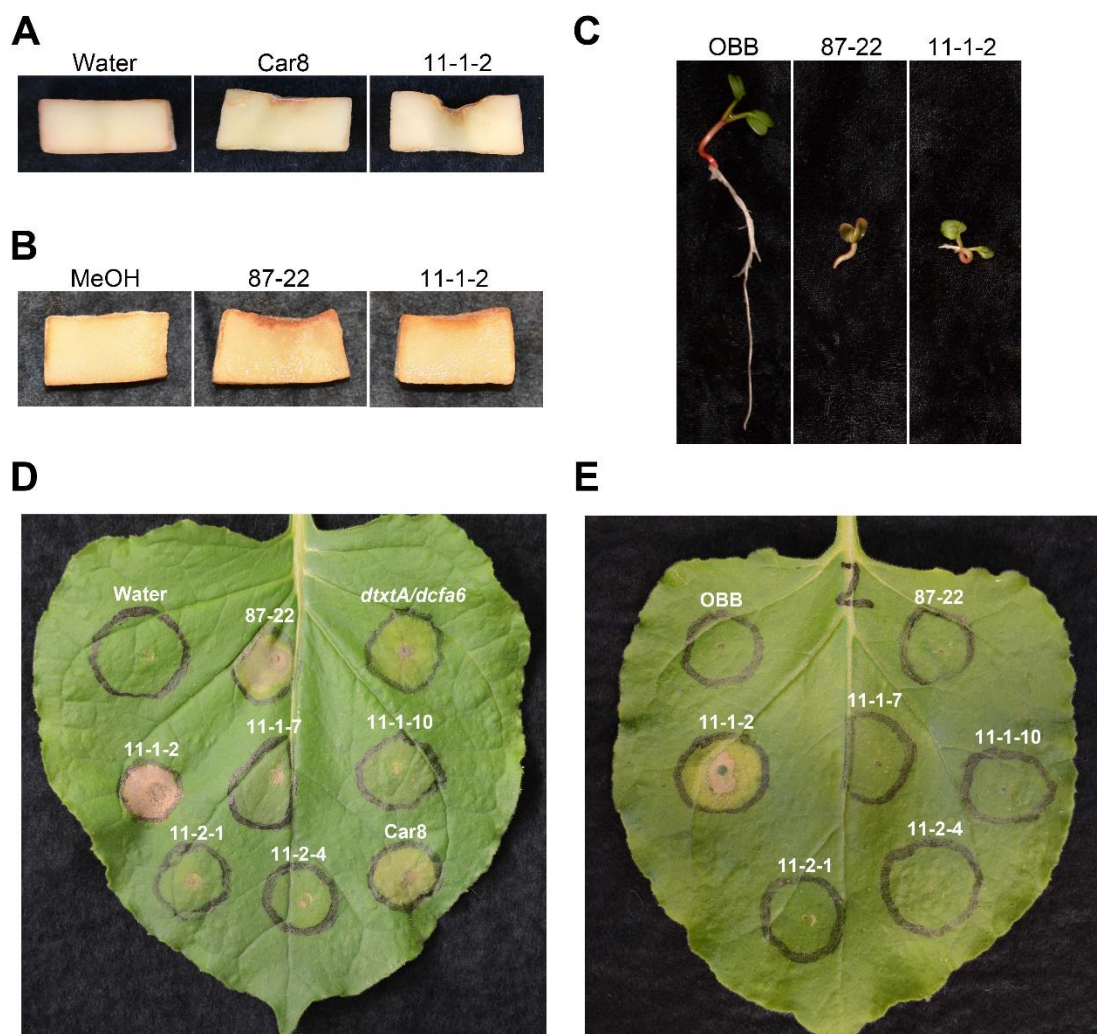


Figure 6.5. Plant pathogenic phenotype of *Streptomyces* sp. strain 11-1-2 on different plant hosts. (A, B) A potato tuber disk bioassay was performed using mycelia (A) or organic culture extract (B) of strain 11-1-2. Mycelia of *S. turgidiscabies* Car8 or culture extract of *S. scabies* 87-22 was used as a positive control while water or methanol (MeOH) was used as a negative control. (C) A radish seedling bioassay was performed using filter-sterilized OBB culture supernatants of *S. scabies* 87-22 and strain 11-1-2. Control seedlings were

treated with sterile uninoculated OBB medium. (D, E) A *Nicotiana benthamiana* leaf infiltration bioassay was performed using spores (D) or filter-sterilized OBB culture supernatants (E) of different *Streptomyces* spp. Treatment with water or with sterile uninoculated OBB medium was included as a negative control.

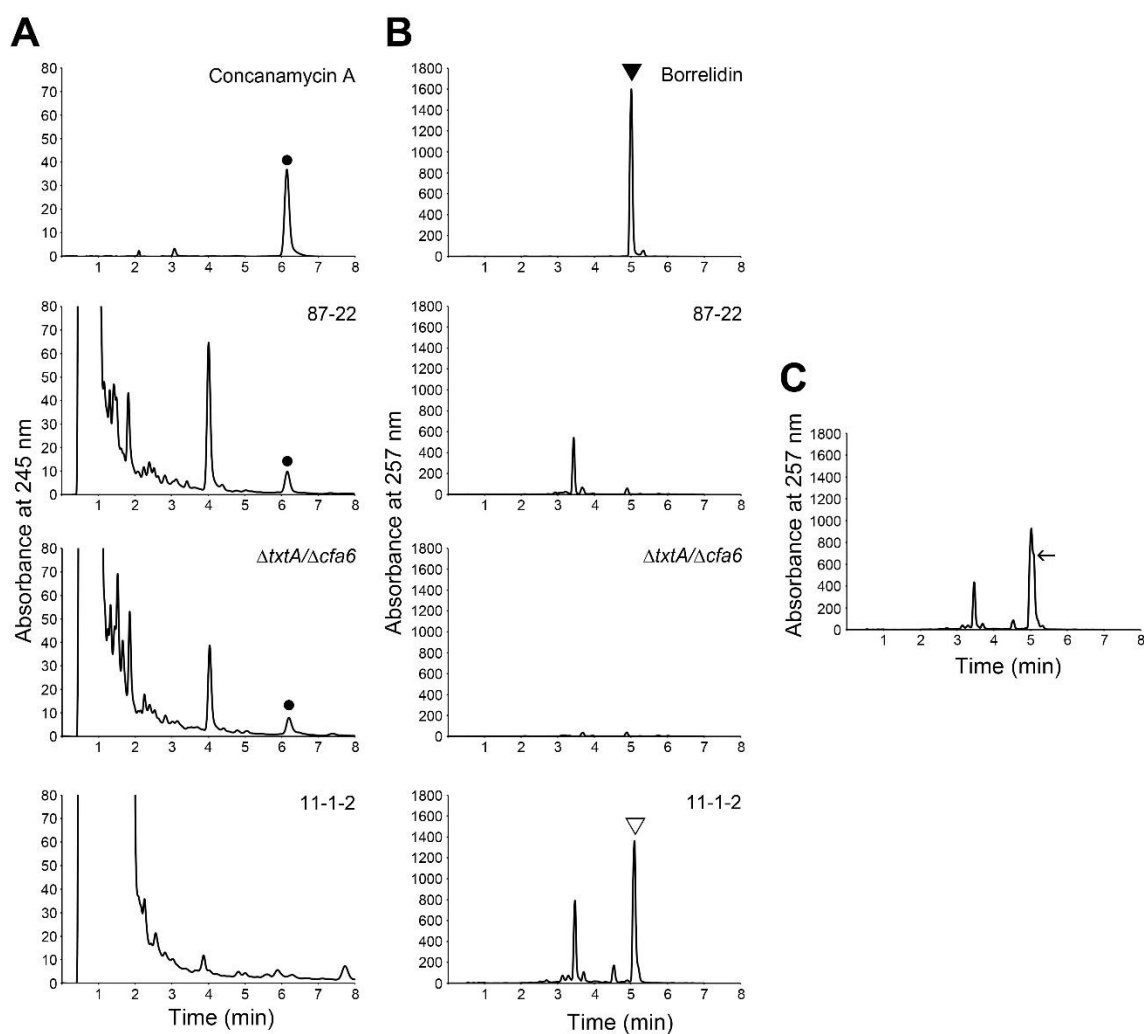


Figure 6.6. Analysis of concanamycin A and borrelidin production by *Streptomyces* spp. OBB culture supernatants of *S. scabies* 87-22, *S. scabies* $\Delta txtA/\Delta cfa6$ and *Streptomyces* sp. strain 11-1-2 were extracted with ethyl acetate, and the resulting extracts were analyzed for the presence of concanamycin A (A) or borrelidin (B) by RP-HPLC. Authentic standards of concanamycin A and borrelidin were included as controls. The concanamycin A peak is indicated by • and the borrelidin peak is indicated by ▼. The peak in the 11-1-2 chromatogram that had a similar retention time as the borrelidin standard is indicated

with ▽. (C) Co-injection analysis of the 11-1-2 culture extract and the borrelidin standard. Equivalent volumes of the extract and standard were combined together, and the mixture was analyzed by RP-HPLC. The shoulder observed on the peak at 5.013 min (indicated by ←) demonstrates that the borrelidin standard did not co-elute with the ▽ peak in the 11-1-2 culture extract.

Table 6.1: Primers used for PCR and sequence analysis of the Newfoundland pathogenic *Streptomyces* isolates

Gene/Region	Primers	Nucleotide Sequence (5' - 3')	Reference
<i>txtA</i>	JKF_txtA_for JKF_txtA_rev	ACACTCGCGCTGTTCGAC CGACAGCCACGACAGCG GCATC	This study
<i>txtD</i>	JKF_txtD_for JKF_txtD_rev	ACTGGAACAGCCTGCGC GTCCCGTGCCCATGTACC AGCCG	This study
<i>nec1</i>	JKF_nec1_for JKF_nec1_rev	ATGAGCGCGAACGGAAG CCCCGGAGCAGGTCGTC ACGAAGGATCG	Bukhalid et al. 1998
<i>tomA</i>	JKF_tomA_for JKF_tomA_rev	GAGGCGTTGGTGGAGTT CTATTGGGGTTGTACTCC TCGTC	St-Onge et al. 2008
<i>rpoB</i>	rpoBF1 rpoBR1	TTCATGGACCAGAACAA CCCGTAGTTGTGACCCTC CC	Guo et al. 2008
16S-23S rDNA ITS	ITS_2F ITS_2R	AAACTTGGCCACAGATG CTCGTCAAGTCATCATGC CCCTT	Song et al. 2004
BOX elements	BOXA1R	CTACGGCAAGGCGACGC TGACG	Clark et al. 1998
ERIC elements	ERIC2 ERIC1R	AAGTAAGTGACTGGGGT GAGCGATGTAAGCTCCT GGGGATTAC	Clark et al. 1998

Table 6.2: Phenotypic and genotypic characterization of the Newfoundland pathogenic *Streptomyces* isolates

Isolate Number	Aerial Hyphae Colour ^a	Melanin Production ^b	Degree of Pathogenicity ^c	Known/Predicted Virulence Genes ^d				Thaxtomin A Production ^e
				<i>txtA</i>	<i>txtD</i>	<i>necI</i>	<i>tomA</i>	
11-1-2	Gray	-	++*	-	-	-	-	-
11-1-7	Gray	-	++	-	-	-	+	-
11-1-10	Green	+	+	-	-	+	-	-
11-2-1	Gray	-	+	-	-	-	-	-
11-2-4	Gray	-	++	-	-	-	-	-
12-2-3	Brown	-	+	-	-	-	-	-
12-4-1	Gray	+	++*	+	+	+	-	+
12-11-1	Gray	+	++*	+	+	+	+	+
12-11-3	Gray	+	++*	+	+	+	+	+
12-11-5	Gray	+	++	-	-	-	-	-
12-15-1	Gray	-	+	-	-	-	-	-
LF12-2-1	Gray	+	++*	+	+	+	+	+
LF12-2-2	Gray	+	++*	+	+	+	+	+
LF12-2-3A	Gray	+	++*	+	+	+	+	+
LF12-2-4	Gray	+	++*	+	+	+	+	+
LF12-3-2	Gray	+	++*	+	+	+	+	+
LF12-4-3	Gray	-	++	-	-	-	-	-

^a Aerial hyphae colour was assessed on the International *Streptomyces* Project medium 4 (ISP-4) after 14-15 days incubation at 28°C.

^b Presence (+) or absence (-) of melanin production was determined by observing brown pigment production in trypticase soy broth medium after 2-4 days incubation at 28°C.

^c Measured using a radish seedling bioassay. (+), average plant size $\geq 50\%$ and $< 100\%$ of average mock-treated plant size; (++) , average plant size $< 50\%$ of average mock-treated plant size. * Indicates that the degree of pathogenicity observed was comparable to that of the control strains *S. scabies* 87-22, *S. acidiscabies* 84.104 and *S. turgidiscabies* Car8.

^d Presence (+) or absence (-) of known or predicted virulence genes was determined using PCR.

^e Production (+) or lack thereof (-) of thaxtomin A was determined by RP-HPLC analysis of culture extracts.

Chapter 7: Draft Genome Sequence of the Plant Pathogen *Streptomyces* sp. 11-1-2

Luke Bown and Dawn R. D. Bignell

Department of Biology, Memorial University of Newfoundland, St. John's, NL, Canada

Address correspondence to Dawn R. D. Bignell, dbignell@mun.ca

7.1 Abstract

Streptomyces sp. 11-1-2 is a Gram-positive filamentous bacterium that was isolated from a common scab lesion on a potato tuber. The strain is highly pathogenic to plants but does not produce the virulence-associated *Streptomyces* phytotoxin thaxtomin A. Here, we report the draft genome sequence of *Streptomyces* sp. 11-1-2.

7.2 Results and Discussion

Members of the *Streptomyces* genus are Gram-positive, filamentous spore forming bacteria that are best known for the ability to produce a wide variety of secondary metabolites with useful biological activities (Bérdy 2005). A small number of *Streptomyces*

spp. can additionally form parasitic relationships with plants and cause economically important crop diseases such as potato common scab (Loria et al. 2006). Most scab-causing streptomycetes produce thaxtomin A, a phytotoxic secondary metabolite that is essential for scab disease development (Bignell et al. 2014). Recently, we isolated *Streptomyces* sp. 11-1-2 from a common scab lesion on a potato tuber harvested in Newfoundland, Canada (Fyans et al. 2016). This strain was shown to be highly pathogenic to plants and produces at least one organic-soluble phytotoxin, but it does not produce thaxtomin A (Fyans et al. 2016).

Genomic DNA was extracted from *Streptomyces* sp. 11-1-2 using the salting out protocol (Kieser et al. 2000) and was sequenced using the Pacific Biosciences RSII platform (Menlo Park, CA, USA) at the McGill University and Génome Québec Innovation Centre (Montreal, Quebec, Canada). This produced a total of 198,563 raw subreads with an average length of 11,877 bp using two single-molecule real-time (SMRT) cells. The reads were assembled using the Hierarchical Genome Assembly Process (HGAP) (Chin et al. 2013) into two contigs totalling 11,655,206 bp, with an average coverage of 230× and an average GC content of 70.85%. The analysis indicated that the genome consists of a single linear chromosome (11,603,877 bp) with a centrally located origin of replication, and a single plasmid (51,329 bp).

Gene prediction and annotation were carried out using the NCBI Prokaryotic Genome Annotation Pipeline version 4.2 (Tatusova et al. 2016). A total of 9,036 protein-coding genes, 64 tRNA and 18 rRNA genes (six 5S, six 16S, six 23S) were identified. Secondary metabolite biosynthetic gene clusters (BGCs) were predicted using antiSMASH

version 4.0 (Blin et al. 2017), which identified 47 putative BGCs in the genome. This includes nine type I polyketide synthase (PKS) gene clusters, one type II PKS gene cluster, five nonribosomal peptide synthetase (NRPS) gene clusters, three hybrid PKS-NRPS gene clusters, and other BGCs for producing siderophores, lantipeptides and terpenes. One BGC was found to be identical to the known gene cluster for producing the polyether ionophore nigericin (Harvey et al. 2007). Also identified was a type I PKS BGC that is highly similar to the gene cluster that produces the phytotoxic ansamycin herbimycin in *Streptomyces hygroscopicus* (Rascher et al. 2005).

Nucleotide BLAST analysis indicated that the *Streptomyces* sp. 11-1-2 chromosome sequence is most similar to that of *Streptomyces violaceusniger* Tü 4113 (96.8% nucleotide identity). It is currently unclear if the sequence differences between *Streptomyces* sp. 11-1-2 and *S. violaceusniger* exist at the strain level or the species level.

The *Streptomyces* sp. 11-1-2 genome sequence will be a valuable resource for characterizing the phytotoxic secondary metabolite(s) produced by this strain as well as other virulence factors that contribute to the plant pathogenic phenotype of the organism.

Accession number(s). The draft genome sequence of *Streptomyces* sp. 11-1-2 has been deposited in DDBJ/ENA/GenBank under the accession numbers CP022545 and CP022546. The version described in this paper is the first version, CP022545.1 and CP022546.1.

7.3 Acknowledgements

This work was supported by a Natural Sciences and Engineering Research Council of Canada Discovery Grant (386696-2010) to D.R.D.B. LB was supported in part through a fellowship from the School of Graduate Studies at Memorial University of Newfoundland.

7.4 References

- Bérdy J. (2005). Bioactive microbial metabolites. *J Antibiot (Tokyo)*, 58:1-26.
- Bignell D.R.D., Fyans J.K., Cheng Z. (2014). Phytotoxins produced by plant pathogenic *Streptomyces* species. *J Appl Microbiol*, 116:223-235.
- Blin K., Wolf T., Chevrette M.G., Lu X., Schwalen C.J., Kautsar S.A., Suarez Duran H.G., de Los Santos E.L.C., Kim H.U., Nave M., Dickschat J.S., Mitchell D.A., Shelest E., Breitling R., Takano E., Lee S.Y., Weber T., Medema M.H. (2017). antiSMASH 4.0-improvements in chemistry prediction and gene cluster boundary identification. *Nucleic Acids Res*, 45: W36-W41.
- Chin C.S., Alexander D.H., Marks P., Klammer A.A., Drake J., Heiner C., Clum A., Copeland A., Huddleston J., Eichler E.E., Turner S.W., Korlach J. (2013). Nonhybrid, finished microbial genome assemblies from long-read SMRT sequencing data. *Nat Methods*, 10:563-9.

- Fyans J.K., Bown L., Bignell D.R.D. (2016). Isolation and characterization of plant-pathogenic *Streptomyces* species associated with common scab-infected potato tubers in Newfoundland. *Phytopathology*, 106:123-131.
- Harvey B.M., Mironenko T., Sun Y., Hong H., Deng Z., Leadlay P.F., Weissman K.J., Haydock S.F. (2007). Insights into polyether biosynthesis from analysis of the nigericin biosynthetic gene cluster in *Streptomyces* sp. DSM4137. *Chem Biol*, 14:703-14.
- Kieser T., Bibb M.J., Buttner M.J., Chater K.F., Hopwood D.A. (2000). Practical *Streptomyces* Genetics. The John Innes Foundation, Norwich, UK.
- Loria R., Kers J., Joshi M. (2006). Evolution of plant pathogenicity in *Streptomyces*. *Annu Rev Phytopathol*, 44:469-87.
- Rascher A., Hu Z., Buchanan G.O., Reid R., Hutchinson C.R. (2005). Insights into the biosynthesis of the benzoquinone ansamycins geldanamycin and herbimycin, obtained by gene sequencing and disruption. *Appl Environ Microbiol*, 71:4862-71.
- Tatusova T., DiCuccio M., Badretdin A., Chetvernin V., Nawrocki E.P., Zaslavsky L., Lomsadze A., Pruitt K.D., Borodovsky M., Ostell J. (2016). NCBI prokaryotic genome annotation pipeline. *Nucleic Acids Res*, 44:6614-24.

Chapter 8: Summary and Future Directions

8.1 Coronafacoyl phytotoxin production by *S. scabies*

The first objective of this study was to further investigate the biosynthetic pathway leading to coronafacoyl phytotoxin production in the CS pathogen *S. scabies* by characterizing the role of the *oxr*, *sdr*, *CYP107AK1*, and *cfl* genes in metabolite biosynthesis. All four genes are located within the CFA-like BGC that is responsible for producing CFA-Ile, the primary coronafacoyl phytotoxin synthesized by *S. scabies* (Fyans et al. 2015). In *Pseudomonas* species, a homologous gene cluster called the CFA BGC is involved in the production of COR, which is the best-characterized coronafacoyl phytotoxin to date (Bender et al. 1996; Bender et al. 1999). COR and CFA-Ile both contain the CFA polyketide that is produced by the CFA and CFA-like BGCs, respectively but they differ in the amino acid moiety that is attached to the CFA polyketide (Bender et al. 1999). Although COR is the primary coronafacoyl phytotoxin produced by *Pseudomonas* spp., other coronafacoyl phytotoxins, including CFA-Ile can be produced by these organisms in minor amounts (Bender et al. 1999).

The *S. scabies* CFA-like BGC is atypical in that it contains several biosynthetic genes that do not have any corresponding homologues in the *P. syringae* CFA BGC, including *oxr*, *sdr* and *CYP107AK1* (Bignell et al. 2010). It had previously been proposed that these additional biosynthetic genes may contribute to the production of novel coronafacoyl phytotoxins by functioning as tailoring enzymes (Bignell et al. 2010). In this

context, the core genes shared between the CFA and CFA-like BGCs would produce the main CFA backbone, and then the novel tailoring enzymes would perform minor structural modifications to the CFA molecule to produce other coronafacoyl phytotoxin family members that may differ in bioactivity. However, this hypothesis was determined to be incorrect based on the discovery that *S. scabies* mainly produces the known coronafacoyl phytotoxin CFA-Ile (Fyans et al. 2015). *oxr*, *sdr* and *CYP107AK1* are co-transcribed with the core phytotoxin biosynthetic genes (Bignell et al. 2010), suggesting that they are somehow involved in the biosynthesis of CFA-Ile. Thus, the role of these genes was further investigated in this study.

Deletion of the *oxr*, *sdr* and *CYP107AK1* genes from the *S. scabies* chromosome showed that all three genes are necessary for full production of CFA-Ile, with *CYP107AK1* being essential (Bown et al. 2016; Bown et al. 2017; Chapters 2 and 3). Structural characterization of the intermediate compounds that accumulated in the $\Delta CYP107AK1$ and Δsdr mutant culture supernatants revealed that both enzymes are involved in the introduction of the keto group onto the bicyclic hydrindane ring of the CFA polyketide. Specifically, the CYP107AK1 P450 monooxygenase introduces a hydroxyl group onto the polyketide backbone, after which the Sdr short chain dehydrogenase/reductase oxidizes the hydroxyl group to form the keto group. It is currently unknown if these modifications take place when the bicyclic hydrindane ring is being constructed and is attached to the Cfa6-7 PKS enzymes, or if they take place after the fully formed polyketide has been released from Cfa7. Given that homologues of Sdr and CYP107AK1 were not found encoded within the CFA BGC or elsewhere in the genome of *Pseudomonas* spp., these findings suggest that

S. scabies and *Pseudomonas* spp. use distinct biosynthetic pathways for producing coronafacoyl phytotoxins. Furthermore, our results demonstrate that the reaction catalyzed by CYP107AK1 during CFA-Ile biosynthesis is critical for the bioactivity of the phytotoxin since the accumulated intermediates in the Δ CYP107AK1 mutant were abolished in bioactivity in our plant bioassay (Bown et al. 2017; Chapter 3).

This study also identified putative coronafacoyl phytotoxin BGCs in other bacteria species, including one not previously known to be pathogenic to plants (Bown et al. 2017; Chapter 3). Several of the identified gene clusters were found to be highly similar in organization and content to the *S. scabies* CFA-like BGC and contained homologues of *oxr*, *CYP107AK1* and/or *sdr*. In addition, such gene clusters were found to encode Cfa7 PKS enzymes that are similar to *S. scabies* Cfa7 in that they harbour the ER domain that is absent from the Cfa7 homologue from *Pseudomonas* spp. This suggests that the novel biosynthetic pathway that we identified in *S. scabies* for production of coronafacoyl phytotoxins may also occur in other bacterial species. Our study also provides convincing evidence that HGT has contributed to the dissemination of coronafacoyl phytotoxin biosynthetic genes among phylogenetically distinct bacteria. While it remains to be determined whether phytotoxin production occurs in all of the organisms in which the biosynthetic genes were found, our study suggests that production of these compounds may be more widespread than previously recognized and that the metabolites may play additional roles for the producing organisms other than as virulence factors.

The function of the *cfl* gene was also investigated as part of this study. *cfl* is one of the core biosynthetic genes that is conserved in all known or predicted coronafacoyl

phytotoxin BGCs (Bown et al. 2017; Chapter 3) and was previously proposed to be responsible for coupling CFA to its amino acid partner in the final step of coronafacoyl phytotoxin biosynthesis (Liyange et al. 1995; Ranaswamy et al. 1998), though this had not been demonstrated experimentally. Our study confirms that the Cfl enzyme is the only enzyme required for the final coupling step as purified *S. scabies* Cfl-HIS₆ was able to synthesize CFA-Ile from the individual components *in vitro* (Chapter 5). Furthermore, we demonstrated that the coupling reaction involves the formation of an adenylated CFA intermediate, and this presumably serves to activate the carboxylic acid prior to the ligation step. This is in agreement with the predicted function of Cfl as an adenylate-forming enzyme based on sequence similarity with several other enzymes that catalyze adenylation reactions (Liyange et al. 1995).

Overall, this research has provided a greater understanding of the biosynthetic pathway leading to production of the CFA-Ile phytotoxin by *S. scabies* 87-22. However, there are still numerous questions that remain to be addressed. While this study has provided insight into the function of the Sdr and CYP107AK1 enzymes in the biosynthesis of CFA-Ile, the function of the Oxr enzyme remains unknown given that no biosynthetic intermediates were detected in the Δoxr mutant culture extracts (Bown et al. 2016; Chapter 2). Sequence homology has suggested that Oxr is a F₄₂₀-dependant oxidoreductase, and these enzymes have previously been associated with chemical reactions including redox transformation of alcohols, imines and carbon-carbon double bonds (Taylor et al. 2013). Based on this, we can predict that Oxr is involved in the introduction of a carbon-carbon double bond in the CFA moiety of the CFA-Ile compound. However, this raises the

question of why this step is necessary in *S. scabies* when there are no Oxr homologues present in *Pseudomonas* spp.? This may be related to the ER domain found in the Cfa7 enzyme of *S. scabies* and other *Streptomyces* spp. that, if active, could allow for the complete reduction of the β -keto ester following extension with the malonate unit (Bown et al. 2016; Chapter 2). In *P. syringae*, the Cfa7 enzyme is predicted to perform an incomplete reduction of the β -keto ester resulting in the formation of the carbon-carbon double bond in the CFA molecule (Bown et al. 2016; Chapter 2). Therefore, if the ER domain of the Cfa7 enzyme in *S. scabies* is active, then the re-introduction of the carbon-carbon double bond via the Oxr enzyme would be necessary to produce CFA-Ile, an idea that warrants further investigation.

Another area of future work includes a more detailed analysis of the substrate specificities of the Cfl homologues in *S. scabies* and *P. syringae*. The main coronafacoyl phytotoxin produced by *S. scabies* is CFA-Ile but the organism is also capable of producing minor coronafacoyl phytotoxins, the nature and activity of which are currently unknown (Fyans et al. 2015). *P. syringae* produces COR as the main coronafacoyl phytotoxin but is also capable of producing small quantities of CFA-Ile, *N*-coronafacoyl-L-valine (CFA-Val) and *N*-coronafacoyl-L-*allo*-isoleucine (Bender et al. 1999). This raises the question of why CFA-Ile and COR are the predominant metabolites produced by *S. scabies* and *P. syringae* respectively, and whether it is related to the substrate preference of the corresponding Cfl enzymes. In addition, there is currently nothing known regarding the amino acid residues in the Cfl protein that are essential for its function. A deeper understanding of the Cfl enzyme is expected to be of broad interest given that Cfl catalyzes a critical step in

phytotoxin biosynthesis and that it is conserved in all of the phytotoxin biosynthetic gene clusters identified (Bown et al. 2017; Chapter 3).

A more detailed examination of the bacteria identified in Chapter 3 that also contain the CFA-like BGC is another aspect of future work that should also be conducted. The discovery of the CFA-like BGC in the genome sequences of non-pathogenic bacteria raises several questions, including whether such bacteria produce coronafacoyl phytotoxins and if so, which ones? Also, what role(s) would the metabolites play for these organisms? Prior to our study, coronafacoyl phytotoxins were exclusively thought of as virulence factors involved in promoting the infection and colonization of plant hosts by different pathogens. However, the results of our work raises the possibility that the metabolites may play other roles that are unrelated to plant pathogenicity. What those roles might be remains to be determined, although it is of note that at least two of the species identified to have the CFA/CFA-like BGC and were not previously known to be pathogens *Pseudomonas psychrotolerans* and *Azospirillum* sp. B510, are reported to be associated with plants, and *Azospirillum* sp. B510 has been shown to promote growth of rice plants and to provide resistance to fungal and bacterial pathogens (Kaneko et al. 2010; Midha et al. 2016).

8.2 Plant pathogenic *Streptomyces* spp. in Newfoundland

The second objective of this study was to further investigate the pathogenic *Streptomyces* spp. associated with CS disease in Newfoundland. At least 10 different *Streptomyces* spp. are associated with CS disease worldwide, of which *S. scabies* appears

to be the most important in North America (Dees and Wanner 2012). With Newfoundland being an island, it was possible that the types and distribution of pathogenic species that exist here are distinct from that on the mainland, and yet no studies had been conducted previously on this subject. This study suggests that *S. europaeiscabiei* may be the predominant species associated with CS in Newfoundland given that it was the primary species that was isolated from CS-infected potato tubers (Fyans et al. 2016; Chapter 6). *S. europaeiscabiei* is commonly found in Europe and is also widely distributed in North America, including Canada (Dees and Wanner 2012; Wanner 2009). Our study also demonstrated the presence of several pathogenic *Streptomyces* isolates that are not related to the known CS pathogens, and thus they may represent novel pathogenic species. Surprisingly, none of the pathogenic isolates recovered were *S. scabies*, though this could be due to the small sample size used in this study.

This study also examined these newly identified pathogenic isolates for the presence of the known or predicted virulence factors associated with CS pathogens. The predominant virulence factor produced by CS-causing species is thaxtomin A which is a cyclic dipeptide (2,5-diketopiperazine) derived from L-phenylalanine and 4-nitro-L-tryptophan (King and Calhoun 2009; Loria et al. 2008). All of the *S. europaeiscabiei* isolates were observed to produce thaxtomin A, however, the overall production levels for the isolates was significantly less than that for *S. scabies* 87-22 (Fyans et al. 2016; Chapter 6). The remaining pathogenic isolates were unable to produce thaxtomin A, and the thaxtomin biosynthetic genes were not detectable by PCR. Most interestingly, one of these thaxtomin A non-producers (*Streptomyces* sp. strain 11-1-2) was observed to display a

severe pathogenic phenotype against multiple plant hosts and produced an unknown phytotoxic substance that is soluble in organic solvent (Fyans et al. 2016; Chapter 6). Whole genome sequencing of the isolate revealed that it is most similar to *Streptomyces violaceusniger* Tü 4113 with a 96.8 % nucleotide identity (Bown and Bignell 2017; Chapter 7). The genome sequence also revealed the presence of multiple putative secondary metabolite BGCs, including one that is highly similar to that involved in production of the phytotoxic metabolite herbimycin in *S. hygroscopicus*. The results of our work provide further evidence that phytotoxins other than thaxtomin A can contribute to CS disease development in the environment.

Several questions have arisen regarding this work and remain to be answered. The nature of the phytotoxic substance that is produced by *Streptomyces* sp. strain 11-1-2 and the role that it plays in the pathogenicity of the strain needs to be further explored. Recent studies from our lab identified culturing conditions that suppress the production of the phytotoxic compound (A. Collins and D. Bignell; unpublished results), and such conditions may be useful for purifying and identifying the compound using LC-MS analysis. The availability of the genome sequence of the organism along with CRISPR/Cas9-based mutagenesis systems for *Streptomyces* spp. may allow for investigations into the role of the phytotoxin as well as other potential virulence factors(s) in the pathogenicity of *Streptomyces* sp. 11-1-2. The final area of future work should be a more comprehensive study of the pathogenic *Streptomyces* spp. that contribute to CS disease on the island of Newfoundland. The small sample size of our study means that the suggestion that *S. europaeiscabiei* may be the predominant pathogenic *Streptomyces* spp. in Newfoundland

is only tentative, and a more detailed study that encompassed a greater geographical area would be useful in determining if this trend was province-wide or localized to the tested sites.

8.3 References

- Bender C., Palmer D. (1996). Biosynthesis of coronatine, a thermoregulated phytotoxin produced by the phytopathogen *Pseudomonas syringae*. *Arch Microbiol*, 166: 71-75.
- Bender C., Rangaswamy V., Loper J. (1999). Polyketide production by plant-associated pseudomonads. *Annu Rev Phytopathol*, 37: 175-196.
- Bignell D.R.D., Seipke R.F., Huguet-Tapia J.C., Chambers A.H., Parry R., Loria R. (2010). *Streptomyces scabies* 87-22 contains a coronafacic acid-like biosynthetic cluster that contributes to plant-microbe interactions. *Mol Plant Microbe Interact*, 23: 161-175.
- Bown L., Altowairish M.S., Fyans J.K., Bignell D.R.D. (2016). Production of the *Streptomyces scabies* coronafacoyl phytotoxins involves a novel biosynthetic pathway with an F₄₂₀ - dependent oxidoreductase and a short-chain dehydrogenase/reductase. *Mol Microbiol*, 101: 122-135.
- Bown L., Li Y., Berrue F., Verhoeven J.T.P., Dufour S.C., Bignell D.R.D. (2017). Coronafacoyl phytotoxin biosynthesis and evolution in the common scab pathogen *Streptomyces scabiei*. *Appl Environ Microbiol*, 83: e01169-01117.

- Dees M.W., Wanner L.A. (2012). In search of better management of potato common scab. *Potato Res*, 55: 249-268.
- Fyans J.K., Altowairish M.S., Li Y., Bignell D.R.D. (2015). Characterization of the coronatine-like phytotoxins produced by the common scab pathogen *Streptomyces scabies*. *Mol Plant Microbe Interact*, 28:443-454.
- Fyans J.K., Bown L., Bignell D.R.D. (2016). Isolation and characterization of plant-pathogenic *Streptomyces* species associated with common scab-infected potato tubers in Newfoundland. *Phytopathology*, 106(2): 123-131.
- Liyanage H., Palmer D.A., Ullrich M., Bender C.L. (1995). Characterization and transcriptional analysis of the gene cluster for coronafacic acid, the polyketide component of the phytotoxin coronatine. *Appl Environ Microbiol*, 61: 3843-3848.
- Loria R., Bignell D.R., Moll S., Huguet-Tapia J C., Joshi M.V., Johnson E.G., Seipke R.F., Gibson D.M. (2008). Thaxtomin biosynthesis: the path to plant pathogenicity in the genus *Streptomyces*. *Antonie Van Leeuwenhoek*, 94: 3-10.
- Kaneko T., Minamisawa K., Isawa T., Nakatsukasa H., Mitsui H., Kawaharada Y., Nakamura Y., et al. (2010). Complete genomic structure of the cultivated rice endophyte *Azospirillum* sp. B510. *DNA Res*, 17: 37-50.
- King R.R., Calhoun L.A. (2009). The thaxtomin phytotoxins: sources, synthesis, biosynthesis, biotransformation and biological activity. *Phytochemistry*, 70: 833-841.
- Midha S., Bansal K., Sharma S., Kumar N., Patil P.P., Chaudry V., Patil P.B. (2016). Genomic resource of rice seed associated bacteria. *Front Microbiol* 6: 1551.

- Rangaswamy V., Mitchell R., Ullrich M., Bender C. (1998). Analysis of genes involved in biosynthesis of coronafacic acid, the polyketide component of the phytotoxin coronatine. *J Bacteriol*, 180(13): 3330-3338.
- Taylor M., Scott C., Grogan G. (2013) F₄₂₀-dependent enzymes - potential for applications in biotechnology. *Trends Biotechnol*, 31: 63–64.
- Wanner L.A. (2009). A patchwork of *Streptomyces* species isolated from potato common scab lesions in North America. *Am J Pot Res*, 86: 247-264.

RESEARCH ARTICLE

Regulation of Coronafacoyl Phytotoxin Production by the PAS-LuxR Family Regulator CfaR in the Common Scab Pathogen *Streptomyces scabies*

Zhenlong Cheng, Luke Bown, Kapil Tahlan, Dawn R. D. Bignell*

Department of Biology, Memorial University of Newfoundland, St. John's, NL A1B 3X9, Canada

* dbignell@mun.ca



OPEN ACCESS

Citation: Cheng Z, Bown L, Tahlan K, Bignell DRD (2015) Regulation of Coronafacoyl Phytotoxin Production by the PAS-LuxR Family Regulator CfaR in the Common Scab Pathogen *Streptomyces scabies*. PLoS ONE 10(3): e0122450. doi:10.1371/journal.pone.0122450

Academic Editor: Paul Jaak Janssen, Belgian Nuclear Research Centre SCK•CEN, BELGIUM

Received: January 10, 2015

Accepted: February 13, 2015

Published: March 31, 2015

Copyright: © 2015 Cheng et al. This is an open access article distributed under the terms of the [Creative Commons Attribution License](https://creativecommons.org/licenses/by/4.0/), which permits unrestricted use, distribution, and reproduction in any medium, provided the original author and source are credited.

Data Availability Statement: All relevant data are within the paper and its Supporting Information files.

Funding: The described work was funded by the Natural Sciences and Engineering Research Council of Canada Discovery Grants Program (386696-2010 to DRDB). Equipment used in this study was purchased with financial assistance from the Research & Development Corporation of Newfoundland and Labrador Ignite R&D Program (5404.1207.102 to DRDB), the Research & Development Corporation of Newfoundland and Labrador Leverage R&D Program (5404.1218.103 to

Abstract

Potato common scab is an economically important crop disease that is characterized by the formation of superficial, raised or pitted lesions on the potato tuber surface. The most widely distributed causative agent of the disease is *Streptomyces scabies*, which produces the phytotoxic secondary metabolite thaxtomin A that serves as a key virulence factor for the organism. Recently, it was demonstrated that *S. scabies* can also produce the phytotoxic secondary metabolite coronafacoyl-L-isoleucine (CFA-L-Ile) as well as other related metabolites in minor amounts. The expression of the biosynthetic genes for CFA-L-Ile production is dependent on a PAS-LuxR family transcriptional regulator, CfaR, which is encoded within the phytotoxin biosynthetic gene cluster in *S. scabies*. In this study, we show that CfaR activates coronafacoyl phytotoxin production by binding to a single site located immediately upstream of the putative -35 hexanucleotide box within the promoter region for the biosynthetic genes. The binding activity of CfaR was shown to require both the LuxR and PAS domains, the latter of which is involved in protein homodimer formation. We also show that CFA-L-Ile production is greatly enhanced in *S. scabies* by overexpression of both *cfaR* and a downstream co-transcribed gene, *orf1*. Our results provide important insight into the regulation of coronafacoyl phytotoxin production, which is thought to contribute to the virulence phenotype of *S. scabies*. Furthermore, we provide evidence that CfaR is a novel member of the PAS-LuxR family of regulators, members of which are widely distributed among actinomycete bacteria.

Introduction

The genus *Streptomyces* consists of hundreds of species of Gram-positive filamentous actinobacteria that are recognized for their ability to produce a large variety of useful secondary metabolites, including many medically and agriculturally important compounds [1]. In addition, some species are notable for their ability to cause important crop diseases such as potato

KT and DRDB) and the Canadian Foundation of Innovation Leaders Opportunity Fund (30482 to KT and DRDB). The funders had no role in the study design, data collection and analysis, decision to publish, or preparation of the manuscript.

Competing Interests: The authors have declared that no competing interests exist.

common scab (CS), which is characterized by the formation of superficial, erumpent (raised) or pitted lesions on the potato tuber surface [2]. Such lesions negatively impact the quality and market value of the potato tubers and cause significant economic losses to potato growers. In Canada, losses associated with CS during the 2002 growing season were estimated at \$15.3–17.3 million dollars [3], and in Australia, the disease has been estimated to cause losses of approximately 4% of the total industry value [4]. Furthermore, it has been reported that CS can also decrease the overall yield of the potato crop and increase the number of smaller tubers in the yield [5].

Streptomyces scabies (syn. *scabiei*) is the best characterized and most widely distributed *Streptomyces* spp. that causes CS disease [2]. The key virulence factor produced by *S. scabies* and other CS-causing pathogens is a phytotoxic secondary metabolite called thaxtomin A, which functions as a cellulose synthesis inhibitor [6–10]. It has been shown by several groups that there is a positive correlation between the pathogenicity of scab-causing organisms and the production of the thaxtomin A phytotoxin [11–15]. Recently, it was demonstrated that *S. scabies* strain 87–22 also produces metabolites that are structurally related to the coronatine (COR) phytotoxin, which contributes to the virulence phenotype of the Gram-negative plant pathogen *Pseudomonas syringae* [16]. COR functions in promoting the invasion and multiplication of *P. syringae* within the plant host, it contributes to disease symptom development during *P. syringae* infection, and it enhances the disease susceptibility of the plant in uninfected regions [17]. In *P. syringae*, COR is produced by linking coronafacic acid (CFA) to coronamic acid (CMA), a reaction that is thought to be catalyzed by the coronafacate ligase (Cfl) enzyme [18]. Although *S. scabies* lacks the ability to produce COR due to the absence of the CMA biosynthetic genes, it does harbour homologues of genes involved in CFA biosynthesis as well as a *cfl* homologue [19]. Recent work from our laboratory demonstrated that this organism produces the coronafacoyl compound CFA-L-Ile as a major product along with other related molecules in minor amounts [16]. Furthermore, mutational studies in *S. scabies* combined with bioactivity studies of the pure CFA-L-Ile molecule support the notion that this molecule functions as a phytotoxin and contributes to the virulence phenotype of *S. scabies* [16, 19].

The biosynthetic gene cluster for production of the coronafacoyl phytotoxins in *S. scabies* is composed of at least 15 genes (Fig 1A), of which 13 are co-transcribed as a single polycistronic mRNA transcript [19]. The remaining two genes are oriented in the opposite direction to the other genes and are co-transcribed as a separate transcript [19]. The first gene in this two-gene operon, *scab79591* (herein referred to as *cfaR*), encodes a 265 amino acid protein belonging to the PAS-LuxR family of transcriptional regulators, which are only found in the actinomycetes. Members of this family contain an N-terminal PAS (PER-ARNT-SIM) domain and a C-terminal LuxR-type domain (Fig 1B), and are often associated with secondary metabolite biosynthetic gene clusters. PAS domains belong to a sensing module superfamily that recognize stimuli such as light, oxygen, redox potential or ligands in order to modulate the regulatory activity of the corresponding protein in which they are present [20]. The LuxR-type domain is named after the *Vibrio fischeri* LuxR protein where the domain was first identified, and it contains a helix-turn-helix (HTH) motif that is typically involved in binding to specific DNA sequences called *lux*-boxes within target promoter(s) for transcription activation [21]. The best characterized PAS-LuxR family member is PimM, which in *Streptomyces natalensis* binds to eight promoters and activates expression of the biosynthetic genes for production of the polyene antifungal antibiotic pimarin (also known as natamycin) [22, 23]. Other family members that have been described include PteF, which controls the production of filipin in *Streptomyces avermitilis* [24], AURJ3M, which is a positive activator of aureofuscin biosynthesis in *Streptomyces aureofuscus* [25] and SlnM, which activates production of natamycin in *Streptomyces lyticus* [26]. In *S. scabies*, the CfaR protein has been shown to function as a transcriptional



Fig 1. Organization of the *Streptomyces scabies* 87–22 coronafacoyl phytotoxin biosynthetic gene cluster and domain structure of the CfaR protein. (A) The block arrows represent the coding sequences within the gene cluster, and the direction of each arrow indicates the direction of transcription. The *cfaR* gene is indicated in black while all other genes are shown in gray. The thin arrows at the top of the image indicate the two transcription units that have been identified [19]. (B) The CfaR protein consists of an N-terminal PAS sensory domain (PF00989) and a C-terminal LuxR-type DNA binding domain (PF00196). The gray shaded boxes below the image show the domain composition of the truncated forms of CfaR (CfaR^{ΔLuxR} and CfaR^{ΔPAS}) that were constructed and used in this study.

doi:10.1371/journal.pone.0122450.g001

activator for CFA-L-Ile phytotoxin production [16, 19]; however, there is currently no information as to how the protein regulates phytotoxin production.

In this study, we set out to characterize the mechanism of regulation of coronafacoyl phytotoxin biosynthetic gene expression by the CfaR protein. We show that the protein binds to a single imperfect palindromic sequence located immediately upstream of the putative -35 hexanucleotide box in the *cfa1* promoter region, which drives the expression of the biosynthetic genes for phytotoxin production. We also show that the DNA binding activity of CfaR depends on both the LuxR and PAS domains, and that the PAS domain is required for the formation of CfaR homodimers. Furthermore, we demonstrate that a high level of CFA-L-Ile production occurs in *S. scabies* when *cfaR* is overexpressed together with the downstream co-transcribed gene, *orf1*. This, together with phylogenetic analyses of CfaR and other PAS-LuxR proteins, indicates that CfaR is a novel member of the PAS-LuxR family of transcriptional regulators.

Materials and Methods

Bacterial strains, cultivation and maintenance

Bacterial strains used in this study are listed in Table 1. *Escherichia coli* strains were routinely cultivated in Luria-Bertani (LB) Lennox medium (Fisher Scientific, Canada) at 37°C unless otherwise stated. Where required, the LB medium was supplemented with kanamycin or apramycin (Sigma Aldrich, Canada) at 50 µg/mL final concentration, or with chloramphenicol (MP Biomedicals North America, USA) at 25 µg/mL final concentration. *E. coli* strains were maintained at -80°C in 20% v/v glycerol [27]. *S. scabies* strains were routinely cultured at 25°C or 28°C on potato mash agar (PMA; 5% w/v mashed potato flakes, 2% w/v agar) solid medium or in trypticase soy broth (TSB; BD Biosciences, Canada), nutrient broth (BD Biosciences, Canada) and soy flour mannitol broth (SFMB) liquid media [28]. When necessary, the growth medium was supplemented with apramycin or thiostrepton (Sigma Aldrich, Canada) at 50 or

Table 1. Bacterial strains and plasmids used in this study.

Strain or plasmid	Description	Resistance [†]	Reference or source
<i>Streptomyces scabies</i> strains			
87–22	Wild-type strain	n/a	[15]
ΔtxtA	<i>S. scabies</i> 87–22 containing a deletion of the <i>txtA</i> thaxtomin biosynthetic gene	Apra ^R	[29]
<i>Escherichia coli</i> strains			
DH5α	General cloning host	n/a	Gibco-BRL
NEB 5-α	DH5 α derivative, high efficiency competent cells	n/a	New England Biolabs
BL21(DE3)	Protein expression strain	n/a	New England Biolabs
ET12567/pUZ8002	<i>dam</i> [−] , <i>dcm</i> [−] , <i>hsdS</i> [−] ; nonmethylating conjugation host	Kan ^R , Cml ^R	[30]
Plasmids			
pET-30b	N- or C- terminal 6 × histidine fusion tag protein expression vector with T7 promoter and <i>lac</i> operator	Kan ^R	Novagen
pET-30b/CfaR	pET-30b derivative carrying a DNA fragment for expression of the CfaR ^{full} –HIS ₆ protein	Kan ^R	This study
pET-30b/CfaR1.1	pET-30b derivative carrying a DNA fragment for expression of the CfaR ^{ΔLuxR} –HIS ₆ protein	Kan ^R	This study
pET-30b/CfaR1.3	pET-30b derivative carrying a DNA fragment for expression of the CfaR ^{ΔPAS} –HIS ₆ protein	Kan ^R	This study
pRLDB50-1a	<i>Streptomyces</i> expression plasmid; carries the strong, constitutive promoter <i>ermEp*</i> and integrates into the φC31 <i>attB</i> site	Apra ^R , Thio ^R	[19]
pRLDB51-1	<i>scab79591</i> (<i>cfaR</i>) overexpression plasmid derived from pRLDB50-1a	Apra ^R , Thio ^R	[19]
pRLDB81	<i>scab79581</i> (<i>orf1</i>) overexpression plasmid derived from pRLDB50-1a	Apra ^R , Thio ^R	This study
pRLDB891	<i>cfaR</i> + <i>orf1</i> overexpression plasmid derived from pRLDB50-1a	Apra ^R , Thio ^R	This study

[†] Apra^R, Thio^R, Kan^R and Cml^R = apramycin, thiostrepton, kanamycin and chloramphenicol resistance, respectively.

n/a = not applicable.

doi:10.1371/journal.pone.0122450.t001

25 μg/mL final concentration, respectively. Seed cultures for RNA extraction were prepared by inoculating 50 μL of a *S. scabies* spore stock into 5 mL of TSB followed by incubation for 24–48 hr until dense mycelial growth was obtained. The seed cultures (0.5 mL) were subsequently used to inoculate 25 mL of SFMB in 125 mL flasks, which were incubated at 25°C and 200 rpm for 4 days. Cultures for small scale CFA-L-Ile extraction were prepared by inoculating TSB seed cultures (200 μL) into 5 mL of SFMB in 6 well plates (Fisher Scientific, Canada) and then incubating at 25°C and 125 rpm for 7 days. *S. scabies* strains were maintained at -80°C as spore suspensions in 20% v/v glycerol [28].

Plasmids, primers and DNA manipulation

Plasmids used in this study are listed in Table 1. Plasmids were manipulated in *E. coli* using standard procedures [27]. All oligonucleotides used in reverse transcription, PCR, sequencing and electrophoretic mobility shift assays were purchased from Integrated DNA Technologies (USA) and are listed in S1 Table. DNA sequencing was performed by The Centre for Applied Genomics (TCAG; Canada). *Streptomyces* genomic DNA was isolated from mycelia harvested from 2-day old nutrient broth cultures using the DNeasy Blood & Tissue Kit as per the manufacturer's protocol (QIAGEN Inc, Canada).

Construction of protein expression plasmids

Three forms of the *cfaR* gene, one encoding the full length protein (CfaR^{full}), one encoding the first 140 amino acids of the protein with the PAS domain (CfaR^{ΔLuxR}), and one encoding the C-terminal 174 amino acids of the protein and harbouring the LuxR domain (CfaR^{ΔPAS}), were amplified by PCR using Phusion DNA Polymerase (New England Biolabs, Canada) according to the manufacturer's instructions, except that DMSO (5% v/v final concentration) was included in the reactions. The resulting products were digested with NdeI and HindIII (New England Biolabs, Canada) and were ligated into similarly digested pET30b to generate the C-terminal 6 × HIS-tagged full length and truncated CfaR expression plasmids. The constructed expression plasmids were sequenced to confirm the fidelity of the inserts, after which they were transformed into *E. coli* BL21(DE3) cells using the one step method [31].

Protein overexpression and purification

For expression of CfaR^{full}-HIS₆ and CfaR^{ΔLuxR}-HIS₆, the *E. coli* cells were grown at 28°C in 500 mL of LB containing kanamycin until an OD₆₀₀ of 0.6 was reached, after which isopropyl 1-thio-β-D-glucopyranoside (IPTG) was added to a final concentration of 1 mM and the cells were incubated for an additional 4 h. To express CfaR^{ΔPAS}-HIS₆, cells were grown at 25°C to an OD₆₀₀ of 0.6, after which they were induced with IPTG (0.25 mM final concentration) and were incubated for an additional 5 h. The cells were harvested and resuspended in buffer consisting of 20 mM sodium phosphate, 500 mM sodium chloride and 30 mM imidazole (pH 7.4), and were lysed using a French press (SLM Instruments Inc., USA). The soluble proteins were purified using an ÄKTA pure FPLC system with a HiTrap IMAC FF 1 mL column at 4°C according to the manufacturer's recommendations (GE Healthcare, Canada). The collected fractions were analyzed by SDS-PAGE on a 12% gel, and those fractions containing protein were pooled and desalted by FPLC using a HiTrap Desalting 5 mL column (GE Healthcare, Canada). The protein concentration in each preparation was determined by the Bradford method [32], and the proteins were stored at -80°C in buffer containing 20 mM sodium phosphate, 150 mM NaCl and 20% glycerol (pH = 7.8).

Total RNA isolation

S. scabiei mycelia from 4-day old SFMB cultures were harvested by centrifugation, and approximately 0.5 g of the cell pellet was placed into a sterile 2 mL microcentrifuge tube. Total RNA was isolated using an innuPREP Bacteria RNA Kit and a SpeedMill PLUS tissue homogenizer (Analytik Jena AG, Germany) as per the manufacturer's instructions. The resulting RNA samples were treated with DNase I (New England Biolabs, Canada) as directed by the manufacturer to remove trace amounts of genomic DNA, after which the DNase-treated RNA samples were quantified using a P300 Nanophotometer (Implen Inc., USA) and were stored at -80°C.

Reverse transcription PCR

Reverse transcription (RT) was performed using SuperScript III reverse transcriptase (Life Technologies, Canada) with 500 ng of DNase-treated total RNA and 2 pmol of the gene-specific primer DRB674. Reactions were set up as per the manufacturer's instructions and were incubated at 55°C for 1 hr. A negative control reaction in which no reverse transcriptase enzyme was added was included to verify the absence of genomic DNA in the RNA samples. PCR was performed using 2 μL of the cDNA template and the primer pairs DRB674-DRB253, DRB674-DRB254a and DRB674-DRB255. Amplification was conducted using Taq DNA polymerase (New England Biolabs, Canada) as per the manufacturer's protocol except that the

reactions included 5% v/v DMSO. The resulting PCR products were analyzed by electrophoresis using a 1% w/v agarose gel and 1× Tris Borate EDTA (TBE) buffer and were visualized by staining with ethidium bromide.

Primer extension analysis

Primer extension was performed using a 6-carboxyfluorescein (FAM)—labeled primer, DRB674, as previously described [33] with modifications. Briefly, a 15 µL reaction containing 40 µg of DNase—treated RNA and 0.6 pmol of 5′-FAM-labeled primer was incubated at 65°C for 5 min and then chilled on ice. Next, 3 µL of SuperScript III reverse transcriptase (600U), 1.5 µL of RNaseOUT Recombinant Ribonuclease Inhibitor (Life Technologies, Canada), 3 µL of dNTPs (10 mM each), 1.5 µL of 0.1M dithiothreitol (DTT) and 6 µL of 5× First-Strand Buffer (Life Technologies, Canada) were added to the reaction, and the reaction was incubated at 55°C for 2 hr. An extra 1 µL of SuperScript III reverse transcriptase (200U) was added after 1 hr of incubation. Then, the reaction was heated at 70°C for 15 min, after which 1 µL (5U) of RNase H (New England Biolabs, Canada) was added and the reaction was incubated at 37°C for 30 min. This was followed by phenol/chloroform extraction and ethanol precipitation of the cDNA. The resulting cDNA pellet was air dried and then sent to TCAG for DNA sizing analysis. The primer extension analysis was performed twice in total.

Electrophoretic mobility shift assay (EMSA)

The DNA probes used for EMSAs were amplified by PCR and were gel-purified using the Wizard SV Gel and PCR Clean-Up System (Promega, Canada). In addition, two pairs of long oligonucleotides (40 nt each), LC12—LC13 and LC14—LC15, were synthesized and used as probes in EMSAs. The complementary oligonucleotides LC12 and LC13 were used to generate probe 1 (P1) and contained the putative CfaR binding site, while the complementary pair LC14 and LC15 were used to generate the negative control probe (P2) and corresponded to the coding region of the *cfaR* gene. The oligonucleotide pairs were incubated at 95°C for 5 min and then slowly cooled to room temperature to allow annealing of the oligonucleotides. The DNA probes were either 3′ end-labeled using the Biotin 3′ End DNA Labeling Kit (Promega, Canada) or were unlabeled. The DNA-protein binding reactions were performed using the Light-Shift Chemiluminescent EMSA Kit (Fisher Scientific, Canada) according to the manufacturer's instructions. Reactions containing unlabeled DNA and protein were analyzed by non-denaturing PAGE and the DNA was visualized afterwards using ethidium bromide. Reactions containing biotin-labeled probe and protein were analyzed by non-denaturing PAGE, after which the DNA was transferred to nitrocellulose membrane by contact blotting and then probed with anti-Biotin-alkaline phosphatase antibodies according to the manufacturer's instructions (Fisher Scientific, Canada). Visualization of the DNA was then performed using the Chemiluminescent Nucleic Acid Detection Module (Fisher Scientific, Canada) and the ImageQuant LAS 4000 Digital Imaging System (GE Healthcare, Canada).

Glutaraldehyde cross-linking of CfaR proteins

Crosslinking reactions consisted of purified CfaR protein (80 pmol) and 20 mM sodium phosphate buffer (pH 7.5) in a final volume of 20 µL. The reactions were initiated with the addition of 1 µL of a 2.3% w/v glutaraldehyde solution and were incubated for 5 minutes at 37°C. Termination of the reactions was achieved by the addition of 2 µL of a 1 M Tris-HCl solution (pH 8.0), after which the cross-linked proteins were separated by SDS-PAGE on a 12% polyacrylamide gel and were visualized by staining with Coomassie brilliant blue.

Construction of *cfaR*, *orf1* and *cfaR+orf1* overexpression plasmids

Construction of the *cfaR* overexpression vector, pRLDR51-1, was described previously [19]. DNA fragments containing *orf1* alone and *cfaR* + *orf1* were amplified by PCR using Phusion DNA Polymerase according to the manufacturer's instructions, except that DMSO (5% v/v final concentration) was included in the reactions. The resulting products were digested with XbaI (New England Biolabs, Canada) and were ligated into similarly digested pRLDB50-1a to generate the *orf1* and *cfaR* + *orf1* overexpression plasmids pRLDB81 and pRLDB891, respectively. The correct orientation of the inserts was confirmed by digestion with BamHI for pRLDB81 and with PstI, SmaI and NcoI for pRLDB891 (New England Biolabs, Canada), after which the constructed plasmids were sequenced to confirm the fidelity of the inserts. The expression plasmids were then introduced into *E. coli* ET12567/ pUZ8002 prior to transfer into *S. scabies* 87–22 by intergeneric conjugation [28].

Extraction and analysis of CFA-L-Ile production

CFA-L-Ile was extracted from SFMB cultures of *S. scabies* and was quantified by analytical HPLC as described previously [16].

Bioinformatics analysis

Identification of protein domains within the CfaR and ORF1 amino acid sequences was performed using the Pfam database (<http://pfam.xfam.org/>) [34]. The logo for the PAS-LuxR protein binding sites was generated using the WebLogo server (<http://weblogo.berkeley.edu/logo.cgi>) [35]. Amino acid sequence alignments of the PAS and LuxR domains from CfaR and other PAS-LuxR proteins in the database were generated using ClustalW within the Geneious version 6.1.2 software (Biomatters Ltd.). The accession numbers for the protein sequences used in the alignments are listed in S2 Table. Phylogenetic trees were constructed from the alignments using the maximum likelihood method in the MEGA 5.2.1 program [36]. Bootstrap analyses were performed with 1000 replicates in each algorithm.

Results and Discussion

CfaR binds to a single site located in the *cfa1* promoter region

Previous transcriptional studies showed that CfaR is required for expression of several coronafacoyl phytotoxin biosynthetic genes [19], and overexpression of CfaR has been demonstrated to enhance phytotoxin production [16]. Given that the biosynthetic genes are expressed as a large polycistronic transcript [19], it was hypothesized that CfaR may control gene activation from the promoter region upstream of *cfa1*, which is the first gene in the operon (Fig 1A). To investigate this further, CfaR was overexpressed and purified from *E. coli* as a C-terminal 6 × histidine tagged protein (CfaR^{full}–HIS₆), after which it was used in EMSAs along with six DNA fragments covering different parts of the intergenic region between *cfaR* and *cfa1* (Fig 2A). As shown in Fig 2B, the CfaR^{full}–HIS₆ could only bind to two of the DNA fragments (*a* and *e*), both of which covered a 264 bp region immediately upstream of the predicted *cfa1* start codon (Fig 2A). Within this region, a 16 bp imperfect palindromic DNA sequence was identified manually (positions -94 to -79 relative to the *cfa1* translation start codon; Fig 2A and 2C), and the sequence was found to be highly similar to the previously described PimM binding site consensus sequence CTVGGGAWWTCCCBAG (Fig 3) [23, 37]. EMSAs using DNA fragments lacking this palindrome confirmed that it is essential for binding of CfaR^{full}–HIS₆ to DNA (Fig 2B). Furthermore, CfaR^{full}–HIS₆ could readily bind to a 40 bp labeled oligonucleotide probe (P1) containing only the palindrome and some DNA flanking sequence (Fig 2C and

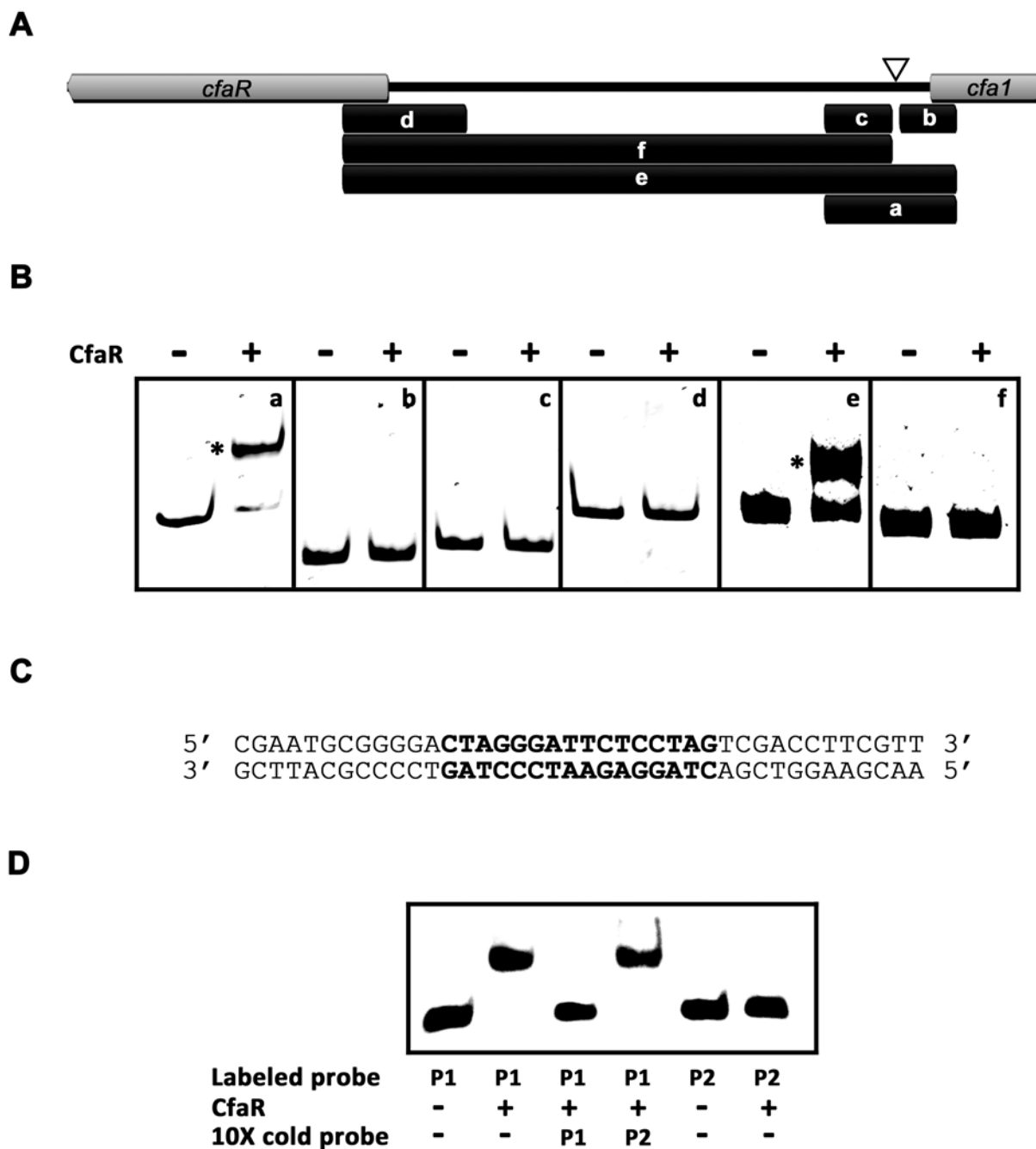


Fig 2. CfaR^{full}-HIS₆ binds to a single site within the *cfaR*–*cfa1* intergenic region. (A) Map of the *cfaR*–*cfa1* intergenic region showing the location of the DNA fragments (indicated by the black bars and labeled a–f) used for EMSAs. The position of the 16 bp palindrome identified upstream of *cfa1* is indicated with the white triangle. (B) EMSA s for CfaR^{full}–HIS₆ with the DNA fragments a–f. Reactions contained 50 ng of DNA with (result+) and without (–) CfaR^{full}–HIS₆ protein (3.7 pmol). DNA-protein complexes observed are indicated with *. (C) Sequence of the 40 bp oligonucleotide P1 probe used for EMSAs. The 16 bp palindromic sequence identified upstream of *cfa1* is shown in bold. (D) EMSA results for CfaR^{full}–HIS₆ with the P1 oligonucleotide probe. Reactions contained 0.1 pmol of biotin-labeled probe with (+) and without (–) CfaR^{full}–HIS₆ protein (2 pmol). Negative control reactions contained the 40 bp biotin-labeled oligonucleotide P2 probe in place of P1. In addition, competition assays were performed in which an excess (10×) of unlabelled (cold) probe (P1 or P2) was included in the reaction. DNA-protein complexes observed are indicated with *.

doi:10.1371/journal.pone.0122450.g002

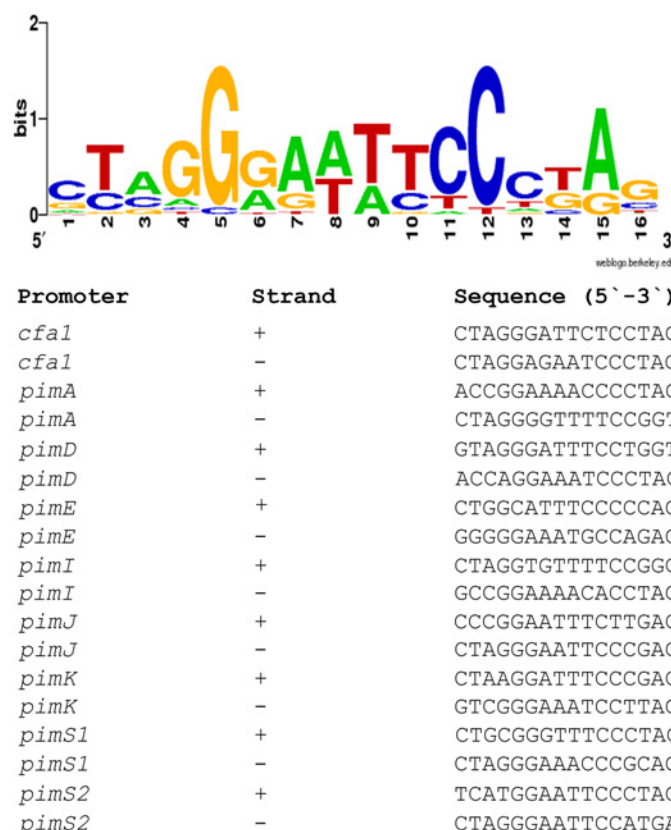


Fig 3. Sequence logo of PAS-LuxR protein binding sites. The logo was constructed using WebLogo [35] with the PimM and CfaR binding sites shown below. The overall height of the stack reflects the sequence conservation at that position, and the height of the letters within the stack designates the relative frequency of the corresponding base at that position [38].

doi:10.1371/journal.pone.0122450.g003

2D) whereas it did not bind to a control 40 bp probe (P2; Fig 2D) corresponding to the *cfaR* coding region (see Materials and Methods). Finally, binding to the labeled P1 probe was abolished when an excess of unlabeled P1, but not P2, was included in the reaction mixture (Fig 2D), indicating that the interaction between CfaR^{full}-HIS₆ and P1 is highly specific.

The location of the CfaR binding site within the *cfa1* promoter was further characterized by mapping the *cfa1* TSS. Total RNA was isolated from a *S. scabiei* strain ($\Delta txtA/pRLDB51-1$) that overexpresses the *cfaR* gene [19] and produces high levels of the coronafacoyl phytotoxins [16], and RT-PCR was performed using a single reverse primer and different forward primers (Fig 4A) in order to identify the approximate location of the TSS. As shown in Fig 4B, two of the forward primers (DRB253 and DRB254a) allowed for amplification of a PCR product from the cDNA template whereas the third forward primer (DRB255) did not, indicating that the TSS was most likely located somewhere between DRB254a and DRB255. This was verified using non-radioactive primer extension analysis, which identified a C residue located 40 bp upstream of the *cfa* translation start site as the TSS. A putative -10 box (TATGGT) and a -35 box (TCGACC) separated by 18 nt is situated upstream of the C residue (Fig 4A), and these features are consistent with the previously described consensus sequence (TTGACN—N₁₆—TASVKT) for streptomycete *E. coli* σ^{70} -like promoters [39]. Interestingly, the palindromic sequence required for CfaR binding is located immediately upstream of the putative -35

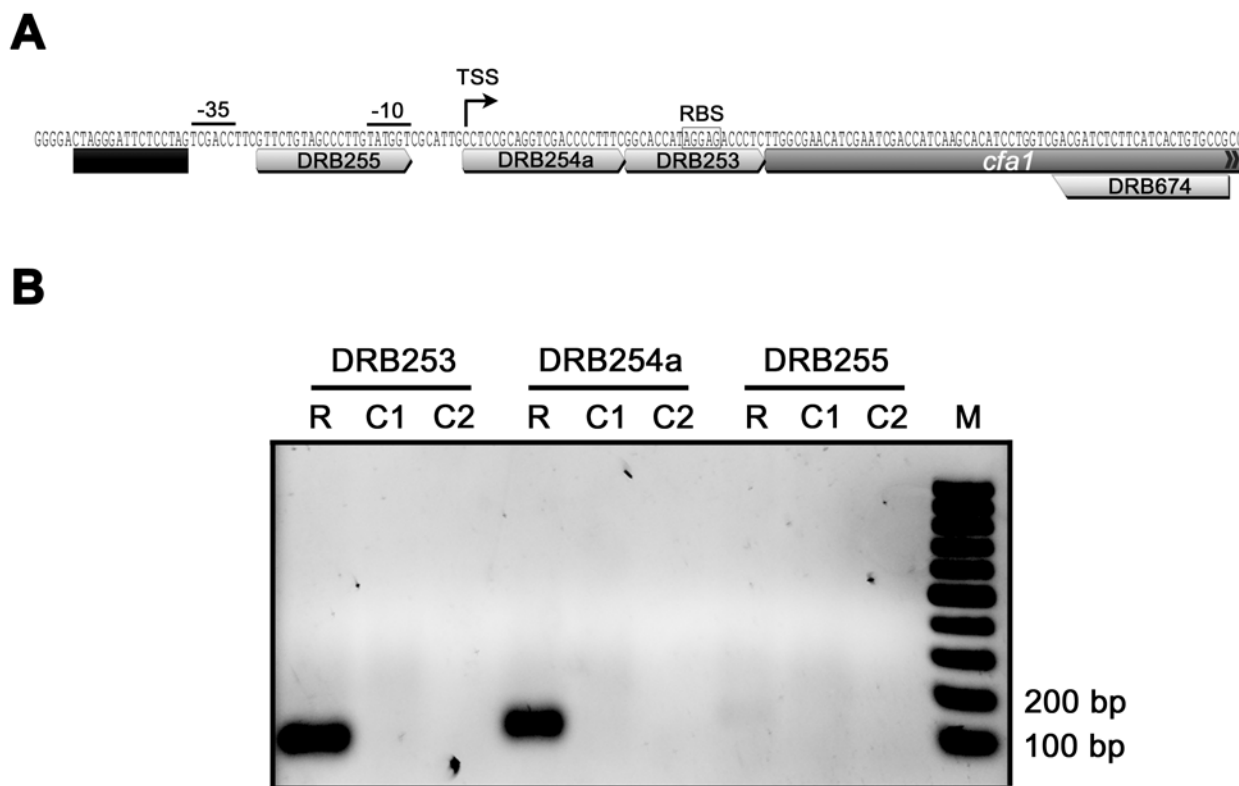


Fig 4. Mapping the transcription start site of *cfa1*. (A) Organization of the *cfa1* promoter region. The putative -10 and -35 hexanucleotide sequence boxes and the putative ribosome binding site (RBS) are shown along with the predicted CfaR binding site, which is indicated by the black bar. Also shown are the binding sites for the primers DRB253, DRB254a, DRB255 and DRB674, which were used for low resolution transcript mapping by RT-PCR. The transcription start site (TSS) as determined by non-radioactive primer extension analysis is also indicated. (B) Results of the low resolution transcription start site mapping by RT-PCR. Reverse transcription was performed using *S. scabies* Δ txtA/pRLDB51-1 total RNA and using the gene-specific primer DRB674. This was followed by PCR using the reverse primer DRB674 and the forward primers DRB253, DRB254a or DRB255. The resulting products were then analyzed by agarose gel electrophoresis. R, PCR reactions using cDNA as template; C1, control PCR reactions using RNA (without reverse transcription) as template; C2, control PCR reactions using water as template.

doi:10.1371/journal.pone.0122450.g004

box (Fig 4A), an arrangement that is similar to what has been described for promoters activated by PimM (the binding site of which typically overlaps the -35 box) [23]. Most likely, this arrangement allows for direct contact between the transcriptional activator and RNA polymerase in order to recruit RNA polymerase to the target promoter [40].

It is noteworthy that the CfaR^{full}-HIS₆ protein did not bind to the DNA fragments *d* and *f*, which cover the promoter region for the *cfaR* gene (Fig 2A and 2B). This suggests that CfaR does not regulate its own expression, a finding that is consistent with previous transcriptional data from *S. scabies* [19] and is also consistent with the observation that PimM does not regulate its own expression [22]. In addition, the entire sequence of the coronafacoyl phytotoxin biosynthetic gene cluster was screened for other potential CfaR binding sites, and although a possible binding sequence was found within the *cfa6* gene, the CfaR^{full}-HIS₆ protein did not bind to this site in EMSAs (data not shown). Therefore, it appears that CfaR regulates coronafacoyl phytotoxin production using a single DNA binding site within the entire gene cluster.

The CfaR PAS domain is required for DNA binding and protein dimerization *in vitro*

In vitro studies on the *S. natalensis* PimM protein have shown that the DNA binding activity of the protein requires the LuxR DNA binding domain but not the PAS domain, and that removal of the PAS domain actually enhances the DNA binding activity of the protein [23]. To investigate the role of the PAS and LuxR domains in the binding of CfaR to DNA, EMSAs were performed using two different truncated forms of the protein, CfaR^{ΔLuxR}-HIS₆ and CfaR^{ΔPAS}-HIS₆, which lack the LuxR and the PAS domain, respectively (Fig 1B). Fig 5A shows that while the CfaR^{full}-HIS₆ protein could bind to the target DNA, neither of the truncated forms showed any DNA binding activity in the assay. This was expected in the case of CfaR^{ΔLuxR}-HIS₆ since the protein lacks the HTH DNA binding motif; however, the lack of binding by CfaR^{ΔPAS}-HIS₆ was surprising based on the previously described results for PimM. Given that transcriptional regulators that bind palindromic sequences normally do so as dimers, we next looked at whether deletion of the PAS domain affected the ability of CfaR to form homodimers using glutaraldehyde crosslinking and SDS-PAGE. As shown in Fig 5B, homodimeric forms of both CfaR^{full}-HIS₆ (59.2 kDa) and CfaR^{ΔLuxR}-HIS₆ (32.8 kDa) could be detected upon treatment with glutaraldehyde whereas only the monomeric form of CfaR^{ΔPAS}-HIS₆ (20.0 kDa) could be observed under similar conditions, suggesting that the lack of DNA binding observed with CfaR^{ΔPAS}-HIS₆ is most likely due to the inability of the protein to dimerize. It is noteworthy that a role for the CfaR PAS domain in protein dimerization is consistent with previous studies on the *Drosophila* circadian rhythm regulator (PER), the mouse aryl hydrocarbon receptor (AHR) and AHR nuclear translocator (ARNT), and the *Drosophila* single minded (SIM) transcription factor, where it was shown that the PAS domain in the respective proteins functions as a mediator of homo- and/or heterodimerization [41–44].

It is currently unclear as to why deletion of the PAS domain had such a drastically different effect on the DNA binding activity of CfaR as compared to PimM. Possibly, it is related to differences in the type and location of the fusion tag used for purifying each protein. In the case of PimM, the full length protein and its truncated versions were purified using an N-terminal GST tag [23], whereas a C-terminal HIS₆ tag was used in the current study for purifying CfaR and its truncated versions. Given that GST fusion proteins have been reported to form dimers most likely due to GST-GST interactions [45–47], it is possible that the presence of the GST protein tag on the N-terminus of the PimM DNA binding domain allowed for dimerization of the protein in the absence of the PAS domain, thereby preserving the DNA binding activity of the truncated protein.

Activation of coronafacoyl phytotoxin production by CfaR is enhanced by ORF1

The *cfaR* gene has been shown to be co-transcribed with a downstream gene, *scab79581* (herein referred to as *orf1*) (Fig 1A), which encodes a protein of unknown function [19]. Given that co-transcribed genes are often involved in similar processes, we hypothesized that the ORF1 protein might also play a role in activating coronafacoyl phytotoxin production in *S. scabies*. To investigate this further, the *cfaR* and *orf1* genes were overexpressed individually and together in wild-type *S. scabies* 87–22, which normally produces undetectable or trace levels of CFA-L-Ile under laboratory conditions [16]. As shown in Fig 6, overexpression of *cfaR* significantly enhanced CFA-L-Ile production when compared to the vector control, a result that is consistent with previous *cfaR* overexpression studies in the *ΔtxtA* thaxtomin A mutant background [16]. Interestingly, overexpression of *cfaR* + *orf1* led to an even greater increase (~10 fold) in CFA-L-Ile production when compared to overexpression of *cfaR* alone, while overexpression of *orf1*

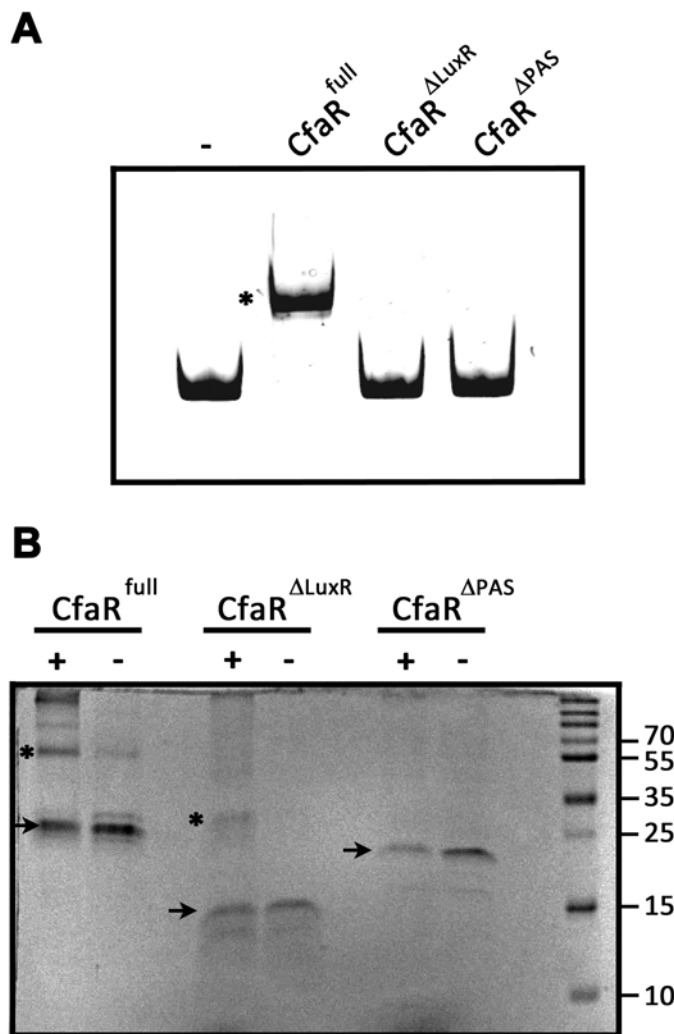


Fig 5. The CfaR PAS domain is required for DNA binding and protein dimerization. (A) EMSA results using CfaR^{full}-HIS₆, CfaR^{ΔLuxR}-HIS₆ and CfaR^{ΔPAS}-HIS₆ with DNA fragment a (Fig 2A). A control reaction (-) in which no protein was added was also included. The DNA-protein complex observed is indicated with *. (B) Analysis of protein dimerization using chemical crosslinking and SDS-PAGE. CfaR^{full}-HIS₆, CfaR^{ΔLuxR}-HIS₆ and CfaR^{ΔPAS}-HIS₆ were either treated with glutaraldehyde (+) or with solvent alone (-), after which the proteins were separated by SDS-PAGE and were visualized by staining with Coomassie brilliant blue. Protein monomers are indicated with black arrows and dimers with *. The sizes (in kDa) of the protein molecular weight marker (M) bands used for size estimation are also shown.

doi:10.1371/journal.pone.0122450.g005

alone had no significant effect on CFA-L-Ile production when compared to the vector control (Fig 6). This suggests that ORF1 somehow augments the activation of CFA-L-Ile production by CfaR, though it is currently unclear as to how this would occur. Analysis of the ORF1 protein sequence using the Pfam database revealed the presence of a ThiF family domain (PF00899.16) and a nitroreductase domain (PF00881.19) situated at the N-terminus and central region of the protein, respectively. Interestingly, the ThiF family domain is found in enzymes such as the eukaryotic ubiquitin activating enzyme E1, the *E. coli* thiamine biosynthetic enzyme ThiF and the *E. coli* molybdenum cofactor biosynthetic enzyme MoeB, all of which are known to catalyze the adenylation of a target polypeptide at the C-terminal end [48]. In the case of ThiF and MoeB, the adenylation of the C-terminus of the target polypeptide is modified further to a

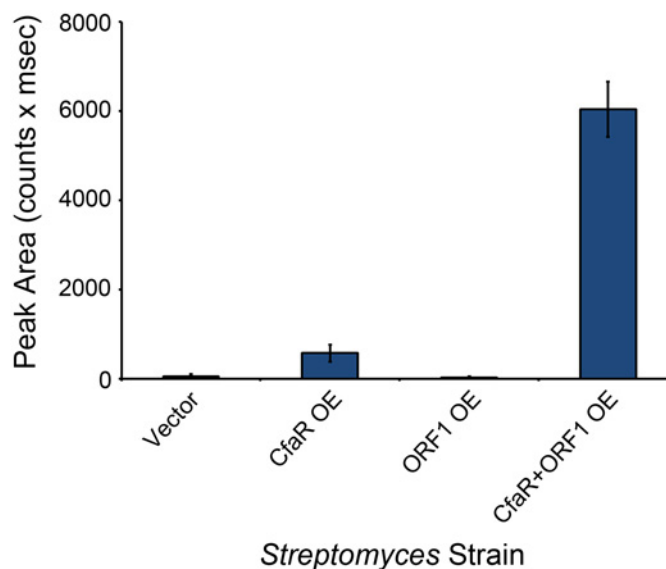


Fig 6. Coronafacoyl phytotoxin production is greatly enhanced by overexpression of both *cfaR* and *orf1*. *S. scabies* strains overexpressing *cfaR* alone, *orf1* alone or *cfaR* + *orf1* were cultured in SFMB medium for 7 days at 25°C, after which the culture supernatants were harvested and extracted with organic solvent. The resulting organic extracts were then analysed for CFA-L-Ile production by HPLC. Shown is the mean area of the CFA-L-Ile peak from six cultures of each strain, with error bars indicating the standard deviation. A *S. scabies* strain containing only the overexpression vector was used as a control in this experiment.

doi:10.1371/journal.pone.0122450.g006

thiocarboxylate, which then serves as a sulfur donor for cofactor biosynthesis [48]. Possibly, ORF1 is involved in some sort of post-translational modification of CfaR in order to enhance the ability of CfaR to elicit transcriptional activation. It is interesting to note that the co-transcription of genes encoding a PAS-LuxR homologue and an ORF1 homologue has not been found in other *Streptomyces* spp., suggesting that the regulation of coronafacoyl phytotoxin production may involve a novel mechanism.

Phylogenetic analysis indicates that CfaR is a novel member of the PAS-LuxR protein family

Previously, it was proposed that CfaR may represent a novel member of the PAS-LuxR protein family based on phylogenetic analysis using the complete amino acid sequence of CfaR and other PAS-LuxR proteins from the database [49]. This analysis demonstrated that CfaR forms a distinct lineage among the different PAS-LuxR family members, though it was unclear as to whether this is mainly due to sequence differences within the PAS domain and/or the LuxR domain, or due to differences within the inter-domain regions only. To examine this further, phylogenetic trees were constructed using only the amino acid sequences of the PAS domain (Fig 7A) or the LuxR DNA binding domain (Fig 7B) from CfaR and other PAS-LuxR family members. Interestingly, the resulting trees showed that both the PAS and LuxR domains from CfaR form a distinct clade among the corresponding domain sequences from other family members (Fig 7A and 7B), indicating that the uniqueness of the CfaR amino acid sequence can be extended into these conserved domains. It is also interesting to note that regardless of the sequence used to generate the tree (PAS domain, LuxR domain or full length protein), the phylogenetic analyses showed that CfaR is distantly related to the previously characterized PAS-LuxR family members PimM, PteF, AmphRIV and NysRIV (Fig 7A and 7B) [49], all of

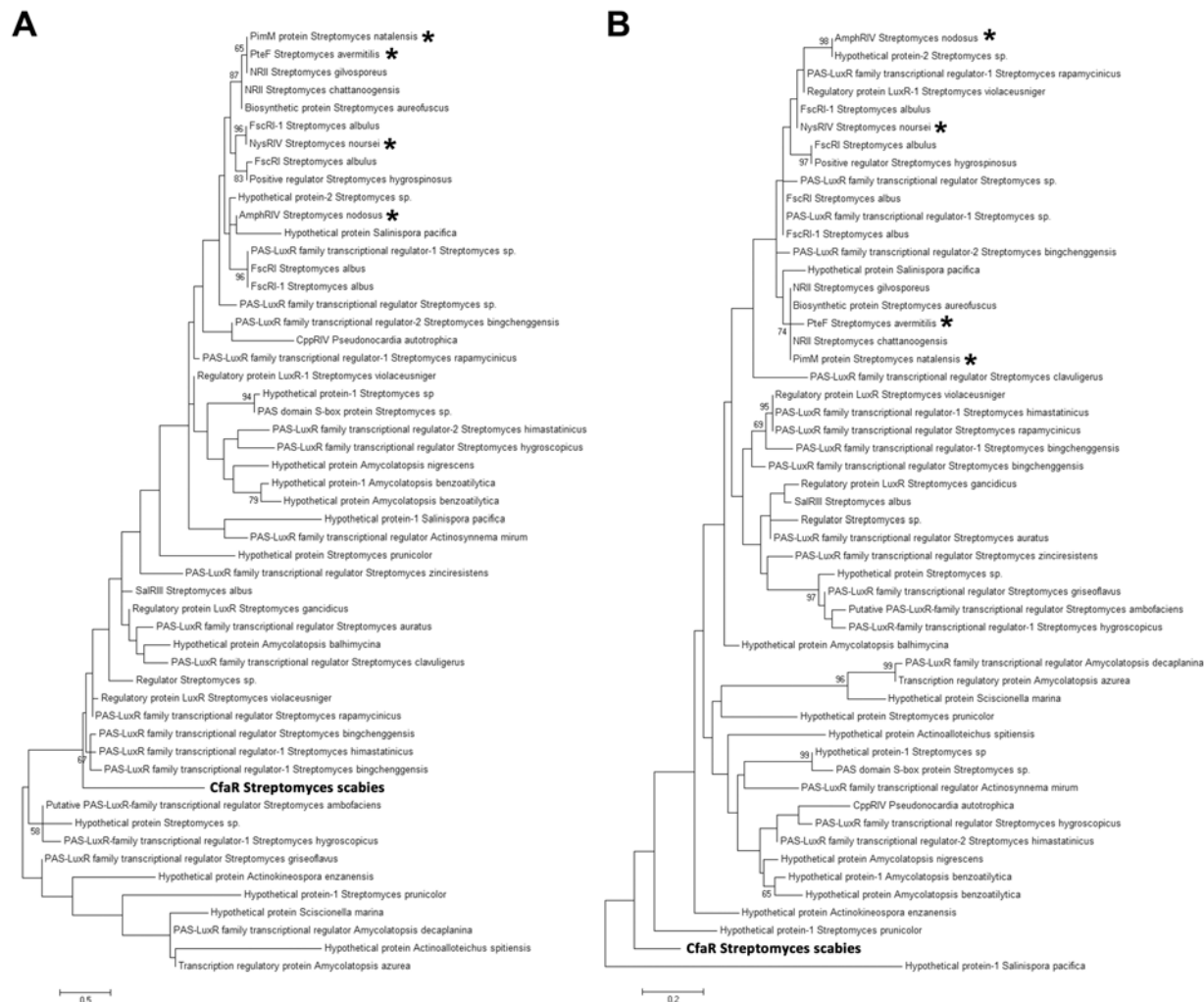


Fig 7. Phylogenetic analysis of PAS-LuxR family proteins from *Streptomyces* and other actinomycetes. The phylogenetic trees were constructed based on the amino acid sequences of the PAS domain (A) and the LuxR DNA binding domain (B). The trees were constructed using the maximum likelihood algorithm, and bootstrap values $\geq 50\%$ for 1000 repetitions are shown. The scale bar indicates the number of amino acid substitutions per site. Family members that have been shown experimentally to be functionally interchangeable are indicated with *.

doi:10.1371/journal.pone.0122450.g007

which are associated with polyene antifungal antibiotic biosynthetic gene clusters [37]. It has been shown that PteF, AmphRIV and NysRIV are able to complement a *S. natalensis* Δ pimM mutant [37] and that PimM is able to complement a *S. avermitis* Δ pteF mutant [24]. In addition, the purified PimM protein can bind to the predicted target sites for PteF, AmphRIV and NysRIV *in vitro* [37]. Together, these results imply that there is functional conservation among these members of the PAS-LuxR family of transcriptional regulators. Whether CfaR is also functionally interchangeable with PimM and similar PAS-LuxR proteins will require further investigation; however, the analyses performed here suggest that CfaR may be functionally distinct from these other family members.

Concluding Remarks

This study has established that CfaR is a novel PAS-LuxR family protein that directly activates the expression of the *S. scabies* coronafacoyl phytotoxin biosynthetic genes by binding to a

single site within the *cfa1* promoter region. This is the first report detailing the mechanism of coronafacoyl phytotoxin biosynthetic gene regulation by CfaR, and other than studies focused on PimM, it is the only other study to date that describes the biochemical characterization of a member of the PAS-LuxR protein family, which is highly represented among *Streptomyces* spp. and other actinomycetes. We also demonstrated that the PAS domain of CfaR is required for DNA binding and protein dimerization, a function that has not been previously described for this domain within the PAS-LuxR protein family. Given that PAS domains are known to function as sensory domains for controlling the regulatory activity of the corresponding protein [20], we suspect that the PAS domain in CfaR has the additional role of controlling the DNA binding activity of the protein in response to a ligand or some other stimulus, and we are currently examining this further. It has been shown that the coronafacoyl phytotoxin biosynthetic genes are expressed during colonization of plant tissues [19] and that production of CFA-L-Ile only occurs in media containing plant-derived components [16], and so it is possible that one or more plant-derived compounds serves as a signal for activating gene expression by CfaR. A particularly interesting finding from this study was the demonstration that the co-transcribed *orf1* gene is also involved in activating phytotoxin production, and we are currently investigating the precise role of the corresponding protein. Furthermore, the involvement of other regulators of *cfaR* via transcriptional or translational control is an area of interest given that a number of the *bld* (bald) gene global regulators that control morphological differentiation and secondary metabolism in *Streptomyces* spp. are known to modulate transcription of the *cfaR* gene or translation of *cfaR* mRNA in *S. scabies* [19, 50].

Supporting Information

S1 Table. Oligonucleotides used in this study.

(DOCX)

S2 Table. Accession numbers of PAS-LuxR protein sequences used for the phylogenetic analyses.

(DOCX)

Author Contributions

Conceived and designed the experiments: DRDB ZC KT. Performed the experiments: ZC LB. Analyzed the data: ZC DRDB. Contributed reagents/materials/analysis tools: DRDB KT. Wrote the paper: ZC DRDB.

References

1. Bérday J. Bioactive microbial metabolites. *J Antibiot* (Tokyo). 2005; 58: 1–26.
2. Dees MW, Wanner LA. In search of better management of potato common scab. *Potato Res.* 2012; 55: 249–268.
3. Hill J, Lazarovits G. A mail survey of growers to estimate potato common scab prevalence and economic loss in Canada. *Can J Plant Pathol.* 2005; 27: 46–52.
4. Wilson CR. A summary of common scab disease of potato research from Australia. In: Naito S, Kondo N, Akino S, Ogoshi A, Tanaka F, editors. *Proceedings of the International Potato Scab Symposium*; 2004 Sept 6–7; Sapporo, Japan.
5. Hiltunen LH, Weckman A, Ylhainen A, Rita H, Richter E, Valkonen JPT. Responses of potato cultivars to the common scab pathogens, *Streptomyces scabies* and *S. turgidiscabies*. *Ann Appl Biol.* 2005; 146: 395–403.
6. Bischoff V, Cookson SJ, Wu S, Scheible WR. Thaxtomin A affects CESA-complex density, expression of cell wall genes, cell wall composition, and causes ectopic lignification in *Arabidopsis thaliana* seedlings. *J Exp Bot.* 2009; 60: 955–965. doi: [10.1093/jxb/ern344](https://doi.org/10.1093/jxb/ern344) PMID: [19269997](https://pubmed.ncbi.nlm.nih.gov/19269997/)

7. Duval I, Beaudoin N. Transcriptional profiling in response to inhibition of cellulose synthesis by thaxtomin A and isoxaben in *Arabidopsis thaliana* suspension cells. *Plant Cell Rep.* 2009; 28: 811–830. doi: [10.1007/s00299-009-0670-x](https://doi.org/10.1007/s00299-009-0670-x) PMID: [19198845](https://pubmed.ncbi.nlm.nih.gov/19198845/)
8. Fry BA, Loria R. Thaxtomin A: evidence for a plant cell wall target. *Physiol Mol Plant Pathol.* 2002; 60: 1–8.
9. King RR, Calhoun LA. The thaxtomin phytotoxins: sources, synthesis, biosynthesis, biotransformation and biological activity. *Phytochemistry.* 2009; 70: 833–841. doi: [10.1016/j.phytochem.2009.04.013](https://doi.org/10.1016/j.phytochem.2009.04.013) PMID: [19467551](https://pubmed.ncbi.nlm.nih.gov/19467551/)
10. Scheible WR, Fry B, Kochevenko A, Schindelasch D, Zimmerli L, Somerville S, et al. An *Arabidopsis* mutant resistant to thaxtomin A, a cellulose synthesis inhibitor from *Streptomyces* species. *Plant Cell.* 2003; 15: 1781–1794. PMID: [12897252](https://pubmed.ncbi.nlm.nih.gov/12897252/)
11. Goyer C, Vachon J, Beaulieu C. Pathogenicity of *Streptomyces scabies* mutants altered in thaxtomin A production. *Phytopathology.* 1998; 88: 442–445. doi: [10.1094/PHYTO.1998.88.5.442](https://doi.org/10.1094/PHYTO.1998.88.5.442) PMID: [18944924](https://pubmed.ncbi.nlm.nih.gov/18944924/)
12. Healy FG, Wach M, Krasnoff SB, Gibson DM, Loria R. The *txtAB* genes of the plant pathogen *Streptomyces acidiscabies* encode a peptide synthetase required for phytotoxin thaxtomin A production and pathogenicity. *Mol Microbiol.* 2000; 38: 794–804. PMID: [11115114](https://pubmed.ncbi.nlm.nih.gov/11115114/)
13. King RR, Lawrence CH, Clark MC. Correlation of phytotoxin production with pathogenicity of *Streptomyces scabies* isolates from scab infected potato tubers. *Am Potato J.* 1991; 68: 675–680.
14. Kinkel LL, Bowers JH, Shimizu K, Neeno-Eckwall EC, Schottel JL. Quantitative relationships among thaxtomin A production, potato scab severity, and fatty acid composition in *Streptomyces*. *Can J Microbiol.* 1998; 44: 768–776. PMID: [9830106](https://pubmed.ncbi.nlm.nih.gov/9830106/)
15. Loria R, Bukhalid RA, Creath RA, Leiner RH, Olivier M, Steffens JC. Differential production of thaxtomins by pathogenic *Streptomyces* species *in vitro*. *Phytopathology.* 1995; 85: 537–541.
16. Fyans JK, Altowairish MS, Li Y, Bignell DR. Characterization of the coronatine-like phytotoxins produced by the common scab pathogen *Streptomyces scabies*. *Mol Plant Microbe Interact.* 2014 Nov 25. doi: [10.1094/MPMI-09-14-0255-R](https://doi.org/10.1094/MPMI-09-14-0255-R)
17. Xin XF, He SY. *Pseudomonas syringae* pv. *tomato* DC3000: a model pathogen for probing disease susceptibility and hormone signaling in plants. *Annu Rev Phytopathol.* 2013; 51: 473–498. doi: [10.1146/annurev-phyto-082712-102321](https://doi.org/10.1146/annurev-phyto-082712-102321) PMID: [23725467](https://pubmed.ncbi.nlm.nih.gov/23725467/)
18. Bender CL, Alarcon-Chaidez F, Gross DC. *Pseudomonas syringae* phytotoxins: mode of action, regulation, and biosynthesis by peptide and polyketide synthetases. *Microbiol Mol Biol Rev.* 1999; 63: 266–292. PMID: [10357851](https://pubmed.ncbi.nlm.nih.gov/10357851/)
19. Bignell DR, Seipke RF, Huguet-Tapia JC, Chambers AH, Parry R, Loria R. *Streptomyces scabies* 87–22 contains a coronafacic acid-like biosynthetic cluster that contributes to plant-microbe interactions. *Mol Plant Microbe Interact.* 2010; 23: 161–175. doi: [10.1094/MPMI-23-2-0161](https://doi.org/10.1094/MPMI-23-2-0161) PMID: [20064060](https://pubmed.ncbi.nlm.nih.gov/20064060/)
20. Taylor BL, Zhulin IB. PAS domains: internal sensors of oxygen, redox potential, and light. *Microbiol Mol Biol Rev.* 1999; 63: 479–506. PMID: [10357859](https://pubmed.ncbi.nlm.nih.gov/10357859/)
21. Fuqua WC, Winans SC, Greenberg EP. Quorum sensing in bacteria: the LuxR-LuxI family of cell density-responsive transcriptional regulators. *J Bacteriol.* 1994; 176: 269–275. PMID: [8288518](https://pubmed.ncbi.nlm.nih.gov/8288518/)
22. Anton N, Santos-Aberturas J, Mendes MV, Guerra SM, Martin JF, Aparicio JF. PimM, a PAS domain positive regulator of pimarcin biosynthesis in *Streptomyces natalensis*. *Microbiology.* 2007; 153: 3174–3183. PMID: [17768260](https://pubmed.ncbi.nlm.nih.gov/17768260/)
23. Santos-Aberturas J, Vicente CM, Guerra SM, Payero TD, Martin JF, Aparicio JF. Molecular control of polyene macrolide biosynthesis: direct binding of the regulator PimM to eight promoters of pimarcin genes and identification of binding boxes. *J Biol Chem.* 2011; 286: 9150–9161. doi: [10.1074/jbc.M110.182428](https://doi.org/10.1074/jbc.M110.182428) PMID: [21187288](https://pubmed.ncbi.nlm.nih.gov/21187288/)
24. Vicente CM, Santos-Aberturas J, Payero TD, Barreales EG, de Pedro A, Aparicio JF. PAS-LuxR transcriptional control of filipin biosynthesis in *S. avermitilis*. *Appl Microbiol Biotechnol.* 2014; 98: 9311–9324. doi: [10.1007/s00253-014-5998-7](https://doi.org/10.1007/s00253-014-5998-7) PMID: [25104037](https://pubmed.ncbi.nlm.nih.gov/25104037/)
25. Wei J, Meng X, Wang Q. Enhanced production of aureofuscin by over-expression of AURJ3M, positive regulator of aureofuscin biosynthesis in *Streptomyces aureofuscus*. *Lett Appl Microbiol.* 2011; 52: 322–329. doi: [10.1111/j.1472-765X.2011.03003.x](https://doi.org/10.1111/j.1472-765X.2011.03003.x) PMID: [21204886](https://pubmed.ncbi.nlm.nih.gov/21204886/)
26. Wu H, Liu W, Dong D, Li J, Zhang D, Lu C. *SlnM* gene overexpression with different promoters on natamycin production in *Streptomyces lydicus* A02. *J Ind Microbiol Biotechnol.* 2014; 41: 163–172. doi: [10.1007/s10295-013-1370-7](https://doi.org/10.1007/s10295-013-1370-7) PMID: [24174215](https://pubmed.ncbi.nlm.nih.gov/24174215/)
27. Sambrook J, Russell DW. *Molecular cloning: a laboratory manual.* Cold Spring Harbor, NY: Cold Spring Harbor Laboratory Press; 2001.
28. Kieser T, Bibb MJ, Buttner MJ, Chater KF, Hopwood DA. *Practical Streptomyces Genetics.* Norwich, UK: The John Innes Foundation; 2000.

29. Johnson EG, Krasnoff SB, Bignell DR, Chung WC, Tao T, Parry RJ, et al. 4-Nitrotryptophan is a substrate for the non-ribosomal peptide synthetase TxtB in the thaxtomin A biosynthetic pathway. *Mol Microbiol.* 2009; 73: 409–418. doi: [10.1111/j.1365-2958.2009.06780.x](https://doi.org/10.1111/j.1365-2958.2009.06780.x) PMID: [19570136](https://pubmed.ncbi.nlm.nih.gov/19570136/)
30. MacNeil DJ, Gewain KM, Ruby CL, Dezeny G, Gibbons PH, MacNeil T. Analysis of *Streptomyces avermitilis* genes required for avermectin biosynthesis utilizing a novel integration vector. *Gene.* 1992; 111: 61–68. PMID: [1547955](https://pubmed.ncbi.nlm.nih.gov/1547955/)
31. Chung CT, Niemela SL, Miller RH. One-step preparation of competent *Escherichia coli*: transformation and storage of bacterial cells in the same solution. *Proc Natl Acad Sci USA.* 1989; 86: 2172–2175. PMID: [2648393](https://pubmed.ncbi.nlm.nih.gov/2648393/)
32. Bradford MM. A rapid and sensitive method for quantitation of microgram quantities of protein utilizing the principle of protein-dye binding. *Anal Biochem.* 1976; 72: 248–254. PMID: [942051](https://pubmed.ncbi.nlm.nih.gov/942051/)
33. Palmer GC, Palmer KL, Jorth PA, Whiteley M. Characterization of the *Pseudomonas aeruginosa* transcriptional response to phenylalanine and tyrosine. *J Bacteriol.* 2010; 192: 2722–2728. doi: [10.1128/JB.00112-10](https://doi.org/10.1128/JB.00112-10) PMID: [20304990](https://pubmed.ncbi.nlm.nih.gov/20304990/)
34. Finn RD, Bateman A, Clements J, Coggill P, Eberhardt RY, Eddy SR, et al. Pfam: the protein families database. *Nucleic Acids Res.* 2014; 42: D222–230. doi: [10.1093/nar/gkt1223](https://doi.org/10.1093/nar/gkt1223) PMID: [24288371](https://pubmed.ncbi.nlm.nih.gov/24288371/)
35. Crooks GE, Hon G, Chandonia JM, Brenner SE. WebLogo: a sequence logo generator. *Genome Res.* 2004; 14: 1188–1190. PMID: [15173120](https://pubmed.ncbi.nlm.nih.gov/15173120/)
36. Tamura K, Peterson D, Peterson N, Stecher G, Nei M, Kumar S. MEGA5: molecular evolutionary genetics analysis using maximum likelihood, evolutionary distance, and maximum parsimony methods. *Mol Biol Evol.* 2011; 28: 2731–2739. doi: [10.1093/molbev/msr121](https://doi.org/10.1093/molbev/msr121) PMID: [21546353](https://pubmed.ncbi.nlm.nih.gov/21546353/)
37. Santos-Aberturas J, Payero TD, Vicente CM, Guerra SM, Canibano C, Martin JF, et al. Functional conservation of PAS-LuxR transcriptional regulators in polyene macrolide biosynthesis. *Metab Eng.* 2011; 13: 756–767. doi: [10.1016/j.ymben.2011.09.011](https://doi.org/10.1016/j.ymben.2011.09.011) PMID: [22001323](https://pubmed.ncbi.nlm.nih.gov/22001323/)
38. Schneider TD, Stephens RM. Sequence logos: a new way to display consensus sequences. *Nucleic Acids Res.* 1990; 18: 6097–6100. PMID: [2172928](https://pubmed.ncbi.nlm.nih.gov/2172928/)
39. Bourn WR, Babb B. Computer assisted identification and classification of streptomyces promoters. *Nucleic Acids Res.* 1995; 23: 3696–3703. PMID: [7478999](https://pubmed.ncbi.nlm.nih.gov/7478999/)
40. Lee DJ, Minchin SD, Busby SJ. Activating transcription in bacteria. *Annu Rev Microbiol.* 2012; 66: 125–152. doi: [10.1146/annurev-micro-092611-150012](https://doi.org/10.1146/annurev-micro-092611-150012) PMID: [22726217](https://pubmed.ncbi.nlm.nih.gov/22726217/)
41. Huang ZJ, Edery I, Rosbash M. PAS is a dimerization domain common to *Drosophila* period and several transcription factors. *Nature.* 1993; 364: 259–262. PMID: [8391649](https://pubmed.ncbi.nlm.nih.gov/8391649/)
42. Lindebro MC, Poellinger L, Whitelaw ML. Protein-protein interaction via PAS domains: role of the PAS domain in positive and negative regulation of the bHLH/PAS dioxin receptor-Arnt transcription factor complex. *EMBO J.* 1995; 14: 3528–3539. PMID: [7628454](https://pubmed.ncbi.nlm.nih.gov/7628454/)
43. Pongratz I, Antonsson C, Whitelaw ML, Poellinger L. Role of the PAS domain in regulation of dimerization and DNA binding specificity of the dioxin receptor. *Mol Cell Biol.* 1998; 18: 4079–4088. PMID: [9632792](https://pubmed.ncbi.nlm.nih.gov/9632792/)
44. Reisz-Porszasz S, Probst MR, Fukunaga BN, Hankinson O. Identification of functional domains of the aryl hydrocarbon receptor nuclear translocator protein (ARNT). *Mol Cell Biol.* 1994; 14: 6075–6086. PMID: [8065341](https://pubmed.ncbi.nlm.nih.gov/8065341/)
45. Maru Y, Afar DE, Witte ON, Shibuya M. The dimerization property of glutathione S-transferase partially reactivates Bcr-Abl lacking the oligomerization domain. *J Biol Chem.* 1996; 271: 15353–15357. PMID: [8663064](https://pubmed.ncbi.nlm.nih.gov/8663064/)
46. Niedziela-Majka A, Rymarczyk G, Kochman M, Ozyhar A. GST-induced dimerization of DNA-binding domains alters characteristics of their interaction with DNA. *Protein Express Purif.* 1998; 14: 208–220. PMID: [9790883](https://pubmed.ncbi.nlm.nih.gov/9790883/)
47. Terpe K. Overview of tag protein fusions: from molecular and biochemical fundamentals to commercial systems. *Appl Microbiol Biotechnol.* 2003; 60: 523–533. PMID: [12536251](https://pubmed.ncbi.nlm.nih.gov/12536251/)
48. Burroughs AM, Iyer LM, Aravind L. Natural history of the E1-like superfamily: implication for adenylation, sulfur transfer, and ubiquitin conjugation. *Proteins.* 2009; 75: 895–910. doi: [10.1002/prot.22298](https://doi.org/10.1002/prot.22298) PMID: [19089947](https://pubmed.ncbi.nlm.nih.gov/19089947/)
49. Bignell DR, Fyans JK, Cheng Z. Phytotoxins produced by plant pathogenic *Streptomyces* species. *J Appl Microbiol.* 2014; 116: 223–235.
50. Bignell DR, Francis IM, Fyans JK, Loria R. Thaxtomin A production and virulence are controlled by several *bld* gene global regulators in *Streptomyces scabies*. *Mol Plant Microbe Interact.* 2014; 27: 875–885. doi: [10.1094/MPMI-02-14-0037-R](https://doi.org/10.1094/MPMI-02-14-0037-R) PMID: [24678834](https://pubmed.ncbi.nlm.nih.gov/24678834/)

Appendix 1: The Coronafacoyl Phytotoxins: Structure, Biosynthesis, Regulation and Biological Activities

Dawn R. D. Bignell*, Zhenlong Cheng† and Luke Bown†

Department of Biology, Memorial University of Newfoundland, St. John's, NL, A1B 3X9, Canada

* Email: dbignell@mun.ca; Phone: +1 709 864 4573

† These authors contributed equally to this work.

© Springer International Publishing

Bignell, D.R.D., Cheng, Z. & Bown, L. *Antonie van Leeuwenhoek* (2018) 111: 649.

The final publication is available at <https://doi.org/10.1007/s10482-017-1009-1>

Abstract

Phytotoxins are secondary metabolites that contribute to the development and/or severity of diseases caused by various plant pathogenic microorganisms. The coronafacoyl phytotoxins are an important family of plant toxins that are known or suspected to be produced by several phylogenetically distinct plant pathogenic bacteria, including the gammaproteobacterium *Pseudomonas syringae* and the actinobacterium *Streptomyces scabies*. At least seven different family members have been identified, of which coronatine (COR) was the first to be described and is the best-characterized. Though nonessential for disease development, coronafacoyl phytotoxins appear to enhance the severity of disease symptoms induced by pathogenic microbes during host infection. In addition, the identification of coronafacoyl phytotoxin biosynthetic genes in organisms not known to be plant pathogens suggests that these metabolites may have additional roles other than as virulence factors. This review focuses on our current understanding of the structures, biosynthesis, regulation, biological activities and evolution of coronafacoyl phytotoxins as well as the different methods that are used to detect the metabolites and the organisms that produce them.

Introduction

Phytotoxins are secondary metabolites that are produced by many phytopathogenic bacteria and fungi. They exhibit adverse effects on plants at very low concentrations and can be critical to the development of disease by pathogenic organisms (Bender et al. 1999; Strange 2007). Phytotoxins can be host specific and affect only those plant species that can

be infected by the producing organism, or they can be non-host specific and exert toxic effects against a broad range of plant species that are not infected by the pathogen. Although some phytotoxins are essential for pathogenicity, many are not required for disease development but instead contribute to the virulence phenotype of the producing organism. In this case, disease may still occur in the absence of the phytotoxin, however the severity of disease symptoms is greatly enhanced when the phytotoxin is present (Bender et al. 1999; Strange 2007).

Coronatine (COR) is a non-host specific phytotoxin that was first described in 1977 by Ichihara and colleagues (Ichihara et al. 1977). It is produced by different pathogenic variants (pathovars or pv) of the Gram-negative plant pathogen *Pseudomonas syringae*, which causes economically important diseases in a variety of plant species (Xin and He 2013). COR belongs to a family of phytotoxins called the coronafacoyl phytotoxins, members of which are now known or suspected to be produced by several phylogenetically distinct plant pathogenic bacteria, including the potato common scab pathogen *Streptomyces scabies* (syn. *S. scabiei*) and the potato blackleg pathogen *Pectobacterium atrosepticum* (Bell et al. 2004; Fyans et al. 2015). Though nonessential for pathogenicity, there is convincing evidence that COR and COR-like molecules are important virulence factors that contribute to the severity of disease symptoms induced by the producing organisms (Bell et al. 2004; Bignell et al. 2010; Panda et al. 2016; Slawiak and Lojkowska 2009; Xin and He 2013). A number of recent studies have provided significant insights into the bioactivity and mode of action of COR and other coronafacoyl phytotoxins, while other studies have focused on understanding the biosynthesis, regulation and evolution of

production of these metabolites in different microorganisms. An updated overview of coronafacoyl phytotoxins is long overdue and is the focus of this review.

Chemical structures and producing organisms

All coronafacoyl phytotoxins characterized to date consist of the bicyclic hydrindane ring - based polyketide coronafacic acid (CFA, Fig. 1A) linked via an amide bond to an amino acid or amino acid derivative. In the case of COR (Fig. 1B), the molecule attached to CFA is coronamic acid (CMA), an ethylcyclopropyl amino acid derived from L-isoleucine via its diastereoisomer L-*allo*-isoleucine (Parry et al. 1994). Production of COR has been demonstrated in three *P. syringae* pathovars (*tomato*, *maculicola*, *actinidiae*) and in *P. coronafaciens* pv *atropurpurea*, *P. cannabina* pv *alisalensis* (formerly *P. syringae* pv *alisalensis*), *P. amygdali* pv *morsprunorum* (formerly *P. syringae* pv *morsprunorum*) and *P. savastanoi* pv *glycinea* (formerly *P. syringae* pv *glycinea*) (Table 1). Other pathovars of *P. syringae*, *P. coronafaciens*, *P. savastanoi*, *P. cannabina* and *P. amygdali* as well as a closely related *Pseudomonas* spp. (*P. temae*) most likely produce COR due to the presence of the biosynthetic genes for CFA and CMA in the respective genome sequences (Table 1). COR production has also been reported in the New Zealand flax pathogen *Xanthomonas campestris* pv *phormiicola* and most recently in a novel plant pathogenic strain of *Pectobacterium cacticidum* (Table 1). *S. scabies* does not produce COR but instead produces *N*-coronafacoyl-L-isoleucine (CFA-Ile; Fig. 1C) as the primary coronafacoyl phytotoxin as well as other minor compounds (Fyans et al. 2015). Coronafacoyl compounds containing the amino acids L-valine (CFA-Val, Fig. 1D), L-isoleucine, L-*allo*-isoleucine (CFA-*a*Ile, Fig. 1E), L-serine (CFA-Ser, Fig. 1F), L-threonine

(CFA-Thr, Fig. 1G) and a methyl-substituted CMA derivative (norcoronatine, Fig. 1H) have also been identified in culture extracts of COR-producing *X. campestris* pv *phormiicola* and/or *Pseudomonas* spp. (Table 1). Studies conducted in *P. savastanoi* pv *glycinea* and *P. syringae* pv *tomato* indicate that COR is the most abundant compound produced, while CFA-Val is usually the second most abundant and the rest are produced as minor components (Mitchell 1991).

Genome sequencing data have revealed that many more bacteria may produce coronafacoyl phytotoxins than previously realized. In 2004, it was reported that the genome sequence of the potato blackleg pathogen *P. atrosepticum* SCRI1043 harbours homologues of the *P. syringae* *cfaI-8* and *cfl* genes (Bell et al. 2004), and since then the genes have been found in the genome sequences of other plant pathogenic *Pectobacterium* spp. and in strains of *Dickeya* spp., *Brenneria* spp. and *Lonsdalea quercina*, all of which are close relatives of *Pectobacterium* (Table 1). Interestingly, a recent analysis of the NCBI database revealed that coronafacoyl phytotoxin biosynthetic genes are not confined to plant pathogenic bacteria species but can also be found in species that are not known to be pathogenic, including *Pseudomonas psychrotolerans*, *Azospirillum* sp. B510, *Streptomyces griseoruber*, *Streptomyces graminilatus*, *Streptomyces* sp. NRRL WC-3618, *Kitasatospora azatica* and *Zymobacter palmae* (Table 1). This suggests that the production of coronafacoyl phytotoxins may serve other purposes rather than functioning exclusively as virulence factors (Bown et al. 2017). Currently, it is not known which specific coronafacoyl phytotoxin(s) is produced by most organisms, though it is likely that the majority do not produce COR due to the absence of the CMA biosynthetic genes.

Biosynthesis

Initial investigations into the biosynthesis of the CMA moiety in *Pseudomonas* spp. led to the discovery of three genes (*cmaATU*; Fig. 2 and Table 2) that are required for the production of CMA (Ullrich & Bender 1994). The *cmaA* gene product appeared to be a didomain protein containing an adenylation (A) domain and a thiolation (T) domain, while the *cmaT* gene product resembled thioesterases and the *cmaU* gene product did not show similarity to any known proteins and its function is currently unknown (Couch et al. 2004; Ullrich and Bender 1994). Subsequent investigations led to the discovery and characterization of additional CMA biosynthetic genes, namely the *cmaBCDE* genes (Fig. 2 and Table 2) (Vaillancourt et al. 2005). Biosynthesis of the CMA moiety begins with CmaA catalyzing the adenylation of L-*a*Ile and attachment of L-*a*Ile to the T domain of CmaA (Fig. 3) (Couch et al. 2004). Recent work identified a gene, *cmaL* (PSPTO4723), which encodes a predicted DUF1330 protein and is likely involved in the biosynthesis of L-*a*Ile from L-Ile (Fig. 3 and Table 2) (Worley et al. 2013). Although *cmaL* is separated from the rest of the *cma* genes by 8.8 kb in *P. syringae* pv *tomato* DC3000, there is evidence that the gene is co-regulated with the other *cma* genes (Worley et al. 2013). The aminoacyl form of L-*a*Ile is then transported to the phosphopantetheinyl arm of the CmaD protein, which is a stand-alone T domain without a corresponding A domain, by the aminoacyltransferase CmaE (Strieter et al. 2007; Vaillancourt et al. 2005). While attached to CmaD, the L-*a*Ile is chlorinated at the γ position to form γ -chloro-L-*a*Ile by the CmaB protein, which is a member of the non-haem Fe²⁺ α -ketoglutarate - dependant enzyme superfamily (Vaillancourt et al. 2005). The CmaC enzyme then catalyzes the cyclization of

the intermediate through the removal of the γ -chloro group by the nucleophilic attack of the α -carbon from L-*a*Ile to produce a cyclopropane ring (Kelly et al. 2007; Vaillancourt et al. 2005). It is believed that the covalent linkage attaching the now cyclised L-*a*Ile is then hydrolyzed by the CmaT thioesterase to release the fully formed CMA substrate (Patel et al. 1998).

The *Pseudomonas* CFA biosynthetic gene cluster is composed of 10 structural genes designated *cfa1-9* and *cfl*, which are organized as a single 19 kb transcriptional unit (Fig. 2 and Table 2) (Bender et al. 1999). *cfa1*, *cfa2* and *cfa3* encode proteins showing significant similarity to acyl carrier proteins (ACP), fatty acid dehydratases (DH) and a β -ketoacyl synthetases (KS) of type II polyketide synthases (PKS), respectively (Penfold et al. 1996). The *cfa4* protein product does not show significant similarity to sequences in the database and its function is unknown, though it has been suggested that it may function as a cyclase (Rangaswamy et al. 1998a). *cfa5* encodes a predicted acyl-CoA ligase, and *cfa6* and *cfa7* encode large, multifunctional enzymes resembling modular type I PKSs (Penfold et al. 1996; Rangaswamy et al. 1998a). The *cfa8* protein product shows similarity to crotonyl-CoA reductase/carboxylase (CCR) enzymes that catalyze the reductive carboxylation of (*E*)-crotonyl-CoA to (2*S*)-ethylmalonyl-CoA, which in turn is used as an extender unit for polyketide biosynthesis (Wilson and Moore 2012). Mutagenesis experiments indicated that *cfa8* is essential for CFA and COR production in *P. savastanoi* pv *glycinea* (Rangaswamy et al. 1998b). The final gene in the CFA biosynthetic gene cluster is *cfa9*, which encodes a protein showing similarity to thioesterases and is dispensable for CFA and COR production (Rangaswamy et al. 1998b).

The exact pathway of CFA biosynthesis in *Pseudomonas* spp. is not well understood, though a hypothetical pathway has been proposed (Rangaswamy et al. 1998a). Precursor feeding studies using ^{13}C – labeled substrates indicated that CFA is synthesized from one unit of pyruvate, one unit of butyrate and three units of acetate (Parry et al. 1994). The theorized starting precursor is α -ketoglutarate, which is generated by carboxylation of pyruvate to form oxaloacetate and then conversion of oxaloacetate to α -ketoglutarate via the TCA cycle (Parry et al. 1996). Rangaswamy and colleagues proposed that α -ketoglutarate is decarboxylated to produce succinic semialdehyde, which is then converted into a CoA ester, possibly by Cfa5. Cfa1, Cfa3, and Cfa4 are then predicted to create enzyme – bound 2-carboxy-3-hydroxycyclopentenone, which is dehydrated by Cfa2 to produce enzyme – bound 2-carboxy-2-cyclopentenone (CPC; Fig. 4) (Rangaswamy et al. 1998a). CPC may then be passed to the loading module of Cfa6, which catalyzes the extension of CPC by a butyrate unit followed by complete reduction of the β -keto ester to form enzyme – bound 2-[1-oxo-2-cyclopenten-2-ylmethyl]butanoic acid (CPE; Fig. 4). The predicted CCR encoded by *cfa8* is thought to provide the (2*S*)-ethylmalonyl-CoA used for extension of CPC by Cfa6 (Rangaswamy et al. 1998b). Next, CPE is transferred to Cfa7, which catalyzes the extension of CPE by a malonate unit. This is followed by an intramolecular 6 - *endo* - trig cyclization of the tethered intermediate to produce the bicyclic hydrindane ring - containing intermediate, which then undergoes ketoreduction and dehydration by the Cfa7 ketoreductase (KR) and DH domains, respectively, to form the complete CFA moiety (Fig. 4) (Strieter et al. 2009). Cfa7 also harbours a thioesterase (TE) domain that would allow for the release of free CFA, which may be enhanced by the

activity of the free Cfa9 thioesterase (Rangaswamy et al. 1998b). The final step in the production of COR is the ligation of the CFA and CMA moieties, which is predicted to be catalyzed by the coronafacate ligase (Cfl) enzyme encoded by the *cfl* gene (Bender et al. 1999).

Sequencing of the *S. scabies* 87-22 genome revealed the presence of a gene cluster that is highly similar to the *Pseudomonas* CFA biosynthetic gene cluster (Table 2 and Fig. 2) (Bignell et al. 2010). Homologues of the *cfa1*-8 and *cfl* genes were identified in a similar arrangement as in *Pseudomonas* spp.; however, no homologues of the *cma* genes were found anywhere in the genome, suggesting that *S. scabies* cannot make COR. Interestingly, six additional genes that are absent from the *Pseudomonas* gene cluster were found associated with the *S. scabies* *cfa* and *cfl* genes. Four of these genes, *SCAB79681* (also known as *oxr*), *SCAB79691* (also known as *CYP107AK1*), *SCAB79711* and *SCAB79721* (also known as *sdr*) were predicted to encode biosynthetic enzymes and were shown to be co-transcribed with the *cfa* and *cfl* genes, while the other two genes (*SCAB79581/orf1*, *SCAB79591/cfaR*) are divergently co-transcribed from the other genes and have been shown to be involved in regulation (Fig. 2) (Bignell et al. 2010; Cheng et al. 2015). The *SCAB79711* gene product shows similarity to 3-hydroxybutyryl-CoA dehydrogenases that are typically involved in the reduction of acetoacetyl-CoA to 3-hydroxybutyryl-CoA, an intermediate in the biosynthesis of crotonyl-CoA (Chan et al. 2009). It is therefore likely that *SCAB79711* works together with the CCR encoded by *cfa8* to produce the (2*S*)-ethylmalonyl-CoA extender unit used for polyketide biosynthesis (Fig. 5) (Bignell et al. 2010). It was initially thought that *oxr*, *CYP107AK1* and *sdr*, which encode a predicted

F₄₂₀-dependent oxidoreductase, a cytochrome P450 and a short chain dehydrogenase/reductase, respectively (Table 2), may function as tailoring enzymes and contribute to the production of one or more novel coronafacoyl phytotoxins in *S. scabies* (Bignell et al. 2010). Although subsequent structural characterization of the primary *S. scabies* phytotoxin indicated that it is the known coronafacoyl phytotoxin CFA-Ile (Fyans et al. 2015), gene deletion analysis revealed that all three genes are required for normal production of CFA-Ile, with *CYP107AK1* being essential (Bown et al. 2016; Bown et al. 2017). Both the $\Delta CYP107AK1$ and Δsdr mutants accumulated biosynthetic intermediates that were purified and structurally characterized, and based on this it was proposed that *CYP107AK1* and *sdr* are responsible for introducing the keto group that is present on the bicyclic hydrindane ring of CFA (Fig. 5) (Bown et al. 2016; Bown et al. 2017). In contrast, no biosynthetic intermediates were isolated from the Δoxr mutant, and so its role in CFA-Ile biosynthesis remains unclear (Bown et al. 2016).

Given the absence of similar genes in the CFA biosynthetic gene cluster and elsewhere in the genome sequences of *Pseudomonas* spp., the involvement of *oxr*, *CYP107AK1* and *sdr* in CFA-Ile biosynthesis suggests that *S. scabies* and *Pseudomonas* spp. utilize distinct biosynthetic pathways for producing the same family of phytotoxins. The proposed hypothetical pathway for CFA biosynthesis in *P. syringae* suggests that the keto group originates from the α -ketoglutarate precursor (Fig. 4). In contrast, studies in *S. scabies* suggest that it is the *CYP107AK1* enzyme that introduces the oxygen via a hydroxyl group, which is then converted to the keto group by the *Sdr* enzyme (Bown et al. 2016; Bown et al. 2017). The scheme shown in Fig. 5 proposes that these steps take place

after polyketide biosynthesis by Cfa6 and Cfa7, though it cannot yet be ruled out that CYP107AK1 and Sdr generate the keto group within an earlier precursor molecule. Although the exact function of the Oxr enzyme in CFA-Ile biosynthesis is currently unknown, it has been suggested that it might introduce the carbon – carbon double bond that is found within the cyclohexene ring of CFA (Fig. 5) (Bown et al. 2016). In *P. syringae*, this double bond results from the reduction and dehydration of the hydrindane ring - containing intermediate by Cfa7 (Fig. 4) (Rangaswamy et al. 1998a; Strieter et al. 2009), whereas the *S. scabiei* Cfa7 enzyme is proposed to contain an extra enoyl reductase (ER) domain that is believed to be functional and would reduce the double bond that is formed by the DH domain (Fig. 5) (Bignell et al. 2010; Bown et al. 2017). If this is the case, then the double bond must be reintroduced at a later step, possibly by Oxr, though further studies are needed to confirm this. The final ligation of CFA to L-Ile by the Cfl homologue was confirmed by deletion of the *S. scabiei* *cfl* gene, which resulted in accumulation of CFA in the mutant culture supernatants (Fyans et al. 2015). Interestingly, the *S. scabiei* Cfl is able to utilize CFA biosynthetic intermediates as substrates for ligation to Ile, suggesting that the enzyme lacks a rigid specificity for the polyketide substrate (Bown et al. 2016; Bown et al. 2017).

Regulation of production

Production of COR in *Pseudomonas* spp. is regulated by multiple nutritional and environmental factors, including pH, carbon sources, osmolarity and nutrient levels (Li et al. 1998; Palmer and Bender 1993). In *P. savastanoi* pv *glycinea* PG4180, temperature has a major effect on COR production as production rates are much higher (more than 60 fold)

at 18°C than at 28°C, the latter being the optimum growth temperature for the organism (Budde et al. 1998; Palmer and Bender 1993; Weingart et al. 2004). The observed thermoregulation of COR production is mainly due to the temperature-dependent transcription of the *cma* and *cfl/cfa* genes (Budde et al. 1998; Liyanage et al. 1995; Rangaswamy et al. 1997), which in the case of the *cma* genes also occurs *in planta* (Weingart et al. 2004). In addition, Budde and colleagues showed that the stability of the CmaB protein is greater at 18°C than at 28°C, indicating that the thermoregulation is also influenced by post-translational factors (Budde et al. 1998). In contrast, the biosynthesis of COR and expression of the *cma* genes is not significantly affected by temperature in *P. syringae* pv *tomato* DC3000 (Weingart et al. 2004), although an earlier study has suggested that it was (Rohde et al. 1998). COR gene expression in *P. syringae* pv *tomato* DC3000 is strongly activated when the cells are cultured *in planta* or in basal medium containing plant extracts (Boch et al. 2002; Li et al. 1998; Ma et al. 1991; Weingart et al. 2004), whereas COR production is not influenced by plant extracts or plant-derived secondary metabolites in *P. savastanoi* pv *glycinea* PG4180 (Palmer and Bender 1993). This suggests that the signals for inducing COR biosynthesis are different in these two organisms.

The DNA region responsible for the thermoregulation of COR production in *P. savastanoi* pv *glycinea* PG4180 is localized in between the CFA and CMA biosynthetic gene clusters and consists of three genes, *corP*, *corS* and *corR*, which encode components of a modified two-component regulatory system (Fig. 2 and Table 2) (Sreedharan et al. 2006; Ullrich et al. 1995). CorR and CorP both show similarity to response regulators that function as mediators of the cellular response in two-component regulatory systems, while

CorS shows similarity to histidine protein kinases that serve as environmental sensors (Ullrich et al. 1995). CorR has the N-terminal receiver domain and the C-terminal DNA binding and effector domain with a helix-turn-helix (HTH) motif that is typical of response regulators (Pao et al. 1994). It has been shown to function as a positive activator of COR gene expression and to bind to the promoter regions controlling expression of the *cfl/cfa* and *cma* genes in a temperature-dependent manner (Fig. 6A) (Penalzo-Vazquez and Bender 1998; Wang et al. 1999). CorP is similar to CorR but it lacks the C-terminal HTH DNA binding domain and does not bind to the promoter regions driving COR production (Wang et al. 1999). Instead, CorP is required for the activation of CorR by CorS at low temperature, though its exact function remains unclear (Fig. 6A) (Wang et al. 1999). CorS is thought to be a membrane-embedded histidine protein kinase that responds to changes in temperature by modulating its conformation within the cell membrane (Braun et al. 2007; Smirnova and Ullrich 2004). Rangaswamy and Bender (2000) demonstrated that CorS can autophosphorylate *in vitro* and can transphosphorylate CorR but not CorP (Fig. 6A), which is consistent with the presence of the conserved receiver aspartate residue in the former protein but not in the latter (Rangaswamy and Bender 2000). Although *corP* and *corR* are expressed constitutively at 18 and 28°C, *corS* expression is highest at 18°C and minimal at 28°C, suggesting that CorS may autoregulate its own expression (Ullrich et al. 1995).

A database search revealed that part or all of the CorRPS two-component regulatory system is conserved in several *Pseudomonas* species that also harbour the *cfl/cfa* and *cma* genes. In *P. syringae* pv *tomato* DC3000, the CorR homolog also functions as a positive activator of CFA and CMA structural gene expression and COR production (Sreedharan et

al. 2006). In turn, *corR* expression is dependent on *hrpL*, which encodes an extracytoplasmic function sigma factor that also regulates the expression of the virulence-associated type III secretion system (Sreedharan et al. 2006). Mutations in *corR* were found to reduce the expression of *hrpL*, and a putative CorR binding site was identified within the *hrpL* promoter, suggesting that CorR may enhance the early expression of *hrpL* (Sreedharan et al. 2006). Whether CorS and CorP are involved in activating CorR via phosphorylation, and what signal(s) is sensed by CorS in *P. syringae* pv *tomato* DC3000 is currently unclear; however, the absence of thermoregulation of COR production in this organism suggests that the signal sensed by CorS is likely different than in *P. savastanoi* pv *glycinea* PG4180.

The regulation of coronafacoyl phytotoxin production has also been studied in *S. scabies*. Production of CFA-Ile was found to mainly occur in media containing plant-based components, with the highest levels observed in soy flour – based media (Fyans et al. 2015). Production levels were also found to be greater at 25°C than at the optimum growth temperature of 28°C (Fyans et al. 2015). The *S. scabies* CFA-Ile biosynthetic genes are transcribed as a single large mRNA transcript from the *cfaI* promoter, and a gene that is divergently transcribed was shown to function as a positive activator of the biosynthetic genes (Bignell et al. 2010). Overexpression of the gene, designated *SCAB79591/cfaR*, leads to enhanced expression of the biosynthetic genes and enhanced CFA-Ile production (Bignell et al. 2010; Fyans et al. 2015). CfaR belongs to a family of actinobacterial transcriptional regulators characterized by an N-terminal PAS (PER-ARNT-SIM) sensory domain and a C-terminal LuxR-type DNA binding domain (Taylor and Zhulin 1999; Fuqua

et al. 1994). Electrophoretic mobility shift assays demonstrated that CfaR binds specifically to a single site located immediately upstream of the -35 hexanucleotide box within the *cfaI* promoter region (Fig. 6B) (Cheng et al. 2015). The binding site identified (5'-CTAGGGATTCTCCTAG-3') is a 16 bp palindromic sequence that is highly similar to the binding site consensus sequence of the PAS-LuxR family regulator PimM, which controls the production of the polyene antifungal compound pimaricin in *Streptomyces natalensis* (Anton et al. 2007; Santos-Aberturas et al. 2011). CfaR DNA binding activity requires both the LuxR and PAS domains, with the latter playing a role in protein homodimer formation (Cheng et al. 2015). Intriguingly, the activation of CFA-Ile biosynthesis by CfaR is significantly enhanced by *SCAB79581/orfI* (Fig. 6B), which is located downstream of and is co-transcribed with *cfaR* (Fig. 2) (Bignell et al. 2010; Cheng et al. 2015). *orfI* encodes a protein with a predicted ThiF family domain and a nitroreductase domain, and while overexpression of *orfI* alone has no effect on CFA-Ile production, overexpression of both *cfaR* and *orfI* leads to significantly greater CFA-Ile production levels than when *cfaR* alone is overexpressed (Cheng et al. 2015). Although the exact function of *orfI* is unclear, it was recently noted that homologues of both *cfaR* and *orfI* are conserved in other Actinobacteria that harbour coronafacoyl phytotoxin biosynthetic genes, suggesting that both genes play a role in regulating metabolite production in multiple species (Bown et al. 2017).

In addition to *cfaR* and *orfI*, other genes appear to regulate the production of CFA-Ile in *S. scabies* (Fig. 6B). Deletion of the *bldA* gene, which encodes the only tRNA that efficiently translates the rare UUA codon in *Streptomyces* mRNA (Chater 2006), led to a reduction in expression of the CFA-Ile biosynthetic genes (Bignell et al. 2010). An analysis

of the *cfaR* coding sequence revealed the presence of a single TTA codon, suggesting that CfaR is not efficiently translated in the *bldA* mutant (Bignell et al. 2010). *bldA* is a member of the *bld* (bald) gene family of global regulators that control both morphological differentiation and secondary metabolism in *Streptomyces* spp. (Barka et al. 2016). Other *bld* genes such as *bldD*, *bldG* and *bldH* were recently shown to control the expression of *cfaR* and/or *cfaI* in *S. scabies* (Fig. 6B) (Bignell et al. 2014).

Biological activities and mode of action

Studies on the biological activity of coronafacoyl phytotoxins have mainly focused on COR, which is the most toxic family member (Bender et al. 1999). One of the most obvious effects of COR is the induction of diffuse chlorosis in various plants, including soybean [*Glycine max*; (Gnanamanickam et al. 1982)], tomato [*Lycopersicon esculentum*; (Uppalapati et al. 2005)] and *Nicotiana benthamiana* (Worley et al. 2013). In *Arabidopsis thaliana* and tomato, COR promotes anthocyanin accumulation and inhibits root elongation (Bent et al. 1992; Uppalapati et al. 2005; Ichihara and Toshima 1999). It also induces hypertrophy of potato tuber tissue (Gnanamanickam et al. 1982; Sakai et al. 1979; Volksch et al. 1989) and it stimulates ethylene production in bean (*Phaseolus vulgaris* L.) and tobacco (*Nicotiana tabacum*) leaves (Ferguson and Mitchell 1985; Kenyon and Turner 1992). Other effects attributed to COR include cell wall thickening, changes in chloroplast structure and accumulation of proteinase inhibitors (Uppalapati et al. 2005; Palmer and Bender 1995). Related phytotoxins such as CFA-Ile and CFA-Val are also biologically active and can induce chlorosis, inhibit root elongation and stimulate potato tuber tissue hypertrophy, though they are not as active as COR in inducing these effects (Fyans et al.

2015; Mitchell 1984; Mitchell and Young 1985; Shiraishi et al. 1979; Uppalapati et al. 2005). In contrast, CFA alone exhibits very little to no biological activity (Shiraishi et al. 1979; Uppalapati et al. 2005) indicating that the attached amino acid is necessary for the observed effects of coronafacoyl phytotoxins.

Several studies have demonstrated that COR is an important virulence factor in *Pseudomonas* spp. COR – deficient Tn5 mutants were shown to still be pathogenic; however, they produced little or no chlorosis and smaller necrotic lesions, and their population sizes were significantly lower *in planta* as compared to COR – producing strains (Bender 1999). It was noted early on by several research groups that COR is structurally similar to the plant hormone jasmonic acid (JA), and more specifically the L-isoleucine conjugate of JA (JA-Ile), which is the most bioactive form (Fonseca et al. 2009; Staswick 2008). JA is a critical phytohormone that is responsible for regulating various biological processes in plants, including defence against necrotrophic pathogens and herbivores (Wasternack and Hause 2013). COR and JA induce similar responses in plants and regulate similar genes, and an *Arabidopsis coi1* (*coronatine insensitive 1*) mutant was shown to be insensitive to both COR and JA (Xin and He 2013). Together, this suggested that COR and JA share a similar mode of action. COI1 is the F-box component of SCF^{COI1}, a member of the Skip/Cullin/F-box (SCF) family of E3 ubiquitin ligases that target proteins for degradation by the 26S proteasome (Staswick 2008). JA-Ile promotes the binding of COI1 to several members of the JAZ (jasmonate ZIM – domain) family of repressor proteins, thereby leading to degradation of the JAZ repressors and activation of JA responsive genes (Chini et al. 2007; Katsir et al. 2008; Melotto et al. 2008a; Thines et al. 2007). Intriguingly,

COR also promotes the formation of COI1-JAZ complexes *in vitro*, but it is ~ 1000 times more active than JA-Ile at promoting this interaction (Katsir et al. 2008). JA-Ile can compete with COR for binding to the COI1-JAZ complexes, and a crystal structure of the COI1-JAZ complex showed that JA-Ile and COR bind to the same ligand binding pocket, indicating that COR functions as a molecular mimic of JA-Ile (Katsir et al. 2008; Sheard et al. 2010). Activation of JA signalling by COR leads to suppression of the salicylic acid (SA) – mediated signalling pathway, which is important for regulating plant defence against biotrophic and hemibiotrophic pathogens like *P. syringae* (Xin and He 2013). More recently, COR was also shown to suppress callose deposition in an SA – independent manner, and it enables bacterial entry into the plant host by overcoming stomatal defenses (Geng et al. 2012; Melotto et al. 2008b). Thus, COR contributes significantly to the virulence of *Pseudomonas* spp. by facilitating host invasion, by promoting bacterial multiplication within the plant through suppression of both SA – dependent and SA – independent defense responses, and by contributing directly to disease symptom development.

Currently, it is not clear whether other members of the coronafacoyl phytotoxin family also contribute to host invasion and/or suppression of plant defense responses during pathogen infection. The structural similarity between JA-Ile and other family members such as CFA-Ile, together with similarities in biological activity between COR and its relatives suggests that they may also function as JA-Ile mimics and induce JA – responsive genes in a COI1 – dependent manner, though likely not with the same efficiency as COR. There is evidence that COR may have additional targets within plant cells other than COI1 (Geng et al. 2012), and the same may apply to the related compounds. Studies of *cfa*

mutants of both *P. atrosepticum* and *S. scabies* have indicated that the resulting coronafacoyl phytotoxins contribute to the virulence phenotype of each organism (Bell et al. 2004; Bignell et al. 2010; Panda et al. 2016), and strains of *P. carotovorum* subsp. *carotovorum* and *Dickeya* spp. harbouring the *cfa/cfl* genes cause more severe disease symptoms than strains that lack these genes (Slawiak and Lojkowska 2009). It therefore appears that the production of COR and COR-like molecules provides an adaptive advantage to a broad range of plant pathogenic bacteria during host colonization and infection, either by stimulating the JA signalling pathway or by interacting with other targets within plant cells. Furthermore, as non-pathogenic bacteria also appear to have the capability to produce coronafacoyl phytotoxins, there are likely additional roles for these metabolites that remain to be discovered.

Evolution of coronafacoyl phytotoxin production

The identification of coronafacoyl phytotoxin biosynthetic genes in phylogenetically distinct bacteria suggests that the production of these compounds is widespread in nature and that horizontal gene transfer has played an important role in the dissemination of the biosynthetic genes. A recent study from our lab attempted to investigate the evolution of coronafacoyl phytotoxin production by examining the genetic architecture and phylogenetic relationships of the CFA biosynthetic gene clusters from different organisms (Bown et al. 2017). A comparison of the gene clusters from members of the *Gammaproteobacteria*, *Alphaproteobacteria* and *Actinobacteria* revealed that the *cfa1-7* and *cfl* genes are conserved among all of the gene clusters, and all but the *cfl* gene were found in the identical arrangement in each gene cluster. Differences were observed

with regards to the presence or absence of other genes, including the CCR – encoding *cfa8* gene and the thioesterase – encoding *cfa9* (Bown et al. 2017). The actinobacterial gene clusters were all found to contain homologues of the *cfaR* and *orf1* regulatory genes as well as the *oxr* and *CYP107AK1* biosynthetic genes from *S. scabies*, and at least one gene cluster additionally contained homologues of *SCAB79711* and *sdr*. Quite possibly, these genes represent subclusters that were recently joined to an ancestral core gene cluster given that they are only found within the actinobacterial CFA biosynthetic gene clusters (Bown et al. 2017). Phylogenetic analysis of the core (*cfa1-7*, *cfl*) biosynthetic genes indicated that the *S. scabies* gene cluster is most closely related to the other actinobacterial gene clusters, and in turn these gene clusters share a common ancestor with the identified cluster from *Azospirillum* sp. B510, an alphaproteobacterium. As further evidence of a close relationship between these clusters, the Cfa7 PKS encoded within these clusters all contain the ER domain that was first identified in the *S. scabies* Cfa7 (Fig. 5), whereas none of the Cfa7 proteins identified from the *Gammaproteobacteria* contain this domain (Bown et al. 2017). The phylogenetic analysis also indicated that the *Pseudomonas* core biosynthetic genes form a distinct clade that shares a common ancestor with the actinobacterial and *Azospirillum* sp. B510 gene clusters (Bown et al. 2017). Analysis of the GC content of the *Pseudomonas* core *cfa/cfl* genes indicated that most of the genes have a significantly higher GC content than the average GC content of the corresponding genomes (Online Resource 1), suggesting that the genes in the pseudomonads may have originated from an actinobacterium or another high GC organism. Although the *cfa/cfl* genes could be identified in phylogenetically distinct bacteria, the *cma* genes were only found in a small subset of known or predicted CFA producers (Bown et al. 2017). This may indicate that

the ability to produce CMA and COR is a more recently acquired trait, a notion that has been suggested previously (Mitchell 1991).

How were the coronafacoyl phytotoxin biosynthetic genes acquired by different bacteria? It was noted early on that the *cfa/cfl* genes in different *Pseudomonas* spp. are localized together with the *cma* genes on large (80 - 100 kb) indigenous plasmids of the pT23A family, which are readily transferred between different strains by conjugation (Bender et al. 1999; Sundin 2007). In *P. syringae* pv *tomato* DC3000, the *cfa/cfl* genes are chromosomally localized and are separated from the *cma* genes by 26 kb, and both regions are rich in mobile genetic elements that could allow for gene transfer (Gross and Loper 2009). Similarly, an analysis of the *S. scabies* 87-22 genome sequence has indicated the presence of mobile genetic elements in the vicinity of *cfa/cfl* genes (Z. Cheng and D. Bignell, unpublished). The *cfa/cfl* genes in *P. atrosepticum* and in blackleg – causing *P. carotovorum* strains are located on a putative horizontally acquired island, HAI2, which is an integrative and conjugative element (Bell et al. 2004; Panda et al. 2016). Studies have shown that HAI2 can excise from the chromosome at low frequency, including *in planta*, providing a means for lateral transfer of the genes that it harbours (Panda et al. 2016; Vanga et al. 2012; Vanga et al. 2015).

Detection of coronafacoyl phytotoxins and toxin – producing organisms

A qualitative bioassay for detecting COR and other coronafacoyl phytotoxins in culture filtrates has been described that makes use of the chlorosis – inducing activity of these compounds in various plants (Gnanamanickam et al. 1982). In addition, the hypertrophy – inducing activity of coronafacoyl phytotoxins on potato tuber tissue has been

used in numerous studies for detecting these compounds and characterizing the activity of biosynthetic intermediates (Fig. 7) (Bown et al. 2016; Bown et al. 2017; Fyans et al. 2015; Gnanamanickam et al. 1982; Valenzuela-Soto et al. 2015). Völksch et al. (1989) demonstrated that the observed hypertrophy – inducing activity could be developed into a semi-quantitative assay for detecting COR in culture filtrates (Völksch et al. 1989). As little as 0.8 nmol of COR can be detected using this bioassay (Fig. 7), though it has been noted that there can be some variability in the hypertrophy response depending on the potato cultivar that is used and the age of the tissue (Bender et al. 1999). Also, the activity of other coronafacoyl phytotoxins in comparison to COR is significantly less in both the chlorosis – inducing bioassay and the hypertrophy – inducing bioassay (Fig. 7) (Fyans et al. 2015; Uppalapati et al. 2005), which reflects the fact that COR is the most toxic family member.

Analytical methods involving small – scale extraction of culture supernatants and HPLC – based detection of coronafacoyl phytotoxin production have been described (Fyans et al. 2015; Panchal et al. 2017). Extractions are typically performed using 0.5 – 1 ml of acidified culture supernatants and either ethyl acetate or chloroform, and the compounds are separated from other components of the extract using a C8 or C18 reverse phase column with a detection wavelength of 208 – 230 nm. Such methods allow for absolute quantitative analysis of phytotoxin production when a standard curve is generated using known amounts of the target compound (Panchal et al. 2017), or relative quantitative analysis when comparing the phytotoxin peak area in a mutant strain with that from a wild-type strain (Bown et al. 2016; Bown et al. 2017; Fyans et al. 2015). Jones and colleagues developed an indirect competitive ELISA assay using monoclonal antibodies specific for COR. The

assay was able to quantify COR with a detection limit of 1 ng/ml and could also detect CFA-Val with similar efficiency and CFA-Ile and CFA-*a*Ile with less efficiency (Jones et al. 1997). More recently, Schmeltz and colleagues described a metabolic profiling approach using vapor phase extraction and GC-MS for directly quantifying COR in *P. syringae* – infected plant tissues. The method requires very little plant material and can be used to simultaneously quantify numerous interacting phytohormones and phytotoxins in plants (Schmelz et al. 2003).

Molecular approaches such as PCR and Southern analysis have been used to detect *Pectobacterium* spp., *Dickeya* spp. and *Streptomyces* spp. that are capable of producing coronafacoyl phytotoxins (Bignell et al. 2010; Slawiak and Lojkowska 2009). Such approaches involved the use of PCR primers or DNA probes specific for the *cfa6*, *cfa7* genes and *cfl* genes (Fig. 2). With the advent of inexpensive next generation sequencing technologies, the search for coronafacoyl phytotoxin producers has now become much easier as entire genome sequences can now be screened for the presence of the CFA and CMA biosynthetic gene clusters. This has led to the identification of bacteria that were not previously known to produce coronafacoyl phytotoxins, including several non-pathogenic species (Table 1) (Bown et al. 2017).

Concluding remarks

Although much has been learned about the coronafacoyl phytotoxin family since the discovery of COR, there are still many interesting questions that remain to be explored. For example, while most predicted coronafacoyl phytotoxin producers cannot make COR due to the absence of the *cma* genes, it is still unclear which specific family members are

made by these organisms. Is there a preference for the production of CFA-Ile and/or CFA-Val over other family members in the absence of CMA, as observed in *S. scabies*? Also, is there an ecological explanation for why COR production appears to be limited to a relatively small number of coronafacoyl phytotoxin producers? There are additionally unanswered questions regarding the coronafacoyl phytotoxin biosynthetic pathway, which largely remains hypothetical in *Pseudomonas* spp. and in other organisms. The role of several genes within the *cfa/cfl* gene cluster have yet to be verified using genetic and/or biochemical approaches. In *S. scabies*, we are particularly interested in whether the ER domain of Cfa7 is active given its absence in the *Pseudomonas* Cfa7 homologs, as well as the precise function of Oxr in the biosynthesis of CFA-Ile. Also, the role of Orf1 in the regulation of CFA-Ile biosynthesis is the subject of ongoing research in our lab. It remains to be determined whether all coronafacoyl phytotoxins function as suppressors of plant defense responses by behaving as JA mimics, or whether there are other roles for these compounds in plant cells. Finally, it will be interesting to establish whether non-pathogenic bacteria can produce coronafacoyl phytotoxins and what role(s) the metabolites play for these organisms. It is noteworthy that at least three of the non-pathogenic organisms that harbour the phytotoxin biosynthetic genes (*Pseudomonas psychrotolerans*, *Azospirillum* sp. B510, *Zymobacter palmae*) are known to be associated with plants, and one (*Azospirillum* sp. B510) has been reported to promote rice plant growth and resistance to fungal and bacterial pathogens (Kaneko et al. 2010; Midha et al. 2016; Okamoto et al. 1993). It is intriguing to speculate that coronafacoyl phytotoxin production by these organisms may contribute to beneficial interactions with plants rather than toxic interactions, an idea worth investigating further.

Compliance with ethical standards

Funding: D.R.D. Bignell acknowledges support from the Natural Science and Engineering Research Council of Canada Discovery Grants program (grant no. 386696-2010), the Canada Foundation for Innovation Leaders Opportunity Fund (project no. 30482) and the Newfoundland and Labrador Research and Development Corporation Leverage R&D program (project no. 5404.1218.103).

Conflict of interest: The authors declare that they have no conflict of interest.

References

- Anton N, Santos-Aberturas J, Mendes MV, Guerra SM, Martin JF , Aparicio JF (2007) PimM, a PAS domain positive regulator of pimarin biosynthesis in *Streptomyces natalensis*. Microbiology 153: 3174-3183.
- Baltrus DA, Nishimura MT, Romanchuk A, Chang JH, Mukhtar MS, Cherkis K, Roach J, Grant SR, Jones CD , Dangel JL (2011) Dynamic evolution of pathogenicity revealed by sequencing and comparative genomics of 19 *Pseudomonas syringae* isolates. PLOS Pathogens 7: e1002132.
- Barka EA, Vatsa P, Sanchez L, Gaveau-Vaillant N, Jacquard C, Klenk HP, Clement C, Ouhdouch Y , Van Wezel GP (2016) Taxonomy, physiology, and natural products of *Actinobacteria*. Microbiol Mol Biol Rev 80: 1-43.
- Bell KS, Sebaihia M, Pritchard L, Holden MT, Hyman LJ, Holeva MC, Thomson NR, Bentley SD, Churcher LJ, Mungall K, Atkin R, Bason N, Brooks K, Chillingworth

- T, Clark K, Doggett J, Fraser A, Hance Z, Hauser H, Jagels K, Moule S, Norbertczak H, Ormond D, Price C, Quail MA, Sanders M, Walker D, Whitehead S, Salmond GP, Birch PR, Parkhill J , Toth IK (2004) Genome sequence of the enterobacterial phytopathogen *Erwinia carotovora* subsp. *atroseptica* and characterization of virulence factors. Proc Natl Acad Sci U S A 101: 11105-11110.
- Bender CL (1999) Chlorosis-inducing phytotoxins produced by *Pseudomonas syringae*. Eur J Plant Pathol 105: 1-12.
- Bender CL, Alarcon-Chaidez F , Gross DC (1999) *Pseudomonas syringae* phytotoxins: mode of action, regulation, and biosynthesis by peptide and polyketide synthetases. Microbiol Mol Biol Rev 63: 266-292.
- Bent AF, Innes RW, Ecker JR , Staskawicz BJ (1992) Disease development in ethylene-insensitive *Arabidopsis thaliana* infected with virulent and avirulent *Pseudomonas* and *Xanthomonas* pathogens. Mol Plant-Microbe Interact 5: 372-378.
- Bignell DRD, Francis IM, Fyans JK , Loria R (2014) Thaxtomin A production and virulence are controlled by several *bld* gene global regulators in *Streptomyces scabies*. Mol Plant-Microbe Interact 27: 875-885.
- Bignell DRD, Seipke RF, Huguet-Tapia JC, Chambers AH, Parry R , Loria R (2010) *Streptomyces scabies* 87-22 contains a coronafacic acid-like biosynthetic cluster that contributes to plant-microbe interactions. Mol Plant-Microbe Interact 23: 161-175.
- Boch J, Joardar V, Gao L, Robertson TL, Lim M , Kunkel BN (2002) Identification of *Pseudomonas syringae* pv. *tomato* genes induced during infection of *Arabidopsis thaliana*. Mol Microbiol 44: 73-88.

- Bown L, Altowairish MS, Fyans JK , Bignell DRD (2016) Production of the *Streptomyces scabies* coronafacoyl phytotoxins involves a novel biosynthetic pathway with an F₄₂₀ - dependent oxidoreductase and a short-chain dehydrogenase/reductase. Mol Microbiol 101: 122-135.
- Bown L, Li Y, Berrue F, Verhoeven JTP, Dufour SC , Bignell DRD (2017) Coronafacoyl phytotoxin biosynthesis and evolution in the common scab pathogen *Streptomyces scabies*. Appl Environ Microbiol 83: e01169-01117.
- Brady CL, Cleenwerck I, Denman S, Venter SN, Rodriguez-Palenzuela P, Coutinho TA , De Vos P (2012) Proposal to reclassify *Brenneria quercina* (Hildebrand and Schroth 1967) Hauben et al. 1999 into a new genus, *Lonsdalea* gen. nov., as *Lonsdalea quercina* comb. nov., descriptions of *Lonsdalea quercina* subsp. *quercina* comb. nov., *Lonsdalea quercina* subsp. *iberica* subsp. nov. and *Lonsdalea quercina* subsp. *britannica* subsp. nov., emendation of the description of the genus *Brenneria*, reclassification of *Dickeya dieffenbachiae* as *Dickeya dadantii* subsp. *dieffenbachiae* comb. nov., and emendation of the description of *Dickeya dadantii*. Int J Syst Evol Microbiol 62: 1592-1602.
- Braun Y, Smirnova AV, Weingart H, Schenk A , Ullrich MS (2007) A temperature-sensing histidine kinase: function, genetics, and membrane topology. Methods Enzymol 423: 222-249.
- Budde IP, Rohde BH, Bender CL , Ullrich MS (1998) Growth phase and temperature influence promoter activity, transcript abundance, and protein stability during biosynthesis of the *Pseudomonas syringae* phytotoxin coronatine. J Bacteriol 180: 1360-1367.

- Bull CT, Manceau C, Lydon J, Kong H, Vinatzer BA , Fischer-Le Saux M (2010) *Pseudomonas cannabina* pv. *cannabina* pv. nov., and *Pseudomonas cannabina* pv. *alisalensis* (Cintas Koike and Bull, 2000) comb. nov., are members of the emended species *Pseudomonas cannabina* (ex Sutic & Dowson 1959) Gardan, Shafik, Belouin, Brosch, Grimont & Grimont 1999. Syst Appl Microbiol 33: 105-115.
- Chan YA, Podevels AM, Kevany BM , Thomas MG (2009) Biosynthesis of polyketide synthase extender units. Nat Prod Rep 26: 90-114.
- Chater KF (2006) *Streptomyces* inside-out: a new perspective on the bacteria that provide us with antibiotics. Philos Trans R Soc Lond B Biol Sci 361: 761-768.
- Cheng Z, Bown L, Tahlan K , Bignell DRD (2015) Regulation of coronafacoyl phytotoxin production by the PAS-LuxR family regulator CfaR in the common scab pathogen *Streptomyces scabies*. PLOS ONE 10: e0122450.
- Chini A, Fonseca S, Fernandez G, Adie B, Chico JM, Lorenzo O, Garcia-Casado G, Lopez-Vidriero I, Lozano FM, Ponce MR, Micol JL , Solano R (2007) The JAZ family of repressors is the missing link in jasmonate signalling. Nature 448: 666-671.
- Cintas NA, Koike ST , Bull CT (2002) A new pathovar, *Pseudomonas syringae* pv. *alisalensis* pv. nov., proposed for the causal agent of bacterial blight of broccoli and broccoli raab. Plant Dis 86: 992-998.
- Couch R, O'connor SE, Seidle H, Walsh CT , Parry R (2004) Characterization of CmaA, an adenylation-thiolation didomain enzyme involved in the biosynthesis of coronatine. J Bacteriol 186: 35-42.
- Ferguson IB , Mitchell RE (1985) Stimulation of ethylene production in bean leaf discs by the pseudomonad phytotoxin coronatine. Plant Physiol 77: 969-973.

- Fonseca S, Chini A, Hamberg M, Adie B, Porzel A, Kramell R, Miersch O, Wasternack C, Solano R (2009) (+)-7-iso-Jasmonoyl-L-isoleucine is the endogenous bioactive jasmonate. *Nature Chem Biol* 5: 344-350.
- Fuqua WC, Winans SC, Greenberg EP (1994) Quorum sensing in bacteria: the LuxR-LuxI family of cell density-responsive transcriptional regulators. *J Bacteriol* 176: 269-275.
- Fyans JK, Altowairish MS, Li Y, Bignell DRD (2015) Characterization of the coronatine-like phytotoxins produced by the common scab pathogen *Streptomyces scabies*. *Mol Plant-Microbe Interact* 28: 443-454.
- Gardan L, Gouy C, Christen R, Samson R (2003) Elevation of three subspecies of *Pectobacterium carotovorum* to species level: *Pectobacterium atrosepticum* sp. nov., *Pectobacterium betavascularum* sp. nov. and *Pectobacterium wasabiae* sp. nov. *Int J Syst Evol Microbiol* 53: 381-391.
- Gardan L, Shafik H, Belouin S, Broch R, Grimont F, Grimont PA (1999) DNA relatedness among the pathovars of *Pseudomonas syringae* and description of *Pseudomonas tremiae* sp. nov. and *Pseudomonas cannabina* sp. nov. (ex Sutic and Dowson 1959). *Int J Syst Bacteriol* 49 Pt 2: 469-478.
- Geng X, Cheng J, Gangadharan A, Mackey D (2012) The coronatine toxin of *Pseudomonas syringae* is a multifunctional suppressor of Arabidopsis defense. *Plant Cell* 24: 4763-4774.
- Gnanamanickam SS, Starratt AN, Ward EWB (1982) Coronatine production *in vitro* and *in vivo* and its relation to symptom development in bacterial blight of soybean. *Can J Bot* 60: 645-650.

- Gross H , Loper JE (2009) Genomics of secondary metabolite production by *Pseudomonas* spp. Nat Prod Rep 26: 1408-1446.
- Han HS, Koh YJ, Hur JS , Jung JS (2003) Identification and characterization of coronatine-producing *Pseudomonas syringae* pv *actinidiae*. J Microbiol Biotechnol 13: 110-118.
- Hauser E, Kampfer P , Busse HJ (2004) *Pseudomonas psychrotolerans* sp. nov. Int J Syst Evol Microbiol 54: 1633-1637.
- Ichihara A, Shiraishi K, Sato H, Sakamura S, Nishiyama K, Sakai R, Furusaki A , Matsumoto T (1977) The structure of coronatine. J Am Chem Soc 99: 636-637.
- Ichihara A , Toshima H (1999) Coronatine: chemistry and biological activities. In: CUTLER, H. G. & CUTLER, S. J. (eds) Biologically Active Natural Products: Agrochemicals. CRC Press.
- Jeong H, Kloepper JW , Ryu CM (2015) Genome Sequences of *Pseudomonas amygdali* pv. *tabaci* Strain ATCC 11528 and pv. *lachrymans* Strain 98A-744. Genome Announcements 3.
- Jones WT, Harvey D, Mitchell RE, Ryan GB, Bender CL , Reynolds PH (1997) Competitive ELISA employing monoclonal antibodies specific for coronafacoyl amino acid conjugates. Food Agr Immunol 9: 67-76.
- Kaneko T, Minamisawa K, Isawa T, Nakatsukasa H, Mitsui H, Kawaharada Y, Nakamura Y, Watanabe A, Kawashima K, Ono A, Shimizu Y, Takahashi C, Minami C, Fujishiro T, Kohara M, Katoh M, Nakazaki N, Nakayama S, Yamada M, Tabata S , Sato S (2010) Complete genomic structure of the cultivated rice endophyte *Azospirillum* sp. B510. DNA Res 17: 37-50.

- Katsir L, Schilmiller AL, Staswick PE, He SY , Howe GA (2008) COI1 is a critical component of a receptor for jasmonate and the bacterial virulence factor coronatine. *Proc Natl Acad Sci U S A* 105: 7100-7105.
- Kelly WL, Boyne MT, 2nd, Yeh E, Vosburg DA, Galonic DP, Kelleher NL , Walsh CT (2007) Characterization of the aminocarboxycyclopropane-forming enzyme CmaC. *Biochemistry* 46: 359-368.
- Kenyon JS , Turner JG (1992) The stimulation of ethylene synthesis in *Nicotiana tabacum* leaves by the phytotoxin coronatine. *Plant Physiol* 100: 219-224.
- Li XZ, Starratt AN , Cuppels DA (1998) Identification of tomato leaf factors that activate toxin gene expression in *Pseudomonas syringae* pv. *tomato* DC3000. *Phytopathology* 88: 1094-1100.
- Liyanage H, Palmer DA, Ullrich M , Bender CL (1995) Characterization and transcriptional analysis of the gene cluster for coronafacic acid, the polyketide component of the phytotoxin coronatine. *Appl Environ Microbiol* 61: 3843-3848.
- Ma S-W, Morris VL , Cuppels DA (1991) Characterization of a DNA region required for production of the phytotoxin coronatine by *Pseudomonas syringae* pv. *tomato*. *Mol Plant Microbe Interact* 4: 69-74.
- Melotto M, Mecey C, Niu Y, Chung HS, Katsir L, Yao J, Zeng W, Thines B, Staswick P, Browse J, Howe GA , He SY (2008a) A critical role of two positively charged amino acids in the Jas motif of Arabidopsis JAZ proteins in mediating coronatine- and jasmonoyl isoleucine-dependent interactions with the COI1 F-box protein. *Plant J* 55: 979-988.

- Melotto M, Underwood W, He SY (2008b) Role of stomata in plant innate immunity and foliar bacterial diseases. *Annu Rev Phytopathol* 46: 101-122.
- Midha S, Bansal K, Sharma S, Kumar N, Patil PP, Chaudry V, Patil PB (2016) Genomic resource of rice seed associated bacteria. *Front Microbiol* 6: 1551.
- Mitchell RE (1984) A naturally-occurring structural analogue of the phytotoxin coronatine. *Phytochemistry* 23: 791-793.
- Mitchell RE (1991) Implications of toxins in the ecology and evolution of plant pathogenic microorganisms bacteria. *Experientia* 47: 791-803.
- Mitchell RE , Young H (1985) *N*-coronafacoyl-L-isoleucine and *N*-coronafacoyl-L-alloisoleucine, potential biosynthetic intermediates of the phytotoxin coronatine. *Phytochemistry* 24: 2716-2717.
- Nishiyama K, Sakai R, Ezuka A, Ichihara A, Shiraishi K, Ogaswara M, Sato H, Sakamura S (1976) Phytotoxic effects of coronatine produced by *Pseudomonas coronafaciens* var. *atropurpurea* on leaves of Italian ryegrass. *Ann Phytopath Soc Jpn* 42: 613-614.
- Okamoto T, Taguchi H, Nakamura K, Ikenaga H, Kuraishi H, Yamasato K (1993) *Zymobacter palmae* gen. nov., sp. nov., a new ethanol-fermenting peritrichous bacterium isolated from palm sap. *Arch Microbiol* 160: 333-337.
- Palmer DA , Bender CL (1993) Effects of environmental and nutritional factors on production of the polyketide phytotoxin coronatine by *Pseudomonas syringae* pv. *glycinea*. *Appl Environ Microbiol* 59: 1619-1626.

- Palmer DA , Bender CL (1995) Ultrastructure of tomato leaf tissue treated with the pseudomonad phytotoxin coronatine and comparison with methyl jasmonate. *Mol Plant Microbe Interact* 8: 683-692.
- Panchal S, Breitbach ZS , Melotto M (2017) An HPLC-based method to quantify coronatine produced by bacteria. *Bio-Protocol* 7: e2147.
- Panda P, Vanga BR, Lu A, Fiers M, Fineran PC, Butler R, Armstrong K, Ronson CW , Pitman AR (2016) *Pectobacterium atrosepticum* and *Pectobacterium carotovorum* harbor distinct, independently acquired integrative and conjugative elements encoding coronafacic acid that enhance virulence on potato stems. *Front Microbiol* 7: 397.
- Pao GM, Tam R, Lipschitz LS , Saier MH, Jr. (1994) Response regulators: structure, function and evolution. *Res Microbiol* 145: 356-362.
- Parry RJ, Jiralerspong S, Mhaskar S, Alemany L , Willcott R (1996) Investigations of coronatine biosynthesis. Elucidation of the mode of incorporation of pyruvate into coronafacic acid. *J Am Chem Soc* 118: 703-704.
- Parry RJ, Mhaskar SV, Lin M-T, Walker AE , Mafoti R (1994) Investigations of the biosynthesis of coronamic acid. *Can J Chem* 72: 86-99.
- Patel J, Hoyt JC , Parry RJ (1998) Investigations of coronatine biosynthesis. Overexpression and assay of CmaT, a thioesterase involved in coronamic acid biosynthesis. *Tetrahedron* 54: 15927-15936.
- Penaloza-Vazquez A , Bender CL (1998) Characterization of CorR, a transcriptional activator which is required for biosynthesis of the phytotoxin coronatine. *J Bacteriol* 180: 6252-6259.

- Penfold CN, Bender CL , Turner JG (1996) Characterisation of genes involved in biosynthesis of coronafacic acid, the polyketide component of the phytotoxin coronatine. *Gene* 183: 167-173.
- Qi M, Wang D, Bradley CA , Zhao Y (2011) Genome sequence analyses of *Pseudomonas savastanoi* pv. *glycinea* and subtractive hybridization-based comparative genomics with nine pseudomonads. *PLOS ONE* 6: e16451.
- Rangaswamy V , Bender CL (2000) Phosphorylation of CorS and CorR, regulatory proteins that modulate production of the phytotoxin coronatine in *Pseudomonas syringae*. *FEMS Microbiol Lett* 193: 13-18.
- Rangaswamy V, Jiralerspong S, Parry R , Bender CL (1998a) Biosynthesis of the *Pseudomonas* polyketide coronafacic acid requires monofunctional and multifunctional polyketide synthase proteins. *Proc Natl Acad Sci U S A* 95: 15469-15474.
- Rangaswamy V, Mitchell R, Ullrich M , Bender C (1998b) Analysis of genes involved in biosynthesis of coronafacic acid, the polyketide component of the phytotoxin coronatine. *J Bacteriol* 180: 3330-3338.
- Rangaswamy V, Ullrich M, Jones W, Mitchell R, Parry R, Reynolds P , Bender CL (1997) Expression and analysis of coronafacate ligase, a thermoregulated gene required for production of the phytotoxin coronatine in *Pseudomonas syringae*. *FEMS Microbiol Lett* 154: 65-72.
- Rohde BH, Pohlack B , Ullrich MS (1998) Occurrence of thermoregulation of genes involved in coronatine biosynthesis among various *Pseudomonas syringae* strains. *J Basic Microbiol* 38: 41-50.

- Sakai R, Nishiyama K, Ichihara A, Shiraishi K , Sakamura S (1979) Studies on the mechanism of physiological activity of coronatine. Effect of coronatine on cell wall extensibility and expansion of potato tuber tissue. *Ann Phytopath Soc Jpn* 45: 645-653.
- Samson R, Legendre JB, Christen R, Fischer-Le Saux M, Achouak W , Gardan L (2005) Transfer of *Pectobacterium chrysanthemi* (Burkholder et al. 1953) Brenner et al. 1973 and *Brenneria paradisiaca* to the genus *Dickeya* gen. nov. as *Dickeya chrysanthemi* comb. nov. and *Dickeya paradisiaca* comb. nov. and delineation of four novel species, *Dickeya dadantii* sp. nov., *Dickeya dianthicola* sp. nov., *Dickeya dieffenbachiae* sp. nov. and *Dickeya zeae* sp. nov. *Int J Syst Evol Microbiol* 55: 1415-1427.
- Santos-Aberturas J, Vicente CM, Guerra SM, Payero TD, Martin JF , Aparicio JF (2011) Molecular control of polyene macrolide biosynthesis: direct binding of the regulator PimM to eight promoters of pimarin genes and identification of binding boxes. *J Biol Chem* 286: 9150-9161.
- Sarris PF, Trantas EA, Baltrus DA, Bull CT, Wechter WP, Yan S, Ververidis F, Almeida NF, Jones CD, Dangl JL, Panopoulos NJ, Vinatzer BA , Goumas DE (2013) Comparative genomics of multiple strains of *Pseudomonas cannabina* pv. *alisalensis*, a potential model pathogen of both monocots and dicots. *PLOS ONE* 8: e59366.
- Schmelz EA, Engelberth J, Alborn HT, O'donnell P, Sammons M, Toshima H , Tumlinson JH, 3rd (2003) Simultaneous analysis of phytohormones, phytotoxins, and volatile organic compounds in plants. *Proc Nat Acad Sci U S A* 100: 10552-10557.

- Sheard LB, Tan X, Mao H, Withers J, Ben-Nissan G, Hinds TR, Kobayashi Y, Hsu FF, Sharon M, Browse J, He SY, Rizo J, Howe GA , Zheng N (2010) Jasmonate perception by inositol-phosphate-potentiated COI1-JAZ co-receptor. *Nature* 468: 400-405.
- Shiraishi K, Konomi K, Sato H, Ichihara A, Sakamura S, Nishiyama K , Sakai R (1979) The structure-activity relationships in coronatine analogs and amino compounds derived from (+)-coronafacic acid. *Agric Biol Chem* 43: 1753-1757.
- Slawiak M , Lojkowska E (2009) Genes responsible for coronatine synthesis in *Pseudomonas syringae* present in the genome of soft rot bacteria. *Eur J Plant Pathol* 124: 353-361.
- Smirnova AV , Ullrich MS (2004) Topological and deletion analysis of CorS, a *Pseudomonas syringae* sensor kinase. *Microbiology* 150: 2715-2726.
- Sreedharan A, Penaloza-Vazquez A, Kunkel BN , Bender CL (2006) CorR regulates multiple components of virulence in *Pseudomonas syringae* pv. *tomato* DC3000. *Mol Plant-Microbe Interact* 19: 768-779.
- Staswick PE (2008) JAZing up jasmonate signaling. *Trends in plant science* 13: 66-71.
- Strange RN (2007) Phytotoxins produced by microbial plant pathogens. *Nat Prod Rep* 24: 127-144.
- Strieter ER, Koglin A, Aron ZD , Walsh CT (2009) Cascade reactions during coronafacic acid biosynthesis: elongation, cyclization, and functionalization during Cfa7-catalyzed condensation. *J Am Chem Soc* 131: 2113-2115.

- Strieter ER, Vaillancourt FH , Walsh CT (2007) CmaE: a transferase shuttling aminoacyl groups between carrier protein domains in the coronamic acid biosynthetic pathway. *Biochemistry* 46: 7549-7557.
- Sundin GW (2007) Genomic insights into the contribution of phytopathogenic bacterial plasmids to the evolutionary history of their hosts. *Annu Rev Phytopathol* 45: 129-151.
- Tamura K, Takikawa Y, Tsuyumu S, Goto M , Watanabe M (1992) Coronatine production by *Xanthomonas campestris* pv. *phormiicola*. *Ann Phytopath Soc Japan* 58: 276-281.
- Taylor BL , Zhulin IB (1999) PAS domains: internal sensors of oxygen, redox potential, and light. *Microbiol Mol Biol Rev* 63: 479-506.
- Thines B, Katsir L, Melotto M, Niu Y, Mandaokar A, Liu G, Nomura K, He SY, Howe GA , Browse J (2007) JAZ repressor proteins are targets of the SCF(COI1) complex during jasmonate signalling. *Nature* 448: 661-665.
- Ullrich M , Bender CL (1994) The biosynthetic gene cluster for coronamic acid, an ethylcyclopropyl amino acid, contains genes homologous to amino acid-activating enzymes and thioesterases. *J Bacteriol* 176: 7574-7586.
- Ullrich M, Penaloza-Vazquez A, Bailey AM , Bender CL (1995) A modified two-component regulatory system is involved in temperature-dependent biosynthesis of the *Pseudomonas syringae* phytotoxin coronatine. *J Bacteriol* 177: 6160-6169.
- Uppalapati SR, Ayoubi P, Weng H, Palmer DA, Mitchell RE, Jones W , Bender CL (2005) The phytotoxin coronatine and methyl jasmonate impact multiple phytohormone pathways in tomato. *Plant J* 42: 201-217.

- Vaillancourt FH, Yeh E, Vosburg DA, O'connor SE , Walsh CT (2005) Cryptic chlorination by a non-haem iron enzyme during cyclopropyl amino acid biosynthesis. *Nature* 436: 1191-1194.
- Valenzuela-Soto JH, Maldonado-Bonilla LD, Hernandez-Guzman G, Rincon-Enriquez G, Martinez-Gallardo NA, Ramirez-Chavez E, Hernandez IC, Hernandez-Flores JL , Delano-Frier JP (2015) Infection by a coronatine-producing strain of *Pectobacterium cacticidum* isolated from sunflower plants in Mexico is characterized by soft rot and chlorosis. *J Gen Plant Pathol* 81: 368-381.
- Vanga BR, Butler RC, Toth IK, Ronson CW , Pitman AR (2012) Inactivation of PbTopo IIIbeta causes hyper-excision of the Pathogenicity Island HAI2 resulting in reduced virulence of *Pectobacterium atrosepticum*. *Mol Microbiol* 84: 648-663.
- Vanga BR, Ramakrishnan P, Butler RC, Toth IK, Ronson CW, Jacobs JM , Pitman AR (2015) Mobilization of horizontally acquired island 2 is induced in planta in the phytopathogen *Pectobacterium atrosepticum*SCRI1043 and involves the putative relaxase ECA0613 and quorum sensing. *Environ Microbiol* 17: 4730-4744.
- Volksch B, Bublit F , Fritsche W (1989) Coronatine production by *Pseudomonas syringae* pathovars: Screening method and capacity of product formation. *J Basic Microbiol* 29: 463-468.
- Wang L, Bender CL , Ullrich MS (1999) The transcriptional activator CorR is involved in biosynthesis of the phytotoxin coronatine and binds to the *cmaABT* promoter region in a temperature-dependent manner. *Mol Gen Genet* 262: 250-260.

- Wasternack C , Hause B (2013) Jasmonates: biosynthesis, perception, signal transduction and action in plant stress response, growth and development. An update to the 2007 review in Annals of Botany. Ann Bot 111: 1021-1058.
- Weingart H, Stubner S, Schenk A , Ullrich MS (2004) Impact of temperature on in planta expression of genes involved in synthesis of the *Pseudomonas syringae* phytotoxin coronatine. Mol Plant Microbe Interact 17: 1095-1102.
- Wilson MC , Moore BS (2012) Beyond ethylmalonyl-CoA: the functional role of crotonyl-CoA carboxylase/reductase homologs in expanding polyketide diversity. Nat Prod Rep 29: 72-86.
- Worley JN, Russell AB, Wexler AG, Bronstein PA, Kvitko BH, Krasnoff SB, Munkvold KR, Swingle B, Gibson DM , Collmer A (2013) *Pseudomonas syringae* pv. tomato DC3000 CmaL (PSPTO4723), a DUF1330 family member, is needed to produce L-*allo*-isoleucine, a precursor for the phytotoxin coronatine. J Bacteriol 195: 287-296.
- Xin XF , He SY (2013) *Pseudomonas syringae* pv. *tomato* DC3000: a model pathogen for probing disease susceptibility and hormone signaling in plants. Annu Rev Phytopathol 51: 473-498.

Figures and Tables

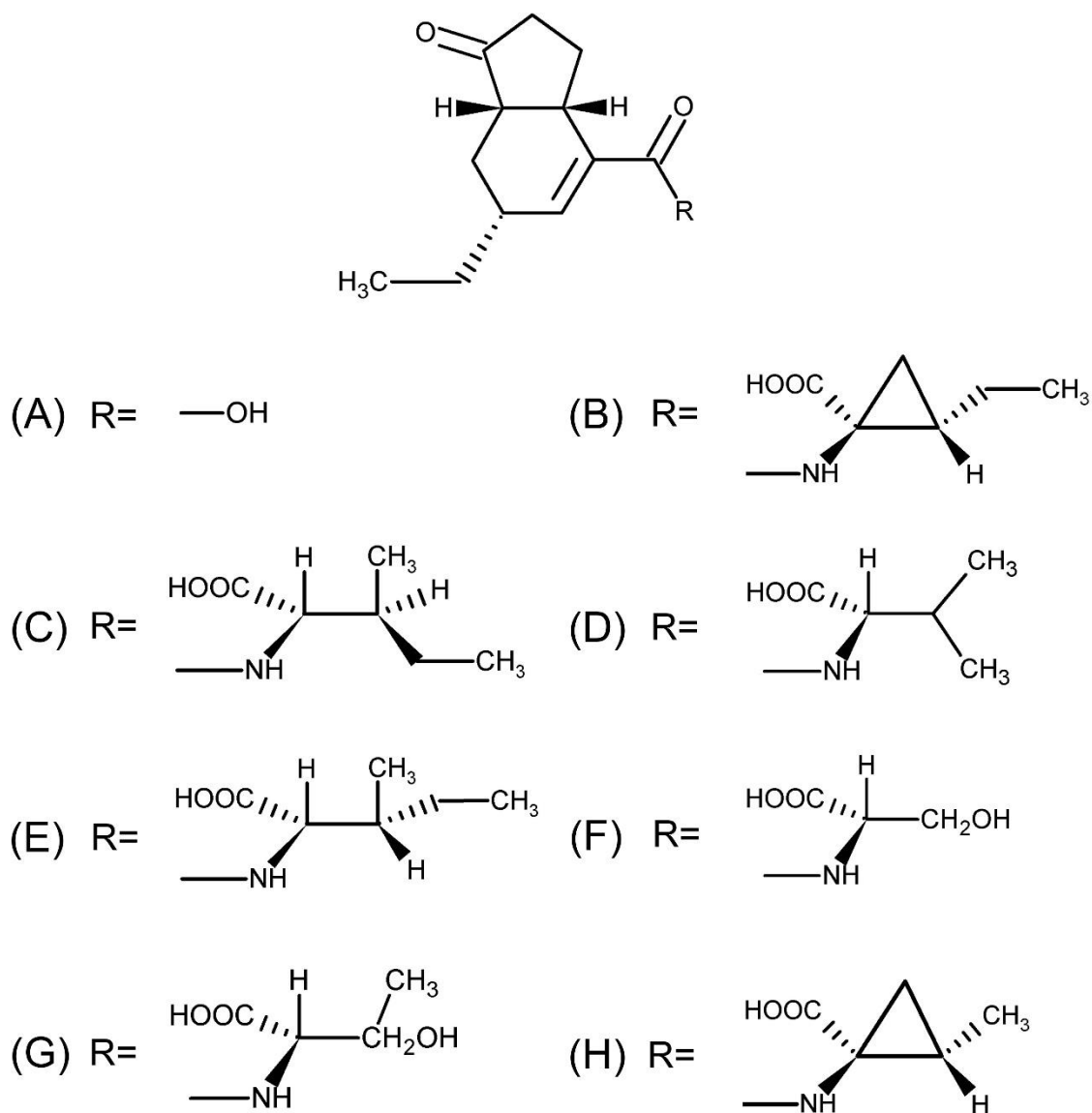


Figure 1. Chemical structure of (A) coronafacic acid (CFA), (B) coronatine (COR), (C) *N*-coronafacoyl-L-isoleucine (CFA-Ile), (D) *N*-coronafacoyl-L-valine (CFA-Val), (E) *N*-

coronafacoyl-L-*allo*-isoleucine (CFA-*alle*), (F) *N*-coronafacoyl-L-serine (CFA-Ser), (G) (D) *N*-coronafacoyl-L-threonine (CFA-Thr) and (G) norcoronatine (norCOR).

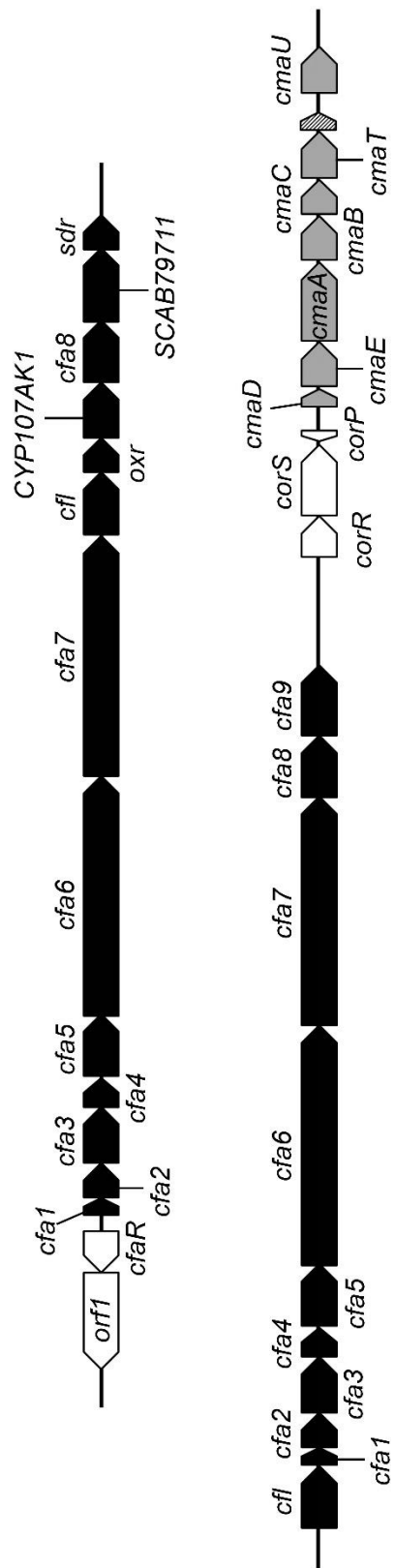


Figure 2. Organization of the gene clusters involved in coronafacoyl phytotoxin biosynthesis in *S. scabies* (top) and *P. savastanoi* pv *glycinea* (bottom). The *cfa/cfl* operon is shown in black, the *cma* operon is in gray, and regulatory genes are in white. The gene within the *cma* operon that is indicated with the hatched lines has not been shown to be involved in CMA biosynthesis.

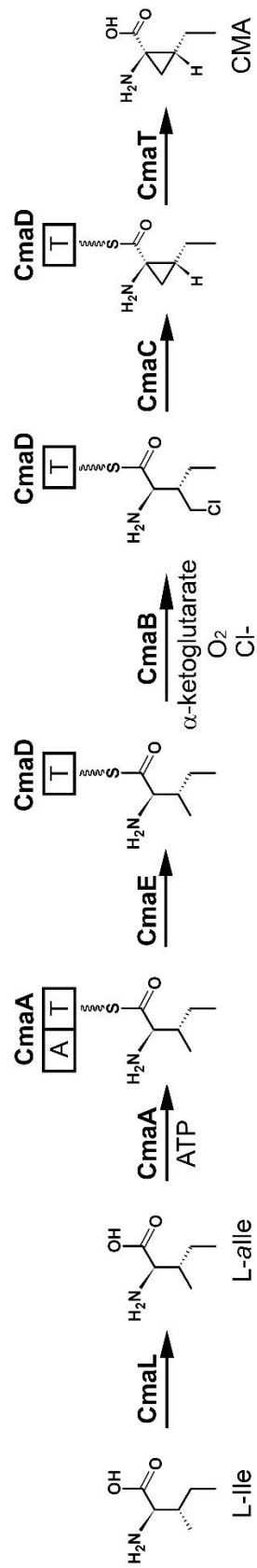


Figure 3. Biosynthetic pathway for production of CMA in *Pseudomonas* spp.

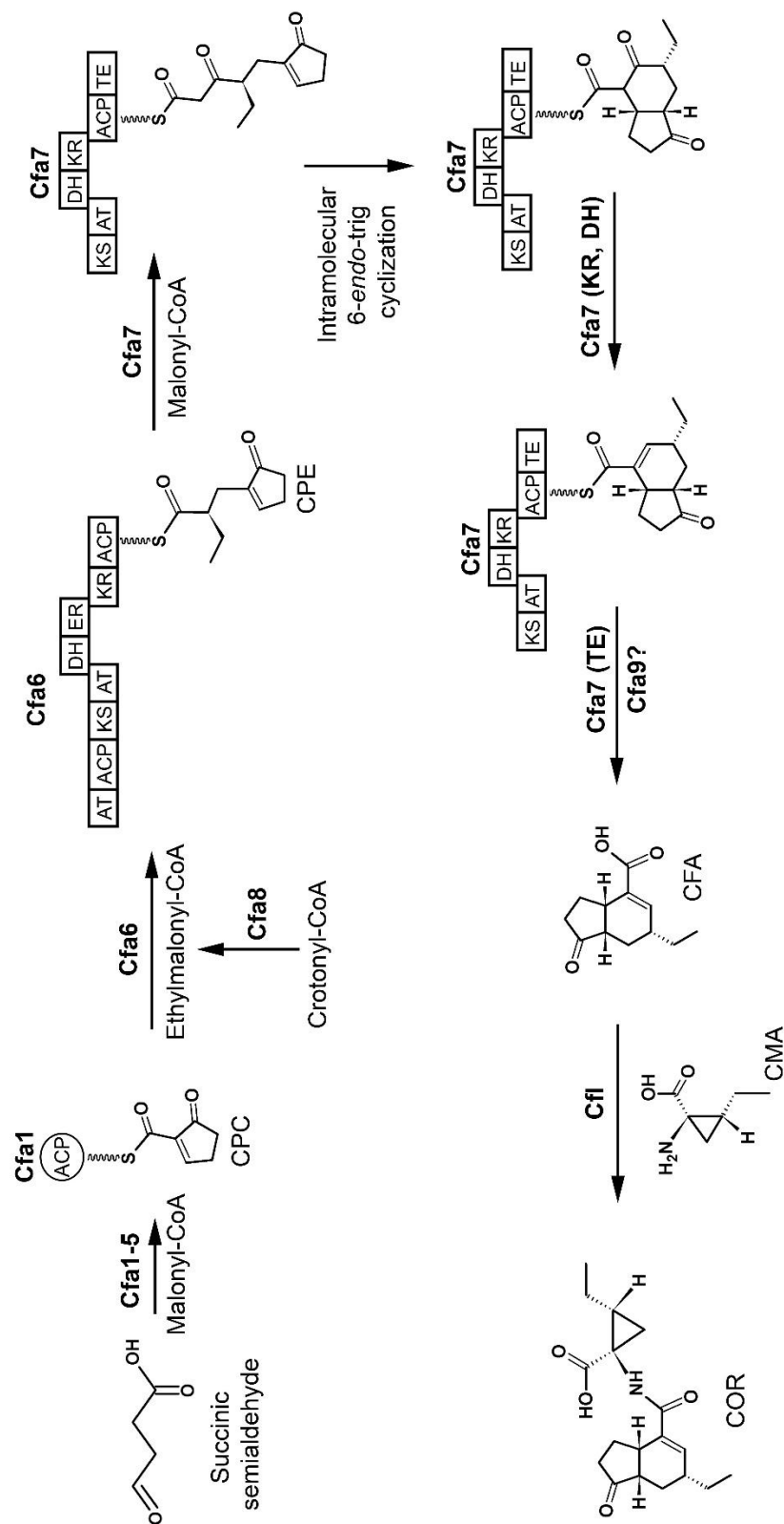


Figure 4. Hypothetic biosynthetic pathway for CFA production and ligation of CFA with CMA to produce COR in *Pseudomonas* spp.

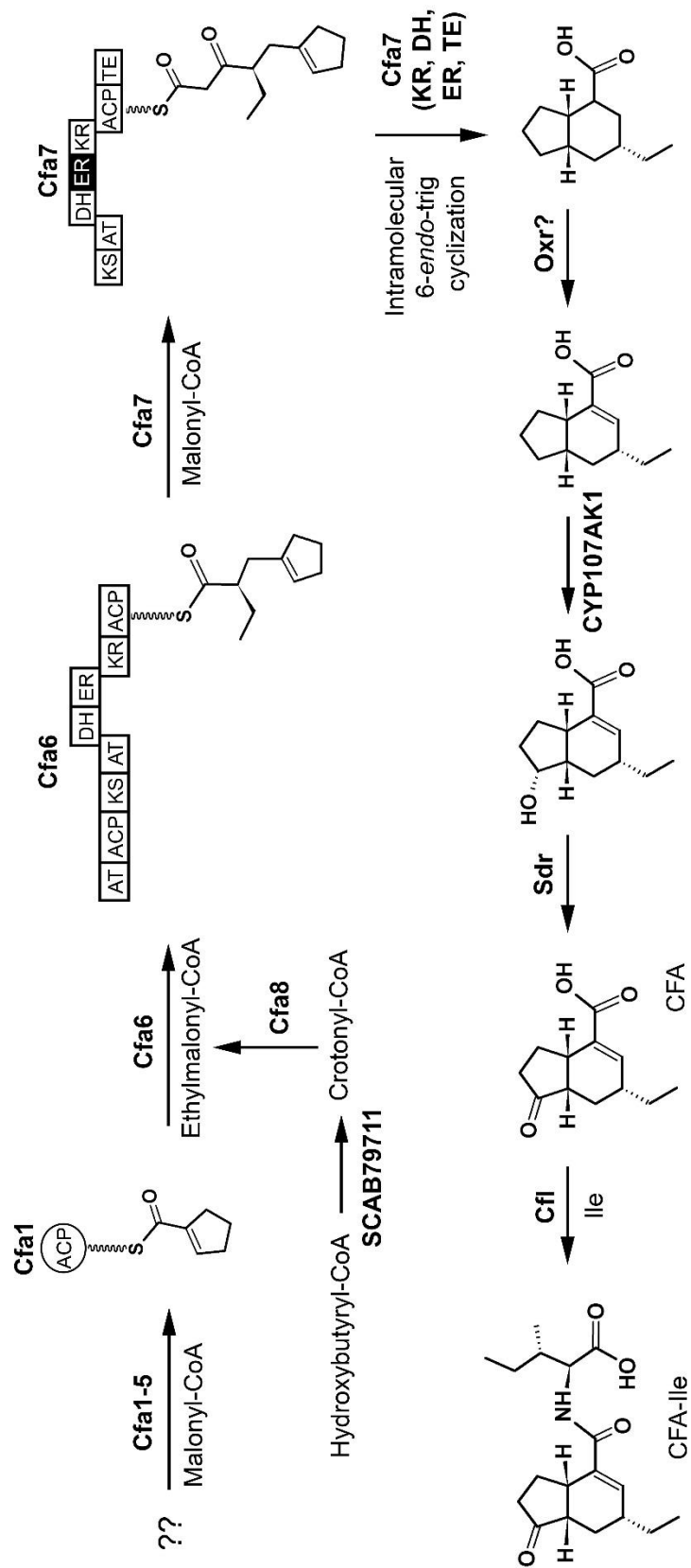


Figure 5. Hypothetical biosynthetic pathway for the production of CFA-Ile in *S. scabies*. The starting precursor may or may not be the same as in *Pseudomonas* spp. and thus is indicated by the question marks. The enoyl reductase (ER) domain that is present in the *S. scabies* Cfa7 and is absent from the Cfa7 homolog in *Pseudomonas* spp. is indicated in black.

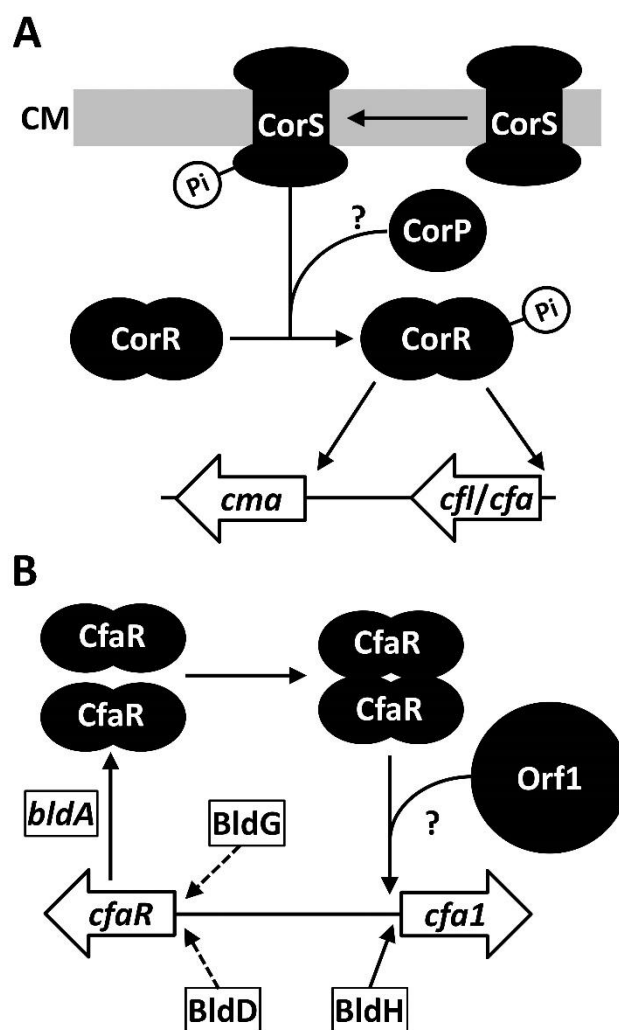


Figure 6. Regulation of coronafacoyl phytotoxin production. (A) The production of COR in *P. savastanoi* pv *glycinea* is regulated by the histidine protein kinase CorS and the response regulators CorR and CorP. CorS is thought to be localized in the cell membrane (CM) and to autophosphorylate in response to changes in temperature. It then transphosphorylates CorR, which in turn activates expression of the *cma* and *cfl/cfa* operons. CorP is required for the activation of CorR by CorS through an unknown

mechanism. (B) The regulation of CFA-Ile production in *S. scabies* involves the PAS-LuxR family regulator CfaR, which binds to the *cfaI* promoter as a dimer and activates expression of the *cfa* operon. The Orf1 protein enhances the activation of CFA-Ile production by CfaR through an unknown mechanism. Several *bld* gene global regulators also modulate the expression of *cfaR* and/or *cfaI*. *bldA* is required for translation of the TTA codon within the *cfaR* coding sequence, while BldD and BldG are predicted to indirectly control the expression of *cfaR*, and BldH is predicted to directly control expression of the *cfaI* promoter (Bignell et al. 2014). Solid arrows in both (A) and (B) are used to indicate direct regulation, while dashed arrows indicate indirect regulation.

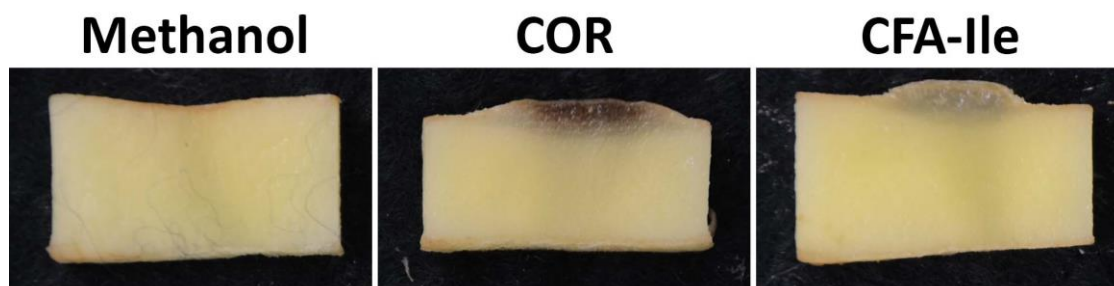


Figure 7. Hypertrophy – inducing activity of coronafacoyl phytotoxins on potato tuber tissue. Tuber disks were treated with pure COR (0.8 nmol), CFA-Ile (16 nmol) or methanol (solvent control).

Table 1. Organisms known or suspected to produce coronafacoyl phytotoxins.

Organism	Subspecies or pathovar	Plant pathogen (host)	Coronafacoyl phytotoxin(s) produced	Reference(s)
<i>Azospirillum</i> sp. B510	NA ^a	No	Unknown, may produce COR due to presence of <i>cfa</i> , <i>cfl</i> and <i>cma</i> genes	(Bown et al. 2017; Kaneko et al. 2010)
<i>Brenneria</i> sp. EniD312	NA	Yes (multiple)	Unknown, harbours <i>cfa</i> genes and <i>cfl</i> , no <i>cma</i> genes present	(Bown et al. 2017; Brady et al. 2012)
<i>Dickeya dadantii</i>	<i>dieffenbachiae</i>	Yes (<i>Dieffenbachia</i> spp)	Unknown, harbours <i>cfa</i> genes and <i>cfl</i> , no <i>cma</i> genes present	(Brady et al. 2012; Samson et al. 2005); this study ^b
<i>Kitasatospora azatica</i>	NA	No	Unknown, harbours <i>cfa</i> genes and <i>cfl</i> , no <i>cma</i> genes present	(Bown et al. 2017)
<i>Lonsdalea quercina</i>	<i>britannica</i> , <i>iberica</i> , <i>quercina</i>	Yes (multiple)	Unknown, harbours <i>cfa</i> genes and <i>cfl</i> , no <i>cma</i> genes present	(Brady et al. 2012); this study ^b
<i>Pectobacterium atrosepticum</i>	NA	Yes (<i>Solanum tuberosum</i>)	Unknown, harbours <i>cfa</i> genes and <i>cfl</i> , no <i>cma</i> genes present	(Bell et al. 2004; Panda et al. 2016; Ślawiak and Lojkowska 2009)
<i>Pectobacterium betavascularum</i>	NA	Yes (<i>Beta vulgaris</i> subsp. <i>vulgaris</i>)	Unknown, harbours <i>cfa</i> genes and <i>cfl</i> , no <i>cma</i> genes present	(Bown et al. 2017; Gardan et al. 2003)
<i>Pectobacterium cacticidum</i>	NA	Yes	COR	(Valenzuela-Soto et al. 2015)
<i>Pectobacterium carotovorum</i>	<i>basiliensis</i> , <i>carotovorum</i> , <i>actinidiae</i>	Yes (multiple)	Unknown, harbours <i>cfa</i> genes and <i>cfl</i> , no <i>cma</i> genes present	(Panda et al. 2016); this study ^b
<i>Pseudomonas amygdali</i>	<i>tabaci</i> , <i>lachrymans</i> , <i>aesculi</i> , <i>ulmi</i> , <i>morsprunorum</i>	Yes (multiple)	COR	(Baltrus et al. 2011; Bender et al. 1999; Gardan et al. 1999; Jeong

				et al. 2015); this study ^b
<i>Pseudomonas cannabina</i>	<i>cannabina</i> , <i>alisalensis</i>	Yes (multiple)	Unknown, may produce COR due to presence of <i>cfa</i> , <i>cfl</i> and <i>cma</i> genes	(Bull et al. 2010; Cintas et al. 2002; Sarris et al. 2013)
<i>Pseudomonas coronafaciens</i>	<i>atropurpurea</i> , <i>porri</i> , <i>zizaniae</i> , <i>oryzae</i>	Yes (multiple)	COR, CFA-Val	(Baltrus et al. 2011; Mitchell 1984; Nishiyama et al. 1976); this study ^b
<i>Pseudomonas psychrotolerans</i>	NA	No	Unknown, may produce COR due to presence of <i>cfa</i> , <i>cfl</i> and <i>cma</i> genes	(Bown et al. 2017; Hauser et al. 2004)
<i>Pseudomonas savastanoi</i>	<i>glycinea</i>	Yes (multiple)	COR, CFA-Val, CFA-Ile, CFA-allo-Ile, CFA-Ser, CFA-Thr, nor COR	(Bender et al. 1999; Qi et al. 2011); this study ^b
<i>Pseudomonas syringae</i>	<i>tomato</i> , <i>maculicola</i> , <i>actinidiae</i> , <i>persicae</i> , <i>berberidis</i> , <i>spinaceae</i>	Yes (multiple)	COR, CFA-Val, CFA-Ser, CFA-Thr	(Bender et al. 1999; Han et al. 2003); this study ^b
<i>Pseudomonas tremae</i>	NA	Yes (<i>Trema orientalis</i>)	Unknown, likely produces COR due to presence of <i>cfa</i> , <i>cfl</i> and <i>cma</i> genes	(Gardan et al. 1999); this study ^b
<i>Streptomyces</i> sp. NRRL WC-3618	NA	No	Unknown, harbours <i>cfa</i> genes and <i>cfl</i> , no <i>cma</i> genes present	(Bown et al. 2017)
<i>Streptomyces graminilatus</i>	NA	No	Unknown, harbours <i>cfa</i> genes and <i>cfl</i> , no <i>cma</i> genes present	This study ^b
<i>Streptomyces griseoruber</i>	NA	No	Unknown, harbours <i>cfa</i> genes and <i>cfl</i> , no <i>cma</i> genes present	(Bown et al. 2017)
<i>Streptomyces scabies</i>	NA	Yes (multiple)	CFA-Ile, other minor compounds	(Fyans et al. 2015)

<i>Xanthomonas campestris</i>	<i>phormiicola</i>	Yes (New Zealand flax)	COR, CFA-Ile, CFA-Val	(Mitchell 1991; Tamura et al. 1992)
<i>Zymobacter palmae</i>	NA	No	Unknown, harbours <i>cfa</i> genes and <i>cfl</i> , no <i>cma</i> genes present	This study ^b

^a NA, not applicable

^b Based on identification of homologues of the *S. scabies* 87-22 and *P. syringae* pv *tomato* DC3000 phytotoxin biosynthetic enzymes using NCBI BlastP

Table 2. Genes and predicted gene function for the CMA and CFA biosynthetic gene clusters in *Pseudomonas* spp. and in *Streptomyces scabies*

Gene	Predicted protein product ^a	Predicted function	Organism
Biosynthetic			
<i>cfa1</i>	Acyl carrier protein (ACP)	Starter unit biosynthesis	conserved
<i>cfa2</i>	Type II fatty acid dehydratase (DH)	Starter unit biosynthesis	conserved
<i>cfa3</i>	Type II β -ketoacyl synthase (KS)	Starter unit biosynthesis	conserved
<i>cfa4</i>	Unknown	Starter unit biosynthesis	conserved
<i>cfa5</i>	Acyl-CoA ligase	Starter unit biosynthesis	conserved
<i>cfa6</i>	Type I PKS	CFA polyketide backbone biosynthesis	conserved
<i>cfa7</i>	Type I PKS	CFA polyketide backbone biosynthesis	conserved
<i>cfa8</i>	Crotonyl-CoA reductase/ carboxylase (CCR)	Ethylmalonyl-CoA biosynthesis	conserved
<i>cfl</i>	Acyl-CoA ligase	Ligation of CFA to amino acid	conserved
<i>SCAB79681/oxr</i>	F ₄₂₀ -dependent oxidoreductase	CFA biosynthesis	<i>S. scabies</i>
<i>SCAB79691/CYP107AK1</i>	P450 monooxygenase	CFA biosynthesis	<i>S. scabies</i>

<i>SCAB79711</i>	Hydroxybutyryl-CoA dehydrogenase	Ethylmalonyl-CoA biosynthesis	<i>S. scabies</i>
<i>SCAB79721/sdr</i>	Short chain dehydrogenase/reductase	CFA biosynthesis	<i>S. scabies</i>
<i>cfa9</i>	Thioesterase	Hydrolysis of thioester bond	<i>Pseudomonas</i> spp.
<i>cmaD</i>	Free standing thiolation (T) protein	Allows formation of cyclopropyl ring	<i>Pseudomonas</i> spp.
<i>cmaE</i>	Aminoacyltransferase	Intermediate shuttle	<i>Pseudomonas</i> spp.
<i>cmaA</i>	NRPS like adenylation-thiolation (A-T) didomain	Adenylation of L- <i>allo</i> -isoleucine	<i>Pseudomonas</i> spp.
<i>cmaB</i>	Non-heme Fe ²⁺ α -ketoglutarate – dependent halogenase	Chlorination of L- <i>allo</i> -isoleucine	<i>Pseudomonas</i> spp.
<i>cmaC</i>	Vicinal oxygen chelate homologue	Cyclopropane ring construction	<i>Pseudomonas</i> spp.
<i>cmaT</i>	Thioesterase	Hydrolysis of thioester bond	<i>Pseudomonas</i> spp.
<i>cmaU</i>	Unknown	Unknown	<i>Pseudomonas</i> spp.
<i>cmaL</i>	Domain of unknown function; DUF1330	L- <i>allo</i> -isoleucine biosynthesis	<i>Pseudomonas</i> spp.
Regulatory			
<i>SCAB79581/orf1</i>	ThiF superfamily protein	Unknown	<i>S. scabies</i>
<i>SCAB79591/cfaR</i>	PAS-LuxR DNA binding protein	Transcriptional activator	<i>S. scabies</i>

<i>corR</i>	Two-component response regulator	Transcriptional activator	<i>Pseudomonas</i> spp.
<i>corS</i>	Two-component histidine protein kinase	Signal transduction	<i>Pseudomonas</i> spp.
<i>corP</i>	Two-component response regulator	Unknown	<i>Pseudomonas</i> spp.

^a CoA = coenzyme A

Appendix 2: Mycobacterial Membrane Proteins QcrB and AtpE: Roles in Energetics, Antibiotic Targets and Associated Mechanisms of Resistance

Luke Bown^{1*}, Santosh K. Srivastava^{1*}, Brandon M. Piercey^{1*}, Clarissa K. McIsaac¹ and Kapil Tahlan^{1Δ}

¹ Department of Biology, Memorial University of Newfoundland, St. John's, NL, Canada
A1B 3X9

** These authors contributed equally*

^Δ Corresponding author: ktahlan@mun.ca

© Springer International Publishing

Bown, L., Srivastava, S.K., Piercey, B.M. et al. J Membrane Biol (2018) 251: 105.

The final publication is available at <https://doi.org/10.1007/s00232-017-9997-3>

Abstract

Infections caused by mycobacteria are difficult to treat due to their inherent physiology, cellular structure and intracellular lifestyle. *Mycobacterium tuberculosis* is a pathogen of global concern as it causes tuberculosis (TB) in humans, which requires 6-9 months of chemotherapy. The situation is further exacerbated in the case of infections caused by drug resistant strains, which necessitate the prolonged use of agents associated with increased host toxicities. Great effort has been invested into the development of new agents for the treatment of drug resistant infections, in addition to novel strategies to reduce treatment time. Energy production using oxidative phosphorylation is essential for the survival of *M. tuberculosis*, even under conditions of dormancy. Many compounds have been recently discovered that inhibit different aspects of energy metabolism in mycobacteria, some of which have been approved for human use or are currently undergoing development. The most successful examples include inhibitors of QcrB and AtpE, which are part of the cytochrome *bc₁* complex and F_oF₁-ATP synthase, respectively. In addition, many of the discovered inhibitors are active against drug resistant strains of *M. tuberculosis*, inhibit nonreplicating cells, and also show potential for the treatment of other mycobacterial infections. In the current review we focus on the discovery of mycobacterial QcrB and AtpE inhibitors, their modes of action and the associated mechanisms of resistance observed to date.

Introduction

Members of the genus *Mycobacterium* are renowned for their complex cell wall structure, intrinsic drug resistance and lipid metabolism (Jackson 2014; Smith et al. 2012). The genus includes pathogens such as *M. tuberculosis* and *M. leprae*, which cause tuberculosis (TB) and leprosy in humans, respectively. Tuberculosis is a major cause of global mortality, with approximately 1.4 million deaths reported due the disease in 2015 (WHO 2016). Drug sensitive forms of the disease are currently treated using a combination of the four front line agents isoniazid (INH), rifampin (RIF), pyrazinamide (PZA) and ethambutol (EMB), over a six to nine month period (Guy and Mallampalli 2008; Villemagne et al. 2012). Due to the inherent physiology of mycobacteria, infections caused by them are often difficult to treat. For example, *M. tuberculosis* can transition between actively growing and nonreplicating states, the latter of which is insensitive to the action of many drugs (Gomez and McKinney 2004). This is a major problem in humans as the bacterium can enter a state of indefinite dormancy after the initial infection event, without causing any symptoms of the active disease (Chao and Rubin 2010). This phenomenon is called latency and the dormant bacteria can reactivate at a later stage to cause active TB under certain circumstances, such as suppression of the host immune system (Gengenbacher and Kaufmann 2012). Currently, it is estimated that approximately 30% of the world's population is latently infected with *M. tuberculosis*. The problem is exacerbated due to TB-HIV co-infections and drug resistant forms of the disease, the latter of which requires up to 2 years of treatment with agents associated with adverse side effects and sometimes high rates of treatment failure (WHO 2016). The prevalence and spread of drug

resistant strains of *M. tuberculosis* (classified as multi-drug resistant: MDR and extensively-drug resistant: XDR, based on resistance profiles) is rising at an alarming rate, beckoning for the development of novel agents for TB treatment and also for strategies to reduce treatment time (AlMatar et al. 2017; Hoagland et al. 2016).

Many species of mycobacteria are widespread in the environment, which include opportunistic pathogens such as nontuberculous mycobacteria (NTM: species other than *M. leprae* or those belonging to the *M. tuberculosis* complex) (Johnson and Odell 2014). The NTM are an emerging cause of concern as *M. kansasii*, *M. abscessus* and members from the *M. avium* complex (MAC) can cause severe infections in humans (Johnson and Odell 2014). Pulmonary infections associated with NTM require 12-18 months of treatment with agents sometimes associated with severe host toxicities, and in the case of *M. abscessus*, treatment often requires surgery in conjunction with chemotherapy. There have been recent reports on the global spread of multidrug resistant strains of different NTM, further highlighting the importance for the development of agents that can target infections caused by different mycobacterial species (Bryant et al. 2016). It should be noted that *M. tuberculosis* and NTM infections are not limited to the lungs and can affect different tissues and organs (Katoch 2004).

The mycobacteria are obligate aerobes which produce ATP via oxidative phosphorylation, even under conditions of dormancy (Rao et al. 2008b). Substrate level-phosphorylation cannot meet their energy requirements and most members from the genus do not perform fermentations under tested conditions (Cook et al. 2014). Their electron transport system (ETS) can utilize various electron donors (e.g. NADH, succinate, fumarate, etc.) to reduce the membrane associated electron carrier, menaquinone (MQ) to

menaquinol (MQH₂) (Bald and Koul 2010; Cook et al. 2014). Menaquinone is the bacterial equivalent of mitochondrial ubiquinone; therefore the two terms are used interchangeably in the current review. Under aerobic conditions, electrons are transferred from menaquinol to reduce the terminal acceptor oxygen (O₂) using either the *aa₃* cytochrome *c* oxidase via the cytochrome *bc₁* complex, or directly by the cytochrome *bd* menaquinol oxidase (Fig. 1) (Bald and Koul 2010; Cook et al. 2014; Preiss et al. 2015; Tran and Cook 2005). During the process of electron transport under aerobic conditions, protons (H⁺) are pumped across the cytoplasmic membrane to establish the electrochemical gradient, which is then used to synthesize ATP by the F₁F₀-ATP synthase (Cook et al. 2017; Preiss et al. 2015; Rao et al. 2008b). Due to the essentiality of the ATP synthase and the requirement of the ETS for survival, there has been great interest in finding inhibitors of proteins from the respective pathways of *M. tuberculosis* (Bald et al. 2017; Cook et al. 2017). Some of the most promising anti-tubercular compounds developed recently include Q203 and bedaquiline (BDQ), which target QcrB (from the cytochrome *bc₁* complex) and AtpE (from the F₁F₀-ATP synthase), respectively. In addition, Q203 is currently in phase Ib clinical trials (Herrmann et al. 2017), whereas bedaquiline is the first dedicated drug approved for TB treatment since 1971 (Preiss et al. 2015), highlighting the importance of their respective targets as druggable proteins. In the current review we specifically discuss important aspects of QcrB and AtpE, the chronology of their identification as antimycobacterial drug targets, along with agents currently under development and the associated mechanisms responsible for the emergence of resistance.

QcrB and the cytochrome bc_1 complex

The *qcrB* gene encodes the β subunit from the cytochrome bc_1 complex, which functions as the menaquinol-cytochrome C oxidoreductase during electron transport (Crofts and Berry 1998). The core protein complex consists of the cytochrome b and c_1 subunits, as well as the Rieske iron sulfur protein (ISP), and is an important component of the mycobacterial respiratory chain (Abrahams et al. 2012; Arora et al. 2014). The complex is highly conserved between the three domains of life, but its composition varies significantly due to the presence of additional supernumerary subunits in eukaryotes (Xia et al. 2013). Structural analysis of the cytochrome bc_1 complex from different organisms has shown that it functions as a dimer (Xia et al. 2013), which catalyzes the transfer of reducing power from low potential menaquinol in the lipid phase to high potential cytochrome c , in the process translocating H^+ across the membrane (Crofts 2004). The cytochrome b protein forms the hydrophobic core, which also functions as the scaffold that interacts with other components of the complex (Kleinschroth et al. 2011). There are two chemically identical *bis-histidine*-coordinated b -type heme groups with high (b_h) and low (b_l) potentials, which are associated with helices 2 and 4 of cytochrome b , respectively (Trumpower 1990; Carter 1981). The two heme groups are organized in the membrane such that b_h is situated on the cytoplasmic face and is involved in menaquinone reduction (called center N or Q_N), whereas b_l is on the exterior face and is involved in menaquinol oxidation (center P or Q_P) (Xia et al. 2013). The bc_1 complex uses menaquinone to shuttle H^+ across the membrane to deposit them on the outer surface using the Q-cycle. This system requires the presence of a menaquinone reduction site on the cytoplasmic face and a menaquinol

oxidation site on the outer face of the membrane, with a branched electron transport system linked to the oxidation site (Cook et al. 2014). The electrons from cytochrome *bc₁* are transferred to the coupled *aa₃* cytochrome *c* oxidase, which then carries out the reduction of oxygen (Trumpower 1990). For every menaquinol molecule oxidized, 2 cytochrome *c* molecules are reduced and 4 H⁺ are released outside of the membrane (Cook et al. 2014; Crofts 2004; Trumpower 1990). In comparison, the alternative cytochrome *bd* complex does not translocate H⁺, but instead generates charge separation via electron transport only (Holyoake et al. 2015). Therefore, it is currently thought that the cytochrome *bc₁* complex functions during aerobic respiration in mycobacteria, whereas the higher affinity *bd* complex is required for growth under hypoxic conditions or under low oxygen tension (Bald and Koul 2010).

Historically, many inhibitors have been found to be active against cytochrome *bc₁* complexes from different organisms and were used in mechanistic and structural studies to understand the functioning of the system (Dong et al. 2011; Jordan et al. 1999; Rotsaert et al. 2008). For example, myxothiazol and stigmatellin are well-known natural products that bind to the Q_P site of cytochrome *b* and block electron transfer (Von Jagow et al. 1984). Myxothiazol has also been used as an antifungal due to its ability to inhibit the mitochondrial cytochrome *bc₁* complex (Gerth et al. 1980; Von Jagow et al. 1984). Antimycin, another natural product, has been shown to bind to the Q_N site of cytochrome *b* to block electron flow from heme *b_h* to ubiquinone (Xia et al. 1997). Numerous other natural products and synthetic compounds have been shown to bind and inhibit the

mitochondrial cytochrome *bc₁* complex, some of which have also been used as fungicides in agriculture (Geier et al. 1994).

Inhibitors of mycobacterial QcrB have been recently discovered using whole-cell phenotypic screening of chemical libraries (Mak et al. 2012; Reynolds et al. 2012). The imidazo[1,2-*a*]pyridines (IPs) were identified in independent studies as potent inhibitors of *M. tuberculosis* and *M. bovis* growth (Fig. 2). The first IP compounds identified were found to be unstable *in vivo* and were therefore deemed unsuitable for direct use (Abrahams et al. 2012). However, the potent anti-tubercular activity, lack of apparent host cytotoxicity and high selectivity lead to further work on this class of compounds, resulting in the development of optimized candidates (Abrahams et al. 2012). IP-3 (Fig. 2a) was found to be one of the most active candidates in a murine infection model, with no apparent signs of host toxicity (Abrahams et al. 2012). Whole genome sequencing (WGS) analysis of spontaneously arising *M. bovis* strains that were resistant to IP-3 identified a single base change at position 937 in *qcrB*. The mutation results in a T313A amino acid substitution in the protein, which suggested that QcrB was the target of IP-3 (Abrahams et al. 2012; Goldman 2013).

Q203 is another IP (Fig. 2b) that was developed following whole-cell screening using infected murine macrophages (Christophe et al. 2010; Pethe et al. 2013). Chemical modifications were made to IP scaffolds identified in the screen to enhance their activity against *M. tuberculosis*. This resulted in the identification of Q203, which is active against MDR and XDR strains and lacks host cytotoxicity on long term administration in murine models (Pethe et al. 2013). Additionally, analysis of spontaneously arising mutants isolated

during the initial screen revealed that single amino acid substitutions (T313A or T313I) in QcrB were responsible for the development of Q203 resistance, again suggesting that the protein was the target of the IPs (Petthe et al. 2013).

Other mycobacterial QcrB inhibitors include the pyrrolo[3,4-*c*]pyridine-1,3(2*H*)-diones (5h, Fig. 2c), which provided a starting point for further optimization. These compounds show promise as they display limited host cytotoxicity and potent activity against *M. tuberculosis* (van der Westhuyzen et al. 2015). Once again, QcrB was identified as the target based on the development of spontaneous resistance, which was attributed to a single point mutation corresponding to an A317T change in the protein (van der Westhuyzen et al. 2015). The currently approved sleep aid Zolpidem (Ambien), an imidazo[1,2-*a*]pyridine-3-acetamide (IPA, Fig. 2d), has also been shown to be active against *M. tuberculosis* (Moraski et al. 2015). To improve its activity, multiple analogues of Ambien were synthesized; one of which displayed higher potency against multiple drug sensitive and resistant strains of *M. tuberculosis*, which even surpassed that of currently used agents (Cheng et al. 2014; Moraski et al. 2015). Q203 resistant *M. tuberculosis* strains harbouring *qcrB* mutations were also found to be cross resistant to the Ambien analogues, suggesting that they share a common target. Further development led to the discovery of the imidazo[2,1-*b*]thiazole-5-carboxamides (17, Fig. 2e), which showed even greater potential as anti-tuberculosis agents (Moraski et al. 2016). These variations of the IP scaffold have been recently tested against drug sensitive and resistant strains of *M. tuberculosis*, as well as actively growing and non-replicating cells. The activities of some of the candidates have been shown to be significantly greater than previously analyzed IP

compounds, with minimum inhibitory concentration (MIC) values of less than 10 nM (Moraski et al. 2016). Some of the compounds from the aforementioned studies were active against NTM, suggesting potential applications in the treatment of other mycobacterial infections. They were also shown to be highly selective against mycobacteria, but were ineffective under hypoxic conditions. This is consistent with the mode of action of the IPs involving the cytochrome *bc₁* complex, which is required for growth during aerobic conditions only (Moraski et al. 2011; Moraski et al. 2016).

It has been noted that SNPs in *qcrB* associated with IP-3 and Q203 resistance are identical, leading to the substitution of T313 in the protein (Abrahams et al. 2012; Pethe et al. 2013). The T313 residue maps to a portion of the quinol oxidation (or Q_P) site in cytochrome *b*, also shown to bind to other nonspecific inhibitors (Pethe et al. 2013). It has been proposed that the T313A change leads to perturbations in the orientation of the side chains of other important amino acids in QcrB (Ko and Choi 2016). Additional point mutations in QcrB that conferred resistance to a diverse set of compounds in another study also mapped to this region (Arora et al. 2014). Therefore, resistance could be caused by a change in the protein that prevents the compounds from acting, and not due to alterations in the mechanism by which the QcrB functions in the cytochrome *bc₁* complex (Abrahams et al. 2012; Ko and Choi 2016). This raises the possibility that the mycobacterial QcrB inhibitors identified so far have similar mechanisms of action to interfere with menaquinol oxidation and electron transport through the cytochrome *bc₁* complex (Abrahams et al. 2012; Ko and Choi 2016), although this hypothesis requires further validation (Cook et al. 2017).

There has also been recent interest in repurposing agents already approved for the treatment of conditions other than TB. A series of 1280 FDA approved compounds were tested in a high-throughput whole-cell based screen designed to detect compounds that protected lung fibroblasts from *M. tuberculosis* cytotoxicity. This led to the identification of the gastric proton-pump (H^+K^+ ATPase) inhibitor lansoprazole (also marketed as Prevacid) (Rybniker et al. 2014) (Fig. 2f), which is used to treat gastric disorders such as ulcers (Bardhan et al. 1995). Lansoprazole is unstable *in vivo*, but lansoprazole sulfide has significantly improved activity and is extremely selective against *M. tuberculosis* (Rybniker et al. 2015). WGS analysis of different isolates showed that a SNP (L176P) in *qcrB* was associated with resistance (Rybniker et al. 2015). The mutation maps to the Q_P site, reminiscent of those identified in previous studies using different QcrB inhibitors (Arora et al. 2014). Lansoprazole (Fig. 2f) and the IP amides are inactive against nonreplicating *M. tuberculosis*, which is likely due to the upregulation of alternative cytochrome *bd* oxidase that replaces cytochrome *bc₁* complex under hypoxic conditions (Arora et al. 2014; Rybniker et al. 2015). Therefore, some strains of mycobacteria have the potential to become resistant to compounds that target the QcrB protein through modification of their ETS, a concern that has also been raised by others previously (Matsoso et al. 2005).

Another class of anti-mycobacterial compounds that inhibit QcrB are the 2-(quinolin-4-yloxy)acetamides (QOAs, Fig. 2g and h) (Phummarin et al. 2016; Pissinate et al. 2016), which were also identified in a *M. tuberculosis* whole-cell based screen (Ballell et al. 2013). Selected compounds from the study were further modified; yielding candidates

with enhanced activities against *M. tuberculosis* under different growth conditions (Phummarin et al. 2016). Moreover, *M. tuberculosis* *bd* oxidase deletion strains were found to be hypersensitive to the compounds, whereas previously isolated *qcrB* mutants were resistant (Arora et al. 2014). In another study, compounds were synthesized based on the initial QOA scaffold and were tested against drug sensitive/resistant strains of *M. tuberculosis* and infected macrophages (Pissinate et al. 2016). These compounds contain a quinoline ring, similar to that found in bedaquiline (Fig. 3a). The lead compounds displayed specificity towards mycobacteria and had little to no measurable toxicity against human epithelial cell lines (Pissinate et al. 2016). The series was not tested against *qcrB* mutants, so further studies to verify the target(s) remain to be conducted. Even though many candidate QcrB inhibitors have been identified to date, details regarding the exact mechanism(s) of inhibition are lacking. Therefore, additional studies are required to thoroughly examine and validate the cytochrome *bc₁* complex as a drug target for future development.

ATP synthase and AtpE

The ATP synthase is an essential transmembrane protein complex that produces ATP using the electrochemical gradient (Abrahams et al. 1994). This makes the ATP synthase of *M. tuberculosis* an attractive target for antibiotic treatment since it is thought to be necessary for maintaining a minimum amount of ATP synthesis, even during periods of dormancy (Rao et al. 2008a). The synthase is comprised of two rotary motors designated as F₁ and F₀, where F₁ is located on the cytoplasmic face of the cell membrane and F₀ is

embedded in the membrane (Fig. 1). The F_1 and F_0 complexes are themselves made up of the $\alpha_3\beta_3\gamma\delta\epsilon$ and ab_2c_{10-15} subunits, respectively (Iino and Noji 2013). The c subunits form c-rings within the F_0 complex in the membrane, which allow the passage of H^+ into the cytoplasm and cause the c-ring to rotate. This rotational motion is transmitted to the α and β subunits from the linked F_1 complex via the connected γ and ϵ subunits (Fig. 1), resulting in the synthesis of ATP from ADP and P_i (Noji et al. 1997). The α and β subunits alternate to form a hexameric structure, where each subunit interface contains a nucleotide binding site, with the β subunit portion of the site also being responsible for catalysis (Iino and Noji 2013). The three β subunits undergo sequential conformational changes due to the rotation of the asymmetrical γ unit, which provides the energy necessary for ATP synthesis to occur (Boyer 1997).

The monomeric c-subunits in the F_0 ring complex have a hairpin structure composed of two α -helices connected by a loop on the cytoplasmic side of the membrane. They are arranged in the c-ring so that their N-terminal helices form an inner ring and the C-terminal helices form the outer ring (Iino and Noji 2013; Pogoryelov et al. 2009). This structural arrangement creates a complex where the inner surface of the ring is hydrophobic, the exception being the region in contact with the outer leaflet of the membrane. The dimeric b-subunit from F_0 contains an N-terminal transmembrane domain that allows it to interact with the δ -subunit from F_1 , thereby acting as a link between the two complexes (Fig.1). This allows the rotation of the c-ring and the γ -subunit during H^+ influx, but prevents rotation of F_1 itself due to its association with the b-subunit from F_0 . Therefore, the γ -subunit rotates within the $\alpha_3\beta_3$ complex, leading to catalysis by β -subunits.

This arrangement is slightly different in mycobacteria as one of the b-subunits is fused to the δ -subunit (b/ δ) through a 110 amino acid bridge (Gajadeera and Weber 2013), whereas the second b-subunit (b') is shorter and lacks the C-terminal segment typically found in other bacteria (Lu et al. 2014). Each c-subunit is used once to transport a H^+ across the membrane during the rotation of the c-ring. Therefore, the number of c-subunits present in the complex can vary depending on the number of H^+ required to drive a single rotation of the c-ring (Preiss et al. 2015). This explains why different bacteria have varying numbers of c-subunits in their respective F_0 complexes. For example, the *M. phlei* c-ring is comprised of nine c-subunits, making it the smallest known complex of bacterial origin for which the structure has been determined (Preiss et al. 2015). The overall basic structure of the ATP synthase complex is similar for bacterial, archaeal, chloroplast and mitochondrial systems. The mycobacterial α and β subunits share between 50-60% sequence identity with *E. coli* and human mitochondrial homologues, suggesting that the majority of differences lie in regulatory regions (Lu et al. 2014). Furthermore, mitochondrial systems have been found to have a more complex arrangement with many additional accessory subunits (Devenish et al. 2000). For example, the F_0 unit in bacteria is comprised of 3 subunits (a, b and c), whereas in *Saccharomyces cerevisiae* it contains at least 12, of which 3 are homologous to the bacterial proteins (Devenish et al. 2000). The exact functions of the extra eukaryotic subunits are not known, but several have been shown to be involved in the structural maintenance and regulation of the mitochondrial ATP synthase (Arnold et al. 1998; Martinez et al. 2003; Nowak and McCarty 2004; von Ballmoos et al. 2008).

The conserved nature of the ATP synthase would seem to preclude its use as a target for antibiotic therapy. However, the success of the diarylquinolines (DAQs) has shown that targeting the complex is a viable option in the case of mycobacteria. The DAQ class of compounds were identified using a *M. smegmatis* whole-cell screening assay, leading to the isolation of R207910 (TMC207 or bedaquiline) (Andries et al. 2005; Koul et al. 2007). Bedaquiline was shown to be highly active against susceptible and MDR strains of *M. tuberculosis* without any observable cross-resistance to other front-line agents, suggesting it has a novel mode of action (Andries et al. 2005). While being effective against mycobacteria (including NTM), bedaquiline has significantly lower activity against other common pathogens, which distinguishes it from the quinoline and fluoroquinolone classes of antibiotics (Andries et al. 2005).

WGS studies consistently identified mutations in the *atpE* gene (encoding the c-subunit from the F₀ complex) in bedaquiline resistant mutants, suggesting that the ATP synthase was the target. This was followed by work on mycobacterial inverted membrane vesicles, which provided detailed mechanistic information. Reconstituted *M. smegmatis* membrane vesicles coupled to a luciferase assay along with NADH and ADP as substrate showed that bedaquiline inhibited the mycobacterial ATP synthase (Haagsma et al. 2009; Haagsma et al. 2011; Koul et al. 2007). These studies also demonstrated the specificity of bedaquiline for the mycobacterial ATP synthase, as excessive concentrations were required to produce any effect on ATP production in eukaryotic cells (Haagsma et al. 2009).

Initially three mutations were identified in *atpE* (corresponding to D32V and A63P in *M. tuberculosis* and I66M in *M. smegmatis*), which contributed to the development of

bedaquiline resistance (Andries et al. 2005; Petrella et al. 2006). The D32, A63 and I66 amino acids are highly conserved throughout the mycobacteria, with the exception of *M. xenopi*, *M. shimoidei* and *M. novocastrense* (where residue 63 is methionine), which confers intrinsic bedaquiline resistance in these species (Huitric et al. 2007; Petrella et al. 2006). Work on human, mouse and bovine mitochondria have also demonstrated that a methionine is present at position 63 in their c-subunits (Haagsma et al. 2009). Additional c-subunit mutations were also reported in bedaquiline resistant strains of *M. tuberculosis* (D28G, L59V, E61D, A63P and I66M), *M. fortuitum* (D28A), *M. smegmatis* (I66M) and *M. abscessus* (D28A and A63P) (Segala et al. 2012). Another study analyzed 97 separate bedaquiline resistant *M. tuberculosis* mutants from clinical samples, which displayed a 4-128 fold increase in resistance (Huitric et al. 2010). *atpE* genes were sequenced from 53 isolates and were found to contain 5 separate point mutations (D28V, A63P, I66M, D28P and E61D). The remaining 38 isolates did not harbour mutations in *atpE* or any gene associated with the F₁-F₀ ATP synthase complex (Huitric et al. 2010), suggesting that other unknown mechanisms can also contribute to resistance development.

M. tuberculosis strains displaying 2-8 fold increase in bedaquiline resistance have also been isolated from some patients, which were attributed to non-target mutations in the *Rv0678* (*mmpR*) gene (Bloemberg et al. 2015). *mmpR* encodes a protein belonging to the multiple antibiotic resistance regulator (MarR) family and is located just upstream of the *mmpS5* gene in *M. tuberculosis* (Milano et al. 2009). MmpR is a negative regulator of *mmpL5* and *mmpS5*, the products of which together comprise an efflux pump capable of causing cross-resistance to different drugs (Andries et al. 2014; Hartkoorn et al. 2014;

Milano et al. 2009). Mutations in MmpR result in a non-functional repressor, which causes de-repression of the *mmpL5* and *mmpS5* gene expression, leading to resistance (Milano et al. 2009). Recently it was also found that *M. tuberculosis* isolates from infected mice treated with bedaquiline, with or without clofazimine, showed a 4 fold increase in resistance to both drugs (Almeida et al. 2016). Antibiotic cross-reactions with clofazimine are currently of interest because of its potential to be used in the short-course treatment for MDR-TB (Piubello et al. 2014; Van Deun et al. 2010). As such, how it will interact with other agents such as bedaquiline in multi-drug therapy is of great importance. Analysis of the isolates demonstrated they had mutations in the *pepQ* gene, which encodes a putative Xaa-Pro aminopeptidase (Bloemberg et al. 2015; Harris et al. 2003). Such proteins catalyze the release of an N-terminal amino acid linked to a proline and are highly conserved across all three domains of life (Dehm and Nordwig 1970; Cottrell et al. 2000). However, the mechanism by which *pepQ* mutations result in increased resistance to bedaquiline is unknown.

Recently, the structure of the c-ring of *M. phlei* was elucidated with and without bound bedaquiline, which provided information regarding its mechanism and specificity (Preiss et al. 2015). AtpE (or c-subunits) from *M. phlei* and *M. tuberculosis* share 83.7% amino acid sequence identity, therefore *M. phlei* was used as a model for structural comparison (Preiss et al. 2015). A single bedaquiline molecule was bound to every c-subunit via a large number of interactions. The hydroxyl group of bedaquiline formed a hydrogen bond with a water molecule along with E65 from the c-subunit. In addition, the dimethylamino (DMA) group of bedaquiline was shown to interact with the ion binding

site of the c-subunit by creating a specific ionic intermolecular hydrogen bond with E65 (de Jonge et al. 2007; Preiss et al. 2015). Mutations in AtpE from bedaquiline resistant mutants were found to directly and indirectly interfere with the structure of the bedaquiline binding site. Direct structural interference was observed in the *M. tuberculosis* E61D, L59V and I66M mutants, while indirect interference was observed in the *M. smegmatis* D32V and in the *M. tuberculosis* D28A, D28G and A63P mutants, respectively (Preiss et al. 2015). For example, the substitution of D32 prevents indirect hydrogen bonding between the bedaquiline and the E65 residue, thereby contributing to resistance (Preiss et al. 2015).

According to the current model, the protonated form of bedaquiline binds with high affinity to the ion binding sites of the c-subunits to interfere with H^+ transfer through the F_0 complex, thereby inhibiting ATP synthesis (Haagsma et al. 2011). When *M. smegmatis* was exposed to bedaquiline, it caused an increase in oxygen consumption and collapsed the ΔpH gradient (Hards et al. 2015). These results are consistent with the uncoupling of ATP synthase due to the inhibitor binding to the c-subunit and disruption of the a-c subunit interaction, causing leakage of H^+ into the cell without eliciting the rotation of the c-ring. The charge gradient ($\Delta\psi$) is unaffected by the disruption, suggesting that the effect is electroneutral due to the coupled exchange of other ions for H^+ (Hards et al. 2015). The mycobacterial specificity of bedaquiline can be explained based on its structure, which allows it to bind to the components of the c-ring by a “lock and key” mechanism (Preiss et al. 2015). In addition, the region of F_0 bound by bedaquiline is highly conserved in mycobacteria, but not in other organisms examined so far. When mutations occur in the mycobacterial c-subunits, there is a change in the structural conformation in the conserved

region, which reduces the number of electrostatic interactions and prevents binding of bedaquiline (Preiss et al. 2015). Bedaquiline is currently only recommended for use in MDR and XDR cases of TB when no other treatment options are available (Field 2015; Gras 2013).

It should be noted that not all mycobacteria are killed by bedaquiline as it was shown to have bacteriostatic activity against *M. avium* when used alone (Lounis et al. 2009). A recent clinical study showed that bedaquiline was effective against both slow and rapidly growing NTM (Pang et al. 2017). 20-40% of isolates were classified as resistant, ~11% of which harboured mutations in *atpE*. However, none of the identified mutations resulted in amino acid changes in the protein and additional genome sequence studies were not performed. Therefore, further work is warranted to identify and compare other potential bedaquiline resistance mechanisms that may exist in NTM.

There are several other potential candidates that target the mycobacterial ATP synthase. The squaramide class of compounds (Fig. 3b) were initially discovered in screens using *M. smegmatis* inverted membrane vesicles for identifying ATP synthesis inhibitors (Tantry et al. 2017). Further optimization studies led to the 3-(4-morpholinophenyl)-4-((pyridin-2-ylmethyl)amino)cyclobut-3-ene-1,2-dione candidate, 31f (Fig. 3b), which selectively inhibited the mycobacterial ATP synthase (Tantry et al. 2017). WGS of resistant strains showed the presence of multiple SNPs, many of which were present in non-essential genes or were not reproducible/consistent between different isolates. Two SNPs were found at high frequency in essential genes, K179N in *atpB* (a-subunit) and D28N in *atpE* (c-subunit) (Tantry et al. 2017). The substitution of D28 has been observed previously in

bedaquiline resistant strains of *M. tuberculosis*, *M. fortuitum* and *M. abscessus* (Segala et al. 2012). Intriguingly, 31f is also active against *M. tuberculosis* strains resistant to bedaquiline, but none of the previously sequenced bedaquiline resistant strains contained SNPs in *atpB*. Therefore, 31f could have a different mechanism by which it binds to the F₀ complex as compared to bedaquiline, making it an attractive candidate for further development (Tantry et al. 2017). Many quinoline compounds have also been evaluated for activity against the mycobacterial ATP synthases. For example, the *N*-(7-chloro-2-methylquinolin-4-yl)-*N*-(3-[(diethylamino)methyl])-4-dihydroxyphenyl)-2,3-dichlorobenzenesulfonamide candidate 9d (Fig. 3d) is active against aerobic and hypoxic cultures of *M. tuberculosis*, but does not display significant activity against other pathogens or ATP synthesis in mammalian cell lines (Singh et al. 2015).

In addition to synthetic compounds, natural product inhibitors of the mycobacterial ATP synthase have also been identified. Trichoderin A1 (Fig. 3c) was isolated from a marine sponge derived fungus and was active against *M. smegmatis*, *M. bovis* (BCG) and *M. tuberculosis* under both aerobic and hypoxic conditions (Kavianinia et al. 2016; Pruksakorn et al. 2010). *M. smegmatis* clones resistant to trichoderin A1 were isolated after transformation with a cosmid library containing random *M. smegmatis* chromosomal DNA fragments. Cosmid clones able to confer trichoderin A1 resistance were analyzed and were found to contain genes for the majority of the ATP synthase complex. Therefore, the target of trichoderin A1 lies somewhere in the ATP synthase, but its exact mode of action or the responsible mechanism of resistance is yet to be determined (Pruksakorn et al. 2011). Based on the described reports, it is apparent that there are a number of mycobacterial ATP

synthase inhibitors currently in the pipeline, some of which should help in further exploiting the vulnerability of this target for anti-TB chemotherapy.

Overview and perspectives

TB chemotherapy is a long and arduous process, which is significantly hampered by the development of drug resistance. Therefore, there is need for the discovery of agents with novel modes of action to overcome prevailing resistance mechanisms. To be broadly applicable, new candidates should also be compatible with currently used front line agents and should not interfere with antiretroviral therapy during TB-HIV treatment (Sacks and Behrman 2009). This review highlights some of the most promising classes of agents developed recently, which target aerobic respiration and ATP synthesis in mycobacteria. As mentioned previously, Q203 is currently in clinical trials and bedaquiline is the first dedicated drug to be approved in over 40 years as one of the last options for inclusion in regimens for the treatment of MDR and XDR-TB (WHO 2016). Q203 and bedaquiline were discovered using whole-cell based screens (Andries et al. 2005; Koul et al. 2007; Pethe et al. 2013), as target based approaches for antibiotic discovery have shown limited success in identifying compounds that have progressed into clinical development (Kana et al. 2014). Two major advantages of the whole-cell based approach include the ability to assess for factors such as drug metabolism and resistance, and accessibility of the target for inhibition by compounds during the screening stage itself (Moreira et al. 2015). While target based methods sometimes play important roles in compound optimization after discovery (Kana et al. 2014), testing against whole-cells is still required at some point to

ensure that lead compounds retain biological activities. The successful development of Q203 and bedaquiline are good examples of how conventional whole-cell screening efforts can lead to the identification of novel agents for antimicrobial chemotherapy.

Due to the essentiality of the ATP synthase and the requirement of the ETS for survival, there has been considerable interest in deciphering the biochemical mechanisms involved in these processes for the purpose of drug discovery (Mak et al. 2012). The search for strategies and agents that not only treat active infections, but can also eradicate latent *M. tuberculosis* reservoirs has been an ongoing challenge. Targeting the ATP synthase in latent TB infections has the potential to eradicate dormant bacteria, which rely on the complex for ATP production and are otherwise insensitive to the action of many other drugs (Yew 2006). The situation with the ETS inhibitors in *M. tuberculosis* seems to be more complex (Cook et al. 2017). Under certain growth conditions *M. tuberculosis* can survive exposure to cytochrome *bc₁* inhibitors due to upregulation of the alternative cytochrome *bd* oxidase (Arora et al. 2014). In addition, *M. tuberculosis* can utilise other terminal electron acceptors under certain conditions, complicating matters further (Cook et al. 2017). It was recently shown that Q203 had bacteriostatic activity against drug-tolerant *M. tuberculosis* persisters, even at 200-fold MIC concentrations (Kalia et al. 2017). Consequently, the use of just cytochrome *bc₁* inhibitors alone might not suffice in completely shutting down electron transport in *M. tuberculosis* to eradicate the bacterium completely. Instead, it is possible that when used together, combinations of cytochrome *bd* (Lu et al. 2015), alternate reductase (Watanabe et al. 2011) and cytochrome *bc₁* inhibitors could completely switch off the pathway, an idea that merits further investigation. It has also been reported that certain mycobacteria have lost the cytochrome *bd* complex and alternate reductases in the

process of genome reduction (Cole et al. 2001; Demangel et al. 2009). Therefore, inhibitors of the cytochrome *bc₁* complex alone could function as candidates for treating infections caused by such species specifically.

Because of their evolutionary relationship, bacteria and mitochondria share many physiological similarities (Margulis 1971). Disruption of bioenergetic pathways in both result in the release of reactive oxygen species (ROS) which cause cellular damage, sometimes leading to cell death (Paradies et al. 2000; Zorov et al. 2006). Therefore, it is imperative that antibacterials should not cross-react with host cell targets to minimize toxicity (Sarver et al. 2012). Fortunately, bedaquiline has very high affinity for AtpE in mycobacteria and does not inhibit mitochondrial function at physiologically relevant concentrations (Haagsma et al. 2009). Assays have also shown that combinations of Q203 and bedaquiline have significant bactericidal activity against *M. tuberculosis*, without damaging host cells (Lamprecht et al. 2016). Despite targeting different membrane proteins, studies suggest that combinations of bedaquiline and Q203 synergistically increase flux through the ETS as feedback inhibition of glycolysis and the tricarboxylic acid cycle is lost (Lamprecht et al. 2016). It was proposed that this increased flux could be exploited by using clofazimine, which accepts electrons from the type 2 NADH dehydrogenase (NDH-2) and reroutes them (Yano et al. 2011). This leads to the formation of an unstable clofazimine intermediate that reacts with O₂, leading to the generation of ROS. Using an infected macrophage model, it was shown that different combinations of Q203, bedaquiline and clofazimine were more efficient in reducing bacterial loads in comparison to each agent when used alone (Lamprecht et al. 2016). These studies highlight the importance of using combinations of agents that have previously unrecognized

synergistic activities, which could also help in devising new treatment regimes (Bollenbach 2015; Caminero et al. 2010).

Bedaquiline has the potential to accelerate treatment when used in combination with other agents (Lu et al. 2017). For example, the frontline anti-mycobacterial drug pyrazinamide has also been shown to decrease the time required to treat TB (Conde and Silva 2011). Interestingly, bedaquiline and pyrazinamide act synergistically against mycobacteria, which has been attributed to the partial inhibition of efflux pumps due to depletion of cellular ATP levels (Lu et al. 2014). The hydrophobic nature of, and the limited number of porins present in the mycobacterial cell wall are partly responsible for the intrinsic antimicrobial resistance observed in these bacteria (Brennan and Nikaido 1995). Efflux systems also contribute to antimicrobial resistance in mycobacteria by actively transporting agents out of the cell (da Silva and Palomino 2011). Recent work with Q203 has shown that its efficacy is also reduced due to an unidentified efflux pump (Jang et al. 2017). When used in conjunction with efflux pump inhibitors (e.g. verapamil) the activities of Q203 and bedaquiline are enhanced significantly (Gupta et al. 2014; Gupta et al. 2015; Jang et al. 2017). *M. tuberculosis* strains resistant to bedaquiline have been detected under clinical settings three years after it was first introduced. This has been attributed in part due to co-treatment with second or third line agents that can induce higher rates of resistance development (Bloemberg et al. 2015; Kalia et al. 2017). A separate study showed that co-administration of verapamil and bedaquiline to infected mice reduced the development of bedaquiline resistance (Gupta et al. 2015). It has also been shown that the efflux pump inhibitor timcodar displays synergism with bedaquiline and other antitubercular drugs (Grossman et al. 2015). Therefore, co-treatment with an efflux pump inhibitors provides

further opportunities to enhance the activities of Q203 and bedaquiline, with the possibly of also reducing the emergence of resistance.

In conclusion, it is evident that the discovery and development of new agents that inhibit the mycobacterial respiratory chain is a very active field of drug research. Many agents have been identified, which are not only confined to the treatment of TB, but can also be used to fight NTM infections. Great discoveries are anticipated in this field, which could provide novel means to treat drug resistant and also possibly latent mycobacterial infections in the future.

Acknowledgements

Research on antibiotic discovery and resistance in KT's laboratory at Memorial University of Newfoundland (MUN) is currently funded by a Discovery Grant (DG) from the Natural Sciences and Engineering Research Council of Canada (NSERC). BMP and CKM were the recipients of a Science Undergraduate Research Award (from MUN) and an Undergraduate Student Research Award (from NSERC), respectively. We would also like to acknowledge the Department of Biology and the Faculty of Graduate Studies (MUN) for additional student support.

References

- Abrahams J.P., Leslie A.G., Lutter R., Walker J.E. (1994). Structure at 2.8 Å resolution of F₁-ATPase from bovine heart mitochondria. *Nature* 370:621-628.
- Abrahams K.A. et al. (2012). Identification of novel imidazo[1, 2-*a*]pyridine inhibitors targeting *M. tuberculosis* QcrB. *PloS ONE* 7:e52951.
- AlMatar M., AlMandea H., Var I., Kayar B., Köksal F. (2017). New drugs for the treatment of *Mycobacterium tuberculosis* infection. *Biomed Pharmacother* 91:546-558.
- Almeida D. et al. (2016). Mutations in *pepQ* confer low-level resistance to bedaquiline and clofazimine in *Mycobacterium tuberculosis*. *Antimicrob Agents Chemother* 60:4590-4599.
- Andries K. et al. (2005). A diarylquinoline drug active on the ATP synthase of *Mycobacterium tuberculosis*. *Science* 307:223-227.
- Andries K. et al. (2014). Acquired resistance of *Mycobacterium tuberculosis* to bedaquiline. *PloS ONE* 9:e102135.
- Arnold I., Pfeiffer K., Neupert W., Stuart R.A., Schägger H. (1998). Yeast mitochondrial F₁ F₀-ATP synthase exists as a dimer: identification of three dimer-specific subunits. *EMBO J* 17:7170-7178.
- Arora K. et al. (2014). Respiratory flexibility in response to inhibition of cytochrome *c* oxidase in *Mycobacterium tuberculosis*. *Antimicrob Agents Chemother* 58:6962-6965.
- Bald D., Koul A. (2010). Respiratory ATP synthesis: the new generation of mycobacterial drug targets? *FEMS Microbiol Lett* 308:1-7.

- Bald D., Villellas C., Lu P., Koul A. (2017). Targeting energy metabolism in *Mycobacterium tuberculosis*, a new paradigm in antimycobacterial drug discovery. *mBio* 8:e00272-00217.
- Ballell L. et al. (2013). Fueling open-source drug discovery: 177 small-molecule leads against tuberculosis. *ChemMedChem* 8:313-321.
- Bardhan K., Hawkey C., Long R., Morgan A., Wormsley K., Moules I., Brocklebank D. (1995). Lansoprazole versus ranitidine for the treatment of reflux oesophagitis. *Aliment Pharmacol Thera* 9:145-151.
- Bloemberg G.V. et al. (2015) Acquired resistance to bedaquiline and delamanid in therapy for tuberculosis. *N Engl J Med* 373:1986-1988.
- Bollenbach T. (2015). Antimicrobial interactions: mechanisms and implications for drug discovery and resistance evolution. *Curr Opin Microbiol* 27: 1-9.
- Boyer P.D. (1997). The ATP synthase-a splendid molecular machine. *Annu Rev Biochem* 66:717-749.
- Brennan P.J., Nikaido H. (1995). The envelope of mycobacteria. *Annu Rev Biochem* 64: 29-63.
- Bryant J.M et al. (2016). Emergence and spread of a human-transmissible multidrug-resistant nontuberculous mycobacterium. *Science* 354:751-757.
- Caminero J.A., Sotgiu G., Zumla A., Migliori G.B. (2010). Best drug treatment for multidrug-resistant and extensively drug-resistant tuberculosis. *Lancet Infect Dis* 10:621-629.
- Carter K.R., Ah-lim T., Graham P. (1981). The coordination environment of mitochondrial cytochromes *b*. *FEBS Lett* 132:243-246.

- Chao M.C., Rubin E.J. (2010). Letting sleeping dogs lie: does dormancy play a role in tuberculosis? *Annu Rev Microbiol* 64:293-311.
- Cheng Y., Moraski G.C., Cramer J., Miller M.J., Schorey J.S. (2014). Bactericidal activity of an imidazo[1, 2-*a*]pyridine using a mouse *M. tuberculosis* infection model. *PLoS ONE* 9:e87483.
- Christophe T., Ewann F., Jeon H.K., Cechetto J., Brodin P. (2010). High-content imaging of *Mycobacterium tuberculosis*-infected macrophages: an *in vitro* model for tuberculosis drug discovery. *Future* 2:1283-1293.
- Cole S. et al. (2001). Massive gene decay in the leprosy bacillus. *Nature* 409:1007-1011.
- Conde M.B., de Silva J.R.L. (2011). New regimens for reducing the duration of the treatment of drug susceptible pulmonary tuberculosis. *Drug Dev. Res.* 72(6):501-508.
- Cook G. et al. (2017). Oxidative phosphorylation as a target space for tuberculosis: success, caution, and future directions. *Microbiol Spectr* 5.
- Cook G.M., Hards K., Vilchèze C., Hartman T., Berney M. (2014). Energetics of respiration and oxidative phosphorylation in mycobacteria. *Microbiol Spectr* 2.
- Cottrell G.S., Hooper N.M., Turner A.J. (2000). Cloning, expression, and characterization of human cytosolic aminopeptidase P: a single manganese (II)-dependent enzyme. *Biochem* 39: 15121-15128.
- Crofts A.R. (2004). The cytochrome *bc*₁ complex: function in the context of structure. *Annu Rev Physiol* 66:689-733.
- Crofts A.R., Berry E.A. (1998). Structure and function of the cytochrome *bc*₁ complex of mitochondria and photosynthetic bacteria. *Curr Opin Struct Biol* 8:501-509.

- da Silva P.E.A., Palomino J.C. (2011) Molecular basis and mechanisms of drug resistance in *Mycobacterium tuberculosis*: classical and new drugs. *Antimicrobial Chemotherapy*. 66 (7): 1417-1430.
- de Jonge M.R., Koymans L.H., Guillemont J.E., Koul A., Andries K. (2007). A computational model of the inhibition of *Mycobacterium tuberculosis* ATPase by a new drug candidate R207910. *Proteins: Struct Funct Bioinform* 67:971-980.
- Dehm P., Nordwig A. (1970). The cleavage of prolyl peptides by kidney peptidases. *Eur J Biochem* 17: 364-371.
- Demangel C., Stinear T.P., Cole S.T. (2009). Buruli ulcer: reductive evolution enhances pathogenicity of *Mycobacterium ulcerans*. *Nat Rev Microbiol* 7:50-60.
- Devenish R.J., Prescott M., Roucou X., Nagley P. (2000). Insights into ATP synthase assembly and function through the molecular genetic manipulation of subunits of the yeast mitochondrial enzyme complex. *Biochim Biophys Acta* 1458:428-442.
- Dong C.K. et al. (2011). Identification and validation of tetracyclic benzothiazepines as *Plasmodium falciparum* cytochrome *bc₁* inhibitors. *Chem Biol* 18:1602-1610.
- Field S.K. (2015). Bedaquiline for the treatment of multidrug-resistant tuberculosis: great promise or disappointment? *Ther Adv Chronic Dis* 6:170-184.
- Gajadeera C.S., Weber J. (2013). *Escherichia coli* F₁F₀-ATP synthase with a b/δ fusion protein allows analysis of the function of the individual b subunits. *J Biol Chem* 288:26441-26447.
- Geier B., Haase U., Von Jagow G. (1994). Inhibitor binding to the Q_p-site of *bc₁* complex: comparative studies of yeast mutants and natural inhibitor resistant fungi. *Biochem Soc Trans* 22: 203-209.

- Gengenbacher M., Kaufmann S.H. (2012). *Mycobacterium tuberculosis*: success through dormancy. *FEMS Microbiol Rev* 36:514-532.
- Gerth K., Irschik H., Reichenbach H., Trowitzsch W. (1980). Myxothiazol, an antibiotic from *Myxococcus fulvus* (Myxobacterales). *J Antibiot* 33:1474-1479.
- Goldman R.C. (2013). Why are membrane targets discovered by phenotypic screens and genome sequencing in *Mycobacterium tuberculosis*? *Tuberculosis* 93:569-588.
- Gomez J.E., McKinney J.D. (2004). *M. tuberculosis* persistence, latency, and drug tolerance. *Tuberculosis* 84:29-44.
- Gras J. (2013). Bedaquiline for the treatment of pulmonary, multidrug-resistant tuberculosis in adults. *Drugs Today (Barc)* 49:353-361.
- Grossman T.H., Shoen C.M., Jones S.M., Jones P.L., Cynamon M.H., Locher C.P. (2015). The efflux pump inhibitor timcodar improves the potency of antimycobacterial agents. *Antimicrob Agents Chemother* 59(3): 1534-1541.
- Gupta S., Cohen K.A., Winglee K., Malga M., Diarra B., Bishal W.R. (2014). Efflux inhibition with verapamil potentiates bedaquiline in *Mycobacterium tuberculosis*. *Antimicrob Agents Chemother* 58: 574-576.
- Gupta S., Tyagi S., Bishai W.R. (2015). Verapamil increases the bactericidal activity of bedaquiline against *Mycobacterium tuberculosis* in a mouse model. *Antimicrob Agents Chemother* 59: 673-676.
- Guy E.S., Mallampalli A. (2008). Managing TB in the 21st century: existing and novel drug therapies. *Ther Adv Chronic Dis* 2:401-408.

- Haagsma A.C. et al. (2009). Selectivity of TMC207 towards mycobacterial ATP synthase compared with that towards the eukaryotic homologue. *Antimicrob Agents Chemother* 53:1290-1292.
- Haagsma A.C., Podasca I., Koul A., Andries K., Guillemont J., Lill H., Bald D. (2011). Probing the interaction of the diarylquinoline TMC207 with its target mycobacterial ATP synthase. *PLoS ONE* 6:e23575.
- Hards K. et al. (2015). Bactericidal mode of action of bedaquiline. *J Antimicrob Chemo* 70:2028-2037.
- Harris J.K., Kelley S.T., Spiegelman G.B., Pace N.R. (2003). The genetic core of the universal ancestor. *Genome Res* 13:407-412.
- Hartkoorn R.C., Uplekar S., Cole S.T. (2014). Cross-resistance between clofazimine and bedaquiline through upregulation of MmpL5 in *Mycobacterium tuberculosis*. *Antimicrob Agents Chemother* 58:2979-2981.
- Herrmann, J., Rybniker, J., & Muller, R. 2017. Novel and revisited approaches in antituberculosis drug discovery. *Current Opinion in Biotechnology*. 48: 94-101.
- Hoagland D.T., Liu J., Lee R.B., Lee R.E. (2016). New agents for the treatment of drug-resistant *Mycobacterium tuberculosis*, *Adv Drug Deliv Rev* 102:55-72.
- Holyoake L.V., Poole R.K., Shepherd M. (2015). The CydDC family of transporters and their roles in oxidase assembly and homeostasis. *Adv Microb Physiol* 66:1-53.
- Huitric E., Verhasselt P., Andries K., Hoffner S.E. (2007). In vitro antimycobacterial spectrum of a diarylquinoline ATP synthase inhibitor. *Antimicrob Agents Chemother* 51:4202-4204.

- Huitric E., Verhasselt P., Koul A., Andries K., Hoffner S., Andersson D.I. (2010). Rates and mechanisms of resistance development in *Mycobacterium tuberculosis* to a novel diarylquinoline ATP synthase inhibitor *Antimicrob Agents Chemother* 54:1022-1028.
- Iino R., Noji H. (2013). Operation mechanism of F₀F₁-adenosine triphosphate synthase revealed by its structure and dynamics. *IUBMB Life* 65:238-246
- Jackson M (2014) The mycobacterial cell envelope-lipids. *Cold Spring Harb Perspect Med* 4:a021105.
- Jang J., Kim R., Woo M., Jeong J., Park D.E., Kim G., Delorme V. (2017). Efflux attenuates the antibacterial activity of Q203 in *Mycobacterium tuberculosis*. *Antimicrob Agents Chemother* doi: 10.1128/AAC.02637-16.
- Johnson M.M., Odell J.A. (2014). Nontuberculous mycobacterial pulmonary infections. *J Thorac Dis* 6:210.
- Jordan D.B. et al. (1999). Oxazolidinones: a new chemical class of fungicides and inhibitors of mitochondrial cytochrome *bc₁* function. *Pest Manag Sci* 55:213-215.
- Kalia N.P. et al. (2017). Exploiting the synthetic lethality between terminal respiratory oxidases to kill *Mycobacterium tuberculosis* and clear host infection. *Proc Natl Acad Sci* 114: 7426-7431.
- Kana B.D., Karakousis P.C., Parish T., Dick T. (2014). Future target-based drug discovery for tuberculosis? *Tuberculosis* 94: 551-556.
- Katoch V. (2004). Infections due to non-tuberculous mycobacteria (NTM). *Indian J Med Res* 120:290.

- Kavianinia I., Kunalingam L., Harris P.W., Cook G.M., Brimble M.A. (2016). Total synthesis and stereochemical revision of the anti-tuberculosis peptaibol trichoderin A. *Org Lett* 18:3878-3881.
- Kleinschroth T., Castellani M., Trinh C.H., Morgner N., Brutschy B., Ludwig B., Hunte C. (2011). X-ray structure of the dimeric cytochrome *bc₁* complex from the soil bacterium *Paracoccus denitrificans* at 2.7-Å resolution. *Biochim Biophys Acta* 1807:1606-1615.
- Ko Y., Choi I. (2016). Putative 3D structure of QcrB from *Mycobacterium tuberculosis* cytochrome *bc₁* complex, a novel drug-target for new series of antituberculosis agent Q203. *Bull Korean Chem Soc* 37:725-73.
- Koul A. et al. (2007). Diarylquinolines target subunit-c of mycobacterial ATP synthase. *Nat Chem Biol* 3:323.
- Lamprecht D.A. et al. (2016). Turning the respiratory flexibility of *Mycobacterium tuberculosis* against itself. *Nat Comm*, 7.
- Lounis N., Gevers T., Van Den Berg J., Vranckx L., Andries K. (2009). ATP synthase inhibition of *Mycobacterium avium* is not bactericidal. *Antimicrob Agents Chemother* 53:4927-4929.
- Lu P. et al. (2015). The cytochrome *bd*-type quinol oxidase is important for survival of *Mycobacterium smegmatis* under peroxide and antibiotic-induced stress. *Sci Rep* 5: 10333.
- Lu P., Lill H., Bald D. (2014). ATP synthase in mycobacteria: special features and implications for a function as drug target. *Biochim Biophys Acta* 1837:1208-1218.

- Mak P.A. et al. (2012). A high-throughput screen to identify inhibitors of ATP homeostasis in non-replicating *Mycobacterium tuberculosis*. *ACS Chem Biol* 7:1190-1197.
- Margulis L. (1971). Symbiosis and evolution. *Sci Am* 225: 48-61.
- Martinez L.O. et al. (2003). Ectopic β -chain of ATP synthase is an apolipoprotein AI receptor in hepatic HDL endocytosis. *Nature* 421:75-79.
- Matsoso L.G. et al. (2005). Function of the cytochrome *bc₁-aa₃* branch of the respiratory network in mycobacteria and network adaptation occurring in response to its disruption. *J Bac* 187:6300-6308.
- Milano A. et al. (2009). Azole resistance in *Mycobacterium tuberculosis* is mediated by the MmpS5–MmpL5 efflux system. *Tuberculosis* 89:84-90.
- Moraski G.C., Markley L.D., Hipskind P.A., Boshoff H., Cho S., Franzblau S.G., Miller M.J. (2011). Advent of imidazo[1, 2-*a*]pyridine-3-carboxamides with potent multi- and extended drug resistant antituberculosis activity. *ACS Med Chem Lett* 2:466-470.
- Moraski G.C. et al. (2015). Putting tuberculosis (TB) to rest: transformation of the sleep aid, Ambien, and “anagrams” generated potent antituberculosis agents. *ACS Infect Dis* 1:85-90.
- Moraski G.C. et al. (2016). Arrival of imidazo[2, 1-*b*] thiazole-5-carboxamides: potent anti-tuberculosis agents that target QcrB. *ACS Infect Dis* 2:393-398.
- Moreira W. et al. (2015). Target mechanism-based whole-cell screening identifies bortezomib as an inhibitor of caseinolytic protease in Mycobacteria. *mBio* 6: e00253-15.

- Noji H., Yasuda R., Yoshida M., Kinosita Jr K. (1997). Direct observation of the rotation of F₁-ATPase. *Nature* 386:299.
- Nowak K.F., McCarty R.E. (2004). Regulatory role of the C-terminus of the ϵ subunit from the chloroplast ATP synthase. *Biochem* 43:3273-3279.
- Pang Y., Zheng H., Tan Y., Song Y., Zhao Y. (2017). In vitro activity of bedaquiline against nontuberculous mycobacteria in China. *Antimicrob Agents Chemother* 61:e02627-02616.
- Paradies G., Petrosillo G., Pistolese M., Ruggiero F.M. (2000). The effect of reactive oxygen species generated from the mitochondrial electron transport chain on the cytochrome *c* oxidase activity and on the cardiolipin content in bovine heart submitochondrial particles. *FEBS Lett* 466: 323-326.
- Pethe K. et al. (2013). Discovery of Q203, a potent clinical candidate for the treatment of tuberculosis. *Nat Med* 19:1157-1160.
- Petrella S., Cambau E., Chauffour A., Andries K., Jarlier V., Sougakoff W. (2006). Genetic basis for natural and acquired resistance to the diarylquinoline R207910 in mycobacteria. *Antimicrob Agents Chemother* 50:2853-2856.
- Phummarin N., Boshoff H.I., Tsang P.S., Dalton J., Wiles S., Barry 3rd C.E., Copp B.R. (2016). SAR and identification of 2-(quinolin-4-yloxy)acetamides as *Mycobacterium tuberculosis* cytochrome *bc₁* inhibitors. *MedChemComm* 7:2122-2127.
- Pissinate K. et al. (2016). 2-(Quinolin-4-yloxy)acetamides are active against drug-susceptible and drug-resistant *Mycobacterium tuberculosis* strains. *ACS Med Chem Lett* 7:235-239.

- Piubello A. et al. (2014). High cure rate with standardised short-course multidrug-resistant tuberculosis treatment in Niger: no relapses. *Int J Tuberc Lung Dis* 18:1188-1194.
- Pogoryelov D., Yildiz Ö., Faraldo-Gómez J.D., Meier T. (2009). High-resolution structure of the rotor ring of a proton-dependent ATP synthase. *Nat Struct Mol Biol* 16:1068-1073.
- Preiss L., Langer J.D., Yildiz Ö., Eckhardt-Strelau L., Guillemont J.E., Koul A., Meier T. (2015). Structure of the mycobacterial ATP synthase F_o rotor ring in complex with the anti-TB drug bedaquiline. *Sci Adv* 1:e1500106.
- Pruksakorn P. et al. (2010). Trichoderins, novel aminolipopeptides from a marine sponge-derived *Trichoderma* sp., are active against dormant mycobacteria. *Bioorg Med Chem Lett* 20:3658-3663.
- Pruksakorn P., Arai M., Liu L., Moodley P., Jacobs Jr W.R., Kobayashi M. (2011). Action-mechanism of trichoderin A, an anti-dormant mycobacterial aminolipopeptide from marine sponge-derived *Trichoderma* sp. *Biol Pharm Bull* 34:1287-1290.
- Rao P.K., Roxas B.A., Li Q. (2008a). Determination of global protein turnover in stressed mycobacterium cells using hybrid-linear ion trap-fourier transform mass spectrometry. *Anal Chem* 80:396-406.
- Rao S.P., Alonso S., Rand L., Dick T., Pethe K. (2008b). The protonmotive force is required for maintaining ATP homeostasis and viability of hypoxic, nonreplicating *Mycobacterium tuberculosis*. *Proc Nat Acad Sci USA* 105:11945-11950.
- Reynolds R.C. et al. (2012). High throughput screening of a library based on kinase inhibitor scaffolds against *Mycobacterium tuberculosis* H37Rv. *Tuberculosis* 92:72-83.

- Rotsaert F.A., Ding M.G., Trumpower B.L. (2008). Differential efficacy of inhibition of mitochondrial and bacterial cytochrome *bc₁* complexes by center N inhibitors antimycin, ilicicolin H and funiculosin. *Biochim Biophys Acta* 1777:211-219.
- Rybniker J. et al. (2014). Anticytolytic screen identifies inhibitors of mycobacterial virulence protein secretion. *Cell Host Microbe* 16:538-548.
- Rybniker J., Vocat A., Sala C., Busso P., Pojer F., Benjak A., Cole S.T. (2015). Lansoprazole is an antituberculous prodrug targeting cytochrome *bc₁*. *Nat Commun* 6.
- Sacks L.V., Behrman R.E. (2009). Challenges, successes and hopes in the development of novel TB therapeutics. *Future* 1:749-756.
- Sarver J.G., Trendel J.A., Bearss N.R., Wang L., Luniwal A., Erhardt P.W., Viola R.E. (2012). Early stage efficacy and toxicology screening for antibiotics and enzyme inhibitors. *J Biomol Screen* 17: 673-682.
- Segala E., Sougakoff W., Nevejans-Chauffour A., Jarlier V., Petrella S. (2012). New mutations in the mycobacterial ATP synthase: new insights into the binding of the diarylquinoline TMC207 to the ATP synthase C-ring structure. *Antimicrob Agents Chemother* 56:2326-2334.
- Singh S. et al. (2015). Novel, potent, orally bioavailable and selective mycobacterial ATP synthase inhibitors that demonstrated activity against both replicating and non-replicating *M. tuberculosis*. *Bioorg Med Chem* 23:742-752.
- Smith T., Wolff K.A., Nguyen L. (2013). Molecular biology of drug resistance in *Mycobacterium tuberculosis*. *Curr Top Microbiol Immunol* 374: 53-80.

- Tantry S.J. et al. (2017). Discovery of imidazo[1, 2-*a*]pyridine ethers and squaramides as selective and potent inhibitors of mycobacterial adenosine triphosphate (ATP) synthesis. *J Med Chem* 60:1379-1399.
- Tran S.L., Cook G.M. (2005). The F₁F_o-ATP synthase of *Mycobacterium smegmatis* is essential for growth. *J Bac* 187:5023-5028.
- Trumpower B.L. (1990). Cytochrome *bc₁* complexes of microorganisms. *Microbiol Rev* 54:101-129.
- van der Westhuyzen R. et al. (2015). Pyrrolo[3, 4-*c*]pyridine-1, 3(2*H*)-diones: a novel antimycobacterial class targeting mycobacterial respiration. *J Med Chem* 58:9371-9381.
- Van Deun A., Maug A.K.J., Salim M.A.H., Das P.K., Sarker M.R., Daru P., Rieder H.L. (2010). Short, highly effective, and inexpensive standardized treatment of multidrug-resistant tuberculosis. *Am J Respir Crit Care Med* 182:684-692.
- Villemagne B., Crauste C., Flipo M., Baulard A.R., Déprez B., Willand N. (2012). Tuberculosis: the drug development pipeline at a glance. *Eur J Med Chem* 51:1-16.
- von Ballmoos C., Cook G.M., Dimroth P. (2008). Unique rotary ATP synthase and its biological diversity. *Annu Rev Biophys* 37:43-64.
- Von Jagow G., Ljungdahl P.O., Graf P., Ohnishi T., Trumpower B. (1984). An inhibitor of mitochondrial respiration which binds to cytochrome *b* and displaces quinone from the iron-sulfur protein of the cytochrome *bc₁* complex. *J Biol Chem* 259:6318-6326.
- Watanabe S., Zimmermann M., Goodwin, M.B., Sauer U., Barry C.E., Boshoff H.I. (2011). Fumarate reductase activity maintains an energized membrane in anaerobic *Mycobacterium tuberculosis*. *PLOS Pathog* 7(10): e1002287.

- WHO (2016). Global tuberculosis report. World Health Organization.
- Xia D., Esser L., Tang W.-K., Zhou F., Zhou Y., Yu L., Yu C.-A. (2013). Structural analysis of cytochrome *bc₁* complexes: implications to the mechanism of function. *Biochim Biophys Acta* 1827:1278-1294.
- Xia D. et al. (1997). Crystal structure of the cytochrome *bc₁* complex from bovine heart mitochondria. *Science* 277:60-66.
- Yano T., Kassoovska-Bratinova S., The J.S., Winkler J., Sullivan K., Isaacs A., Schechter N.M., Rubin H. (2011). Reduction of clofazimine by mycobacterial type 2 NADH: quinone oxidoreductase. *J Biol Chem* 286: 10276-10287.
- Yew W. (2006). Development of new antituberculosis drugs. Nova Science Publishers: New York
- Zorov D.B., Juhaszova M., Sollott S.J. (2006). Mitochondrial ROS-induced ROS release: an update and review. *Biochim Biophys Acta* 1757:509-517.

Figures

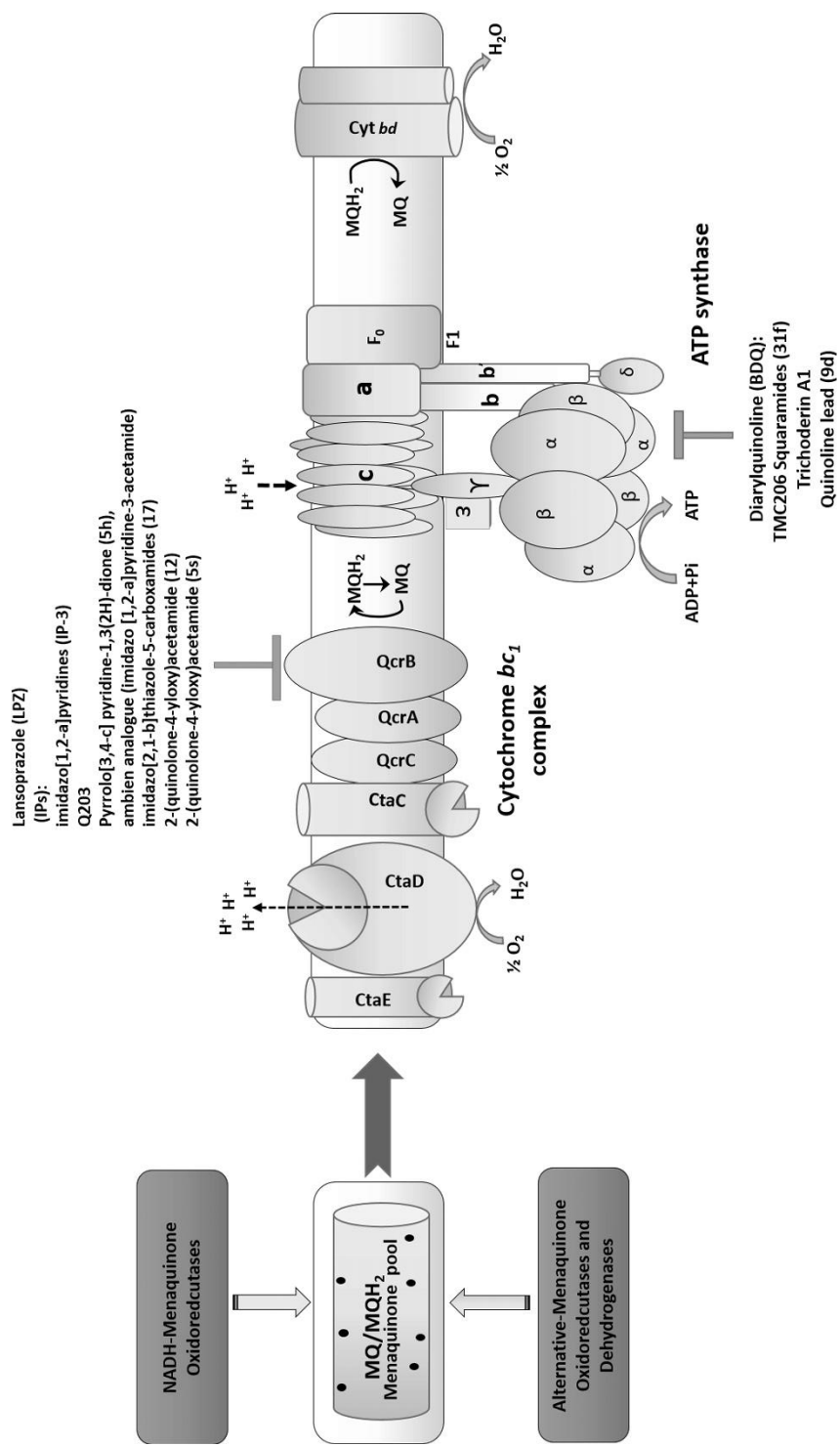


Figure 1. The core respiratory components of mycobacteria and their drug targets (primarily focusing on *M. tuberculosis*): NADH-menaquinone oxidoreductase (NDH1 and NDH2) and alternate-menaquinone oxidoreductases transfer reducing power from electron donors to menaquinone (MQ), which is reduced to menaquinol (MQH₂). From the menaquinol pool, electrons can be transferred to the cytochrome *bc₁* complex (*b* subunit is composed of QcrA, QcrB and QcrC). The cytochrome *bc₁* complex forms a super-complex with the cytochrome *aa₃*-type terminal oxidase, which transfers electrons to reduce oxygen (terminal electron acceptor). During the process protons (H⁺) are deposited outside of the membrane and help to establish/maintain the electrochemical gradient. Under low oxygen tension or hypoxic conditions, electrons from menaquinone can be directly transferred to oxygen by the cytochrome *bd*-type menaquinol oxidase. ATP synthesis by the F₁F₀-ATP synthase is driven by the translocation of H⁺. The F₁ and F₀ complexes are made up of the α₃β₃γδ_ε and ab₂c₉ subunits, respectively. Cytochrome *bc₁* complex inhibitors shown: lansoprazole (LPZ), imidazo[1,2-*a*]pyridines (IPs), Q203, pyrrolo[3,4-*c*]pyridine-1,3(2*H*)-dione, 2-(quinolin-4-yloxy)acetamide (5s), Ambien analogue (5), 2-(quinolin-4-yloxy)acetamide (12). ATP synthase inhibitors shown: bedaquiline (BDQ), squaramides, trichoderin A1.

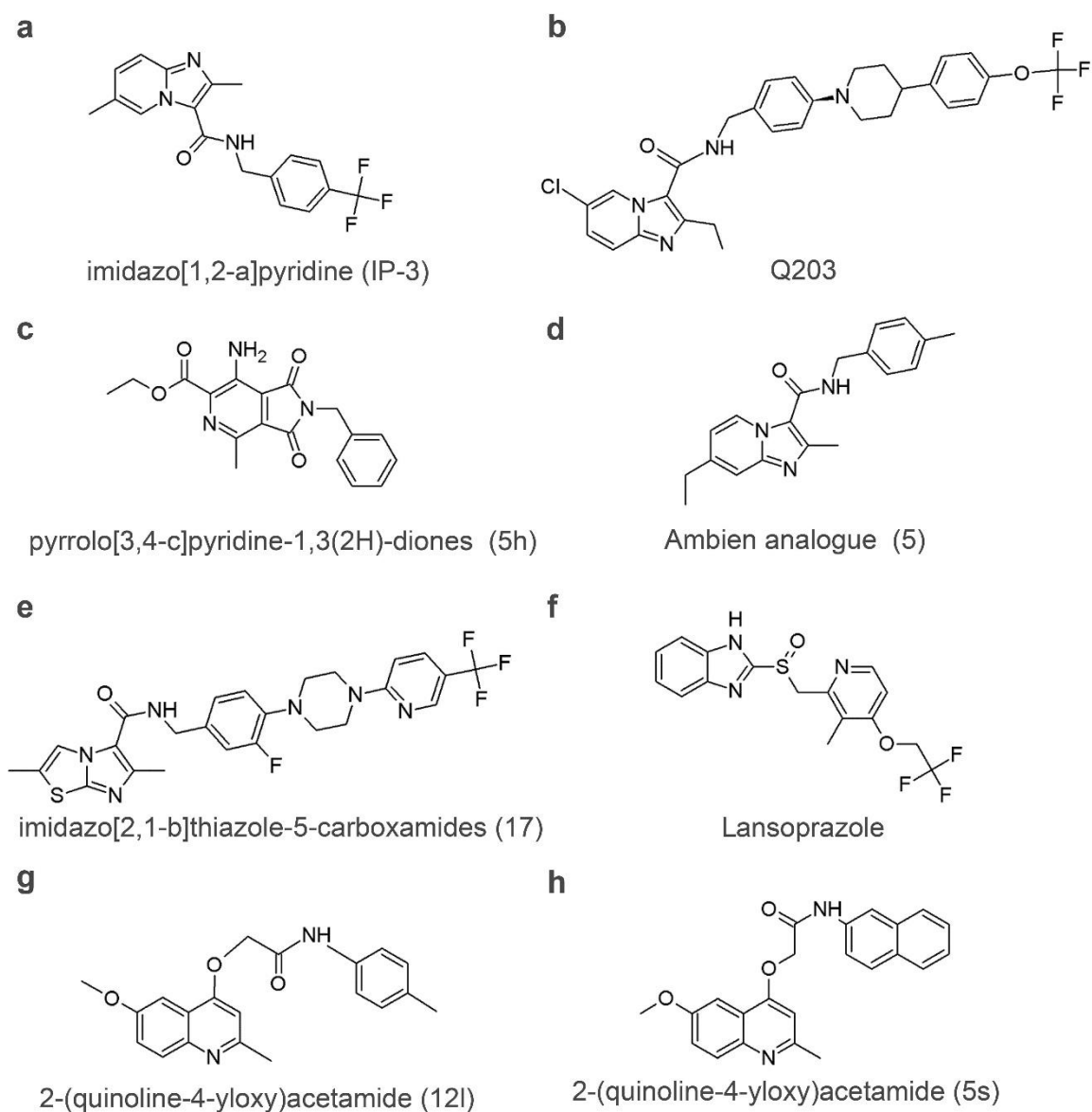


Figure 2. Chemical structure of mycobacterial QcrB inhibitors. **(a)** imidazo[1,2-*a*]pyridine (compound IP-3; Abrahams et al. 2012), **(b)** Q203 (Petthe et al. 2013), **(c)** pyrrolo[3,4-*c*]pyridine-1,3(2*H*)-diones (compound 5h; van der Westhuyzen 2015), **(d)** Ambien analogue (compound 5; Cheng et al. 2014; Moraski et al. 2015), **(e)** imidazo[2,1-*b*]thiazole-

5-carboxamides (compound 17; Moraski et al. 2016), **(f)** lansoprazole (Rybniker et al. 2015), **(g)** 2-(quinolin-4-yloxy)acetamide (compound 12l; Phummarin et al. 2016), **(h)** 2-(quinolin-4-yloxy)acetamide (compound 5s; Pissinate et al. 2016).

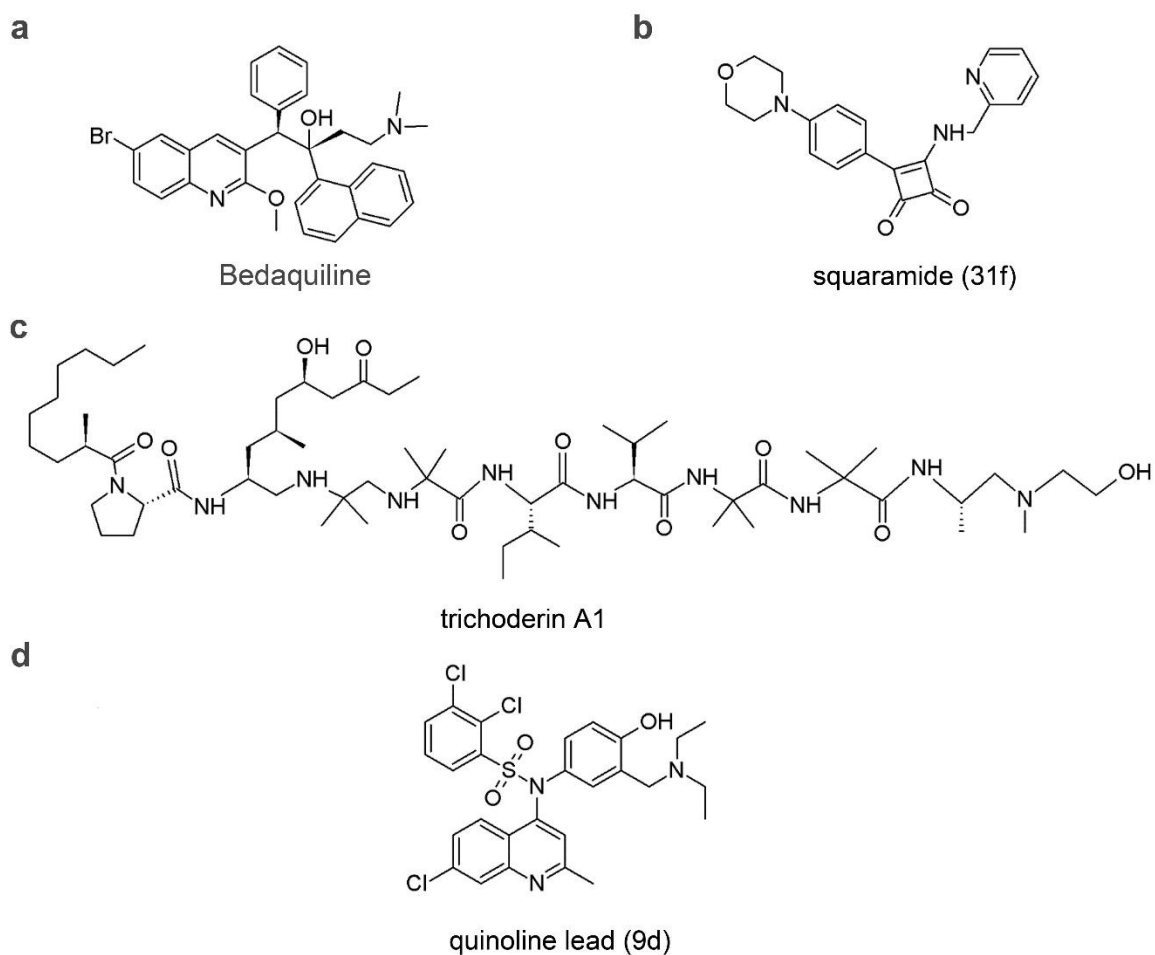


Figure 3. Chemical structure of mycobacterial AtpE inhibitors. **(a)** bedaquiline (Andries et al. 2005), **(b)** squaramide (compound 31f; Tantry et al. 2017), **(c)** trichoderin A 1 (Pruksakorn et al. 2010), **(d)** quinoline lead (compound 9d; Singh et al. 2015).